Investigation of Decommissioning of Offshore Wind Mono-Pile Foundations

Ahmed AbdulHameid Al Mowafy

Renewable Energy Marine Structure Centre of Doctoral Training
Department of Naval Architecture, Marine and Ocean Engineering [Civil and Environmental Engineering]
University of Strathclyde

21 August 2023

A thesis submitted in fulfilment of the requirements for the degree of Doctorate of Philosophy

Supervisor
Professor Feargal Brennan

Declaration of Authenticity & Author's Rights

This thesis is the result of the author's original research. It has been composed by the author and has not been previously submitted for examination which has led to the award of a degree.

Ahmed Al Mowafy

21/08/2023

Abstract

Decommissioning process intricacy level varies depending on the offshore wind turbine components. Decommissioning superstructure components -blades, nacelle, tower, etc.- is a straightforward process, which is the reverse of the installation. The full removal decommissioning strategy that applies to the superstructure extends to include a few offshore wind foundations. For instance, the decommissioning of suction bucket foundation is through release and extract by applying pressure. Nonetheless, for the pile foundation, which is the most common type, with a total installation of more than 7,000 [4,914 single and 2,934 group piles], the decommissioning is complicated; one reason is that excavation is required in the two strategies - full and partial removal [cutting the pile externally]. However, the current industry-proposed methods may not always be adopted, and developing novel foundation decommissioning methods such as extraction [full removal] becomes mandatory/ beneficial. The reason is that offshore wind currently initiated to alter the method for decommissioning some of its turbine components, e.g., blades, from landfilling the material to recycling. For extraction method feasibility validation, an investigation was carried out through an experimental campaign and a techno-economic assessment.

For the experimental campaign, a series of 1g model pile extraction tests using displacement and force control and 400mm long open-ended steel piles with diameters of 88.9 and 101.6 mm were conducted in unsaturated and saturated soil. Experimental campaign results showed the tensile capacity of both piles had reduced by up to 90% compared to the compression capacity in both conditions.

In the unsaturated case, with maintaining the soil density constant, results had evident the impact of extraction rate -by reducing- the tensile capacity of the pile regardless of diameter. Nonetheless, in the saturated soil, the tensile capacity decreased due to the pore water pressure; for the 101.6 mm pile, the decline was by 50 and 18% for displacement and force extraction applications, respectively.

Compared with displacement extraction application, the tensile capacities of the 88.9 and 101.6 mm piles under force decreased [lowest] by 25 and 23% in unsaturated soil and saturated soil by 6 and 11%, respectively. Despite higher capacity under displacement extraction, the application exhibited local shear failure -partial drainage occurrence due to the application mechanism- where piles had extracted soil-free, which was not the case for the force

application. The experimental results validated the theoretical method developed in aiding extraction of OWPile foundations and demonstrated the feasibility and efficiency of extraction application, displacement, and required total energy [velocity and time].

For the techno-economic assessment, a model developed to determine the most economical decommissioning strategy and method for offshore wind foundations in terms of timing and costs by comparing the industry-preferred strategy [partial removal] with the novel-proposed one. The model inputs' parameters included foundation removal operations duration, wait-on-weather, and vessels' strategies and types, which are key drivers that significantly influence the total decommissioning costs. Additionally, sensitivity analysis was carried out for the input parameters because are subject to a high degree of uncertainty. For the sensitivity analysis, the parameters' baseline estimated values had increased by conservative percentages; offshore wind foundations decommissioning methods activities' estimated duration by 100%, ranging the weather adjustment factor by 50 – 100%, and vessels' day rate by ± 20%.

The model results showed that the economical vessels' strategy, regardless of decommissioning strategy/ method, is the transiting -utilising two vessels of the same type- compared to the sender one. Analysing results further, heavy lift vessels (HLV) carry out decommissioning activities in less time than wind turbine installation vessels (WTIV), nevertheless increasing the costs due to their low availability. The sensitivity analysis results showed that despite increasing weather factor adjustment factor and vessels' day rate, the total cost for the novel decommissioning proposed method is more economical than the industry-proposed one. Including the learning curve in the analysis, the total cost of offshore wind foundations decommissioning, regardless of methods, could reduce by up to 35%.

Contents

Declaration of Authenticity & Author's Rights i
Abstract ii
Contents iv
List of Figures vii
List of Tables xii
Acknowledgements xiv
1 Introduction 1-1
1.1 Background 1-1
1.2 Research Aim 1-3
1.3 Research Objectives 1-3
1.4 Thesis Structure 1-4
2 Literature Review 2-1
2.1 Background 2-1
2.2 Global Wind Overview 2-5
2.3 Offshore Wind Industry 2-11
2.4 Offshore Wind Technology 2-18
2.5 Offshore Wind Fixed Substructures 2-20
2.5.1 Mono-pile Structure 2-22
2.5.2 Tri-pod Structure 2-23
2.5.3 Tri-pile Structure 2-24
2.5.4 Jacket Structure 2-25
2.6 Offshore Wind End-of-Life Scenarios 2-26
2.6.1 Life Extension Scenario 2-27
2.6.2 Repowering 2-27
2.6.3 Decommissioning 2-30
2.7 Offshore Wind Pile Foundations Decommissioning Operations 2-35
2.7.1 Partial Removal Strategy 2-36
2.7.2 Full Removal Strategy 2-38
2.8 Case Study 2-41
2.8.1 Literature Review 2-41
2.8.2 Industrial Criteria 2-42
3 Experimental Campaign 3-1
3.1 Background 3-1
3.2 Pile Foundation Classifications 3-2

3.2.1 Design 3-2
3.2.2 Material and Construction 3-3
3.2.3 Installation Methods 3-4
3.3 Structure [Pile]-Soil Interaction Mechanism: Pile Installation Influence 3-6
3.4 Extraction Theory Mechanics 3-10
3.4.1 Failure Surface Shape 3-11
3.4.2 Skin Friction 3-14
3.4.3 Suction Force 3-16
3.5 Experimental Components 3-17
3.5.1 Model Pipe Pile 3-18
3.5.2 Perspex Model Box 3-20
3.5.3 Supporting Frame 3-22
3.5.4 Soil Properties 3-24
3.5.5 Semi-submersible pressure transducer 3-25
3.6 Experimental Investigation Setup 3-28
3.7 Experimental Investigation Procedures 3-35
3.8 Experimental Investigation Results 3-40
3.8.1 Pile Installation 3-40
3.8.2 Validating The Experimental Investigation Results 3-43
3.8.3 Tension Versus Compression 3-48
3.8.4 Extraction in Unsaturated Soil 3-52
3.8.5 Extraction in Saturated Soil 3-63
3.8.6 Suction Force 3-75
3.8.7 Failure Surface Shape 3-86
3.9 Conclusion 3-88
4 Decommissioning Techno-Economic Assessment of Offshore Wind Fixed Foundations 4-1
4.1 Background 4-1
4.2 OWFoundations' Removal Operations Duration 4-8
4.3 Wait-on-Weather 4-14
4.4 Vessels 4-17
4.4.1 Background 4-17
4.4.2 Vessel Strategies 4-20
4.4.3 Vessel Types 4-21
4.4.4 Vessels Costs 4-26
4.4.5 Vessels in Offshore Wind Decommissioning 4-27
4.5 Cost and Time Modelling for OWFoundations Decommissioning 4-28

4.5.1 Transiting Strategy 4-33
4.5.2 Sender Strategy 4-37
4.6 Results 4-39
4.7 Sensitivity Analysis 4-42
4.7.1 OWFoundations' Removal Operations Duration 4-42
4.7.2 Wait-on-Weather 4-44
4.7.3 Vessel Day Rates 4-45
4.7.4 Learning Curve 4-46
4.8 Conclusion 4-49
5 Conclusion 5-1
5.1 Decommissioning By Extraction 5-2
5.2 Decommissioning Techno-Economic Assessment 5-5
5.3 Future Research 5-6
6 Reference 6-1
7 Appendix 7-1
7.1 Appendix A 7-1
7.2 Appendix B 7-3
7.3 Appendix C 7-4

List of Figures

Figure 2-1. Renewable energy sources' cumulative installed capacity globally—source: author edited based on [18].....2-3
Figure 2-2. Renewable energy technologies' electricity generation cumulative percentages concerning renewable's total share in the global electricity generation mix – source: author edited based on [5], [22].....2-4
Figure 2-3. Global wind cumulative installed capacity - source: author edited based on [1], [18]. 2-7
Figure 2-4. Geographical regions' on-shore wind cumulative installed capacity - source: author edited based on [1], [18]. 2-7
Figure 2-5. Geographical regions' off-shore wind cumulative installed capacity - source: author edited based on [1], [18]. 2-8
Figure 2-6. Europe's current offshore wind's cumulative installed capacity, 28GW, and turbines - source: author edited based on [41], [45].....2-12
Figure 2-7. The impact of wind turbine blades fabricating materials [resin/ fibre glass] on decommissioning; a top view of the Casper landfill, Wyoming. 2-14
Figure 2-8. The industry's proposed/ preferred offshore wind foundations decommissioning strategy impact -partial removal- on the seabed – created by the author.....2-14
Figure 2-9. Offshore wind foundations' full removal strategy impacts on the seabed – created by the author. 2-15
Figure 2-10. The impact of offshore wind bottom-fixed foundations decommissioning strategies concerning seabed availability on the industry's long-term development sustainability. 2-16
Figure 2-11. The average turbine capacity installed and forecasted from 2015 - 2020 and 2020 - 2016, respectively - source: author's analysis for various resources. 2-19
Figure 2-12. Offshore wind farms' average water depth from 2015 to 2021 and forecasted depths from 2021 to 2026 - source: author's analysis for various sources. 2-19
Figure 2-13. Schematic view of mono-pile structure.....2-23
Figure 2-14. Schematic view of tri-pod structure. 2-24
Figure 2-15. Schematic view of tri-pile structure. 2-25
Figure 2-16. Schematic view of jacket structure.....2-26
Figure 2-17. The potential sequence of end-of-life scenarios. 2-30
Figure 2-18. Break down the offshore wind farm decommissioning process stages. 2-31
Figure 2-19. The capacities and the number of offshore wind farms and their turbines projected for decommissioning, the default option, over the next two decades.....2-34
Figure 2-20. When the decommissioning will occur, following the adoption of life extension and repowering scenarios. 2-34
Figure 2-21. The percentage of OWFoundations decommissioning methodologies supported by offshore oil & gas and wind industries' experts.....2-36
Figure 2-22. A simplified comparison of activities for partial removal and extraction methodologies. 2-40
Figure 2-23. The installed Cumulative Offshore Wind Capacity By sea basin.....2-42
Figure 2-24. UK in-operation OWFs by sea basin.....2-44
Figure 2-25. UK in-operation OWFs by total capacity. 2-44
Figure 2-26. The UK in-operational OWFs by area. 2-45
Figure 2-27. The UK in-operational OWFs by distance to shore. 2-45
Figure 3-1. The types of steel pipe piles. 3-3
Figure 3-2. The three modes of pile penetration; from left to right, fully coring, partially plugged and fully plugged. 3-8
Figure 3-3. The two assumed shapes of the failure surface for extracting a pile; [A] dense sand and stiff clay and [B] loose sand and soft clay.....3-13

Figure 3-4. The components of shaft resistance - internal and external friction. 3-15
Figure 3-5. The assumed zone of suction occurrence for extracting open-ended piles. 3-16
Figure 3-6. The utilised two piles' diameters. 3-19
Figure 3-7. Piles lengths of 88.9 [left] and 101.6mm [right]. 3-19
Figure 3-8. The piles' dimensions - diameters [left] and wall thicknesses [right]. 3-19
Figure 3-9. The [altered] hole diameter on piles-surface [left] and piles weights [right]. 3-19
Figure 3-10. The pile-machine attachment setup, including the pin's insertion location. 3-20
Figure 3-11. A schematic diagram of the perspex box. 3-21
Figure 3-12. The supporting frame schematic view. 3-23
Figure 3-13. The supporting frame design and assembly. 3-23
Figure 3-14. The soil's grain-size distribution, provided by i2 Analytical Ltd. 3-25
Figure 3-15. The semi-submersible pressure transducer dimensions; cross-section dimensions adopted from Omega (no date b). 3-26
Figure 3-16. The transducer setup before installation. 3-26
Figure 3-17. The transducer wiring [left] and its output wires attached to the strain gauge wiring box [right]; [+] white & [-] green are outputs signal wires, [+] red & [-] black are excitation wires, ground wire and [transparent] drainage wire. 3-27
Figure 3-18. iNet-600 and iNet-512 assembly. 3-27
Figure 3-19. The ZwickRoell testing machine. 3-30
Figure 3-20. Testing schematic machine's front and side views. 3-30
Figure 3-21.Experiments' schematic setup; testing machine, Perspex box and support frame. 3-31
Figure 3-22. The dimensions of the Perspex box to the machine testing area; the images from left to right are front sides [left and right] for length and left [front] and right front] sides for width. 3-31
Figure 3-23. The support frame dimensions-to- the machine testing area; images from left to right are front [left] and back [right] sides for length and left [front] and right [front] for width. 3-32
Figure 3-24. The final position of the Perspex box [left] and the support frame [middle and right] within the testing area. 3-32
Figure 3-25. The poured soil layer before and after levelling and compacting. 3-32
Figure 3-26. The positioning of the semi-submersible pressure transducer in the soil. 3-33
Figure 3-27. The 101.6mm pile diameter distance to the Perspex box's inner wall in saturated soil [experiment #]; the images from left to right are front, back, left, and right sides. 3-33
Figure 3-28. Starting positions for embedding piles' diameters in the two soil conditions; images from left to right are unsaturated and saturated soil for 88.9 and 101.6 mm. 3-33
Figure 3-29. A close-up view of the distance tightness between the pile and machine load cell for accessing and measuring the developed soil column during and after the embedment. 3-41
Figure 3-30. The height of the soil column resulting from the 88.9 mm pile installation in the unsaturated soil. 3-41
Figure 3-31. The soil column height developed inside the 101.6 mm pile in the unsaturated soil during installation. 3-41
Figure 3-32. The hammering effect on the soil column developed in 88.9 [left] and [right] 101.6 mm piles in saturated soil. 3-43
Figure 3-33. Load-displacement curves for the extracting 88.9 mm pile showing failure displacement consistency in testing extraction applications; [A] displacement and [B] force. 3-45
Figure 3-34. Load-displacement curves for the extracting 101.6 mm pile showing failure displacement consistency in testing extraction applications; [A] displacement and [B] force. 3-46
Figure 3-35. Load-displacement curves for installing and extraction of the tested piles' diameters in two soil conditions; A [88.9 mm] and B [101.6 mm] in unsaturated, and C [88.9 mm] and D [101.6 mm] in saturated. 3-51
Figure 3-36. The load-displacement curve of displacement-extracting application testings for the 88.9mm pile in unsaturated soil. 3-52

Figure 3-37 presents the load-displacement response to the impact of soil densification on the rate of extracting the 88.9 mm pile in unsaturated soil. 3-53
Figure 3-38. The load-displacement response for the impact of extracting the 88.9 mm pile with a higher velocity than 50 mm/min on the tensile capacity in the unsaturated soil.....3-54
Figure 3-39. The load-displacement curve of each applied velocity to extract the 101.6 mm pile in unsaturated soil. 3-55
Figure 3-40. The load-displacement response to different rates of extracting the 101.6 mm pile in unsaturated soil with constant density.....3-55
Figure 3-41. The response of the load-displacement curve when applying high displacement velocity, 100 mm/min, for 101.6 mm pile extraction in unsaturated soil. 3-56
Figure 3-42 The load-displacement response for the impact of increasing the extraction rate on the tensile capacity of the 101.6 mm pile in unsaturated soil with lower density. 3-56
Figure 3-43. The load-displacement curves of the applied forces for extracting the 88.9 mm pile in unsaturated soil; two curves from displacement extraction tests had used for comparison. 3-57
Figure 3-44. The load-displacement curves resulting from the applied rates to extract the 101.6 mm pile in unsaturated soil; for comparison, three curves were adopted for displacement extraction testing. ...3-58
Figure 3-45. The peak tensile capacity of the 101.6 mm pile resulting from the employed force and displacement extraction applications in unsaturated soil. 3-59
Figure 3-46. The load-displacement response to the influence of soil densification on the 101.6 mm pile's tensile capacity with a constant extraction force rate. 3-61
Figure 3-47. The response of the load-displacement curves at and after exceeding a specific force rate, 150 N/min, for 88.9 mm pile extraction in unsaturated soil. 3-62
Figure 3-48. The effect of force-extracting rates at and surpassing 100 N/min on the tensile capacity of a 101.6 mm pile in unsaturated soil. 3-62
Figure 3-49. The load-displacement response for extracting the 88.9mm pile diameter in saturated soil by applying various displacement velocities. 3-64
Figure 3-50. The response of the load-displacement curves for extracting the 88.9 mm pile with 50 mm/min or higher displacement. 3-65
Figure 3-51. The load-displacement response for 101.6mm pile diameter extraction tests in saturated soil employing the displacement-control method. 3-66
Figure 3-52. The influence of applying 50 and 100 mm/min extraction velocities on the 101.6 mm pile's tensile capacity in saturated soil.....3-67
Figure 3-53. The load-displacement curves' response for extracting both piles' diameters in unsaturated and saturated soil with almost constant density; [A] 88.9 and [B] 101.6 mm piles. 3-68
Figure 3-54. the load-displacement response in saturated soil for 88.9 mm pile extraction tests through the force-control method. 3-70
Figure 3-55.The 101.6 mm pile's load-displacement curve in saturated soil for the force-extracting method. 3-71
Figure 3-56. The impact of the weight and length of the soil plug pulled with the pile on the tensile capacity of the pile; [top] 88.9 mm and [bottom] 101.6 mm piles.....3-73
Figure 3-57.In testing force extraction application, the load-displacement curves for extracting both piles' diameters in unsaturated and saturated soil with almost constant density; [A] 88.9 and [B] 101.6 mm piles.....3-74
Figure 3-58. The pore pressure-time curve for extracting the 88.9 mm pile in saturated soil with a 5 mm/min velocity. 3-76
Figure 3-59. The pore pressure-time curves for the three velocities applied for extracting the 88.9 mm pile in saturated soil. 3-76
Figure 3-60. The pore pressure-time curve response for a 5 mm/min extraction velocity in testing the 88.9 mm pile in saturated soil. 3-77

Figure 3-61. The pore pressure-time curves for the applied velocities for extracting the 101.6 mm pile in saturated soil. 3-77
Figure 3-62. The elevation level of the plug to the soil surface for extracting both piles' diameters by applying various displacement velocities; [top] 88.9 mm and [bottom] 101.6 mm piles. 3-78
Figure 3-63. The pore water pressure level during extracting both piles' diameters under 50 and 100 mm/min displacement velocity; [top] 88.9 mm and [bottom] 101.6 mm pile. 3-79
Figure 3-64. The response of the pore pressure-time curves for extracting the 88.9 mm pile in saturated soil under various force rates. 3-82
Figure 3-65. The response of the pore pressure-time curves for extracting the 101.6 mm pile in saturated soil under various force rates. 3-83
Figure 3-66. The pore pressure-time curve response for extracting the 88.9 mm pile under the rate of 150 N/min in saturated soil. 3-83
Figure 3-67. The pore pressure-time curve for extracting the 101.6 mm pile in saturated soil with 50 N/min rate. 3-84
Figure 3-68. The conditions of the soil and 88.9 mm pile after terminating force-extraction application testing. 3-84
Figure 3-69. The conditions of the soil and 101.6 mm pile after terminating force-extraction application testing. 3-85
Figure 3-70. The top view of the failure surface shape and its diameter in unsaturated soil; [top] 88.9 mm -force- and [bottom] 101.6 mm piles –[left] displacement and [right] force. 3-86
Figure 3-71. The top view of the failure surface shape [vertical] and its diameter in saturated soil; [top] 88.9 mm, [bottom] 101.6 mm piles, [left] displacement and [right] force. 3-87
Figure 3-72. An overview of a few factors of the processes that influence extraction. 3-89
Figure 3-73. The potential influencing factors on the extraction load of open-ended piles in different soils; [A] dense sand and stiff clay and [B] loose sand and soft clay. 3-90
Figure 4-1. Offshore wind expenditures' percentage breakdown. 4-2
Figure 4-2. Offshore wind cost elements' contribution percentage to levelised cost of Energy (LCOE). 4-2
Figure 4-3. Some of the decommissioning stages' activities. 4-3
Figure 4-4. The increase in decommissioning cost per MW. 4-5
Figure 4-5. Breakdown of decommissioning costs. 4-5
Figure 4-6. How likely each of the covered decommissioning methodologies will reduce foundations removal costs. 4-7
Figure 4-7. How likely offshore oil & gas and wind industries' experts consider removal operations duration in their decision-making process? 4-8
Figure 4-8. How offshore O&G and wind industries experts will likely utilise existing and proposed removal methodologies for offshore wind foundations, relying on their durations. 4-11
Figure 4-9. The percentage of OWFoundations decommissioning methodologies supported by offshore oil & gas and wind industries' experts. 4-12
Figure 4-10. The stages where the utilised vessels could experience potential delays due to wait-on-weather. 4-14
Figure 4-11. The impact of Hs on-site on completing offshore activities utilising Wind Turbine Installation Vessels. 4-15
Figure 4-12. The number of in-operation Jack-Ups capable of installing wind turbine capacities. 4-19
Figure 4-13. Vessels' cost breakdown for the offshore wind decommissioning phase. 4-26
Figure 4-14. The time and cost of a single vessel for transit strategy for foundations partial removal options by cutting the pile at or 1 to 2m below the seabed. 4-40
Figure 4-15. The time and cost of a single vessel for transit strategy for foundations full removal option by extraction. 4-40
Figure 4-16. The time and cost of multi vessels for transit strategy for foundations partial removal options by cutting the pile at or 1 to 2 m below the seabed. 4-41

Figure 4-17. The time and cost of multi vessels for transit strategy for foundations full removal by extraction.....4-41
Figure 4-18. The impact of incrementing removal methodologies operations duration for offshore wind foundations utilising two WTIVs on decommissioning cost and time. 4-43
Figure 4-19. The impact of incrementing removal methodologies operations duration for offshore wind foundations utilising two HLVs on decommissioning cost and time. 4-43
Figure 4-20. The time and cost of the sensitivity of the wait-on-weather factor for decommissioning removal strategies utilising two WTIVs. 4-44
Figure 4-21. The time and cost of the sensitivity of the wait-on-weather factor for decommissioning removal strategies utilising two mooring HLVs. 4-44
Figure 4-22. Impact of setting vessels day rates on foundations partial removal options costs. 4-45
Figure 4-23. Impact of setting vessels day rates on foundations full removal option [extraction] costs. 4-46
Figure 4-24. Hypothetically, the learning rates' impact on the total decommissioning cost.....4-47
Figure 4-25. The effects of learning rates on OWFs decommissioning cost and time utilising transit strategy. 4-48
Figure 4-26. The impact of WOW and removal methodologies' operations on vessels. 4-50
Figure 4-27. Decommissioning expenditures reduction and increment factors. 4-51
Figure 7-1. Up-to-date [2021] global wind cumulative installed capacity - source: author analysis edited based on [GWEC, 2022]. 7-1
Figure 7-2. Geographical regions cumulative wind installed capacity, on and offshore – source: author edited based on [GWEC, 2022]. 7-2

List of Tables

Table 2-1. An estimate of wind total installation capacity (GW) in various geographical regions by 2050. 2-10
Table 2-2 summarises substructure and foundation types.....2-22
Table 2-3 defines the water depth ranges of most offshore wind fixed substructures. 2-22
Table 2-4 presents decommissioned offshore wind farms/ turbines. 2-32
Table 2-5 displays the error percentage of the number of turbines. 2-35
Table 2-6 summarises the proposed decommissioning strategies and methodologies for OWFoundations. 2-37
Table 2-7 summarises the partial removal strategy's methodologies differences. 2-38
Table 2-8 summarises the offshore wind farms/ turbines' reference adoption in the existing literature. 2-42
Table 2-9 summarises Horn Rev 1 wind farm specifications.....2-43
Table 2-10 summarises the criteria for the case study selection. 2-43
Table 2-11 summarises the availability Status for DP and ES of the eligible nine offshore wind farms. 2-46
Table 2-12 summarises GGOWF specifications. 2-47
Table 3-1 summarises a few of the various piles employed in the available experimental investigations. 3-6
Table 3-2 represents the dimensions of some of the open-ended piles. 3-6
Table 3-3 summarises the dimensions of model piles. 3-18
Table 3-4 illustrates a few of the suggested pile-to-model box or to-centrifuge ratios. 3-21
Table 3-5 summarises the Perspex box dimensions. 3-21
Table 3-6 indicates pile-to-box ratios.....3-21
Table 3-7 summarises the dimensions of the supporting frame. 3-24
Table 3-8 summarises Kiln Dried Sand's primary properties. 3-25
Table 3-9 represents experiments' schematic setup. 3-31
Table 3-10 exhibits the logged measurements for piles' distance to the perspex box's inner wall over different experimental tests. 3-33
Table 3-11 summarises the executed stages' aim in the experimental campaign tests. 3-35
Table 3-12 summarises the sets' variables of the experimental campaign. 3-35
Table 3-13 depicts the number of tests carried out for each set. 3-37
Table 3-14 exhibits extraction repeatability tests in sets one to four. 3-37
Table 3-15 shows the record of experiments.....3-39
Table 3-16 summarises the ratio of reduction in pore water pressure from the start of the extraction process until failure in testing displacement extraction application. 3-80
Table 3-17 summarises the ratio of reduction in pore water pressure from the start of the extraction process until failure in testing force extraction application. 3-81
Table 3-18 summarises parameters for future investigation. 3-92
Table 4-1 summarises estimated decommissioning expenditures of offshore wind farms. 4-3
Table 4-2 summarises the estimated time for the first two decommissioning stages' activities. 4-4
Table 4-3 summarises DecEx estimation by scholars. 4-6
Table 4-4 summarises decommissioning strategies and methodologies adopted by the studied sources. 4-6
Table 4-5 summarises the proposed decommissioning strategies & methodologies for OWFoundations. 4-9
Table 4-6 demonstrates proposed excavating equipment for partial removal methodologies in the offshore oil and gas industry. 4-10

Table 4-7 summarises the proposed equipment for cutting piles internally and externally in offshore oil & gas and wind industries. 4-10
Table 4-8 compares removal activities proposed for cutting the pile internally. 4-10
Table 4-9 summarise the estimated duration for offshore wind foundations removal operations. 4-11
Table 4-10 categorises the duration range for the existing and proposed removal methodologies for OWFoundations. 4-13
Table 4-11 compares feeding and transiting strategies. 4-21
Table 4-12 compares self-propelled jack-up types....4-23
Table 4-13 summarises the specifications of MPI resolution. 4-24
Table 4-14 compares a few specifications of JUB and SPJU. 4-25
Table 4-15 summarises a few specifications for HLVs' four types. 4-26
Table 4-16 illustrates proposed vessel strategies and types for offshore wind farms' foundations decommissioning. 4-27
Table 4-17 summarises data availability status in the studied sources. 4-29
Table 4-18 summarises the average WTIV fundamental specifications. 4-34
Table 4-19 summarises WTIVs technical specifications utilised by the decommissioning programme and the literature review available. 4-35
Table 4-20 summarises WTIVs costs. 4-35
Table 4-21 summarises the WTIVs implemented values in vessels' cost and time model. 4-36
Table 4-22 summarises mooring HLV cranes fundamental specifications based on Seaway Yudin specifications. 4-36
Table 4-23 summarises mooring HLV cranes available technical specifications and costs. 4-36
Table 4-24 summarises self-elevating jack-up barges fundamental specifications based on JB-117 specifications. 4-38
Table 4-25 summarises self-elevating jack-up barges costs. 4-38
Table 4-26 summarises floating sheerleg fundamental specifications. 4-39
Table 4-27 summarises floating sheeleg vessels costs. 4-39
Table 5-1 summarises the required future work for decommissioning offshore wind mono-pile foundations. 5-7

Acknowledgements

I would like to express my gratitude to my supervisor, Professor Feargal Brennan, for believing in me and the project, and for the support, time, and resources he has provided me throughout my study.

I want to extend my gratitude to my family. To my parents, Dr Abdulhameid Almowafy and Ragaa Rabie, thank you for your belief in me and your love which has been my strength throughout this journey. Your sacrifices and support have not gone unnoticed and have been influential in my reaching this point. To my siblings, Sanaa, Yasser, and Hussam Almowafy, thank you for your constant disturbing and always being there for me. To my lively niece, Jana Sameh, whose boundless energy and good-natured mischief have been a constant source of amusement and frequent distraction.

In order to obtain this milestone within my professional journey, I would like to offer my sincerest thank you for Dr Manpreet Puri, Miss Fatemeh (Diba) Bazargani and Mr Nikolas G. Tsamalis for offering their support through the peaks and troughs of this thesis, and completing this to the high standard and expectations I have set for myself.

I would like to thank Dr Saeid Lotfian and the University of Glasgow members, Dr Mohammad Fotouhi and Dr Sakineh Fotouhi, for allowing the usage of the testing machine in the Rankine Building. The ability to use the laboratory was instrumental in conducting my experiments and contributed to the successful completion of my research.

Chapter One

1 Introduction

1.1 Background

Offshore wind has rapidly grown in development since the first offshore wind farm commissioned in 1991. In the last three decades, Europe was leading the market with a cumulative global wind installed capacity of 35 GW [1]. Offshore wind plays a pivotal role in the recent energy transition sector which is forecasted to generate 10% of global electricity by 2050 which can be equated to an installation capacity of 1,400 GW [2]. Additionally, continents such as Europe consider offshore wind a core source to become carbon-neutral by 2050. They are installing capacity ranging from 230 to 450 GW, proving it to be one of the leading sources of clean, renewable energy [3]. To ensure long-term sustainable development and achieve 2050 targets, the current focus of offshore wind is on overcoming the challenges of development, including their duration and activities -from leasing to installation. However, there seems to be little to no focus on post-operational stages, especially decommissioning, which is the current default option from end-of-life scenarios.

Decommissioning began to be viewed as a broader phase, with abandonment being just one of its constituent processes or activities. While the overarching objective of decommissioning has remained consistent, adjustments have been introduced to accommodate exceptions to the full removal of offshore installations. These exceptions allow for strategies like partial removal or leaving installations in-situ, provided they pose no risks posed to navigation, marine ecosystems, or other sea users. Intriguingly, these updated regulations were swiftly incorporated and applied to marine projects with structural designs similar to offshore oil and gas, such as offshore wind, without accommodating potential industry-specific variations like purpose, risk, or scale.

Onshore wind has proven the critical importance of decommissioning in long-term sustainable development, with efforts ranging from banning the landfill of decommissioned wind turbines to recycling its materials. As the wind industry takes steps to alter the method for decommissioning, it is expected that these changes will eventually extend to include other

components, particularly in the offshore wind sector. One component believed to be impacted is the fixed steel pile foundations.

Up to mid-2022, the offshore wind industry's dominant foundation type was the fixed-steel open-ended pile, totalling 7,848 installations. Categorising fixed-steel open-ended pile types solely, single piles [mono-pile substructure] account for 62.6%, while group piles [jacket, tri-pod and tri-pile substructures] account for 37.4%. When comparing decommissioning strategies of offshore wind foundation types, the industry's preferred approach for pile foundations is partial removal, in contrast to suction bucket and gravity-base foundations, where full removal is favored.
Considering the rapid growth of offshore wind, the predominance of pile foundations, and the application of the industry's proposed decommissioning strategy, among other factors, the long-term consequence could be a reduction in seabed availability, leaving no space for sustainable development.

The preceding text demonstrates the absence of a decommissioning method capable of fully removing fixed-steel pile foundations with minimum environmental impact. Investigating and developing a novel decommissioning method for the complete removal of pile foundations is essential, as it may become mandatory and beneficial in the future. The proposed novel decommissioning method focuses on extraction, primarily applying to offshore wind's single fixed-steel pile foundations - mono-piles.

Applications of extraction for fixed-steel pile removal are gradually starting to emerge and be adopted in the offshore energy research space, both in industrial and academic settings. However, the applications have been limited to two methods: vibro-extraction and hydraulic pressure. Unfortunately, the data related to the industry's use of these methods remains confidential.

In the context of offshore wind, vibro-extraction was employed once to remove the four pile foundations of a small-scale demo wind farm called Lely, which is one of the ten decommissioned wind farms to date. As for offshore oil and gas, an academic small-scale experimental investigation was conducted to test vibro-extraction for removing jacket platforms' piles [4]. Therefore, to facilitate the extraction of offshore wind's single fixed-steel pile foundations [mono-piles] and to expand the proposed method's scale, the research project aims to investigate the engineering and economic feasibility of extraction techniques.

1.2 Research Aim

The aim of the research is to investigate, develop and analyse a novel method for decommissioning offshore wind's single fixed-steel pile foundations. The proposed method is extraction and will fall under the full removal strategy, along with excavation at the end of the engineering lifecycle. The proposed extraction applications are displacement and force control.

The research and development of the method are focused on two of the three aspects of decommissioning, namely engineering and economics [excluding the environment]. It specifically targets single open-ended piles embedded in the soft seabed soil [e.g., sand]. The proposed method is expected to support the long-term sustainability of offshore wind development.

1.3 Research Objectives

For achieving the research's aim, the following objectives have been adopted in this research project:

- Carry out a comprehensive review of the state-of-the-art applications recently tested to extract mono-piles in the industry, as well as the industry's developed economic modelling approaches for offshore wind decommissioning.
    - Decommissioning by Extraction
- Study the mechanics of extraction theory across industries to define the baseline influencing factors on the extraction force.
- Investigate the effectiveness of the novel extraction applications, displacement, and force, to define the optimum application for offshore wind single open-ended fixed steel piles extraction.
- Test in unsaturated and saturated soils to determine the impact of soil conditions, e.g., pore water pressure, on the tensile capacity of open-ended piles.
    - A decommissioning techno-economic assessment
- Build an analytical model to estimate the total expenditures of the adopted removal methods, cutting at or below the seabed [partial removal, the industry's preferred] and extraction [full removal, the novel proposed method] for decommissioning offshore wind single fixed-steel pile foundations.

- Develop a decommissioning techno-economic model to define the most effective method for decommissioning offshore wind's single fixed-steel pile foundations, in terms of cost and time, by comparing the adopted removal methods.
- Conduct a sensitivity analysis of the adopted decommissioning methods to define the influence of changing the models' input parameter values on the decommissioning expenditures.

1.4 Thesis Structure

The research presented herewith in the subsequent chapters will focus on the following aspects of the novel mono-pile extraction method:

- Chapter Two presents the general justification for focusing on wind energy, particularly offshore wind, with a background on energy transition, its contribution among renewables to achieving the Paris Agreement's aims, and its gaps and challenges. The chapter reviews the installed offshore wind statistics globally to determine the location, scale, and time for decommissioning. It also demonstrates foundation technologies and end-of-life scenarios of offshore wind, decommissioning strategies, and methods for offshore wind's mono-pile foundations. Lastly, the chapter reviews the case study adopted in the experimental campaign (e.g., pile type, soil type) and techno-economic assessment (e.g., specifications and scale).
- Chapter Three demonstrates a detailed description of the conducted experimental campaign, validating the feasibility of novel extraction applications, defining the optimum application amongst the tested ones, and identifying influencing factors on extraction force. It further identifies pile classifications (e.g., design, material, construction, and installation methods) and structure-pile interaction mechanisms in terms of installation influence solely. The chapter also presents the experimental components, setup, procedures, constraints, and results.
- Chapter Four presents a novel decommissioning techno-economic assessment for offshore wind single fixed-steel pile foundations. The assessment combines all the wind farm's foundations numbers and specifications (e.g., dimensions, distance to shore, depth) and the vessels' strategies, types, and costs. The assessment further includes the processes and duration of the pile foundations' removal methods. Detailed results are presented and discussed for the preferred and novel methods.

- Chapter Five demonstrates research outputs and provides recommendations for future policies and works.

Chapter Two

2 Literature Review

2.1 Background

Energy - regardless of its sources - has been an enduring debate topic since the onset of the industrial revolution. The reason is that energy availability and its transition have changed humankind's course in terms of production, consumption quantity, and the adoption of new energy sources. Energy is the backbone of human evolution, and its importance has been evident throughout the ages.

Wind, for thousands of years, has been a versatile source of energy for humanity. It started with propelling boats/ships along the Nile around 5,000 B.C., and it has played numerous roles since then, including food production and water pumping for agriculture. However, it has become a primary source in the global energy mix since the 1980s [5], despite the first known wind turbine being developed over a century ago, in 1887, by James Blyth[1] [6].

Nonetheless, before briefly illustrating the energy transition phases and specifying its current phase/pathway, it's essential to define the meaning of energy transition, mix, consumption, and sources. Furthermore, we will explore the global renewable energy sources' cumulative installed capacity and their share in the global energy mix and electricity mix.

In a simple phrase, energy transition is the change in how humankind develops, utilises, and benefits from energy - environmentally, economically, and socially [7], [8]. In other words, it is the structural change in the primary energy supply/system, gradually shifting from a specific form of energy provision to a new state of an energy system. The energy mix refers to the mixture of the usage of various primary sources to meet global and/or geographic energy demands.

[1] References for further reading [223]–[225].

Energy sources are categorised into two groups: primary and secondary. Primary sources include renewables [e.g., hydro, wind, solar], nuclear, fossil fuels (non-renewable) such as oil, natural gas, and coal – all of which are harvested from natural sources. The secondary sources, produced or generated by converting primary sources, comprise electricity, hydrogen, liquid biofuels, gasoline, and heat, to name a few. These secondary sources are utilised in energy consumption sectors such as electricity, transportation, and heating and cooling.

Energy throughout time has undergone tremendous and critical transitional phases, beginning with the shift from using traditional biomass, e.g., solid fuels [wood, charcoal, or crop waste] to coal, followed by coal to hydrocarbons [natural gas and oil]. As a result, fossil fuels dominated the energy mix - which was homogeneous to some extent - in the first transition.

Following the addition of hydropower and nuclear energy throughout the 20^{th} century, the energy mix became more diverse. Nevertheless, the global energy sector is currently on a shifting path towards zero or low-carbon sources for energy production and consumption instead of fossil fuels [9], [10]. In other words, the world is transitioning from fossil fuels to zero or low-carbon sources for energy dominance by the second half of the current century [9].

Zero or low-carbon sources, generally, are renewables and nuclear energies [5]. Renewable energy sources are categorised into three aspects, depending on their greenhouse gas emissions during operation. Wind, hydro and solar are considered zero-emission sources, biomass is neutral, and geothermal is low [11].

The main reason for the current shift, aside from the crises that led to former energy transitions [to fossil fuels], is to commit to and achieve the 2015 Paris Agreement's global climate action framework. The Paris Agreement aims to limit global temperature warming below 2°Celsius(C), seeking to keep it to 1.5°C [12], [13] by reducing greenhouse gas (CO2) emissions to net-zero by 2050 [14], [15].

Carbon dioxide (CO_2), nitrous oxide, and methane, to name a few, are the greenhouse gases that cause global climate change. The global prime focus is on carbon dioxide reduction because it represents the highest proportion of emitted gas by human activities, three-quarters, amongst greenhouse gases [5], [16]. The main reason for emitting a high proportion of CO_2 is fossil fuels combustion for energy consumption sectors [electricity & transportation], industrial processes, land use, and forestry, to name a few. Energy consumption sectors and industrial

processes [e.g., cement & lime, iron & steel] emit sizable CO_2 [17] and account 80% or more [16].

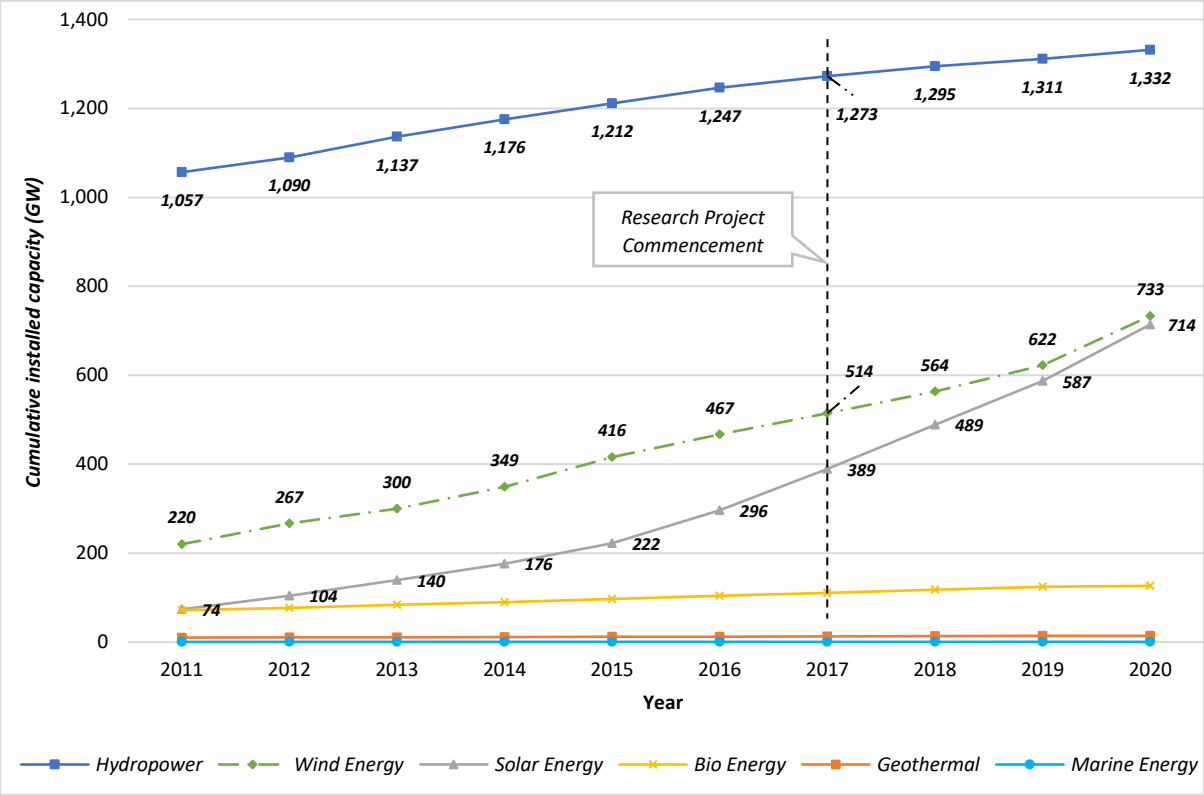

Figure 2-1. Renewable energy sources' cumulative installed capacity globally—source: author edited based on [18].

As a result, renewable energies gained strength globally and are still gaining momentum, as illustrated in Figure 2-1[2]. One reason is that renewable energy can reduce CO_2 emissions by 90% by the 2050 target, as set by the EU Directive [19].

Renewable energies' strength has been enhanced by contributing to the electricity generation mix with a higher share than the total energy mix. However, in the total energy mix, renewables' share is less due to the challenges in decarbonising other energy consumption sectors such as transport, heating and cooling [5].

The share of renewable energies in the global electricity generation mix was 24.9% [20], 26% and 29% [5], [11], [21] in 2018, 2019 and 2020, respectively, representing a total increase of 4.1%. Even so, their share in the global total energy mix was roughly 11% in 2019 [5], [11].

[2] Renewable energies, in figure [1], hydropower [mixed plants and pure pumped storage], wind [off and on-shore], solar [solar photovoltaic and concentrated solar power], and bio energy [solid biofuels and renewable waste - e.g., bagasse, renewable municipal waster, other solid biofuels- liquid biofuels, and biogas].

Unfortunately, data for renewables' share in the global total energy mix for 2020 and 2021 was not available or published.

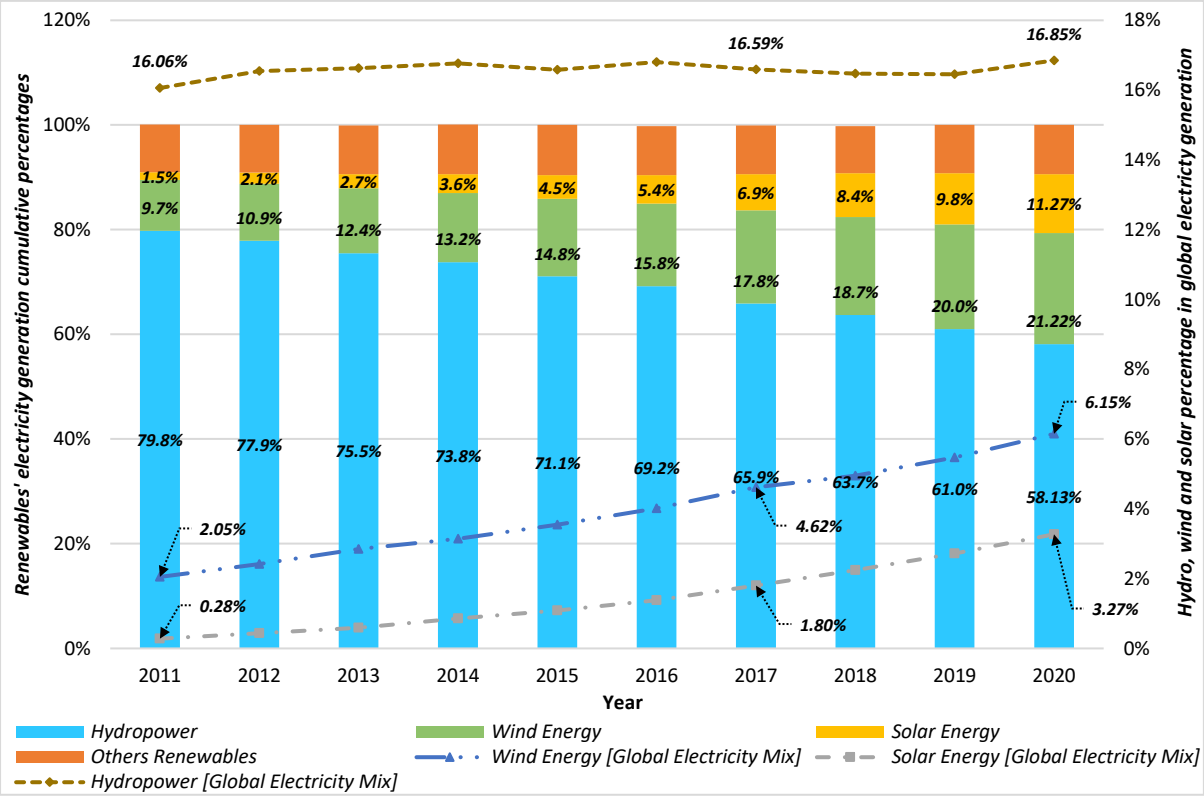

Figure 2-2. Renewable energy technologies' electricity generation cumulative percentages concerning renewable's total share in the global electricity generation mix – source: author edited based on [5], [22].

Wind and solar - especially PV - power (as shown in Figure 2-1 and Figure 2-2), or so-called modern renewables, are the fastest-developing renewables technologies globally in terms of electricity generation mix share and installed capacity over the last decade. The total share of these two technologies in the global electricity generation mix was slightly over 9%, up from 2% in 2010 [23]. Wind accounted for roughly 6% [1], [5] and solar accounted for approximately 3% in 2020, as shown in Figure 2-2.

In other words, modern renewables have contributed and will continue to contribute to the growth of renewable energies' share in the electricity generation mix. For instance, in 2050, modern renewables are expected to account for 68% of the electricity generation mix [23]. On the other hand, hydropower, the oldest renewable energy source in the electricity generation mix with the highest percentage share (around 17% in 2020), had increased only by a fraction of a percentage.

The cumulative installed capacity for modern renewables has drastically increased compared to other renewable sources, mainly hydropower. Wind and solar capacities have increased by 233% and 865%, respectively, over the last decade, while hydropower increased by 26% [Figure 2-1].

The preceding justifies the research project's focus on modern renewable energy technology - wind power. In other words, although solar power had significantly increased and was slightly behind wind power from the research project's commencement (in 2017, Figure 2-1) to its writing-up (beginning of 2022), wind power has remained the second-largest renewables technology regarding capacity and electricity mix share. The preceding relied on 2020 statistics because [up-to-date] 2021 statistics were not published during the writing-up. Wind energy technologies, both off-shore and on-shore, up-to-date global statistics, and outlook installation capacity, to name a few, are briefly discussed in the following subsequent sections.

2.2 Global Wind Overview

The [modern] wind industry has been continuously exploring and emerging in new global markets and locations since the development of the first commercial on-shore [Crotched Mountain] wind farm in the U.S at the end of 1980 [24]–[26]. Some reasons, regardless of the aforementioned ones, are that wind technologies, both on and offshore wind turbines, are constantly developing in several attributes, such as capacity and size, to name a few.

The capacities of on and offshore wind turbines have dramatically increased since their first commercial emergence. On-shore wind capacity has increased from 0.03MW [Crotched Mountain] to 6MW [e.g. GE's Cypress & SG 6.6-155] [27], [28] and 7MW [e.g. Enercon E-126/7.5MW] [29] wind turbines. This represents a 19,990% to 23,233% increase compared to the Crotched Mountain wind turbines. On the other hand, the turbine capacity for offshore wind has increased from 0.45MW [the Vindeby wind turbine] to 14MW [GE Haliade-X prototype] [30], a 3,011% increase.

Additionally, numerous non-commercial locations/sites have become commercial for wind development [24]. The wind industry, for instance, has expanded and developed offshore because the wind flow is consistent, constant and powerful, resulting in massive energy potential gains. Furthermore, locations with favourable wind onshore may become limited/scarce over time due to the growing population and ecological demand on the land [6],

[31]. In other words, the amount of harvested power from wind depends on the turbine's specifications and location, which justifies the latter.

The onshore wind market, following the U.S., emerged in Germany, Denmark, Spain, and various countries [24]. For the offshore wind market, the first demonstration offshore wind farm developed globally was in Denmark in 1991 [32], followed by the Netherlands and the UK. Nonetheless, it should be noted that the first erected offshore wind turbine was Nogersund - Svante 1 (demonstrator) in Sweden commissioned in 1990.

Since the first emergence of the wind market, it has been deployed across four geographical regions onshore and three geographical regions[3][4] offshore respectively, with a cumulative installed capacity of more than 700GW in 2020. Figure 2-3, Figure 2-4 and Figure 2-5 illustrate the global wind cumulative installed capacity, and cumulative installed wind capacity per region for on and off-shore, respectively.

[3] ***"Geographical region"*** herein refers to combining two or more contients, under one region, for simplicity and consistency. The reason is that the studied wind statistic reports -Global Wind Energy Council (GWEC) and International Renewable Energy Agency (IRENA)- are adopting different analysing methodologies. IRENA, for instance, analysed North America, Central America plus Caribean, and South America separately. In comparison, GWEC had analysed and categorised the three-above regions as Americas.

[4] ***"Eurasia"*** region -Russia, Turkey, Georgia, Armenia and Azerbaijan- had classified under Europe only for the on-shore wind market. Asia-Pacific comprises Asia and Oceania countries.

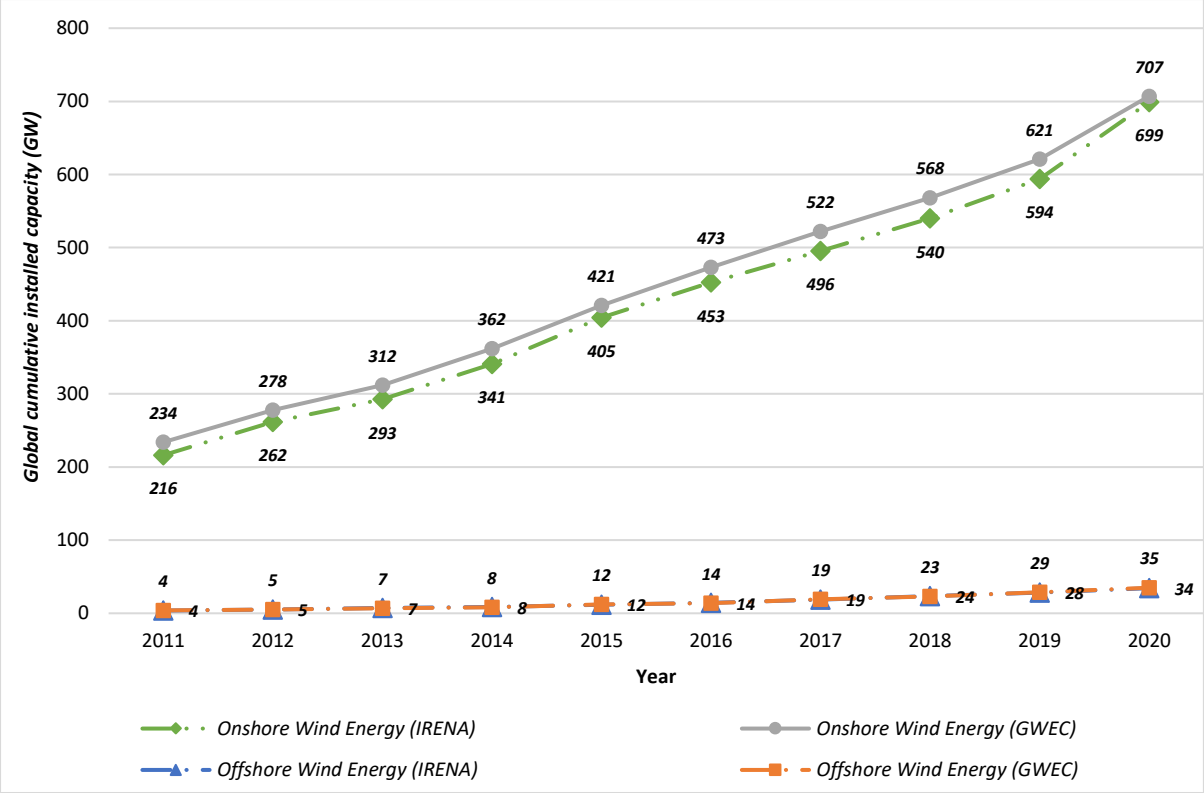

Figure 2-3. Global wind cumulative installed capacity - source: author edited based on [1], [18].

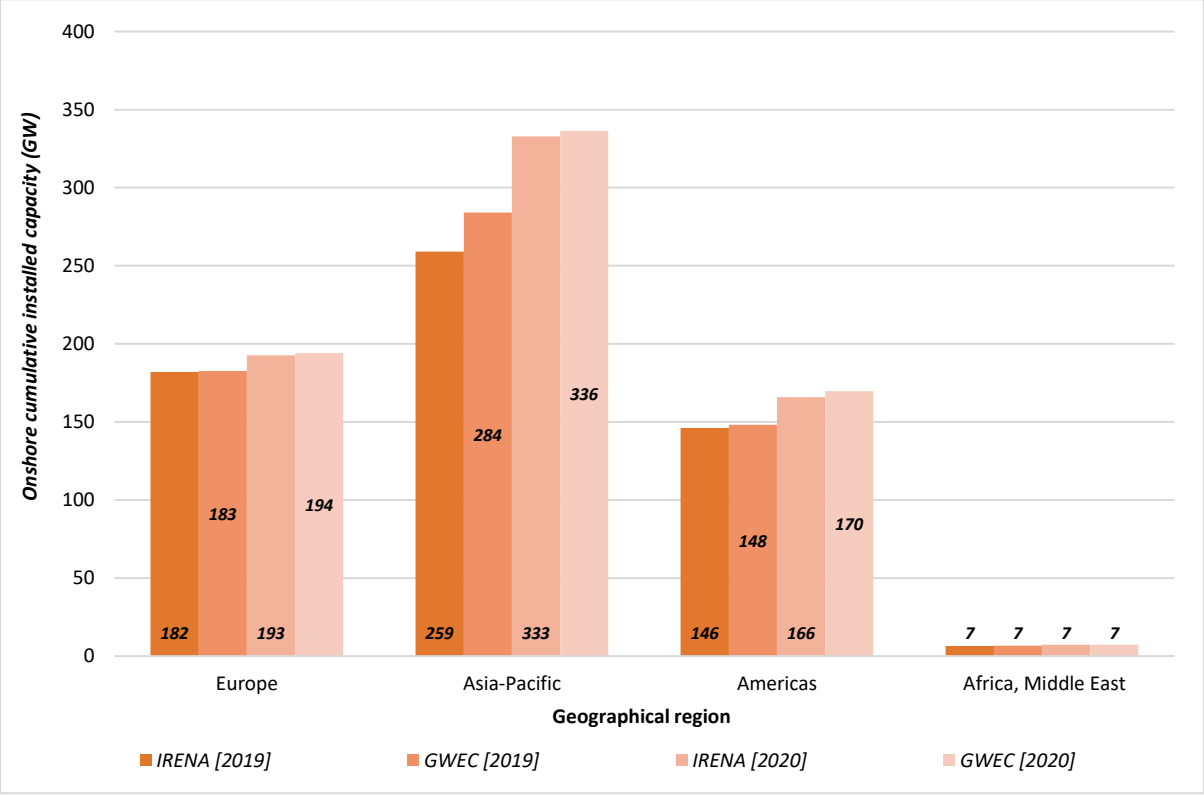

Figure 2-4. Geographical regions' on-shore wind cumulative installed capacity - source: author edited based on [1], [18].

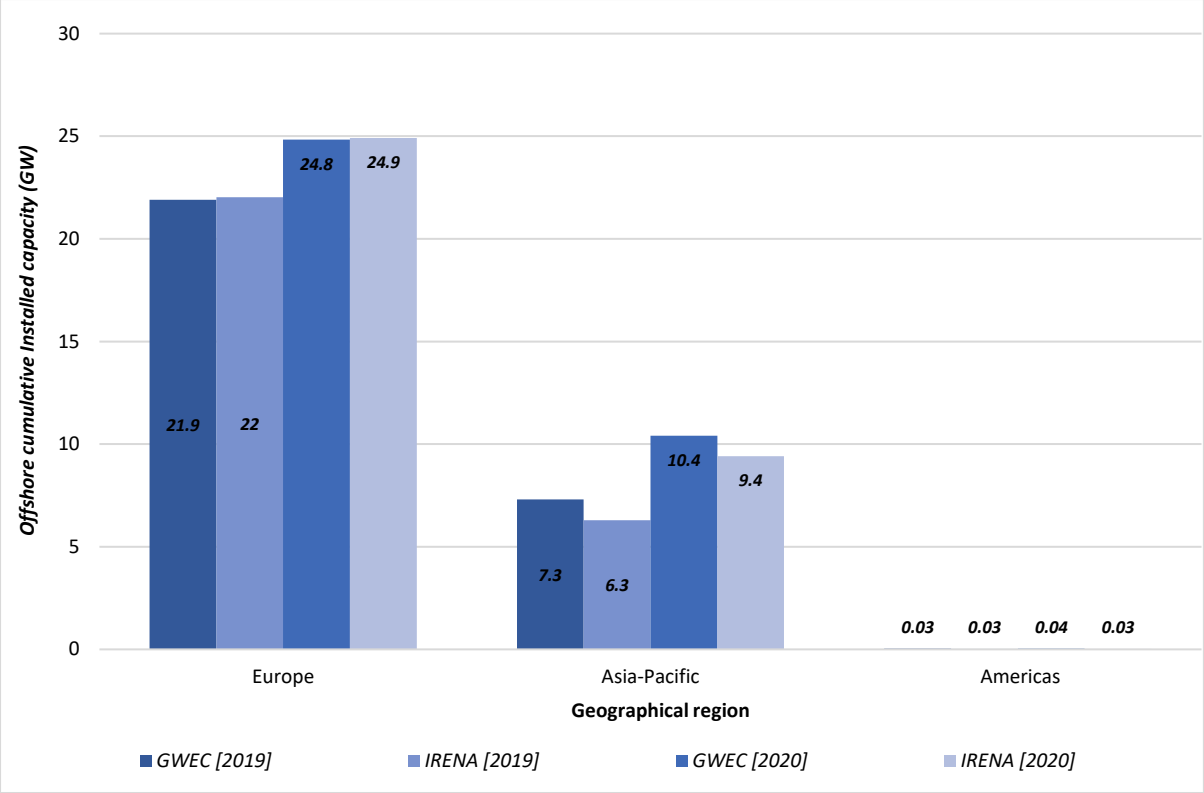

Figure 2-5. Geographical regions' off-shore wind cumulative installed capacity - source: author edited based on [1], [18].

Figure 2-3 indicates a 1% and 3% error percentage between GWEC and IRENA wind statistics for onshore and offshore cumulative installed wind capacity, respectively. Hypothetically, the error might be due to the adopted analyse methodology, analysis period, or data sources. As a result, BP statistics were studied [33], where its statistics were in line with IRENA regarding wind cumulative installed capacity, both onshore and offshore, at 733 GW.

The Asia-Pacific region, as shown in Figure 2-4, is the leader in the onshore wind market with 47 - 48% (330 – 336 GW). In terms of countries, China accounted for 39% (273 – 278 GW) of total onshore installations, followed by the USA at 17% (118 – 122 GW). In contrast, the offshore wind market is led by the Europe region with more than 70% (25 GW). The UK represented 29% (10 GW), followed by China and Germany with 26% - 28% (9 -10 GW) and 22% - 23% (8 GW), respectively. All the presented data - percentages and gigawatts (GW) – are rounded up to the nearest number; numbers below and above 0.5 show 0% and 1%, respectively.

The global wind had a record year for installations, with over 90 GW [87 GW onshore and 6 GW offshore] of installed capacity in 2020. The installation of renewables, especially wind, is

forecasted to grow year-on-year (YoY) following the 2020 record, which is described as the new normal [1], [34]. The reason, along with the Paris Agreement, is that wind energy is projected to lead the global electricity mix by supplying over 30% of the total electricity demand by 2050 [35], [36].

As a result, the annual global wind installation capacity is exptected to witness a tremendous increase in the coming decades, reaching roughly 178 – 180 GW (∼150 GW onshore and 28 GW offshore) per year by 2030 and over 245 GW (>200 GW onshore and 45 GW offshore) per year by 2050 (IRENA, 2019; GWEC, 2021). It should be noted that the latter figures indicate the target that wind needs to reach; however, currently it is heading towards 1,455 GW and 2,434 GW by 2030 and 2050, respectively. In comparison, under IEA Net-Zero by 2050 scenario [37], wind is projected to reach an annual installation capacity of 390 GW (310 GW onshore and 80 GW offshore) by 2030.

The current published long-term scenarios set by intergovernmental energy agencies, international organisations, and others [mentioned above]; will undergo amendments over time, particularly for wind and renewables. Even so, these scenarios/goals are inevitably expected to be revised upward. IRENA's 2050 scenarios support this notion; under IRENA's world energy transitions outlook – 1.5° pathway [14], total wind installation capacity is projected to exceed 8,100 GW. Additionally, according to IRENA's Global Renewables Outlook – Energy Transformation 2050 [35], the wind installation capacity is expected to reach 6,044 GW.

After providing a brief overview of global wind technologies' development, expansion, and up-to-date statistics, and its projected electricity mix share, the research project focuses on offshore wind technology. There are numerous motivations for this focus, including the fact that offshore wind provides a complementary alternative to address onshore wind deployment challenges, either currently (e.g., Europe) or in the future due to concerns related to land availability and transmission congestion [36].

Offshore wind is rapidly maturing and is expected to play a vital role in future energy systems. Although it currently contributes only a fraction to the global electricity mix (0.3% in 2018 [38]) compared to onshore wind, its significance is growing. OREAC has set a 1,400 GW target of offshore wind capacity by 2050, which will generate 10% of global electricity [2]. On the other hand, IRENA projects that offshore wind will represent roughly 17% (1,000 GW) of the global total installed wind capacity,, which is projected to be 6,044 GW by 2050 [36].

Table 2-1. An estimate of wind total installation capacity (GW) in various geographical regions by 2050.

Geographical region/ reference	***Asia***	***Europe***	***North America***	***Latin America and the Caribbean***	***Oceania***	***Africa and the Middle East***
[36]	613	215	164	5	3	-
[39]	720	640	360	120	80	40

Offshore wind has the capability to tap its full potential and generate over 420,000TWh of electricity per year globally [38], which is more than 15 times the electricity demand in 2021 (27,521TWh) [5]. Additionally, the IEA estimates that the technical potential of offshore wind worldwide exceeds 120,000 GW.

Regarding the geographical region studied in this research project, the focus is on Europe. The reason for this choice is that Europe has been at the forefront of the global offshore market for three decades in terms of technology development and installed capacity. It holds the distinction of installing the world's first turbine and demonstration wind farm. Consequently, Europe is the geographical region where decommissioning is expected to occur first on a large scale. It should be noted that decommissioning has already taken place in a few small-scale offshore wind farms in Europe, which will be discussed in the subsequent sections.

It is worth noting that in 2021, China was undergoing construction of more than 10 GW offshore wind capacity, known as the "installation rush", to connect to the grid before the year's end, surpassing or meeting Europe's installed capacity level [40]. GWEC's latest global wind statistics, detailed in Appendix A, support this claim [41]; Europe and China's cumulative offshore wind installed capacity is 28.15 GW and 27.68 GW, respectively (17 GW in 2021).

Nonetheless, Europe is expected to dominate offshore installation capacity for approximately a decade; after that, China is projected to outpace Europe's capacity (less than two decades from 2019) [36]. However, according to the IEA, Europe will remain the offshore wind technology leader until 2040 [38].

Statement 2-1

The various targets set by organisations for global renewables' total installation capacity, with a specific focus on wind, by 2030 and 2050, as demonstrated above, indicate the current prime focus on renewable energy and the significant future increase in renewable energy capacities. This increase will be evident in terms of reliance on renewables, their deployment, and technological development, among other aspects. As a result, upcoming targets and statistics - not included herein due to the writing -up time - will likely show even greater year-on-year growth compared to the ones presented above.

2.3 Offshore Wind Industry

The offshore wind notion, when it first developed in the world in Europe, was simple; a few onshore turbines installed on concrete gravity-based foundations in shallow water (Vindeby wind farm [32]). Despite the notion's simplicity and in its third decade, offshore wind is still a challenging industry due to being relatively new and maturing regarding its development stages, including its lifecycle.

Consequently, it is essential to define the industry roadmap, focussing on the key challenges before delving into offshore wind farm's technical aspects, such as lifespan, technology components, installation methods, and industries' similarities and differences. By defining the industry's maturity extent, we can determine and reflect its awareness and attention to decommissioning aspects.

Offshore wind is one of Europe's primary sources to become carbon-neutral by 2050. To fulfil this role, offshore wind requires an installation capacity of 300 GW [42]–[44] or 230 to 450 GW [3] in the North Seas, Mediterranean and other seas.

Translating the 2050 target into an installation capacity rate per year, Europe needs to install roughly 7 GW per year by the Quarters 3 & 4 of the 2020s, increasing to 20 GW by 2030, based on WindEurope data availability and with the highest target. These required installation capacity rates are around two and six times Europe's current (as of 2020) and estimated installation rate per year until 2025, approximately 3 GW.

Although the 2050 target is ambitious, regardless of the installation capacities mentioned above, as it is sixteen times Europe's current cumulative installed capabity of offshore wind [Figure 2-6], it is still considered feasible. However, the target poses challenges due to the

growth magnitude and rate of offshore wind being determined by its development stages, activities, and duration, rather than vice versa. The development stages for offshore wind farms, whether for demonstration or commercial purposes on a small or large scale, include leasing, consenting, financial, and installation/construction.

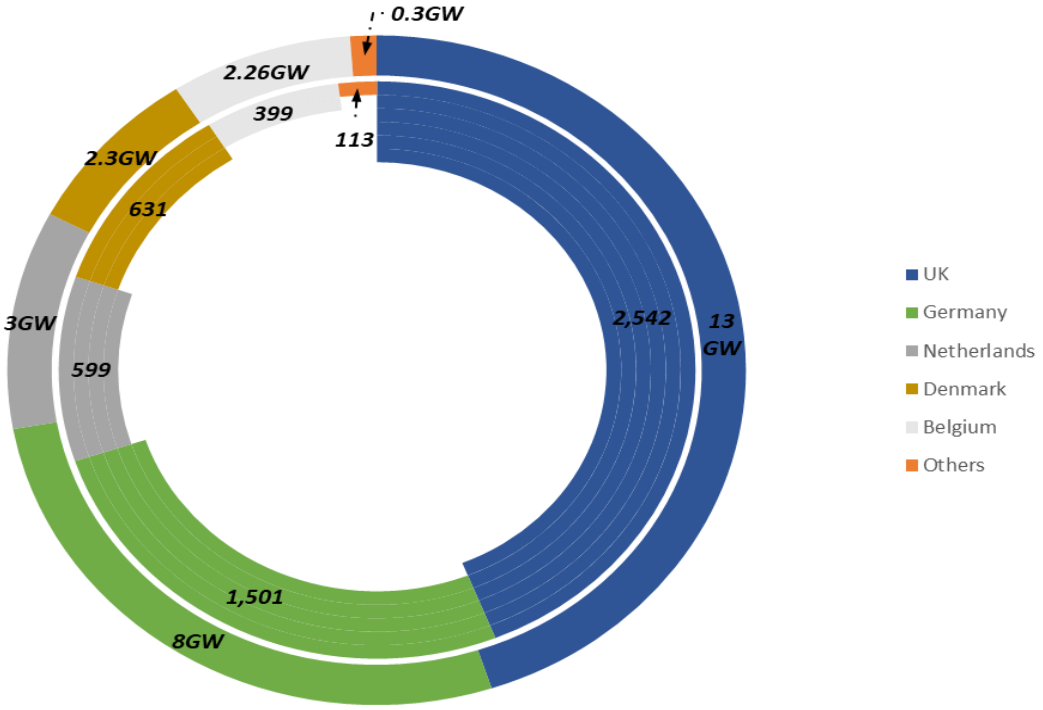

Figure 2-6. Europe's current offshore wind's cumulative installed capacity, 28GW[5], and turbines - source: author edited based on [41], [45].

One of the challenges is the Maritime Spatial Planning (MSP) in the leasing stage. In Europe, offshore wind could develop in roughly 40% of the North Seas' total area (the North Sea, Baltic Sea, and the Atlantic Ocean) of 2,762,772 km^2. The remaining area of 1,700,000 km^2- is set for other sea users, marine developments, and environmental reasons. As a result, the levelised cost of energy varies, leading to a potential shortage in the number of offshore wind farm developments compared to spatial planning without exclusions/constraints.

Spatial planning without exclusions, dedicating more areas for offshore wind, can have a positive impact investment, particularly in the supply chain, and lowers the risks and capital costs [3], [46]. It is worth noting that most spatial exclusions will probably remain the same until 2050. On the other hand, regardless of competition from other marine sectors, offshore

[5] The presented cumulative installed capacities, GW, rounded up to the nearest number; numbers below and above 0.5 show 0 and 1, respectively.

wind farms enter under spatial exclusions after the installation's completion, decreasing the industry's dedicated area.

Along with spatial planning, permitting (the consenting stage) poses challenges for the industry, particularly to achieve the 2050 targets, due to the complexity of regulations/rules, procedures, and lack of experience, among other factors. This may result in the permitting magnitude not matching the required annual installation capacity rates mentioned earlier. Additionally, the costs and risks associated with permitting can deter investment in development, leading to delays [3], [47], [48].

The challenges related to permitting may extend to impact offshore wind farm end-of-life scenarios, particularly repowering. However, consent, if granted, comes with a condition, requiring developers to prepare and submit an initial decommissioning program before construction. This condition is outlined in the Energy Act 2004 Section (105), meaning that construction cannot commence unless a decommissioning program is submitted [49], [50].

The European Commission has proposed solutions to overcome some of the offshore wind challenges, including adopting a multiuse/multipurpose approach in maritime spatial planning to coexist with other activities [3], [51]. Additionally, the duration of permitting renewable energy installations, under the Renewable Energy Directive (2018/2001/EU) Article 16, should not exceed two years and one year for repowering [47], [52].

Statement 2-2

To this extent, the focus of offshore wind, either from industry or academia, on decommissioning is limited, as its entire focus is to overcome the challenges (e.g., regulations, technology, installation) associated with its future targets.

Despite the focus on overcoming future offshore wind targets' challenges, little attention is given to decommissioning. However, sustaining offshore wind's long-term development lies in its decommissioning, particularly concerning its foundations. The decommissioning strategy and method for offshore wind foundations have a significant impact on seabed availability. Figure 2-8 and Figure 2-10 justify this, as they demonstrate the impact of adopting the industry's current preferred decommissioning strategy (partial removal) for fixed foundations. Applying this strategy will lead to a decrease in seabed availability until there is no space left

for further development, And the appearance will be similar to landfills[6] of decommissioned wind turbine blades [Figure 2-7].

The impacts of bottom-fixed foundations' decommissioning strategies, partial and full-removal, on seabed availability are compared in Figure 2-8, Figure 2-9 and Figure 2-10. For simplicity, the North Seas' total area (without exclusion) is dedicated to offshore wind development, excluding the removal strategies' methods.

Figure 2-7. The impact of wind turbine blades fabricating materials [resin/ fibre glass] on decommissioning; a top view of the Casper landfill, Wyoming.

Figure 2-8. The industry's proposed/ preferred offshore wind foundations decommissioning strategy impact - partial removal- on the seabed – created by the author.

[6] Landfilling the decommissioned wind turbines' blades is currently one [and the onset] of the wind industry's end-of-life challenges, whereby the industry called for banning by 2025 across Europe [226].

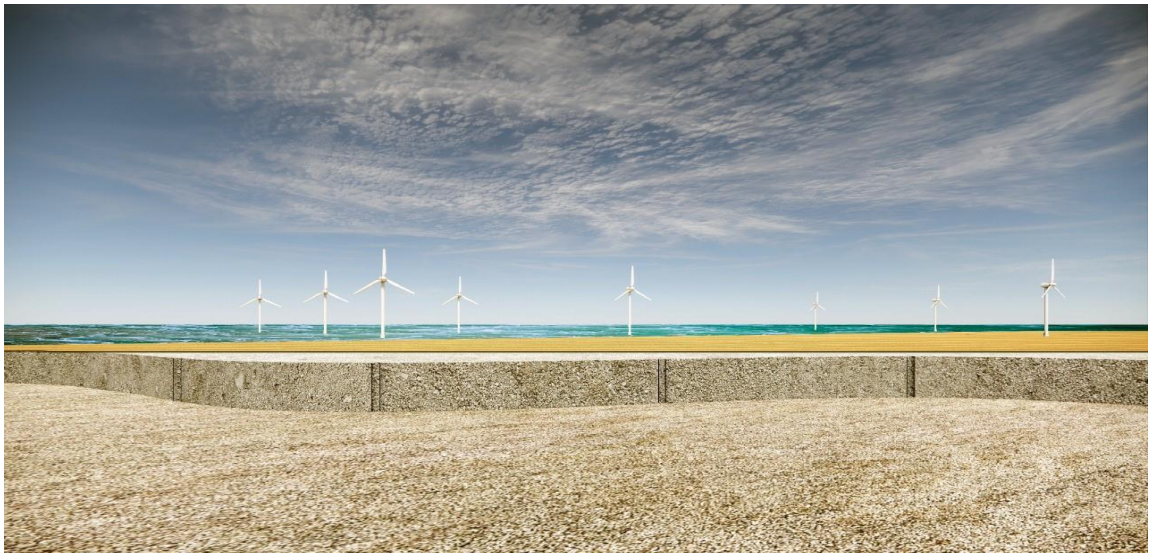

Figure 2-9. Offshore wind foundations' full removal strategy impacts on the seabed – created by the author.

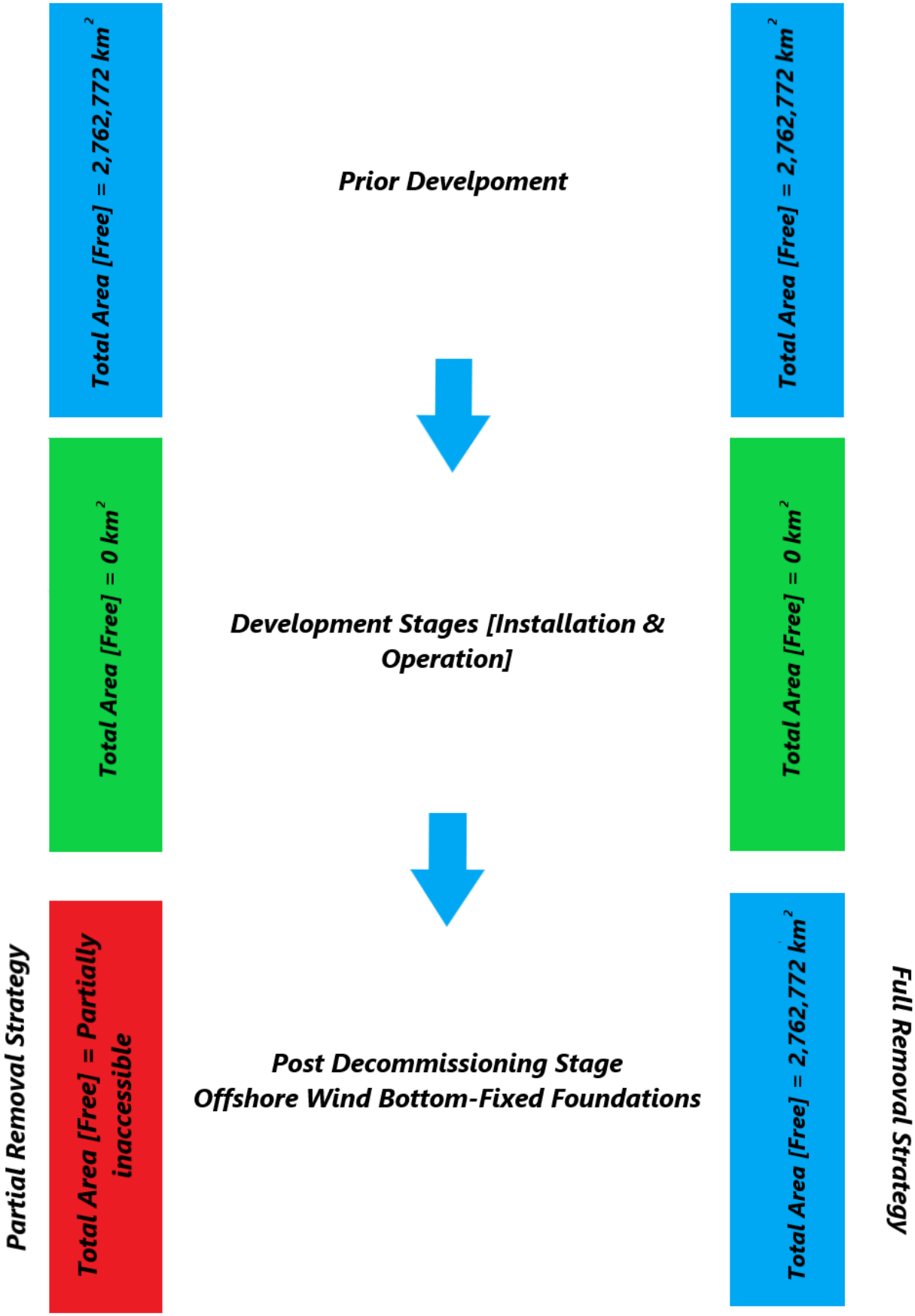

Figure 2-10. The impact of offshore wind bottom-fixed foundations decommissioning strategies concerning seabed availability on the industry's long-term development sustainability.

Motivation 1

Offshore wind, particularly the bottom-fixed foundations, is on the brink of encounrtering various challenges by the farms' end-of-life. Therefore, there is a motivation and requirement to investigate and develop a distinct decommissioning path for bottom-fixed foundations, aligning with [Arup, 2018]. Factors such as hypothetical changes in spatial planning and/or stricter regulations during the time lag between installation and decommissioning, as well as landfill banning, justify the need for such investigations and developments by Siemens Gamesa [54]. Ensuring the long-term development of offshore wind is essential.

Contributing to partially solving offshore wind's near-future decommissioning challenges was necessary to study and possibly adopt well-established industries with similar structures to the offshore wind, considering the dissimilarities. These industries include offshore oil and gas, with a focus on installation and decommissioning strategies, methodologies, and technologies.

An offshore wind turbine structure is a combination of onshore wind for superstructures and offshore oil and gas sub-structures. Since this research project focuses on offshore wind foundations, offshore oil and gas was adopted for comparison, while onshore wind was excluded. It's important to note that this section only briefly discusses the similarity with and adoption extent of offshore wind from offshore oil and gas to justify the impact of the later on offshore wind.

Most offshore wind foundations, regardless of technologies and types (except for tri-pile), are extensions of the experience from offshore oil and gas. Therefore, it is logical that offshore wind will follow a similar path for its foundation decommissioning. The term "technology(ies)" in this context refers to both bottom-fixed and floating foundations.

Offshore wind development has followed similar steps as offshore oil and gas regarding water depth and distance to shore. Offshore oil and gas fields/wells were initially located near the shore and in shallow water (e.g., the Creole field[7] [55], [56] or Kerr-McGee drilling platform[8] [57]), gradually increasing in depth and distance. The timeline for the first developed offshore

[7] Creole field, which represented the offshore industry's birth, was located 1.5 miles from the shore at a water depth of 4m.

[8] Kerr-McGee drilling platfrom -or so-called McGee's Kermac Rig No.16- was the first "out of sight of land" offshore well, was at a water depth of 6m and 10 miles from the coast.

wind substructures and foundation technologies and their distance to shore has been demonstrated by Schneider and Senders (2010).

2.4 Offshore Wind Technology

Offshore wind farms' development and growth were slow for approximately a decade following the construction of the Vindeby wind farm, with only a few demonstration projects around Europe. The largest initial demonstration wind farm was located at Middelgrunden, Denmark, comprising of twenty 2 MW turbines on gravity-base foundations with a 40 MW total capacity [58], [59]. During the development of Middelgrunden, the political focus within Western Europe was on technical feasibility rather than the costs [32].

The transition from demonstration to commercial offshore wind farms occurred through projects like Horns Rev 1 wind farm in Denmark, which marked the industry's first large-scale project. Horns Rev 1 wind farm was commissioned in 2002 with a total output of160 MW with eighty 2 MW turbines on monopile foundations [60], [61]. After this, offshore wind farms developed rapidly, with greater emphasis on components, foundation specifications, water depth, and distance to shore.

Regarding offshore wind foundation technologies, whilst China has exceeded the UK's total installed capacity, the UK leads in floating offshore wind technology [41], making Europe home to the largest operational wind farms for foundation technologies. At the same time, wind turbines have shifted from onshore versions to ones designed specifically for offshore, with an increase in average installed capacity and water depth by seventeen times [0.45MW to 8MW] and is projected to increase further two times by 2026 [Figure 2-11]. Concurrently, the average water depth has increased by eleven times from 4 m to 44 m and is forecasted to increase further as showcased in [Figure 2-12].

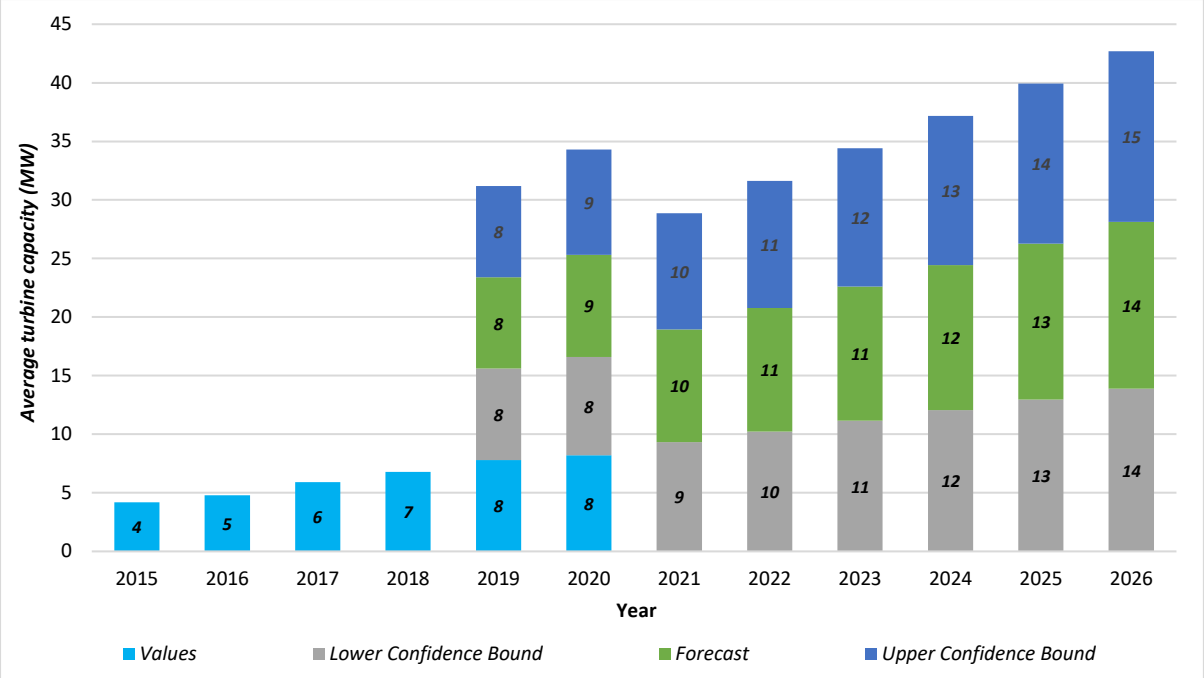

Figure 2-11. The average turbine capacity installed and forecasted from 2015 - 2020 and 2020 - 2016, respectively - source: author's analysis for various resources.

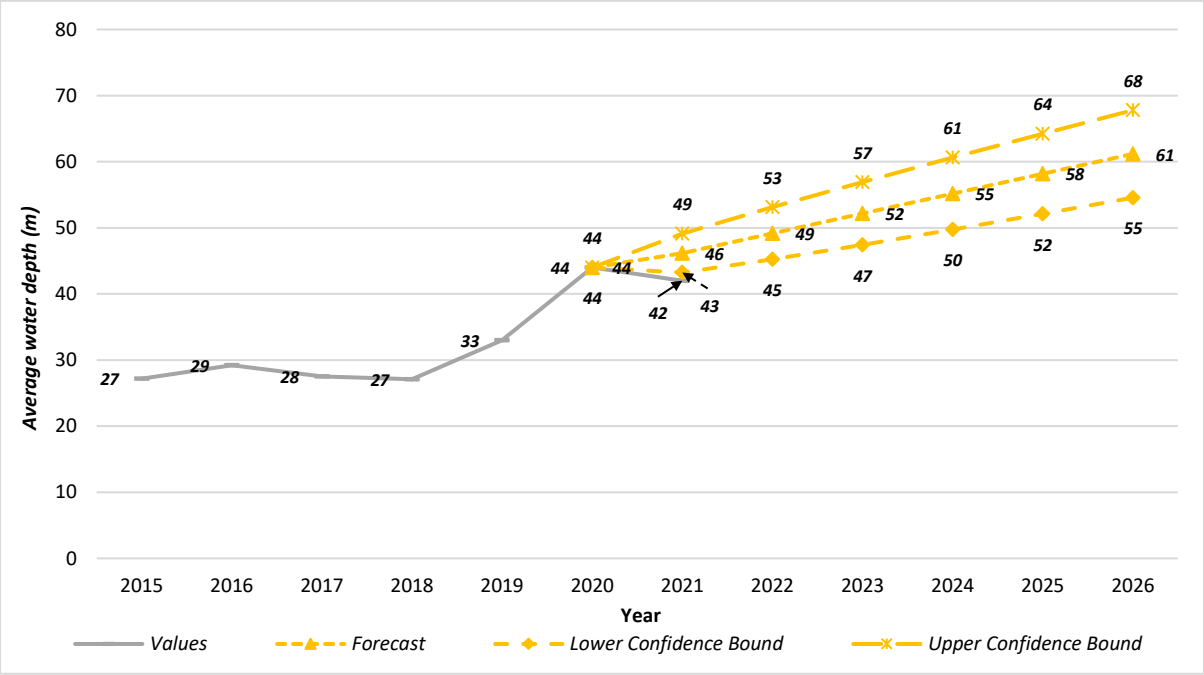

Figure 2-12. Offshore wind farms' average water depth from 2015 to 2021 and forecasted depths from 2021 to 2026 - source: author's analysis for various sources.

To forecast actual values from 2016 to 2021 from WindEurope, statistics have been implemented in MS Excel and depicted as a graph in Figure 2-11 and Figure 2-12 [45], [62]–[67].

Statement 2-3

The focus, whether from the industry in general or owners, developers, and operators, is on maturing offshore wind technology, such as specifications, installation methods and operational efficiency. Owners expect turbines to operate at their maximum designated lifetime of approximately 25 years without becoming obsolete [68]. Meanwhile, there are up to six developed methods for turbine installation [69].

In comparison, offshore wind technology decommissioning experience is limited, almost non-existent. For instance, the decommissioning process at Yttre Stengrund wind farm had to refine the adopted method along the process, which was different from the installation process [Bagner, 2016]. The industry's current decommissioning knowledge/experience level has remained stagnant since its development 30 years ago.

Offshore wind farms (OWF) typically comprise turbines, foundations, transformer platforms (or offshore substations), and transmission cabling (inter-array and export). OWF superstructure components, existing installation methods and supply chains are discussed in detail in the literature referenced [69]–[71] and organisational reports are available from [68], [72]. Whilst offshore winds various substructures have been researched, documented and described, the main focus of this thesis will be structures mounted on fixed steel pile foundations.

The lifetimes of these components vary, with turbines having the lowest lifetime of 20 to 25 years, while substations and transmission cabling can last 35 and 40+ years, respectively [73]. Foundations' lifetime depends on their type and loads, with gravity-based foundations estimated to endure 100+ years [74]. The designated lifetime for an offshore wind farm is typically 20 years, with turbines playing a critical role in this.

2.5 Offshore Wind Fixed Substructures

In the literature, the terms "substructures", "support structures," and "foundation" are often used interchangeably, which creates confusion. Therefore, it was essential to distinguish between these terms before defining the substructure types. For instance [70] divided offshore wind turbine structures into a wind turbine and a support structure system whereby the support structure was composed of a transition piece, foundation, and scour protection. Another example is where [31] stated that the offshore wind turbine support structure consisted of a

tower and foundation, with the foundation extension initiating from the water level and continuing below the water level.

[75] broke the offshore wind turbine structure system into two key parts: the support structure and the foundation. The wind turbine's support structure is located between the seabed and the wind turbine's nacelle. On the other hand, DNV considered the foundation as a different or separate structure, describing it as a structure, geotechnical component, or both, extending from the seabed downwards. However, neither of the definitions above included or defined the term "substructure".

[76] expanded the support structure term definition by including substructure and defining it as a part of the support structure, extending from the tower's lower part to the foundation. Additionally, the support structure term included foundation and tower. In other words, the support structure term encompasses the tower, substructure, and foundation. For simplification, the term ***"substructure"*** herein refers to the part between the tower's lower part and the seabed, while ***"foundation"*** refers to the part embedded and in direct contact with the soil, extending from the seabed downward.

Offshore wind encompasses various substructure and foundation types, with many adopted from offshore oil and gas, and they can be categorised by various factors such as structural configuration, construction material, and installation method. These variations in substructure and foundation result in numerous combination opportunities. For instance, a tri-pod structure can mount either on a conventional pile or suction bucket foundations [75]. The available substructure and foundation types currently or in the future fall under two categories, fixed (or so-called bottom mounted) or floating support structures, as presented in Table 2-2. Table 2-3 shows water depth ranges for offshore wind fixed substructures.

According to WindEurope's latest published statistics [45], there are 6,032 installed substructures for turbines with and without grid connection. Offshore wind fixed and floating structures represent 99.49% (5,999) and 0.28% (17), respectively, while other unspecified substructures represent 0.26% (16).

The most common installed substructure is the mono-pile, accounting for 81.5% (4,914), followed by the jacket with 9.6% (579), gravity base with 5% (300), tri-pod 2.1% (126), and

tri-pile 1.33% (80). Floating semi-submersible, spar, and barge account for 0.15% (9), 0.12% (7), and 0.017% (1), respectively.

Table 2-2 summarises substructure and foundation types.

Fixed support structure		***Floating support structure***	
Substructure	***Foundation***	***Substructure***	***Foundation***
Gravity-based	Gravity-based	Tension leg platform (TLP)	Anchor[9]
Mono-pile	Suction cassion/ bucket	Semi-submersible	
Jacket	Pile	Spar	
Tri-pod		Barge	
Tri-pile			

Table 2-3 defines the water depth ranges of most offshore wind fixed substructures.

Structure	[77]	[78]	[71]	[75]
Gravity-based	Up to 30 m	<10 m	15 – 25 m	0 – 25 m
Mono-pile	Up to 40 m	20 – 40 m	Up to 25 m	
Tri-pod	Up to 50 m	10 – 35 m	25 – 50 m	20 – 50 m
Jacket	Up to 60 m	5 – 50 m	-	

After defining common offshore wind substructure and foundation types and presenting their latest share in the European offshore wind market, decommissioning will occur on a large scale for pile foundations, mainly mono-pile structures. Consequently, the focus of this study hereinafter is solely on offshore wind substructures mounted on pile foundations. In contrast, gravity-based and suction bucket foundations have been excluded; however, references to them will be made if required. The exclusion is due to the foundations' structural design, material, methods, and percentage of their installation.

Mono-pile, tri-pod, tri-pile and jacket structures penetrate the seabed and mount on pile foundations, regardless of essential selection factors for substructure types, such as seabed condition and water depth. Pile-mounted substructures differ in piling scales and numbers due to their structural design, as briefly discussed in the following subsections.

2.5.1 Mono-pile Structure

The mono-pile is a single rigid, robust hollow steel cylindrical/tubular/circular pile with various diameters (> 10 m), supporting the tower directly or through a transition piece. The mono-pile is manufactured from single steel plates, bending/rolling separately to form cans and conical shapes. The single shapes are jointly welded together, forming a tubular segment. The tubular segments are welded together to form one long cylinder pipe. In simple words, mono-pile

[9] Pile, plate, gravity, free-fall, suction, prestressed, and fluke are anchor foundations' types for floating support structures [142].

fabrication is from steel plates, which are rolled and welded together to form one cylindrical section [31], [79].

For clarity, the mono-pile comprises a pile foundation and transition piece (more often than not). The mono-pile is the most installed structure compared to the others due to its cost-effectiveness and simplicity in manufacturing and installation. Figure 2-13 shows a schematic view of mono-pile foundation.

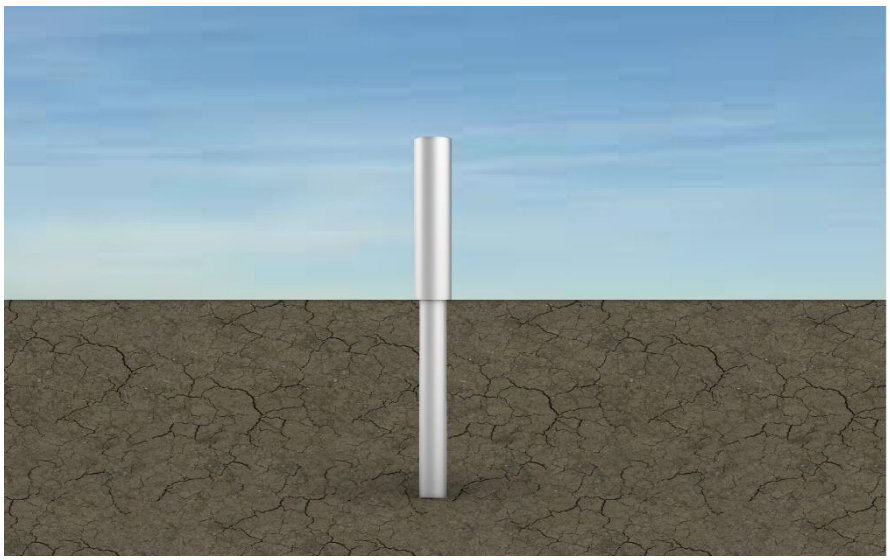

Figure 2-13. Schematic view of mono-pile structure.

The mono-pile structure installation method is predominately defined by the seabed condition/formation. A mono-pile is installed by driving (conventional) through vibration or hammering in the sand, clay or chalk seabed strata; or drilling or boring in rocky strata [31]. It is worth noting that the mono-pile structure is laterally loaded. Mono-piles' water depth range is relatively shallow, up to 40 m [Table 2-3], which could be seen as one of the mono-pile's possible disadvantages [75], [76].

2.5.2 Tri-pod Structure

The tri-pod is a three-leg structure of steel cylindrical tubes - forming a wide seabed base - with a central (vertical) steel shaft for the tower transition [75], [76], Figure 2-14. In other words, it is a steel substructure that comprises a central (single) shaft protruding from sea level that three legs branched from to their particular locations on the seabed [31], [70], [71].

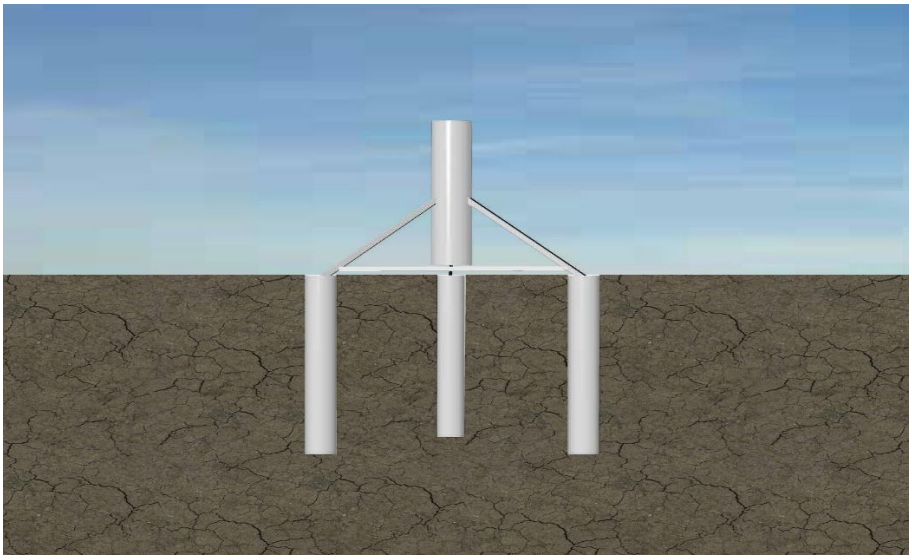

Figure 2-14. Schematic view of tri-pod structure.

Tri-pod legs end with pile sleeves at the corners, whereby pile foundations, in an equilateral triangle form, anchor the substructure to the seabed. Pile sleeves can be vertical or inclined. The substructure pile foundation's diameter and length are smaller than the mono-pile foundation [69]; the range is approximately 0.8 – 2.5 m [80]. Alpha Ventus, Germany, justifies the latter; the 60 MW wind farm comprises twelve turbines, six installed on tri-pod structures with a pile diameter of 2.48 m [81].

The pile foundations' installation methods for tripod and mono-pile structures are similar, either by driving or drilling [80], whereas the tri-pod structure, along with its foundations, is axially loaded. A tri-pod structure is inherently installed at intermediate/medium to deep water with a depth range of up to 50 m [Table 2-3].

2.5.3 Tri-pile Structure

The tri-pile is a tripod cross transition piece anchored to the seabed by mounting on three individual steel tubular piles, as the name implies, arranged in an equilateral triangle [82]–[84], Figure 2-15. The tri-pile is a relatively new offshore wind substructure, first utilised for the prototype/demonstrator project Hooskiel (decommissioned), followed by Bard Offshore 1 wind farm located in Germany during 2008 and 2013, respectively [85]–[87].

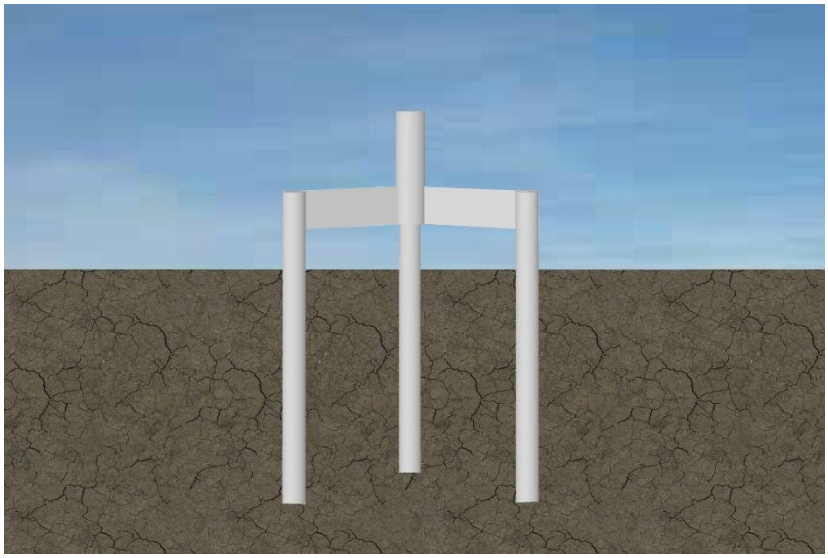

Figure 2-15. Schematic view of tri-pile structure.

Tri-pile is an alternative concept of the tri-pod structure. The substructures differ in the following attributes, but not limited to, the transition piece shape, the pile's top location and diameter. The piles' tops for tri-pile and tripod structures are above [77], [88] and below sea level [71]. Regarding the diameter, the tri-pile pile foundation is 3.9 m (standard) [83], bigger than the tri-pod structure foundations. However, the water depth range for both substructures is the same, up to 50 m.

2.5.4 Jacket Structure

The jacket, or so-called space-frame or truss tower, is a three or four-legged structure connected by (welded) bracings - the substructure made of small-diameter steel circular tubes [71], [76]. The substructure extends from the seabed/mudline to above the sea (water) level [70], Figure 2-16. The jacket structure comprises a centralised large steel tube transition piece; on its top to support the tower [76]. The substructure anchors to the seabed through pile foundations/ sleeves or suction buckets, also known as suction piles or suction caissons. Suction buckets were excluded herein because the foundations' decommissioning strategy is full removal - release and extract through applying pressure.

For pile foundations, the substructure anchors to the seabed by pre-piling or post-piling, depending on, but not limited to, the design of substructure legs. Pre-piling - or so-called preinstalled piles - as the name suggests, pile foundations secure/install first into the seabed with exact distance (centre-to-centre) as jacket structure legs. The distance between piles is maintained by using a piling template, called pile installation frame. Following pile

foundations' installation, the substructure legs are placed on/stabbed in the pile foundations and secured by grouting, e.g., cement [89], [90].

The pre-piling method was adopted for the first time in installing Alpha Ventus wind farm jacket structures [81], [91]. Conventional post-piling is the same as the tripod structure installation method; pile foundations install inside the pile sleeves [71].

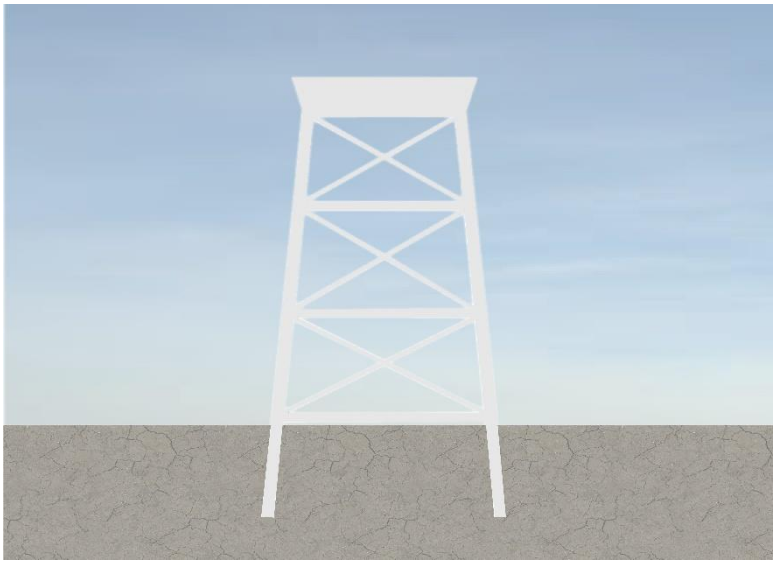

Figure 2-16. Schematic view of jacket structure.

Pile foundations' diameter range for jacket and tripod structures is the same, from 0.8 m to 2.4 m. Beatrice and Alpha Ventus wind farms justify the latter; the 588 MW and 60 MW farms encompass 336 (84 jackets) and 24 (six jackets) piles with 2.2 m and 1.8 m diameters, respectively [81], [90]. The jacket structure installs in deep water with a depth range of up to 60 m [Table 2-3]. For simplification, the mono-pile structure will be referred to as a single pile in the subsequent chapters. Whereas tri-pod, tri-pile, and jacket structures will be referred to as group piles.

2.6 Offshore Wind End-of-Life Scenarios

Offshore wind farms' end-of-life scenarios [EoLs] recognised are life extension, repowering - fully or partially - and decommissioning [73], [92]. The EoLs' definitions in the literature were interchangeable; however, that did not prolong decommissioning. The indistinguishability between repowering, life-extension, or refurbishment definitions - although terms explain themselves - is due to, in layperson's terms, their aim compatibility. The aim is to extend/utilise

the offshore wind farm past its designated lifespan, regardless of the duration, which is not the case for decommissioning [detailed hereafter].

[WindEurope (2017)], for instance, defined partially repowering as life-extension, or so-called re-activation, refurbishment, or enhancement. On the other hand, [Gokhale (2021)] considered refurbishment a scenario along with the other recognised three. Consequently, it was essential to establish a generic baseline concept to distinguish repowering and life-extension definitions, regardless of cost and/or investment impact.

2.6.1 Life Extension Scenario

Life extension aims to extend the wind turbine operation beyond its designated lifespan through minor repairs. A Life-extending feasibility decision relies on assessments, analytical and practical (on-site), and so-called life-extension assessment. In simplistic terms, prior to any repairs/maintenance is executed, assessments on components, e.g., rotor to the foundation, will be completed and successfully passed.

Life extension assessment[10] is conducted through the final years of the operational life to define the wind turbine's (most recent) state [92], [95]. According to DNV (no date), extending wind turbine lifespan relies in conducting an assessment periodically at the beginning and throughout the project lifecycle. From this, one is able to develop and improve the maintenance activity.

When discussing life-extension scenario feasibility, dependent on the above, can be summarised in the following; the structures safety, along with quality and management of operation, maintenance activities and inspection [97]. In the case of adopting the scenarios, the operational life will be extended from five (25%) [98] to ten years (50%) [73] of the lifespan average/certified (estimated 20 years).

2.6.2 Repowering

Repowering is a scenario that counts, along with new projects, for meeting Europe's future electricity generation targets from renewables [93]. This can be encapsulated in two options,

[10] The assessment requires documents availability, not limited to, are repair, inspection and maintenance, construction, and commissioning, and operating and yield data, to name a few.

to provide the wind farm's second life by upgrading its old components to next-generation high output technology; options are full or partial.

For partial repowering, minor components in the superstructure, depending on the case, are upgraded with efficient and advanced components with keeping in situ the tower, substructure, and cables. Components may include gearboxes, rotors, and drivetrains, to name a few [36]. Some literature, such as [99] considered the tower as a key component to upgrade. An answer to the literature contradiction regarding the tower was clarified by the Bockistigen wind farm demonstration case study, which will be examined later in this section.

In comparison, for full repowering, the whole superstructure and cabling are replaced and upgraded including the turbine, tower, and array cables. The replacement can include installation of larger foundations. Whilst electrical infrastructure, such as substations and export cables are unchanged.

Typically, adopting either of the repowering scenario's options, will increase the capacity of a wind farm and its turbines by an amount/fold. The increment assumption is more than double and four times, respectively, relying on [48] analysis of 60 repowering onshore projects. In contrast, under fully repowering, the number decreases by roughly 30%+ due to decommissioning [48], [73].

The repowering scenario had been adopted for the first time, and only to date, in Bockstigen wind farm which is the world's third commissioned offshore wind farm, whereby the project was partially repowered in 2018. Bockstigen wind farm commenced operation in 1998, Sweden, with a 0.55 MW total capacity and five turbines operating for two decades. The following components: blades, nacelle, and control systems for the five turbines were replaced from five refurbished turbines, V47-660 kW, with reusing the original foundations, towers and cables [100], [101]. As a result of partial repowering, Bockstigen wind farm's life expectancy was extended by 15 years, and its operational capacity was increased to 3.3MW [102]. It is worth noting that Bockstigen wind farm's initial plan is to decommission and install ten 4 or 5 MW turbines.

Considering and adopting the repowering option is dependent on the following characteristics: regulations applicable, project size, and site characteristics [73]. Furthermore, the price evolution of the wholesale electricity market, end of leasing or operation and maintenance

contract, or public support are additionally decision-affecting factors [48], [93]. The majority of offshore wind farms in operation have site leases for 40 to 50 years by the Crown Estate in the UK, allowing two entire lifecycles of operation: Thanet and Lincs (40 yrs), London Array and Greater Gabbard (50 years). Under leasing Round 4 (the latest), the lifecycle duration was extended from 50 to 60 years [103].

The repowering decision will be taken at or after the wind farm operation mid-life, around 15 years from commencement, considering the initial adoption of a life extension scenario. Nonetheless, repowering a wind farm can be planned well before its lifetime, e.g., nine years into operation [48]. The prime drivers for this are; economic gains and resource utilisation purposes at the older, best resource sites with improved technology designs potential [36].

Repowering is a more attractive end-of-life scenario than decommissioning but it is heavily reliant on the above. One reason for this attraction is that the location is in utilisation and has the best wind energy resource profile. However, repowering is not always a feasible option, instead decommissioning becomes the preferred route, as proved by Yttre Stengrund wind farm. The Yttre Stengrund was the world's first decommissioned offshore wind farm, located in Sweden and operating since 2001 with a total capacity of 10 MW – consisting of five 2 MW turbines for over a decade (15 years).

Yttre Stengrund wind farm's decommissioning process occurred from Quarter 4 of 2015 to Quarter 3 of 2016 [104]. Despite achieving granted permission, repowering Yttre Stengrund wind farm was not feasible due to the turbines being a manufactured early model and had limited production availability (50 in total) [105]. In other words, sourcing spare parts and managing obsolescence was the wind farm's ongoing challenge.

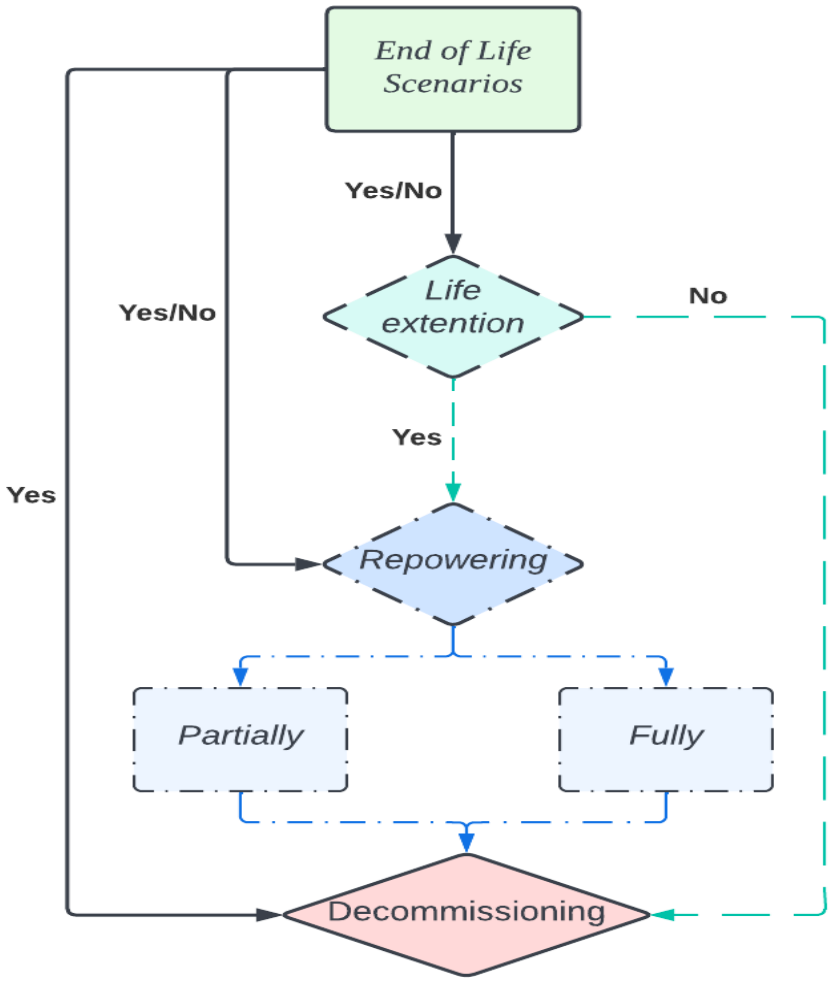

Figure 2-17. The potential sequence of end-of-life scenarios.

Adopting life extension or repowering, or a hybrid approach does not avert decommissioning being an inevitable final phase of the project's lifecycle, as illustrated in Figure 2-17.

2.6.3 Decommissioning

In layman terms, decommissioning is the final stage of a project's lifecycle. Decommissioning aims to reinstate the site to its initial 'natural' condition, as far as practicable, prior to the project construction/installation. Furthermore, decommissioning aims to clear the site from any risk created through the project's lifecycles, which may impact society and/or the environment. Within the following sections we will investigate the provision stated under Acts/Regulations in the energy sector, nuclear, oil & gas and wind.

For offshore wind, an initial decommissioning plan, as depicted in Section 2.3, is a permit required for project consenting, developed and submitted prior to construction. The plan among other aspects, demonstrates the decommissioning process, feasibility (how it will carried out),

and assurance of sufficient funds allocation to cover its costs. Figure 2-18 illustrates a simple sequence of OWF decommissioning phases, adopted from the publicly published decommissioning programmes.

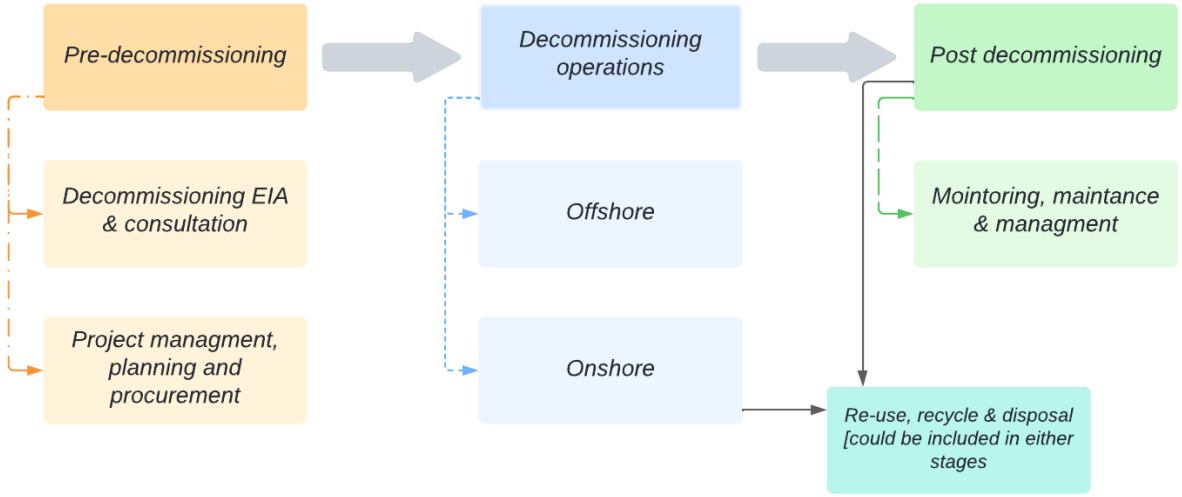

Figure 2-18. Break down the offshore wind farm decommissioning process stages.

Throughout the project's installation and operation stages, the initial decommissioning plan expands to a detailed one through review and modification, including changes, e.g., regulatory regime, technology or costs, market conditions, and international standards. In other words, reviewing, modifying and/or developing a periodic detailed plan is to minimise or avoid any uncertainties and issues that might arise once decommissioning initiates. The motivation for this is to ensure the decommissioning measures, along with the factors mentioned above, may vary at the actual commencement of the decommissioning phase [106]. The UK Energy Act 2004 justifies the latter by stating that reviews and revisions of decommissioning programmes under section (108) are mandated [49].

Decommissioning operations, strategies and methodologies for a wind turbine are simplistic and straightforward for some components when compared to others. The turbine superstructure should be removed in its entirety from the site. Dismantling its components is the linear reversal of the installation process with the following overview: blades removal, followed by the nacelle and tower (in one or more sections). Without altering the process, various superstructure components' dismantling methodologies will be developed, adopted, and employed, as with the platform installation. However, the proposed methodology will be the one that involves minimal dismantling of operations offshore and maximum onshore as it reduces the variables of safety risk, time, resources, and expenditures offshore.

For offshore wind foundations, decommissioning operations are complicated, depending on foundation type and equipment/technology available. In other words, foundation decommissioning utilises different operations from sub-structure installation, particularly the pile foundation. Pile foundations can be removed either fully through excavation or partially by cutting internally or externally at or below the seabed, as described in Section 2.7. In comparison, for suction bucket foundations, the full removal strategy is adopted where the process is the inherent reversal of the installation; release and extract by applying pressure. Consequently, the selection of the decommissioning operations relies on the site's specific factors, such as available vessels, equipment/technology, foundation type, weather conditions, distance to ports, and water depth.

To date, decommissioning is the default option, and it has already been carried out for 10 offshore wind farms/turbines across Europe with the most recent being 2022 as illustrated in Table 2-4. Apart from the adapting decommissioning experience from offshore oil and gas, these projects learned, modified, developed, and accumulated decommissioning experience and knowledge within the industry. Albeit offshore wind will need experience spanning a few decades to draw upon in order to make accurate and precise decisions. One reason for this observation is that the decommissioned projects so far have been relatively small when compared to those currently in operation when taking into account the turbine numbers, specifications, water depth, and distance to shore.

Table 2-4 presents decommissioned offshore wind farms/ turbines.

OWF name	***Country***	***Comm yr***	***Decom yr***	***Operat yrs***	***Total cap (MW)***	***Foun. [Turb. No]***	***Area (km2)***
Nogersund	Sweden	1990	2007	14 [2004]	0.22	TPod [1]	0.25
Vindeby	Denmark	1991	2017	26	4.95	GBS [11]	0.45
Lely	Netherlands	1994	2016	22	2	MP [4]	0.04
Irene Vorrink		1996	2022	26	17 [16.8]	MP [28]	0.4
Blyth	UK	2000	2019	13 [2013]	4	MP [2]	0.4
Utgrunden 1	Sweden	2000	2018	18	10.5	MP [11]	0.45
Yttre Strengrund		2001	2015	14	10	MP [drilled] [5]	0.06
Hooksiel	Germany	2008	2016	8	5	TPile [1]	N/A
Robin Rigg[11]	UK	2010	2015	-	6	MP [2]	N/A
WindFloat	Portugal	2011	2016	6	2	Floating [1]	3.11

[11] Robin Rigg's two 3MW turbines decommissioned due to grouted connections failure between mono-pile and foundation [227], damaging the bedrock beyond possible remedial work or shifting sands [228].

From the second half of the 2020s to the next decade(s), the decommissioning volume will drastically increase as the default option, since the current in-operation wind farms are either reaching their mid or end of their designed lifetime. However, adopting the other two end-of-life scenarios will postpone decommissioning to 2046. The results derived from the analysis of these two scenarios, in terms of time and volume (capacity, farms, and turbines), are displayed in Figure 2-19 and Figure 2-20.

Wind farms installed and fully commissioned after Middelgrunden wind farm were researched, and the analysis and conclusions are included within this study. However, any pilot projects have been excluded. Although Middelgrunden is a demo project, it was selected as a baseline because it was the first-largest wind farm installed at the time, as mentioned in 2.4. Data for wind farms included in the analysis were mainly extracted from 4C offshore [107] and implemented in MS Excel.

The analysis focused on EU countries with the highest installed wind capacities, including the UK, Germany, Netherlands, Denmark, and Belgium. For wind farm estimated end of life, decommissioning will occur either after 20 years, as the default option, or 45 years by adopting life extension (5 years) and repowering (20 years) scenarios.

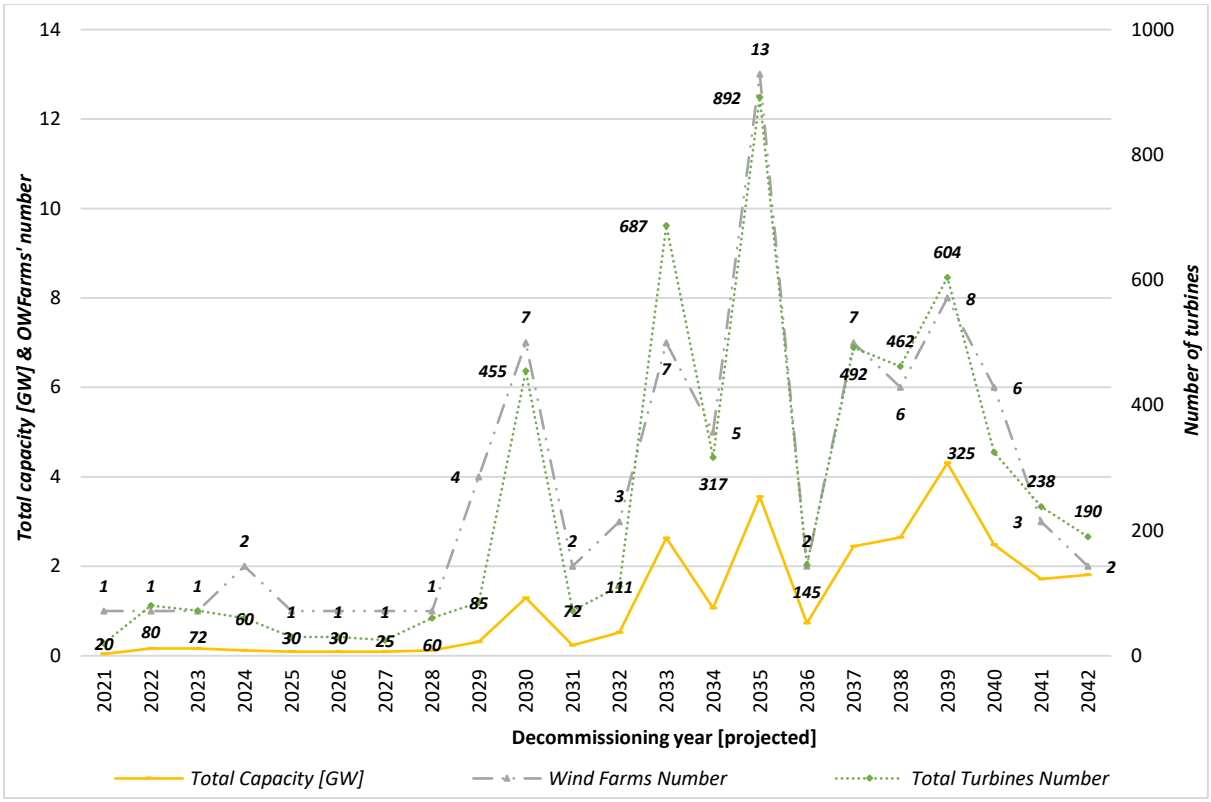

Figure 2-19. The capacities and the number of offshore wind farms and their turbines projected for decommissioning, the default option, over the next two decades.

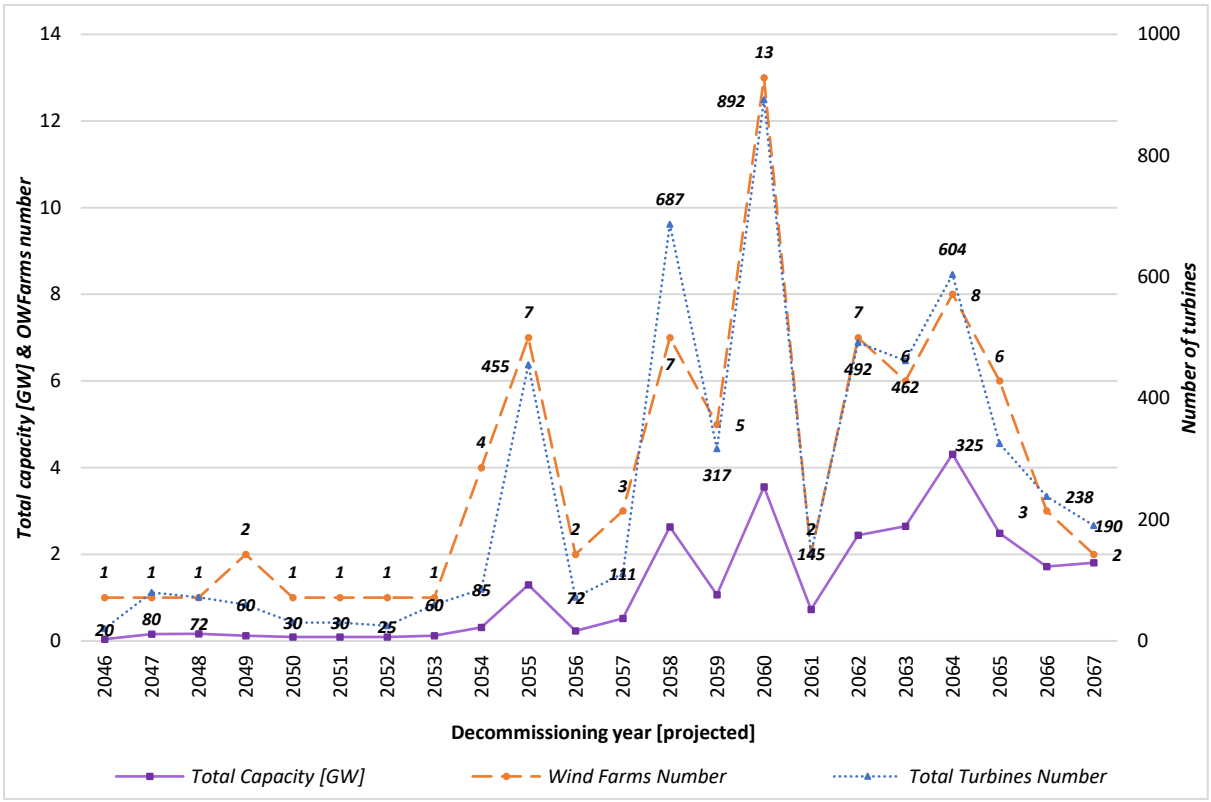

Figure 2-20. When the decommissioning will occur, following the adoption of life extension and repowering scenarios.

Table 2-5 displays the error percentage of the number of turbines.

Reference/ Country	***Number of turbines***				
	UK	***Germany***	***Denmark***	***Netherlands***	***Belgium***
[45]	2,542	1,501	631	599	399
Author	2,457	1,450	585	561	399
Error percentage [%]	3%	3%	7%	6%	0%

To validate the analysis herein, the studied data (installed capacity and number of turbines) was compared with WindEurope 2022 statistics [45]. An error percentage was observed between the two statistics, displayed in Table 2-5; solely looking at the number of turbines.

The above has shown that EoL scenarios will occur closer than ever in coming future. However, all or few were and continue to remain a challenge for long-term consideration by the industry when compared to the industry's current focus which is to establish itself as a reliable energy source of choice.

Motivation 2

The time lag between the installation and decommissioning stages of a project lifecycle is evidence hypothetically and with high probability that decommissioning of offshore wind foundations could transform entirely or partially regarding regulations, operations, and technologies. Accordingly, it was one of the motivations to investigate and develop a novel fixed steel pile-foundation removal strategy, extraction which looks to expand current decommissioning boundaries (options). Furthermore, to expand the decommissioning process definition, incorporating the reversal of the installation process is to include pile foundations, which is the most installed foundation type to date.

2.7 Offshore Wind Pile Foundations Decommissioning Operations

The in-operation OWFs deploy on a total area of over 4,000 km^2, relying on the analysis carried out in Section 2.6. The UK has the largest area, with 2,398 km^2, followed by Germany, Denmark, Netherlands, and Belgium, with 831, 529, 385 and 183 km^2, respectively. Re-using or excluding such areas for sustainable development will depend mainly on which strategy is utilised to decommission the current foundations. Consequently, the following question was proposed and distributed to industrial and academic experts in offshore oil & gas and wind to obtain the industry's long-term perspective. What technology or methodologies will be developed for offshore wind single fixed steel pile foundations in the coming years, whether existing, proposed, or new?

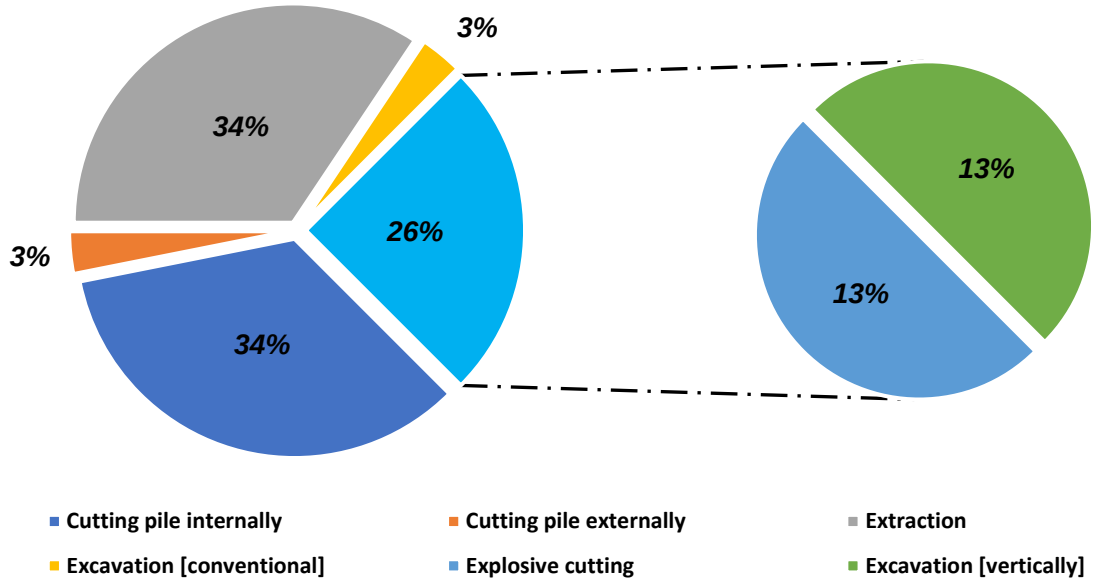

Figure 2-21. The percentage of OWFoundations decommissioning methodologies supported by offshore oil & gas and wind industries' experts.

The collected responses, shown in Figure 2-21, showcased that the cohort selected new methodologies to develop, such as vertically excavating and explosive cutting, along with improving the existing and proposed ones. The majority of experts (34%) supported the internal extraction and cutting of the pile methodologies equally.

Regardless of the methods depicted in Figure 2-21, the industry will adopt the strategies, methodologies and technologies that are economical, easy to use, and minimise marine site disturbance. For simplicity, scour protection, along with components connected and/or attached to foundations, such as transition piece and J-tube, have been removed prior to the foundations' removal.

2.7.1 Partial Removal Strategy

Partial removal, by consensus, is the industry's preferred decommissioning strategy, relying on open published decommissioning programs, as depicted in Table 2-6. Some reasons behind this preference include being less disturbing to the site, maintaining practical integrity, commercial viability, and safety. The partial removal strategy involves cutting the foundation at or to a certain depth below the seabed (mudline), leaving the rest in situ. In a nutshell, the removal process for the partial removal strategy, regardless of the methodology, involves excavation, cutting and lifting.

Table 2-6 summarises the proposed decommissioning strategies and methodologies for OWFoundations.

OWFoundations' decommissioning - Authors	[108]	[109]	[110]	[111]
Wind farm name	Lincs	Sheringham Shoal	Greater Gabbard	Burbo Bank Extension
Decommissioning Strategy	Partial removal	Partial removal	Partial removal	Partial removal
Cutting method	Internally	Internally	Externally	-
Excavation method – depth(m)	Internally – 2m	Internally – 2m	Externally – 2m	Internally & externally – 1.5m
Cutting depth (m)	1m (initial)	1m (initial)	1m (initial)	1m (initial)

Despite the theoretical simplicity, cutting depths change based on localised factors at each site, such as soil conditions, resulting in variation in excavation depth [108], [110]. For piles embedded in hard rock and sandbank, the cutting depth is 1 - 2m and 5 - 10m below the seabed, respectively. The is due to the potential movement of sand over a long period [112], exposing structures/materials in situ. The excavation depth will initially be 1m below the cutting depth for all seabed conditions. It is logical to indicate that cutting methodology and depth, along with seabed conditions, affect soil excavation's method and equipment.

Although excavation occurs, cutting the pile internally is the preferred methodology over cutting it externally because it causes less damage to the seabed. In other words, the excavation diameter for cutting the pile externally increases by 2m for every 1m indepth, resulting in higher cost, personnel risk, and environmental impact. Excavation below 1m depth is damaging and intrusive. It is worth noting that partial removal methodologies may involve installation techniques such as a vibratory hammer to overcome or separate soil-structure interaction (frictional forces). These partial removal methodologies have been demonstrated in Table 2-7.

Table 2-7 summarises the partial removal strategy's methodologies differences.

Parameters	***Partial Removal Methodologies***	
	Cutting Internally	***Cutting Externally***
Soil excavation method	Inside the pile	Around/ outside the pile[12]
Soil excavation technique	Drilling/ milling, OR high-pressure water jetting (HPWJ)	Excavate
Soil excavation equipment	Drill string (drill pipe, bottom hole assembly & drill or mill bit)	Subsea/ seabed dredger; supported by ROV for restricted are
Cutting technique[13]	[Abrasive] water jetting (WJ)	[Abrasive] diamond wire cutting (DWC)
Cutting deployment	Lowering from the vessel	ROV or sea crawler
Reference(s)	[108], [109], [113]	

2.7.2 Full Removal Strategy

2.7.2.1 Excavation

Excavating is a proposed method by the industry. Its concept is analogous to partial removal methodologies' excavation activity, but on a larger scale. For every 1m in-depth, the diameter increases by 2m resulting in a truncated cone shape. The openly published decommissioning programmes have limited information/data on the method; hypothetically, the industry will not adopt it as a first option.

The reason for this is that excavating along the pile foundation penetration depth in such a shape and area would be too damaging to the marine environment, risky and expensive, requiring specialised equipment over long periods. Nevertheless, full removal via excavating is more beneficial than partial removal methodologies in terms of sustainable development and maximising material reuse.

2.7.2.2 Extraction

Extracting and re-using is a common method in the onshore environment, particularly in the piling industry for temporary casings and piles. Extraction is carried out through various methods, such as pulling, vibration, and rotation, to name a few [114]. For offshore wind, extraction may develop and become essential or beneficial and profitable in the future

[12] Excavated pits will partially backfill with the previously excavated pit's clean soil; storm waves and natural seabed sediments' movements would further fill pits.

[13] Explosive is one of the proposed cutting techniques; however, did not include herein because not expected to be the first choice.

compared to the industry's currently preferred strategy, where structures are designed for decommissioning.

A few reasons are that piles will be fully re-used/recycled instead of partially. Pile foundations, regardless of type, are steel fabricated, which is 100% recyclable, making it a fundamental part of the circular economy and reducing decommissioning expenditures. Apart from monitoring, maintaining, and managing left in situ cables, extraction will hypothetically eliminate the foundations' post-decommissioning stage, involving monitoring surveys over a duration. Surveys occur once at the time of decommissioning completion, annually for the following two years, and once after five- and ten- year intervals. Figure 2-22 compares the processes between partial removal strategy methodologies and extraction methodology.

Pile extraction has already been completed and tested experimentally and on a small-scale project. The Dieseko Group (PVE Offshore) successfully extracted Lely wind turbines' pile foundations, becoming the first wind farm decommissioned via a full removal strategy. Lely, located in Denmark, was a 2 MW total capacity wind farm with four 0.5 MW turbines mounted on mono-pile foundations. It was built, commissioned, and decommissioned in 1992, 1994, and 2016, respectively. The Lely pile foundations were 26 m long with a diameter range of 3.2 to 3.7 m. The Dieseko Group extracted the four foundations using the vibration technique, utilising vibro-hammer (PVE 500M). The removal process took 180 minutes (3 hours), approximately 45 minutes for each foundation [115].

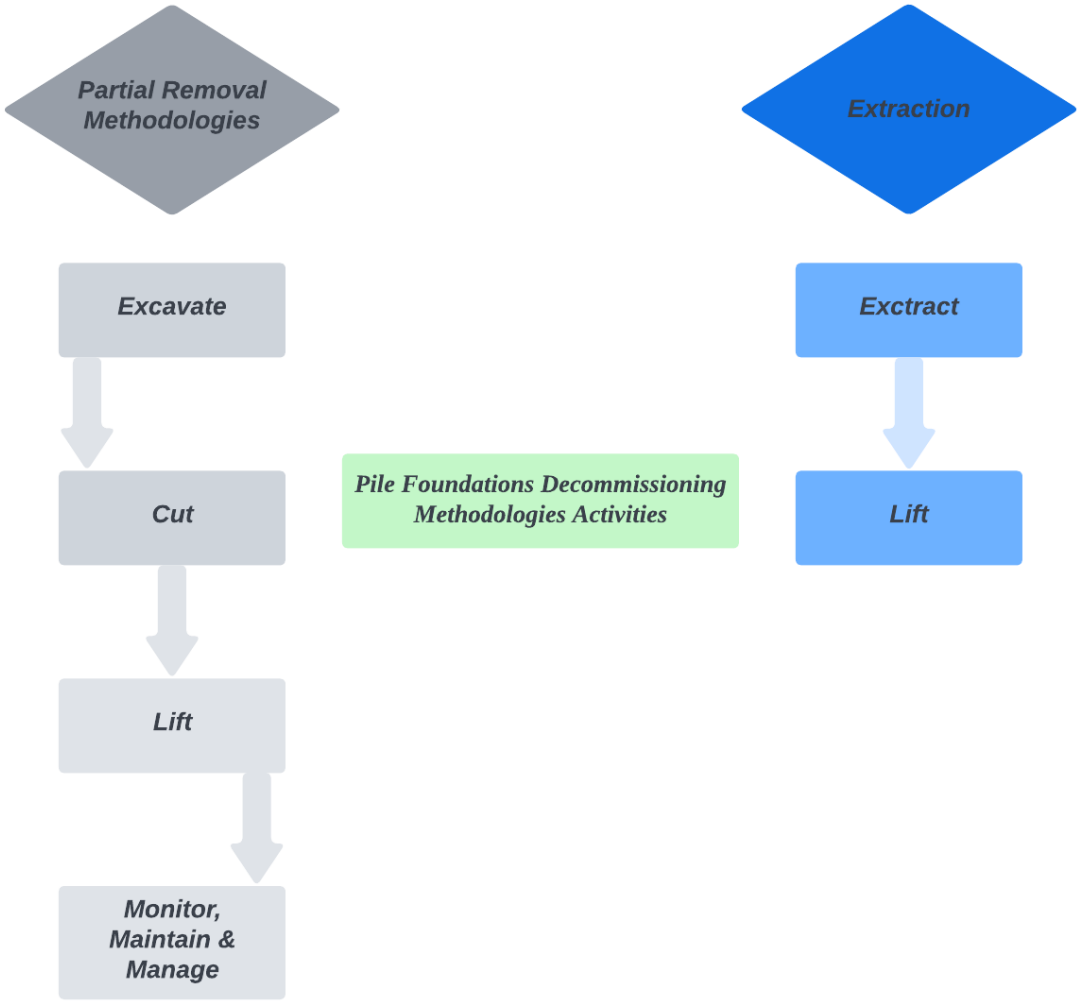

Figure 2-22. A simplified comparison of activities for partial removal and extraction methodologies.

On the experimental scale, under Hydraulic Pile Extraction Scale Tests research (HyPE-ST[14]) project, hydraulic using water pressure was investigated as an extraction technique. The experimental project took place in Deltares water-soil flume facility. The proposed technique requires sealing the pile's top and pressuring water inside its void, forcing the pile upwards [116]. The results of experiment -1:20 and 1:30 scale piles- demonstrated the feasibility of extraction via hydraulic pressure [117].

Floating Offshore Installation (FOX[15]) of XXL wind turbines is a demonstration project that aims to test novel installation methods[16] of various wind turbine components. The project utilised a mono-pile foundation, which was installed using a novel method in 2018, as part of the Slip Joining Offshore Research (SJOR) project. The method involved a vibro-lifting tool

[14] HyPE-ST is part of the Growth through research, development & demonstration in offshore wind (GROW) program and a joint industry initiative of Delfares, Innogy, IHC IQIP, Jan De Nul Group, DOT BV and ECN.
[15] FOX was collaborative project between Heerma, TU Delft and DOT.
[16] Methods include rotor and nacelle assembly (RNA) and slip joint.

with a dynamically positioned (floating) vessel, without utilising a gripper frame or impact hammer (or equivalent) [118]. After the completion of the FOX project, the mono-pile installation process was reversed for removal [119].

Statement 2-4

On a small scale, extraction methods were initiated to develop and will continue to emerge in the foreseeable future, along with the existing decommissioning methodologies proposed by the industry. However, upto this point, the tested extraction methods have been limited to vibration and hydraulic techniques. Therefore, the research project aims to expand and include various extraction methods, such as force and displacement controls.

2.8 Case Study

Adopting a case study is essential for conducting a parametric and sensitivity analysis experimentally and economically to validate the novel decommissioning method proposed for single fixed-steel pile foundations, namely extraction. The identification, selection and justification of the case study are based on two main criteria: literature review and industrial viewpoints. Various factors, such as Europe's offshore wind market statistics, sea basins, and openly published documents (e.g., decommissioning programs, environmental statements and environmental impact assessments), were taken into account.

The adoption and analysis of these mentioned industrial criterion factors help narrow down the specification and characteristics range of existing in-operation OWFs. Consequently, a reliable baseline for each factor will be set to justify the selection of the case study.

2.8.1 Literature Review

Numerous authors have studied and utilised various OW turbines' references, as depicted in Table 2-8, to fulfil diverse aims. These references include, but are not limited to, the National Renewable Energy Laboratory (NREL) 5MW [120], LeanWind (LW) 8MW [121], and the Technical University of Denmark (DTU) 10MW [122].

The OWF baseline capacity, as derived from Table 2-8, is +500 MW based on the mutual literature. Defining and analysing in-depth industrial criteria will further verify the baseline case study. If two OWFs qualified, one from each criterion, the selection would rely on industrial criterion factors due to the technical justifications.

Table 2-8 summarises the offshore wind farms/ turbines' reference adoption in the existing literature.

Author	*Wind Turbine Capacity Reference*	*Wind Farm Total Capacity Reference*
[123]	5.5 MW	5.5 MW
[124]	DTU 10 MW	10 MW
[125]	NREL 5 MW	500 MW
[126]	3.6 MW	504 MW
[68]	10 MW	1000 MW

2.8.2 Industrial Criteria

As previously mentioned, Europe is the research focus for the project's geographical region baseline. The selection of the sea basin and case study depended on the country with the highest cumulative installed wind capacity, the UK, as demonstrated in Section 2.3.

2.8.2.1 Sea basin Baseline

The sea basin factor aims to define the seabed soil conditions and characteristics, whether rock or sand. North Seas and Southern European waters are the sea basins for offshore wind farms in operation and development. WindEurope's latest statistics [45] demonstrate that the North Sea has the highest cumulative installed capacity (see Figure 2-23). Consequently, the North Sea is chosen as the baseline sea basin for identifying and selecting the case study.

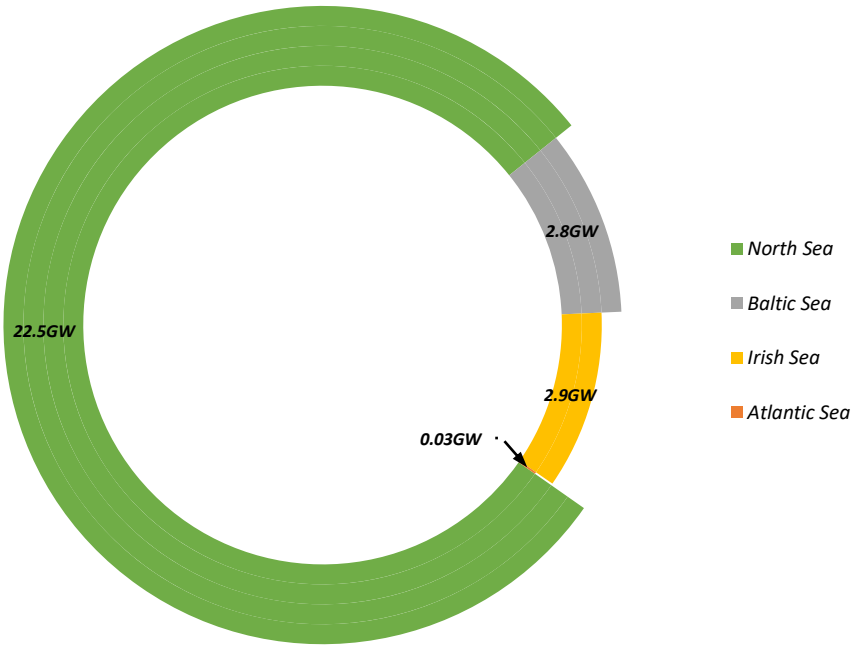

Figure 2-23. The installed Cumulative Offshore Wind Capacity By sea basin.

2.8.2.2 Offshore Wind Farm Baseline

The criteria for establishing the wind farm baseline rely on, but are not limited to, total capacity, distance to shore, and area. It also ensures that the selected OWF scale links between small and large projects. Accordingly, Horns Rev 1 wind farm was a feasible selection because it represents the offshore wind's turning point from pilot to commercial (small to large scale) projects (see Table 2-9). The case study's specification must be equal to or beyond Horns Rev 1 wind farm specifications.

Table 2-9 summarises Horn Rev 1 wind farm specifications.

Wind Farm Specifications	***Values***
Country	Denmark
Commissioning year	2002
Sea basin	North Sea
Turbine Capacity (MW)	2
Total capacity (MW)	160
Number of turbines	80
Foundation	Mono-pile
Area (km^2)	20.7 ~ 21
Distance to shore (km)	Average 17.9 ~ 18
Water depth (m)	6 – 14 (average 10)
Reference/s	[60], [127]–[129]

2.8.2.3 Greater Gabbard Wind Farm

The number of UK in-operation grid-connected OW farms/turbines is 42, with 35 commercial projects and 7 demo projects, as researched by the author. Based on the other baselines (see Table 2-10), UK OWFs have been segmented accordingly. Figure 2-24 to Figure 2-27 illustrate the analysis of UK in-operational OWFs regarding sea basin, capacity, area, and distance to shore, respectively.

Table 2-10 summarises the criteria for the case study selection.

No.	***Criteria***	***Baseline***
1.	Country	UK
2.	Sea Basin	North Sea
3.	Wind Farm	Horns Rev 1
3.1.	Total Capacity (MW)	≥160
3.2.	Distance to shore (km)	≥18
3.3.	Area (km^2)	≥21

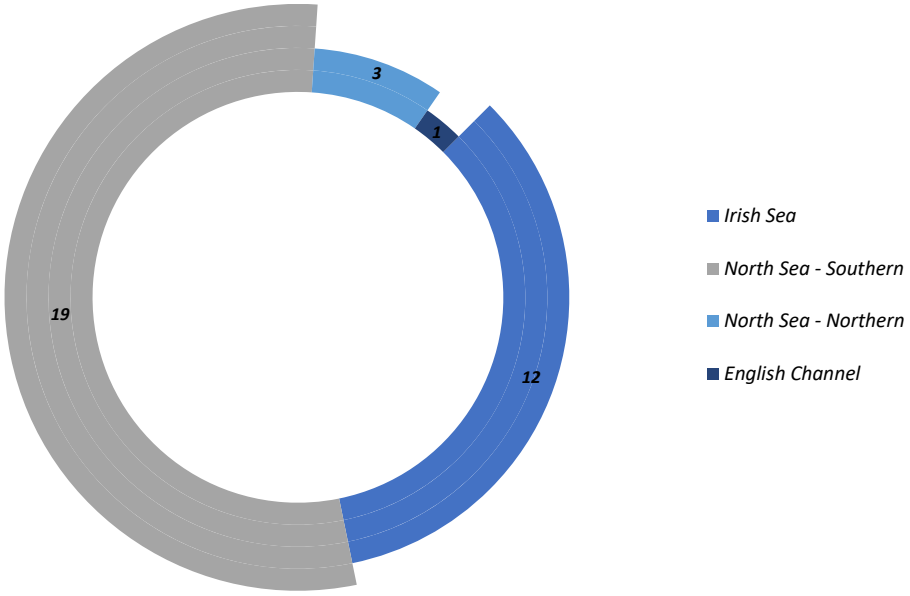

Figure 2-24. UK in-operation OWFs by sea basin.

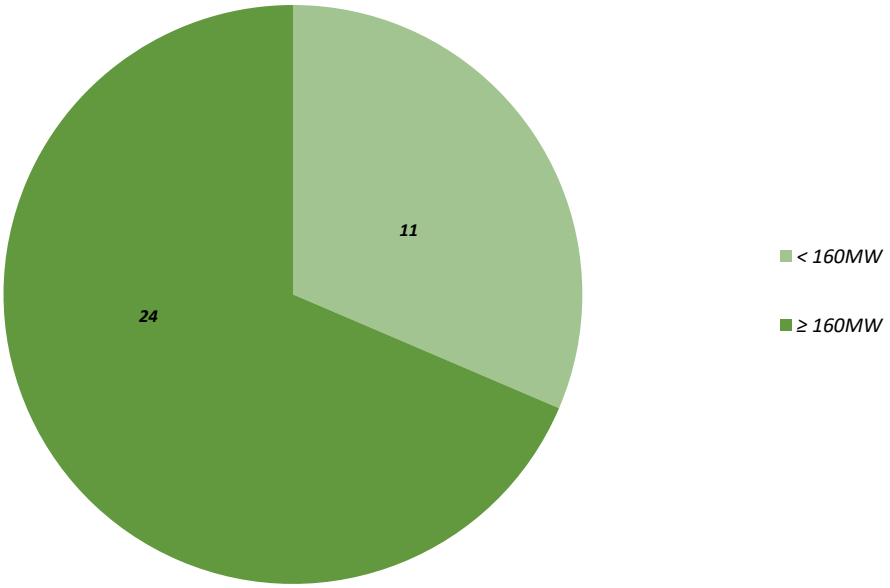

Figure 2-25. UK in-operation OWFs by total capacity.

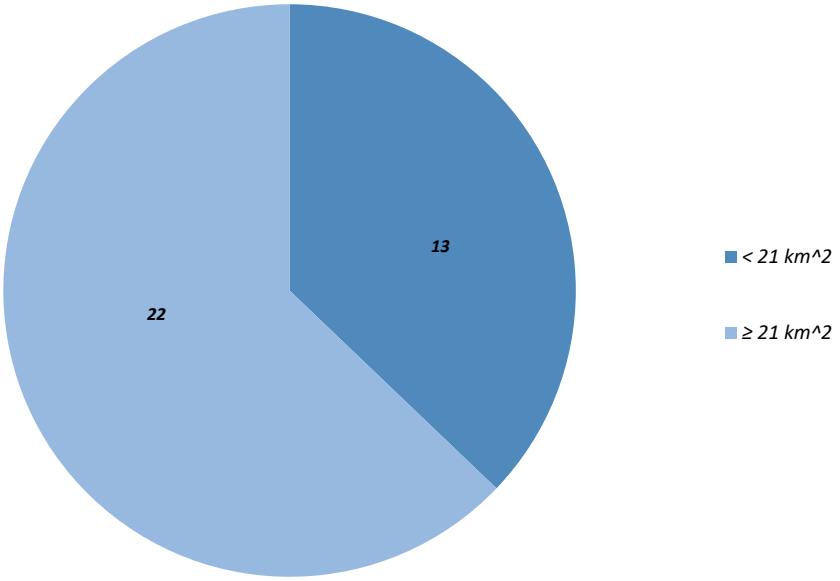

Figure 2-26. The UK in-operational OWFs by area.

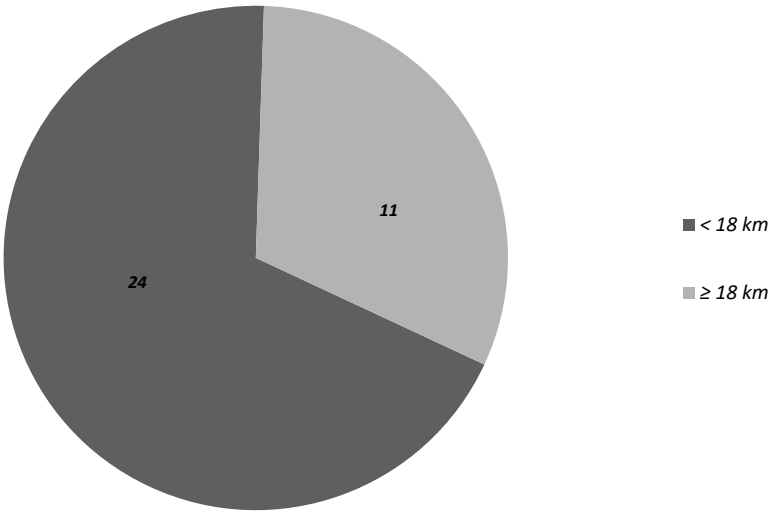

Figure 2-27. The UK in-operational OWFs by distance to shore.

The criteria analysis indicated that 9 OWFs qualified to be adopted as a case study, and the selection relied on openly published documents, as shown in

Table 2-11. The required documents for the case study selection are as follows: decommissioning programme/plan (DP) and environmental statement (ES). In the table, the letters Y and N refer to the available and unavailable documents, respectively.

Table 2-11 summarises the availability Status for DP and ES of the eligible nine offshore wind farms.

No.	***Offshore Wind Farm***	***Total Capacity (MW)***	***(DP)***	***(ES)***	***Reference***
1.	Dudgeon	402	Y	N	DP[130]
2.	Greater Gabbard	504	Y	Y	DP[110]; ES[131]
3.	London Array	630	Y	N	DP[132]
4.	Race Bank	573.3	N	N	-
5.	Sheringham Shoal	316.8	Y	Y	DP[109]; ES[133]
6.	Galloper	353	N	Y	ES[134]
7.	East Anglia One	714	N	N	-
8.	Hornsea Project One	1216	N	N	-
9.	Triton Knoll	857	N	N	-

The decommissioning programme and environmental statements are publicly available for two farms, Greater Gabbard and Sheringham Shoal. The selected case study for this research project is Greater Gabbard, as it aligns with the installed capacity, distance to shore and area. Furthermore, Greater Gabbard's capacity is in line with the OWF capacity adopted by [125] and [126], in terms of capacity and distance to shore attributes.

The specifications for Greater Gabbard wind farm [GGOWF], as shown in Table 2-12, have been extracted from various resources, including the publicly published decommissioning programme prepared by Greater Gabbard Offshore Wind Farm Limited[17] [110], the owner(s) [135], developer(s) [136] and consultancy and market research organization(s) [137], [138].

[17] Greater Gabbard Offshore Wind Limited (GGOWL), a jointly owned company, founded specifically to develop, finance, construct, operate and decommission GGOWF.

Table 2-12 summarises GGOWF specifications.

GGOWF Specifications	
Other Name/s	GGOWL
Country	United Kingdom
Round	Two
Lease term (yrs)	50
Construction year	2008
Commissioning year	2012 - 2013
Site Characteristics	
Sea basin	North Sea – Southern North Sea
Distance to shore (km)/ (Nm) [Location]	20 - 36/ 10.8 – 19.44 [off the Suffolk coast]
Area (km^2)	146.13 ~ 147
Water Depth (m)	20 - 34
Geological Characteristics	A thick sequence of London Clay Formation of Eocene age [firm to stiff silty clay, clayey, sandy silts and subordinate sands]
Wind Turbine Characteristics	
OWFTubrines number	140
Turbine type	SWT-3.6-107
Max. height (m)	170
Rotor diameter (m)	107 - 130
Rotor weight (T)	95
Nacelle weight (T)	~125
Tower weight (T)	*250 - 255*
Total Capacity (MW)	500 - 504
Transition Piece (TP) Characteristics	
Weight (T)	230 - 300
Total weight (T)	32,200 - 42,000
Foundation Characteristics	
Foundation type	Hollow Steel Mono-pile
Foundation length (m)	62 – 65
Foundation diameter (m)	6.5
Weight (T)	600 - 700
Total weight (T)	84,000 – 98,000
Embedment depth (m)	30 - 35
End of Life Scenarios	
Re-powering	
Expected Decommissioning year	40 yrs: 2052 – 2053 50 yrs: 2062 - 2063
Decommissioning	
Stated Decommissioning year (25 yrs)	2037 - 2038
Expected Decommissioning year (20 yrs)	2032 - 2033

Chapter Three

3 Experimental Campaign

3.1 Background

In engineering, a foundation is a crucial part of the structure that connects the superstructure to the soil/ground, whether onshore or offshore. Its primary purpose is to support the superstructure by transferring or directing its load to the soil. Foundations are conventionally categorised into shallow and deep [139]. However, the “shallow” and “deep” differ in the onshore and offshore environments.

In onshore engineering, deep foundations include piles, caissons, and piers, while shallow foundations (or footings) include strips, pads and rafts [140], [141], with the terms referring to the types of foundations. In the offshore context, the terms shallow and deep primarily refer to the water depths and substructures, rather than foundations. This observed deviation is commonly seen within offshore wind technology publications. For instance, mono-pile and jacket structures are installed at shallow and deep-water depths, respectively, even though both substructures are mounted on pile foundations.

Offshore wind foundation technologies, as discussed in Section 2.5, can be categorised as fixed and floating. Fixed foundations include piles, gravity-base, and suction caisson/bucket. On the other hand, floating foundations comprise anchor foundations with various configurations, such as pile, suction, plate, gravity and free-fall anchors [142].

There are currently more than 6,000 installed offshore wind substructures, with over 5,000 of them mounted on piles, as analysed in the literature review in Section 2.5. Consequently, the number of installed piles exceeds 7,000 (7,848 in total), consisting of 4,914 single piles and 2,934 piles grouped together. For simplicity, jacket structures are considered to be mounted on four piles. As a result, this research project solely focuses on the decommissioning of offshore wind’s fixed single steel pile/piled foundations.

Decommissioning piled foundations utilising the research project's proposed method, extraction, requires investigating the impacts of various factors. These factors include, but are not limited to, the design/type, angularity, and installation methods of piles, as well as soil plug and operational duration. In general, a pile is a long steel-made cylinderical column with a slim diameter (e.g., jacket structure) or a wide diameter (e.g., mono-pile) with an open or closed end. Pile/piled foundations, mainly open-ended, have been the most common foundation for offshore fixed substructures since the 1940s [75], as they facilitate installation to the desired penetration depth.

A foundation is defined as “piled” when its depth is more than three times its diameter(width). Piled foundations are classified according to design function (type), installation method, and material. However, these classifications are somewhat indistinguishable/intertwined to some extent. For example, closed-ended piles, although the name is self-describing, differ onshore and offshore. Onshore, a closed-ended pile is one that has a steel plate, or end cap, sealing/covering its bottom end. For offshore, at a certain penetration level or during the operation phase, the open-ended pile would act as a closed-ended pile due to the formation of the soil plug, as discussed in the subsequent sections. In other words, the term “closed-ended” is used to describe an open-ended pile when the soil column inside causes a perfect full plug.

3.2 Pile Foundation Classifications

3.2.1 Design

Pile foundation design is based to resisting overturning moments, uplift/tension, lateral forces, and other factors. In general, pile foundations can be categorised as friction piles, end-bearing piles, laterally loaded piles and tension piles [143]. In this context, the term "design" refers to the process of pile foundations bearing the applied load. The load-bearing capacity of piles to the applied loads is generated through end-bearing, skin friction, or a combination.

End-bearing resistance relies on the soil’s bearing capacity, especially in hard, impenetrable stratum such as very dense sand, rock, and gravel, underlying or at reasonable depth the base of the pile. On the other hand, skin friction develops the load-bearing capacity/resistance through shear stresses along the pile sides. In simpler terms, the pile foundation transfers the applied loads to the surrounding soil by friction or adhesion between its surface or material and the soil, for sandy or clay soils, respectively. For simplicity, the entire pile surface is assumed to transmit the load to the soil. It is evident that soil conditions define the higher proportion of

the pile load-bearing capacity process, whether it is end-bearing or skin friction, in transferring/absorbing the applied load [141], [144], [145].

3.2.2 Material and Construction

A pile is primarily classified based on the material and, in some cases, on the construction method utilised, as both determine installation methods. Pile materials can include steel, timber, concrete, or composites formed by combining at least two materials. However, for the scope of this research, construction methods and their impact, along with concrete and timber piles, have been excluded.

Steel piles come in various shapes, with H-section, sheet piles (both excluded), and pipe piles being the most common examples. Steel pipe piles can be either closed or open-ended. Open-ended pipe piles can be flush or joined with various accessories, such as splicers, points (both excluded), and they may have a driving shoe [146]. The driving shoe, a sleeve or shoe accessory attached to the bottom of the open-ended pile internally or externally, comes in different configurations and dimensions, and is defined as a shoe pile. Its aims include increasing capacity, protecting the toe from damage, facilitating installation, and allowing soil dilation [147]–[149].

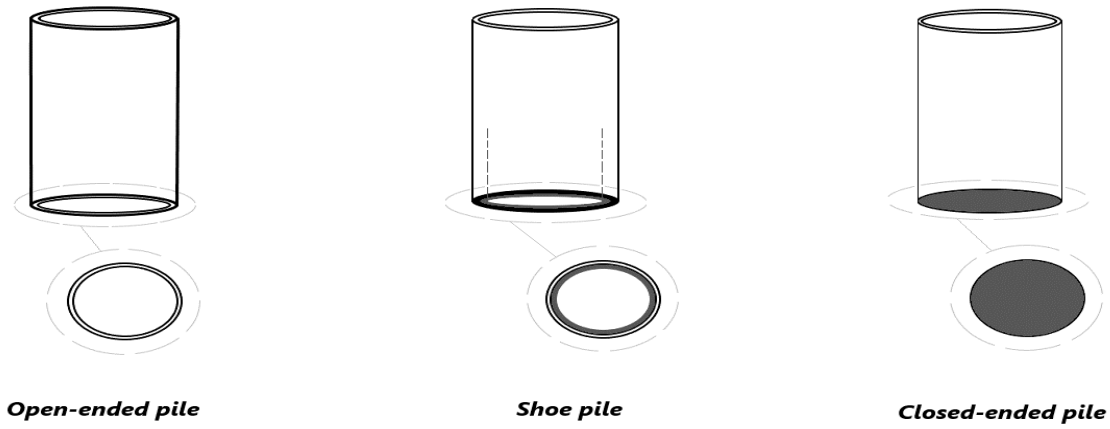

Figure 3-1. The types of steel pipe piles.

Open-ended pipe pile models, both with and without a shoe, as well as closed-ended pipe pile models, Figure 3-1, have been utilised on various scales by several researchers/scholars [4], [148], [150], [151] to study and examine numerous behaviours in different soil conditions. These behaviours include, but are not limited to, pile-soil interaction, soil plugging, suction, pull-out, uplift and breakout resistance, and extraction methods. On the other hand, other

researchers, such as [152], [153] and [154] have studied the same behaviours utilising different offshore foundations, such as spudcan and suction cassion.

The references cited above have been discussed in detail, along with several others, in the relevant subsequent sections. In summary, the focus will mainly be on open-ended piles, with some consideration for closed-ended ones. One of the reasons for this approach is that both types of pipe piles, as previously mentioned, exhibit similar behaviours under certain conditions.

3.2.3 Installation Methods

A steel pipe pile can be installed using either displacement or boring methods, also known as replacement or non-displacement methods. Based on the installation method used, a steel pipe pile can be classified as a displacement or a bored pile. It is worth noting that this classification generally extends to include all pile types mentioned in section 3.2.2.

Displacement and bored methods fundamentally differ in their installation approach. In the bored method, for instance, the pile is installed or positioned in a hole or pit following the removal of soil by grabbing (percussion boring) or augering (rotary boring or drilling)]. As a result, the soil will not densify due to the absence of displacement. In the offshore environment, this method mainly applies to rock or very hard soil sediments [55]. However, the investigation of the method's impact on pile extraction was not accounted for herein due to time and equipment limitations. Consequently, the focus of this research is solely on displacement methods.

Utilising the displacement method, the pile is driven, jacked, or vibrated into the soil, displacing it radially outwards and vertically downwards for unsaturated soil, along with its densification and compaction. For saturated soil, the soil will heave. During the process, the soil, regardless of the type, will enter from the pile bottom-end opening, forming a plug/column, increasing pile toe bearing capacity. This is described in further detail within the preceding sections. However, the latter phenomenon does not apply to closed-ended piles.

Displacement methods, as mentioned above, including driving, jacking, or vibrating, whereby each method utilises one or more applications. The driving method is executed through various impact hammering applications, such as hydraulic (dominant in single offshore wind pile installation), compressed air, dropping, or diesel hammering. The fundamental

form/mechanism of driving applications is the drop hammer; nonetheless, one of the distinctions is the energy delivered in a single blow and by the number of blows per time unit.

In comparison, vibrating– (or so-called vibratory driving) is a modern method that employs a vibratory hammer for driving the pipe pile into the soil. The vibratory hammer *is a mechanical sine-wave oscillator with weights rotating eccentrically in opposite directions. The effect of vibrations is an oscillating vertical force classified by frequency and amplitude* [155]. This implies that the vibrational impact can be controlled in terms of force and wavelength.

In simple words, vibratory driving comprises of rotating eccentric weights powered either hydraulically or electrically, whereby the weights transmit only vertical vibrations to the pile, classified by amplitude and frequency. Along with placing the pipe pile, the vibrating method also extends to extraction. Some advantages of vibratory driving over conventional impact hammering are time and noise emission reduction. This also leads to mitigating the environmental impacts of noise dispersal and corresponding shockwave within the water. However, the jacking method produces lower to no noise and vibration compared to the other methods during installation.

The jacking method (or so-called jack-in or pressing) in simple terms, uses load (dead weight) to press/pressure the pile to place into the soil. The method utilises hydraulic rams to generate static load [114], [156]. Consequently, the pile displacement methods can be classified as dynamic (impact hammering and vibro driving) and static (jacking).

Table 3-1 summarises a few pipe piles and installation methods depicted in the literature, and the dimensions of open-ended piles are in Table 3-2.

Table 3-1 summarises a few of the various piles employed in the available experimental investigations.

Reference	***Open-ended pile [Flush]***	***Shoe pile***	***Closed-ended pile***	***Instrumented***[18]	***Installation method***
[157][19]	✓	✓		✓	Dynamic[20]
[147]	✓	✓	✓	✓	Dynamic (impact-hammering)
[150]	✓	✓		✓	Jacked & dynamic
[151]	✓		✓		Impact-hammering (Hammer blow)
[158]	✓		✓	✓	Jacked
[159]	✓			✓	Dynamic (impact-hammer (falling))
[4]	✓				Jacked

Table 3-2 represents the dimensions of some of the open-ended piles.

	Material & Dimensions [mm] – outside diameter [OD], wall thickness [T], length [L]l
References	*Open-ended pile [Flush]*
[157]	Steel - 70, 2, 2,500
[147]	Steel – 51.1, 1.6, 2,200
[150][21]	Aluminium – 16, 0.55, 350
[159]	Steel – 42.7, 6.2, 908
[4]	Steel – 60.3, 2.77, 400

3.3 Structure [Pile]-Soil Interaction Mechanism: Pile Installation Influence

In simple terms, the structure-soil interaction concept means that before placing a structure or object on the soil, the soil is assumed to be stable and undisturbed. Once the structure is placed on or in the soil, regardless of how it's done (using displacement or resting methods), a bond or interaction between the structure and the soil will develop and strengthen over time as the structure becomes more embedded or settled in the soil. This bond between the structure and the soil is essential for the stability and support of the structure.

In simpler terms, when you place an object on saturated soil, like the seabed, the force of its weight will naturally push into the soil, causing interaction between the object and the soil. Initially, this interaction might be weak, but over time, both the soil and the object will strengthen their bond [160]. This concept remains the same, but the degree of interaction can

[18] "***Instrumented***" term defines the status of the piles utilised by the authors, not as a different type of pile.

[19] The authors used [four] large-scale piles, along with model piles, with 324mm in diameter and [two] 12,000mm and [two] 24,000mm in length.

[20] Model and large-scale piles' installation methods were free falling ram operated by mechanical apparatus and hydraulic hammer, respectively.

[21] The pile dimensions -outside diameter and length- scale by a factor of 100.

vary due to different factors. These factors include the shape, size, and specifications of the object, the method use to install it, the condition of the soil, the loads applied, the depth of placement, and the time it spends in the soil. However, due to the complexity of considering all these factors, the investigation of structure-soil interaction has been mostly limited to studying the impact of installing open-ended piles into the soil column or plug.

When a pile is driven into the soil, the soil enters the pile from the tip, creating a cylindrical column inside the pile. Initially, at the beginning of penetration, the length of the soil column is equal to the depth of penetration. As the driving process continues, the pile can penetrate in three different ways (as showcased in Figure 3-2):

1. Fully Unplugged: The pile penetrates without any significant soil entering the pile, leaving the internal column empty and open.
2. Partially Unplugged: The pile penetrates with some soil entering the pile, but not enough to completely fill the internal column.
3. Fully Plugged: The pile penetrates with the soil entering the pile develops a sufficient frictional resistance develops at a certain penetration level/s preventing intrusion of any new soil. As a result, the pile acquires the closed-ended pile tip resistance.

The degree of frictional resistance that the soil develops inside the pile is one of the determining factors in these penetration modes. If the soil develops enough frictional resistance at a certain depth, it can prevent the intrusion of new soil, and the pile becomes fully plugged. Another situation where the pile becomes fully plugged is when it drives through a transition from dense to a softer material [150]. When the pile is fully plugged, it acquires additional closed-ended pile tip resistance bearing capacity and significant displacement of the surrounding soil [161].

Indeed, during the driving process, the pile typically penetrates in a partially plugged mode, where the rate of pile penetration is higher than the rate at which the soil enters the pile [150]. On the other hand, for fully unplugged piles, both rates are equal [151]. However, under static or operational loading, the pile becomes fully plugged. It's important to note that regardless of the condition of the soil column during penetration, it is generally referred to as the soil plug. In summary, the advancement of the soil column concerning the pile penetration mode, which has implications for the interaction between the pile and the soil during and after the installation process [157].

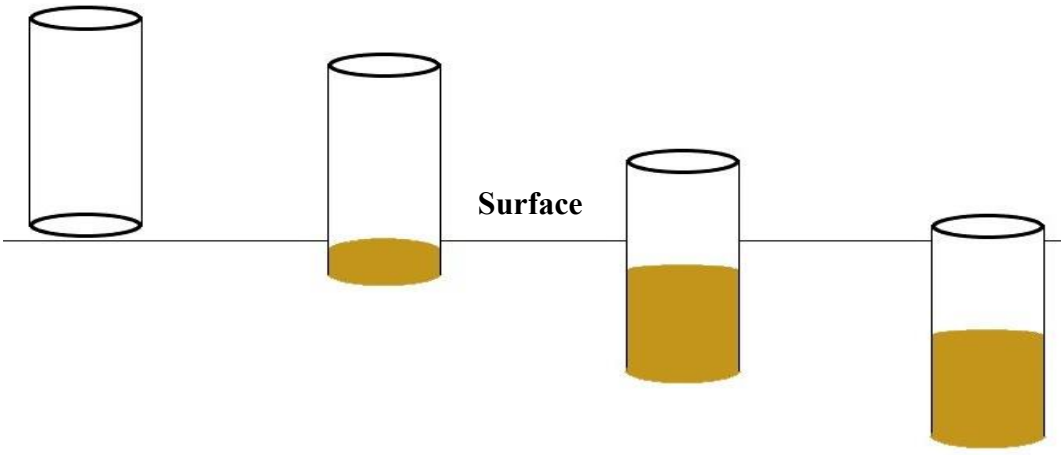

Figure 3-2. The three modes of pile penetration; from left to right, fully coring, partially plugged and fully plugged.

To accurately measure the soil column penetration in the pile and determine the degree of soil plug or plugging, the incremental filling ratio (IFR) is suggested as a reliable method [150], [157], [159], [161]. While one-dimensional analysis of the soil plug[22] or plug length ratio[23] (PLR) is an option, IFR offers a more comprehensive approach. Measuring the PLR is easier in the field compared to IFR, but IFR can be estimated from PLR using the equation proposed by [159]. The IFR is defined as the ratio of the incremental increase in the soil plug length concerning the increment of penetration depth. The authors [159], [161] have presented the IFR equation. For fully coring mode, the IFR equals 100% and for fully plugging mode, it is 0. A value between 0 and 100% indicates a partially plugged pile. To calculate the IFR, it is crucial to measure the soil column length and the pile penetration depth continuously throughout the penetration process and at regular intervals to ensure accuracy. Various measurement methods have been employed on scale models [150], [158], [159] and large models [151], [157]. These measurements help in understanding the interaction between the pile and the soil during the installation process more comprehensively.

Different factors influencing the degree of soil plug formation have been identified, relying on model and field-scale tests. At four sandy sites, [157] drove open and sleeve-ended piles with 70 mm (model) and 324 mm (large) diameters using mass falling, diesel hammering, and free fall hammering. The authors identified several factors that influence the degree of soil plug formation, including the compressibility and density of the soil entering the pile, as well as the

[22] The 1-D analysis of the soil plug is not easy to use; one reason is due to the method's sensitivity to the lateral earth pressure coefficient challenging to estimate, which De Nicola and Randolph (1997) had addressed [159].
[23] Plug length ratio is the ratio of the soil plug length to pile penetration (L/D).

pile diameter and installation method (involving mechanisms, total energy concerning velocity and height, among others).

By installing open and sleeve-ended piles with a 16 mm outside diameter in saturated sand, [150] found that driving the piles resulted in a higher soil column for the open-ended piles than sleeve-ended ones. However, the results were different when installing the piles by jacking. The authors attributed this difference to the low penetration depth achieved during the jacking process. To investigate further, the authors conducted tests in different relative densities ranging from 68% to 95%. They defined relative density as one of the controlling factors influencing the length of the soil column for driven piles. They observed that the soil column length increases with increasing density for driven piles. In contrast, for the jacked piles, the length of the soil column decreases with increasing density. This difference is attributed to the development of sufficient friction by soil column internal stresses, which is affected by the bearing resistance of the soil beneath the pile tip. Notably, one reason for this disparity is the absence of dynamic effects during jacking.

Jacking open-ended piles with diameters ranging from 40 mm - 114 mm and thickness from 1.2 mm - 14.6 mm in loose sand, [158] indicated some factors controlling the plugging. These factors include relative density and the ratio of pile inside diameter to wall thickness - the higher the ratio, the longer the column. Using hammer impact (falling) to install a pile with an outside diameter of 42.7 mm in dry sand with relative densities of 23% – 90%, [159] defined the relative density, along with horizontal stress, are the factors that control soil plug degree. For a 450 mm embedment depth, with an increase in relative density from 23% to 90% - data captured from the study – IFR (Incremental filling ratio) increased to approximately 73% from 56.5%.

The overall conclusion from the prior studies is that the method of pile installation is a more controlling factor than any other, particularly the soil. When installing the pile using displacement applications, the soil properties change in and around the pile; the sand will densify if loose and dilate if dense, impacting the structure-soil interaction during and after penetration.

3.4 Extraction Theory Mechanics

In the field of ocean and offshore engineering, the process of extracting objects embedded in the ocean or seabed sediments has been a relatively understudied issue, despite having knowledge of the physical characteristics of the objects and the soil's resistance to compression/installation. The lack of understanding applies to various offshore industries, such as salvage, and oil and gas operations, among others. [160] experience in salvage revealed that sometimes, embedded objects never break out due to a lack of comprehension of the breakout phenomenon mechanism. Understanding this phenomenon is crucial in designing submersibles and operations to determine the minimum force required to break the submersible free from the bottom mud after a specific duration of rest. This required force for extraction/lifting/pulling an embedded object has been defined as breakout force [162] or mud suction [160], [163]. When applying extraction force for a specific time, it is referred to as breakout time [163]. [164] emphasised that two of the least understood components of the breakout force are soil suction and the adhesion between an object and the surrounding soil. Similarly, [165] acknowledged the lack of full understanding of the phenomena that generate suction forces when extracting offshore oil and gas platforms' foundations, particularly gravity-based structures. Therefore, it is crucial to define the influencing factors on the breakout force in order to gain a better understanding of this phenomenon and improve the knowledge and techniques related to object extraction in ocean and offshore engineering.

According to [160], the breakout phenomenon encompasses various parameters, including object mass, displacement, velocity, water and soil viscosity , permeability, shear strength of soil, and hydrostatic pressure, among others. These parameters constitute the main influencing factors of the breakout phenomenon. [164] provided a general definition of the influencing factors, which encompass the (effective) weight of the soil mass and object, including the force transmission instrument, adhesion force between the object surface and surrounding soil, soil resistance along the failure surface, and soil suction force. To elaborate on the latter, parameters like soil permeability, shear strength, velocity, and hydrostatic pressure contribute to the soil suction force. These parameters and factors remain constant while also varying based on the soil condition. For example, in unsaturated soil, authors [166] and [167] have indicated that a combination of weight and mobilised soil shear strength within the failure surface boundary, along with the pile weight, are contributing resistance factors for extraction/uplift, [4] calculated the net extraction (tensile) load by deducting the pile's weight and the force

transmission instrument, the vibrator. The factors influencing breakout force have been extensively discussed in subsequent sections, excluding the weight factor.

3.4.1 Failure Surface Shape

Understanding the precise configuration of the failure surface, commonly referred to as the "slip surface", is crucial for determining the volume of soil involved in a breakout phenomenon. Numerous assumptions and variations regarding the shape of the failure surface, informed by experimental or analytical testing, have been presented in the literature (e.g., [167]–[169]). These investigations build upon [Balla's[24]] pioneering research [164]. The exploration of failure surface shapes has primarily focused on scenarios involving the uplift of anchor plates encompassing geometries such as square, circular or rectangular (strip) shapes. However, an exception is found in [166] work, where they analytically studied the shape arising from extraction of circular piles. Authors, [168] displayed the different shapes of failure surfaces assumed to estimate the pull-out capacity of anchor plates in cohesionless soil, along with the geometrical overview of each shape. Throughout these investigations, the emphasis has been on comprehending various failure surface shapes and their implications, with a specific focus on scenarios involving the uplifting of anchor plates.

In Balla's method, which focussed on shallow circular plates embedded in dense sand, the shape of the failure surface exhibited circular elevation characteristics. The shape originated with a vertical angle (90 degrees) at the edge of the plate and curved outward from the vertical axis until it intersected the soil surface at an angle of $45 - \emptyset/2$ [164], [167], [168], [170]. [168] model testing results, involving circular plates with 24 mm - 76 mm diameters and a thickness of 6 mm in dense sand, aligned with Balla's findings, particularly when the embedment ratio was less than 6. However, this alignment was not observed for an embedment ratio ≥ 6 (indicating deeper embedment), as the authors noticed a slight elevation in the soil surface around the anchor's tie rod. For example, when dealing with anchor diameters of approximately 25 mm (1 inch) and 51 mm (2 inches) at a depth of 345 mm (14 inches), which corresponds to an embedment ratio ≥ 6; the failure surface did not become apparent until the foundation was relatively shallow.

[24] To clarify, although there was developed work/ theories before 1960 around the failure surface shape (e.g., Majer's method), Balla's proposal had been considered modern research on the subject, which was the foundation for the following investigations [168], [229], [230].

[167] semi-empirical theory, which is based on simplified assumptions and comparison with experimental data, to some extent corroborates [168] findings regarding the extent of the failure surface for deep footings. Their theory was developed by testing model anchors (metal discs) with diameters ranging from 25 mm ([1 inch) to 101.6 mm (4 inches) at various depths. For deep anchors embedded in dense sand, the failure shape was less conspicuous, initially curving and then transitioning to a predominately vertical orientation before reaching the soil ground surface. In contrast, in loose sand, the failure surface appeared as a vertical plane with limited extension, not reaching the ground surface due to the compressibility of the soil mass above the footing and its deformation. In the case for shallow anchors in loose sand, the failure shape resembled that of deep anchors (vertical), yet it extended all the way to the ground surface. This phenomenon also occurred in soft clays [164]. For shallow anchors in dense sand, [167] observed that the failure surface extended from the anchor's edge to the ground surface from the anchor edge in a shallow arc (curved shape), which was consistent with the results obtained by [Balla and [168]. The authors further noted that the failure in the shallow depths generally occurred in shear with a more global distribution, a conclusion supported by [164] theoretical analysis. On the other hand, failure in deep depths was characterised by localised shear. Through their developed general theory, [167] defined the failure surface in the shallow depths as having a truncated pyramidal shape. This theory provides valuable insights into the complex behaviour of failure surfaces in different soil conditions and anchor depths.

In the cone method, also referred to as the Mors method, the assumed shape of the failure surface is that of a truncated cone. The angle of the apex of this cone is considered to be 90 degrees plus the angle of shear resistance of the soil, denoted as ∅. Alternatively, in the frictional cylinder method, often referred to as the vertical surface method, the name itself provides a clear description. Failure is anticipated to occur along the cylinderical surface of the soil, accounting for friction, with the diameter of the cylinder being equivalent to that of the foundation [168], [170]. However, it is important to note that relying solely on these methods, as proposed by various authors (such as [167]–[170]), can yield conservative estimates and may not provide highly accurate pull-out capacities. For example, in the cone method, the capacity is defined as the weight of the soil within the failure surface, disregarding frictional resistance. This approach is generally conservative for shallow depths and the opposite for larger depths. In contrast, when calculating capacity, the frictional resistance is considered in conjunction with the weight of the soil in the frictional cylinder model. In essence, these methods provide simplified approximation that can be useful but should be employed with

caution, as they might not capture all the complexities of the actual behaviour of soil-anchor interactions in real-world scenarios.

In the case of a vertically embedded circular pile within unsaturated soil, [166] proposed a failure shape resulting from the extraction process. They postulated that this failure shape would resemble those predicted by the methods employed by [Balla and [167]]. Through the research, [166] determined that the pile's embedment ratio and friction angle exert a significant influence on the lateral horizontal extent of the failure shape. This relationship is characterised by a direct correlation, meaning that changes in the embedment ratio and friction angle will directly impact the lateral spread of the failure shape.

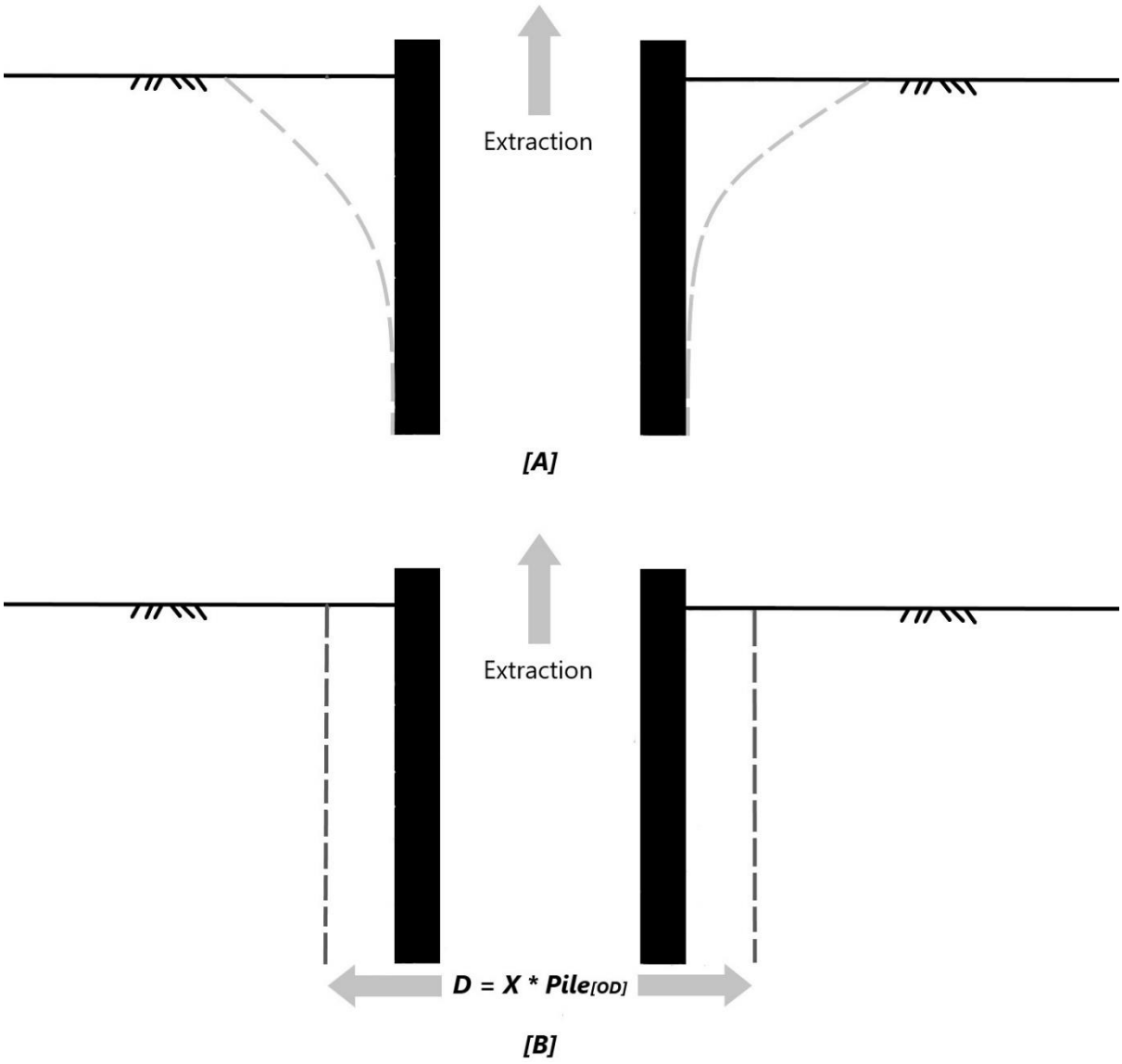

Figure 3-3. The two assumed shapes of the failure surface for extracting a pile; [A] dense sand and stiff clay and [B] loose sand and soft clay.

A preliminary assumption was undertaken, as depicted in Figure 3-3, to ascertain the shape of the failure surface resulting from the extraction of a pile at shallow depths across various soil conditions. Through analysis, it was determined that factors such as the embedment ratio and soil properties, as well as the prevailing soil conditions, exert an influence on the the extent to which the failure surface shape extends to the ground surface. Additionally, the embedment ratio and pile's friction angle were identified as parameters affecting the horizontal spread of the failure shape. When considering the impact of the failure surface shape on the pull-out capacity, studies in this regard have been limited. This limitation persists despite the structural configuration, and it pertains to the geometry of the failure zone.

3.4.2 Skin Friction

Skin friction, as previously mentioned, constitutes a component of pile-bearing capacity and is also regarded as a significant resistance factor during pile extraction. It contributes to the overall extraction force required. The failure mechanism of an object or foundation is more straightforward along its sides, attributed to the presence of skin friction, in comparison to its base [162]. During extraction processes, skin friction can also be referred to as uplift skin friction, shaft friction or resistance and adhesion, particularly in saturated soil conditions. Similarly, to pile installation, skin friction represents a form of resistance along the pile's internal and external surfaces. During failure conditions, the contribution of internal friction to the overall shaft friction may differ from that of external friction. This discrepancy is contingent on the length of the soil column that has formed within the pile, as illustrated in Figure 3-4. In essence, total shaft friction encompasses both internal and external friction until the pile's tip reaches the top of the soil column developed within the pile. This concept is supported by previous studies [4], [147], [157].

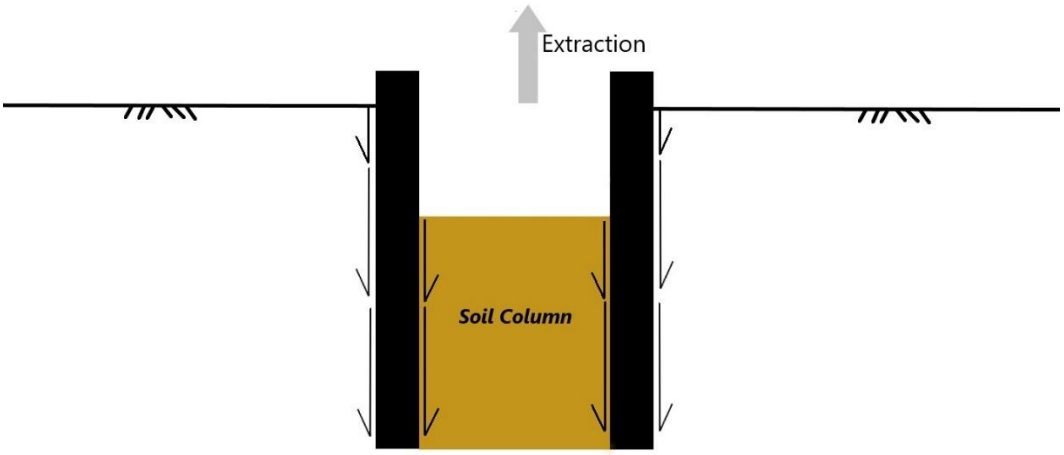

Figure 3-4. The components of shaft resistance - internal and external friction.

The resistance encountered when extracting or uplifting a vertical cylindrical pile, commonly referred to as a straight shaft, from cohesionless soil (sand) which is the primary focus of the research project - is generally believed to be contingent on the concept of limiting skin friction between the pile and soil [166], [167], [171]. Limiting skin friction refers to the point at which the average skin friction reaches its maximum value at a specific embedment ratio, known as the critical embedment depth [172]. Using a rough model pile with a diameter of 25.4 mm in dry silica sand of varying densities at different depths and embedment ratios up to 12 [173] established a direct linear relationship between the embedment ratio and the average uplift skin friction. Expanding on this work and considering embedment ratios up to 24 with the same parameters, [174] discovered that beyond the critical embedment ratio, which is influenced by both relative density and pile surface characteristics, the average skin friction stabilises. However, this stabilization occurs only after the critical embedment ratio is surpassed, a value that varies based on the relative density of the soil [166]. On the contrary, the analytical approach employed by the latter authors revealed results contrary to [174] findings. In this case, the average skin friction decreases gradually beyond the critical embedment depth. This decrease can be attributed to factors such as diminishing earth pressure coefficient values and a reduction in the friction angle (due to stress level changes) with increasing depth. These combined effects contribute to the gradual decline in average skin friction beyond the critical embedment depth.

[166] emphasised that several factors contribute to the determination of average skin friction, including the embedment ratio, soil-pile friction angle (δ), as well as the soil's shear resistance angle. In summary, the average skin friction is influenced by factors such as embediment ratio, relative soil density, the friction angle between the soil and pile, and the soil's shear resistance

angle. These factors collectively play a role in defining the skin friction experienced during pile extraction or uplifting processes.

3.4.3 Suction Force

Suction force, also known as mud suction, is closely related to the pore water pressure level within the soil. Similar to skin friction, suction represents a resistance component during pile extraction that contributes to the breakout force. This force emerges between the base or bottom of the pile and the seabed, as illustrated in Figure 3-5. The resistance encountered during extraction is a result of the development of negative pore water pressure within the soil column inside the pile and at its base. The initial reduction in pore water pressure is attributed to the fact that the soil's pore pressure bears a significant portion of the extraction load as soon as it's applied. This load is subsequently gradually transferred to the surrounding soil, as observed during installation [162], [165].

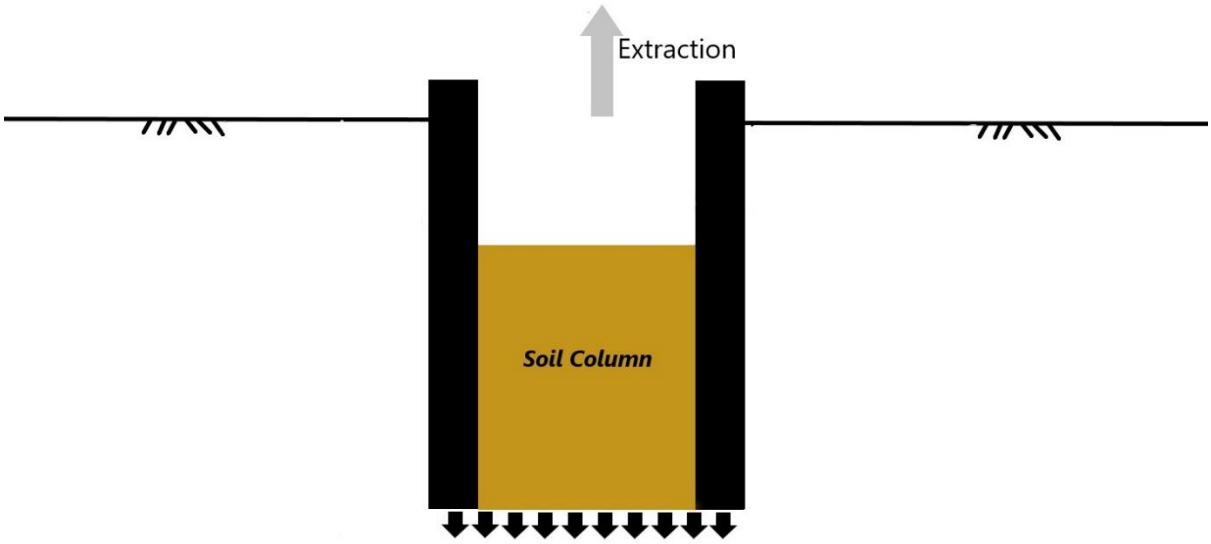

Figure 3-5. The assumed zone of suction occurrence for extracting open-ended piles.

Various foundation configurations have been explored to investigate the factors impacting the reduction in pore pressure (suction degree) during the extraction process. These investigations have been conducted through theoretical, analytical or experimental means, and the findings have been published by researchers such as [162], [163], [175], [154]. [162] validated their proposed explanation of the breakout phenomenon through experimental testing. They utilised a 25.4 mm diameter circular brass model with a 6.35 mm deep skirt (referred to as a suction caisson) in saturated clay soil. Their study established a correlation between extraction force and suction. As magnitude of the extraction force is increased, significant changes occurred in

the negative pore pressure, leading to conditions of undrained behaviour. It was observed that extending the extraction process allowed ample time for the negative pore pressure to dissipate (drainage behaviour), thereby reducing suction and the required extraction force. In a different analytical approach, [163] examined the development of negative pore pressure under an object during its extraction from the ocean bed. His analysis concluded that soil permeability and firmness play pivotal roles in influencing suction. Notably, Foda's findings aligned with the results of [162], indicating that the duration over which the extraction force is applied is as significant as the magnitude of the extraction force itself.

[175] conducted an investigation involving a 100 mm diameter caisson model tested in saturated clay soil. The study aimed to assess the impact of long and short-term loading, specifically the dissipation of negative pore pressure, on extraction capacity. Two different loading scenarios were considered: one involving displacement and one force control with an incremental load of 22 kN applied at a rate of 0.0169 mm/s, and the other utilising displacement control at a rate of 25 mm/s. When subjected to long-term (slow) loading conditions, the extraction capacity ranged between 0.31 kN to 0.155 kN. This variation in capacity was observed across different waiting periods, spanning from of 30 to 180 mins. During this process, the soil exhibited a tendency to remain behind, indicative of local shear failure. In contrast, the situation was distinct under short-term (fast) loading conditions, yielding a capacity of 0.38 kN. Notably, in this case, the soil plug was extracted along with the caisson, implying a general shear failure occurrence. The findings of both El-Gharbawy and Olson's study were consistent with those of the previously mentioned authors. It was evident that the rate and duration of the extraction process significantly influence the extraction capacity.

In summary, the research focused on the influence of suction force on extraction force has been limited, primarily centered on specific foundation configurations, without much exploration into pile foundations. Alongside various foundation setups, the parameters governing the degree of suction include soil properties, the velocity or rate of extraction, and the duration of the extraction process.

3.5 Experimental Components

To assess the credibility of the theoretical method devised to assist in the extraction of single fixed-steel pile foundations (mono-piles) for offshore wind installations, initial 1g experimental tests were carried out using scaled models. These tests encompassed two distinct soil

conditions. Importantly, it is worth mentioning that potential scaling challenges, including factors like boundary effects, were fully considered when selecting components, described in the succeeding sections.

3.5.1 Model Pipe Pile

The experimental tests employed open-ended mild steel pipes as the model piles. Initially, the experimental plan aimed to use piles with three diameters: 60.3 mm, 88.9 mm and 101.6 mm. Accordingly, the scales of piles diameters to the case study's mono-pile are 1:108, 1:73 and 1:64, respectively. Because of these varying diameters, the piles were identified with the labels (small) S, (medium) M and (large) L for 60.33 mm, 88.9 mm and 101.6mm diameters, respectively. Additionally, the letter S denoted the material as steel. The original length of all piles was 3200 mm, which were subsequently divided into four sections of 800 mm each to facilitate the experimental setup.

Table 3-3 summarises the dimensions of model piles.

	MS pile	***LS pile***
Pile numbers	Three	Three
Length [mm]	400	400
Outside diameter [mm]	88.9	101.6
Wall thickness [mm]	3	3.25
Embedment ratio [L/D]	4.5	3.9
Weight [kN]	0.02 [2.38 kg]	0.03 [2.78kg]

The dimensions of the piles were tailored to match the specifications of the equipment initially designated for use in the Advanced Material Research laboratory at Strathclyde University. However, due to changes in laboratory setups, locations, and equipment, certain modifications were made to the lengths, structures, and the attachment of the piles to the machinery.

The length of each pile was reduced from 800 mm to 400 mm, resulting in a total of eight piles for each diameter. All the pertinent dimensions of the model piles utilised in the study are stated in Table 3-3 and visually represented in **Error! Reference source not found.** to Figure 3-9. In terms of the pile structures, two holes were drilled into the walls of the piles. These holes were intended for inserting a pin that rigidly attached the piles to the load cell frame of the testing machine. The diameter of the holes in the piles' walls, as indicated in Figure 3-9 (left), the connection hole on the load cell frame, and the pin itself were all set at 30 mm. A depiction of the pile suspended from the machine, along with the attached pin, is presented in Figure 3-10 prior to the commencement of testing.

Piles with a diameter of 66.3 mm were excluded from the testing due to the apparatus constraints. The diameter of the load cell base exceeded the diameter of the 66.3 mm pile, preventing proper attachment. Consequently, a total of six piles were used for testing in both unsaturated soil conditions. For mild steel (MS) and low strength (LS), three piles each were employed.

Figure 3-6. The utilised two piles' diameters.

Figure 3-7. Piles lengths of 88.9 [left] and 101.6mm [right].

Figure 3-8. The piles' dimensions - diameters [left] and wall thicknesses [right].

Figure 3-9. The [altered] hole diameter on piles-surface [left] and piles weights [right].

Figure 3-10. The pile-machine attachment setup, including the pin's insertion location.

Because of equipment constraints, the surface roughness of the piles could not be measured. Accordingly, the potential impact of pile surface characteristics on the extraction load was not taken into account and was intentionally excluded from the scope of the research project.

3.5.2 Perspex Model Box

The design of the model box for testing is typically shaped by several factors, including handling capacities, equipment accessibility (as noted in reference [176]), and the dimensions of the components involved. For the purposes of the testing objectives, the design of the model centered solely around the dimensions of the pile, particularly its diameter and embedment depth. In more technical terms, this design approach was found on two ratios: the ratio of the pile's diameter to the box wall's diameter, and the separation between the pile tip and the base of the box. The design strategy was employed to mitigate the influence of boundary effects, encompassing both lateral/side and bottommost aspects, on the resistance encountered during the pile installation process.

Boundary effects refer to the impact of a model box's or centrifuge chamber's geometry and size on the behaviour of soil. For instance, these effects can include stress confinement, which does not replicate the conditions present at full scale due to the fact that the generated stresses disperse throughout the surrounding soil. It's important to acknowledge that the consideration of boundary effects primarily revolves around the relative density of the soil. For densely packed specimens, this consideration is crucial. However, this significance diminishes in the case of loosely packed specimens, as indicated by references [158] and [177]. Researchers have proposed various ratios to minimise the influence of boundary effects, regardless of the pile

configuration or whether the testing is conducted within a model box or a centrifuge. A selection of these ratios is outlined in Table 3-4.

Table 3-4 illustrates a few of the suggested pile-to-model box or to-centrifuge ratios.

Reference	***Pile to box wall diameter ratio***	***Separation ratio***
[4]	**7.76**	**4.44**
[176]	**8**	**3.3**
[177]	**5**	**>10**

Adhering to the proposed ratios, the internal dimensions of the model box were configured to achieve a minimum ratio of 4 to the dimensions of the two model piles. This alignment is summarised in Table 3-5. However, it's worth noting that if either ratio falls below 4, the effects will become evident. This situation has been observed by researchers such as [178].

Table 3-5 summarises the Perspex box dimensions.

Perspex box dimensions	
Internal width [mm]	670
Internal length [mm]	670
Inner height [mm]	835
Thickness [mm] – base and four sides	15 [each]

Table 3-6 indicates pile-to-box ratios.

	Model Piles	
Ratio	***MS***	***LS***
Pile to box wall diameter	7.87	6.88
Pile tip to the box base	4.72	4.13

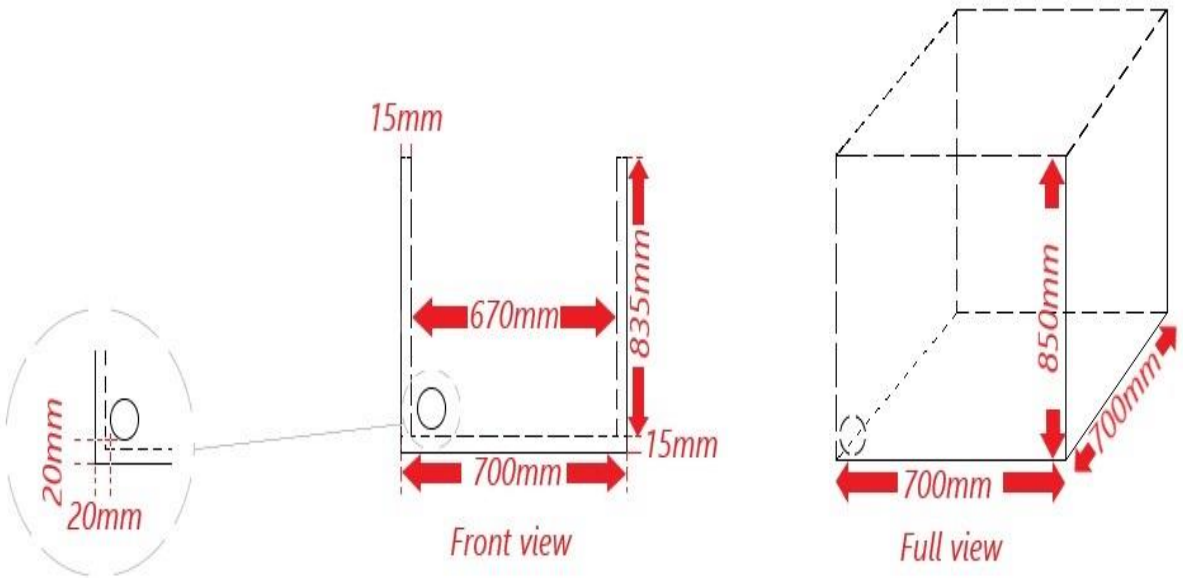

Figure 3-11. A schematic diagram of the perspex box.

Despite modifying the dimensions of the model box from the initial height of 1,277 mm to 850 mm, due to technical restrictions in testing equipment, the ratios did not exhibit a notable impact. The final dimensions of the setup are detailed in Figure 3-11 and Table 3-6. The model box utilised for all tests was entirely constructed using transparent acrylic, subsequently referred to as the Perspex box. One of the motivations for utilising acrylic was to facilitate the observation of soil movement resulting from the advancement of the pile, if applicable. Additionally, this choice of material was made to facilitate future investigations. This includes the examination of surface failure shapes using an axis-symmetric pile setup, as well as exploring the influence of the friction coefficient of the fabrication material on boundary effects (such as frictional resistance at the soil-material interface) when compared to other materials, for instance, aluminium.

To facilitate drainage and minimise potential risk to personnel and equipment resulting from the dimensions and height of the box from the ground, a drainage channel was incorporated at the left portion of the front side of the Perspex box. This channel was designed to effectively manage the discharge of soil and/or water after the completion of testing.

3.5.3 Supporting Frame

The utilization of the supporting frame during testing served as a precautionary measure to address and mitigate specific risks. In addition to the potential risk of drainage channel leakage as outlined in section 3.5.2, there were other risks, notably the likelihood of Perspex box breakage. This risk was particularly pronounced in the case of saturated soil conditions due to the inherent complexity of its formation. The risk of Perspex box breakage carries a range of potential impacts, including but not limited to, harm to personnel, damage to equipment, and financial loses. Given these considerations, the decision was made to employ the supporting frame exclusively during testing conducted in saturated soil conditions. This approach was intended to enhance the stability of the setup and thereby minimise the risk associated with Perspex box breakage.

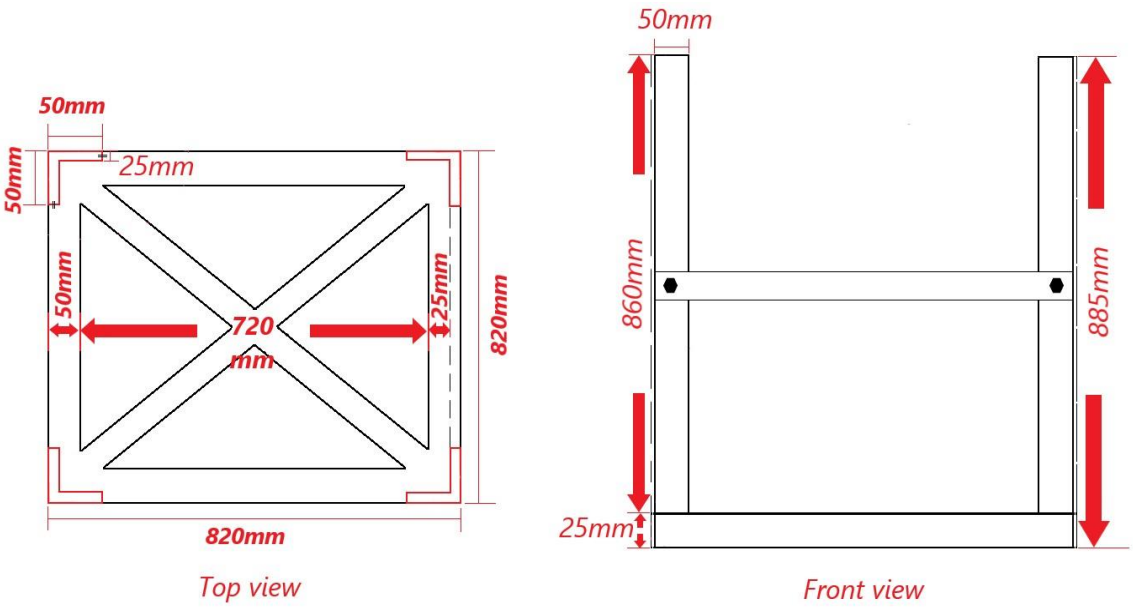

Figure 3-12. The supporting frame schematic view.

Figure 3-13. The supporting frame design and assembly.

A straightforward design was chosen for the supporting frame to achieve several objectives. The design aimed to minimise the weight of the frame, ensuring easy insertion and removal from the testing machine. Additionally, it was intended to simplify the process of installing and removing the Perspex box from the frame. Another key consideration was to avoid impeding the movement of the testing machine's moving crosshead, as this movement directly influences the separation distance between components.

Table 3-7 summarises the dimensions of the supporting frame.

Supporting Frame Dimension	
Internal width [mm]	720
Internal length [mm]	720
Inner height [mm]	860
Base thickness [mm]	25
L – shape thickness [mm]	15

The frame design was structured as a hollow assembly, consisting of a base, four L-shaped sections, and four flat bar sections, all of which were constructed from steel. Comprehensive details about these components can be found in Table 3-7, along with visual representations presented in Figure 3-12 & Figure 3-13. Each of these sections were devised to be fastenable and detachable from both the base and the adjacent sections through the use of bolts. To ensure additional protection, the internal width and length dimensions of the frame were intentionally made larger by 20 mm compared to those of the Perspex box. This extra space was utilised to incorporate a soft material, such as a sponge, in between the frame and the box. This measure served as a safeguard, designed to cushion, and stabilise the sides of the box in the event of an unexpected incident.

3.5.4 Soil Properties

Kiln Dried sand was uniformly utilised in all testing procedures, and its comprehensive characterization was undertaken by an independent laboratory, i2 Analytical Ltd. The characterization process is summarised and visually shown in Figure 3-14, with specific parameter detailed in Table 3-8. The decision to collaborate with i2 Analytical Ltd stemmed from a variety of constraints, including the closure of the University's geotechnical laboratory and time limitations. The former factor led to the exclusion of conducting cone penetration tests (CPT) to further define the soil profile, including attributes such as the soil friction angle. It's important to note that the grain size of the sand was not proportionally scaled in alignment with the model's other geometric aspects. This deliberate decision was taken to uphold consistent material properties throughout the testing process. The method employed for the preparation of the soil beds is elaborated upon in subsequent sections.

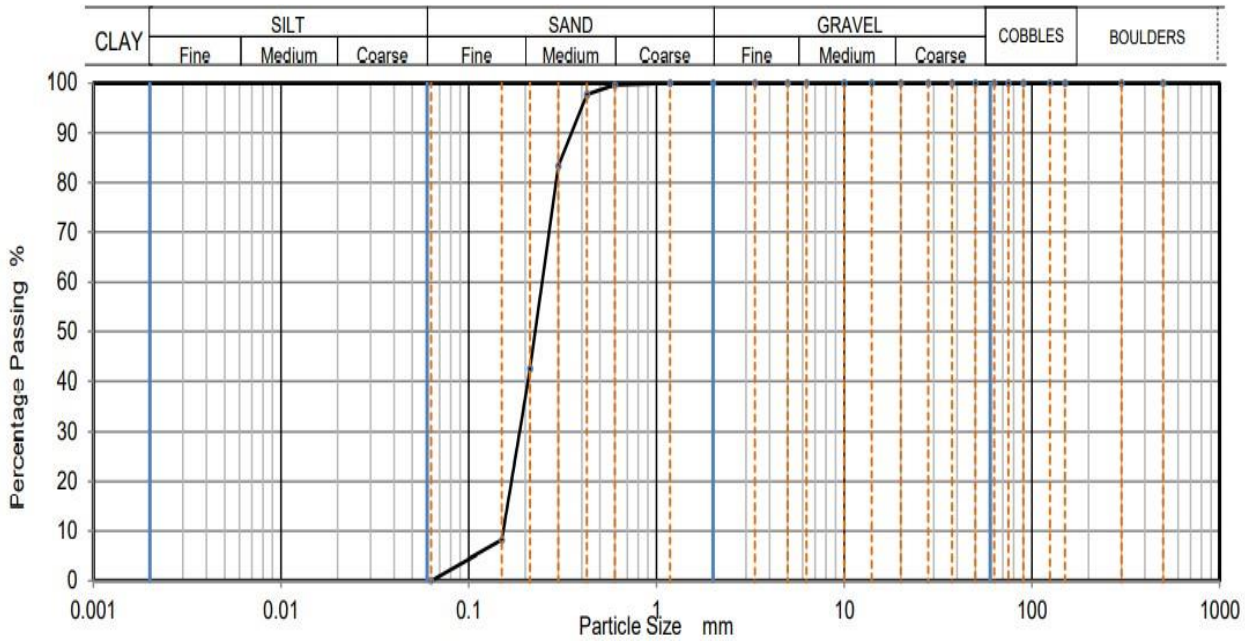

Figure 3-14. The soil's grain-size distribution, provided by i2 Analytical Ltd.

Table 3-8 summarises Kiln Dried Sand's primary properties.

Soil Property	***KD Value***
D_{10} [mm]	0.153
D_{30} [mm]	0.187
D_{60} [mm]	0.246
Uniformity Coefficient, C_U	1.6
Minimum dry density, ρ_{min} [kg/m^3]	1,010
Maximum dry density, ρ_{max} [kg/m^3]	1,630

3.5.5 Semi-submersible pressure transducer

As mentioned earlier, the experimental campaign consisted of a series of tests conducted in saturated soil conditions. To monitor the pore water pressure levels of the soil during both installation and extraction processes, a semi-submersible pressure transducer was employed. The specific model used was the PX709GW-2.5G5V by Omega. The primary objective was to gauge the influence of different extraction rates on the pore water pressure, a key factor impacting the tensile load. Detailed dimensions of the transducer are depicted in Figure 3-15.

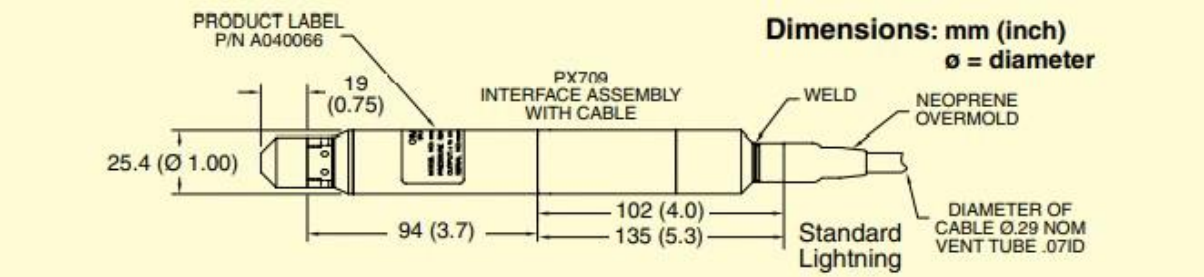

Figure 3-15. The semi-submersible pressure transducer dimensions; cross-section dimensions adopted from Omega (no date b).

Figure 3-16. The transducer setup before installation.

Before embedding the transducer into the soil, a precautionary measure was taken by covering its five nozzles with pieces of cotton, as showcased in Figure 3-16. This step was advised to minimise the risk of soil intrusion. The transducer underwent calibration by the manufacturer, a process that was validated through an attached calibration certificate. As per recommendations, the transducer was installed within a stilling well and oriented vertically. It's notable that fastening the transducer to a pipe was discouraged due to potential risks. In accordance with this recommendation, the transducer was positioned independently to avoid the possibility of displacement and damage, as outlined in reference [180].

The transducer was equipped with a standard 3-meter flexible Polyurethane cable capable of bending. At the cable's end, there were four electrical outputs: two for output signals and two for excitations. The excitation wires were responsible for providing power to the transducer. To achieve this, these wires were connected to an external power supply. It's worth noting that the external supply power of 2 A and a voltage of 10 V, as stipulated in reference [180].

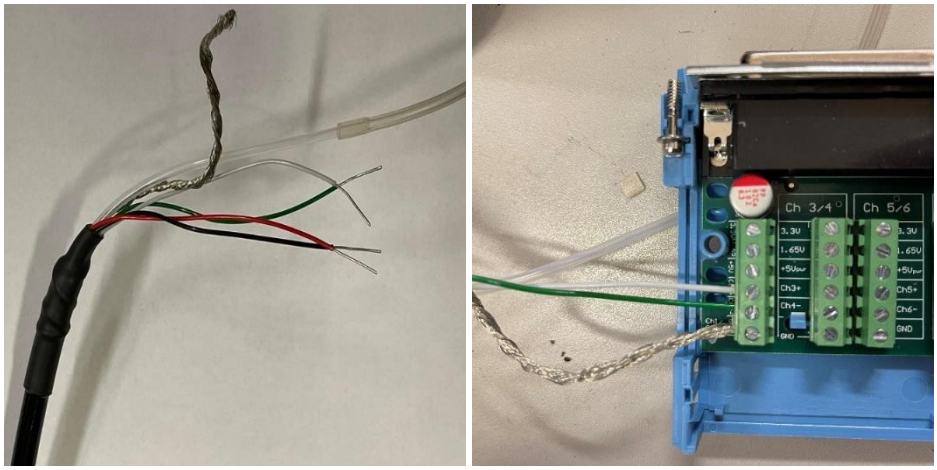

Figure 3-17. The transducer wiring [left] and its output wires attached to the strain gauge wiring box [right]; [+] white & [-] green are outputs signal wires, [+] red & [-] black are excitation wires, ground wire and [transparent] drainage wire.

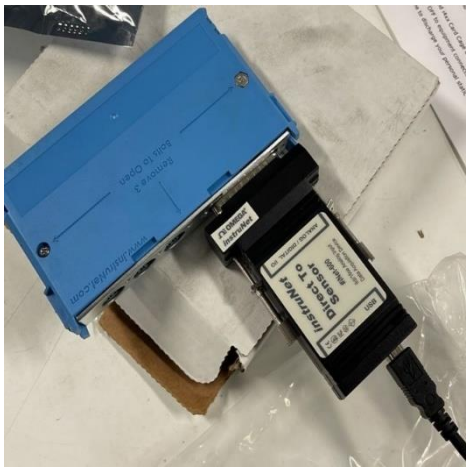

Figure 3-18. iNet-600 and iNet-512 assembly.

The process of translating the pressure readings into a signal was accomplished by connecting and securing the transducer's two output signal wires to the iNet512 8-banks (16 channels) strain gauge wiring box [181], illustrated in Figure 3-17. Specifically, the output wires were attached to iNet-512 channel 1/2. Subsequently, the acquisition of data from the transducer's signals was conducted using the iNet-600 8-channel standalone USB data acquisition system.

The iNet-600 data acquisition system was securely connected to both the iNet-512 wiring box and the PC using two thumbscrews, as depicted in Figure 3-18. Additionally, a USB connection was established between the iNet-600 and the PC. It is worth noting that while it was feasible to capture the signal from the testing machine's load cell through one of the iNet-512 channels, this option was deliberately omitted in this context to uphold accuracy, consistency, and simplicity in the setup.

To facilitate the recording of transducer signals, the instruNet world software was installed on the PC using the CD provided by Omega. This software package includes a setup record dialog encompassing a range of settings related to digitising signals. This includes setting of parameters such as the sensor type, timebase, display options, and more. In the context of the sensor setting, pressure was selected with a Pascal unit and display ranging between -5,000 Pa (minimum) to 5,000 Pa (maximum)]. This selection aimed to prevent potential errors in the data, ensuring accurate capturing and recording of the pressure measurements.

In the timebase settings, there were several parameters to configure: sample rate, points per scan, and the number of scans. The sample rate aims to capture the base sample rate in units per channel, typically measured in samples per second per channel. For the testing, a sample rate of 10 samples per second per channel was designated. The points per scan parameter determines the quantity of data collected in each individual () scan. Throughout most of the testing, the range of points per scan spanned from 100,000 to 1,000,000 with only two instances utilising 10,000 points per scan. As for the number of scans, this parameter essentially dictates the number of individual scans that will be conducted. For the testing, a total of 100 scans were set to be performed. It should be noted that the number of scans was set to 100 as precautious. However, the installation process, waiting period and extraction process were captured in one scan.

The decision to adjust the timebase settings (Pts/S) stemmed from the combination of limited knowledge with the transducer and its operation, along with the time constraints (a span of four days)[25]. Despite these factors, all data was effectively captured and recorded. Throughout the testing, a series of trials and adjustments were performed on the timebase settings. This was done to ensure that the scales for data collection were sufficiently higher than the anticipated duration of the extraction testing in saturated soil. By default, all recorded data is saved in a text file format that can be opened using software like Notepad. To facilitate further processing, the data was extracted, inserted, and saved in the MS Excel format.

3.6 Experimental Investigation Setup

The process of installing and extracting model piles in the two soil conditions was facilitated through the utilisation of a floor standing ZwickRoell Z250 universal testing machine,

[25] Four days were the time window to familiarise with the transducer and its software, along with carrying out the testing sets in saturated soil.

equipped with a 250kN load cell. These operations were conducted at the University of Glasgow. Visual representations of the employed ZwickRoell machine, along with its dimensions, can be observed in Figure 3-19 & Figure 3-20. It's important to acknowledge that there were variations in the dimensions of the testing area with the machine, the Perspex box, and the supporting frame. While the testing area's width and length were larger and smaller, respectively, compared to the two components, It became imperative to ensure proper centering of the Perspex box and the support frame within the machine prior to conducting the tests. This alignment served to centralise the pile within the machine's loading cell, without influencing the pile-to-box wall diameter ratio. A schematic design illustrating the dimensions and positioning of the components within the machine's testing area was developed prior to setting up the experiment, as depicted in Figure 3-21 and Table 3-9. Figure 3-22 to Figure 3-24 capture the final setup of the components for the two different soil conditions. It's worth noting that the process of setting up the box within the machine was performed a total of three times. Two iterations were carried out before preparing the unsaturated soil, while one iteration preceded the preparation of the saturated soil. This occurred due to the shared usage of the machine by other researchers.

After confirming the appropriate positioning of the components within the machine's testing area, the process of preparing soil-beds commenced for both unsaturated and saturated conditions. Researchers have employed a variety of methods to prepare soil beds, such as tamping, pluviation, vibration and stirring, each requiring different equipment. However, due to the equipment limitations, the manual pouring technique was employed for all conditions. This technique was previously employed by [173] for preparing sand beds with different densities; loose, medium and dense.

Figure 3-19. The ZwickRoell testing machine.

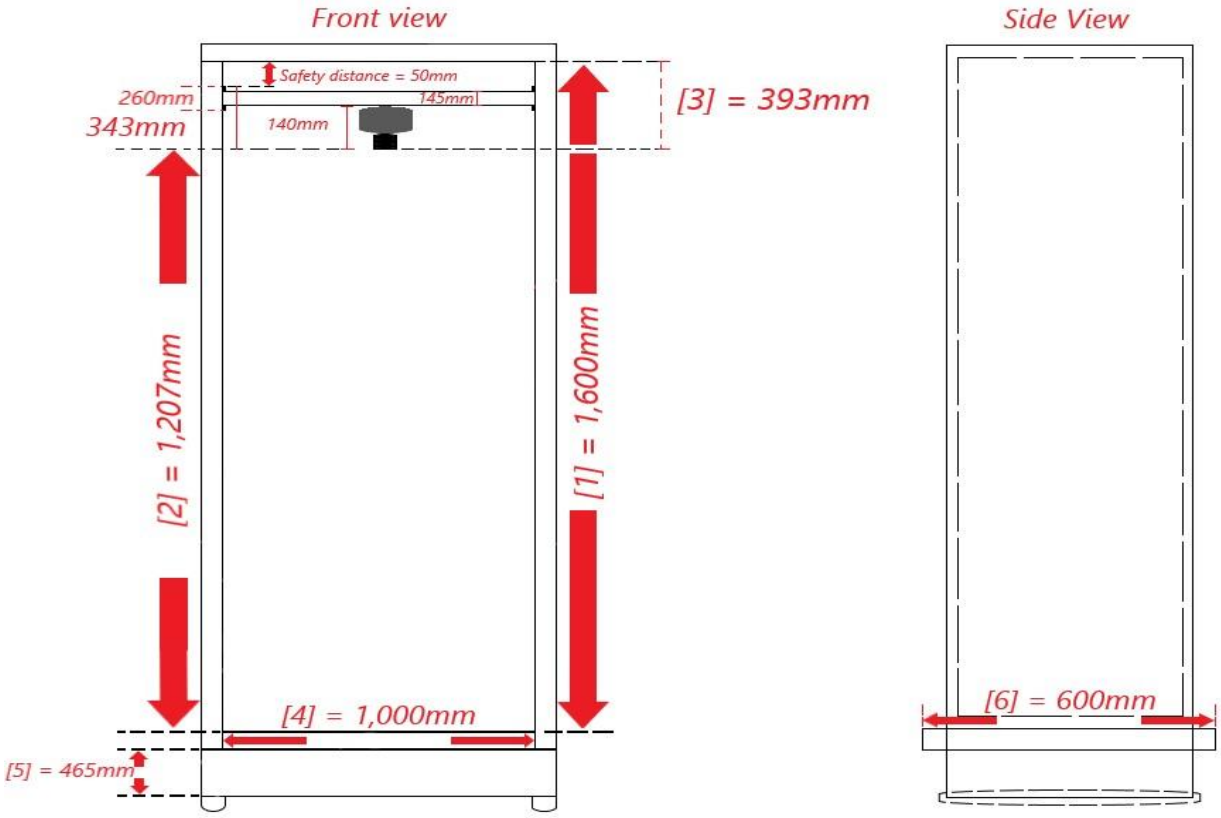

Figure 3-20. Testing schematic machine's front and side views.

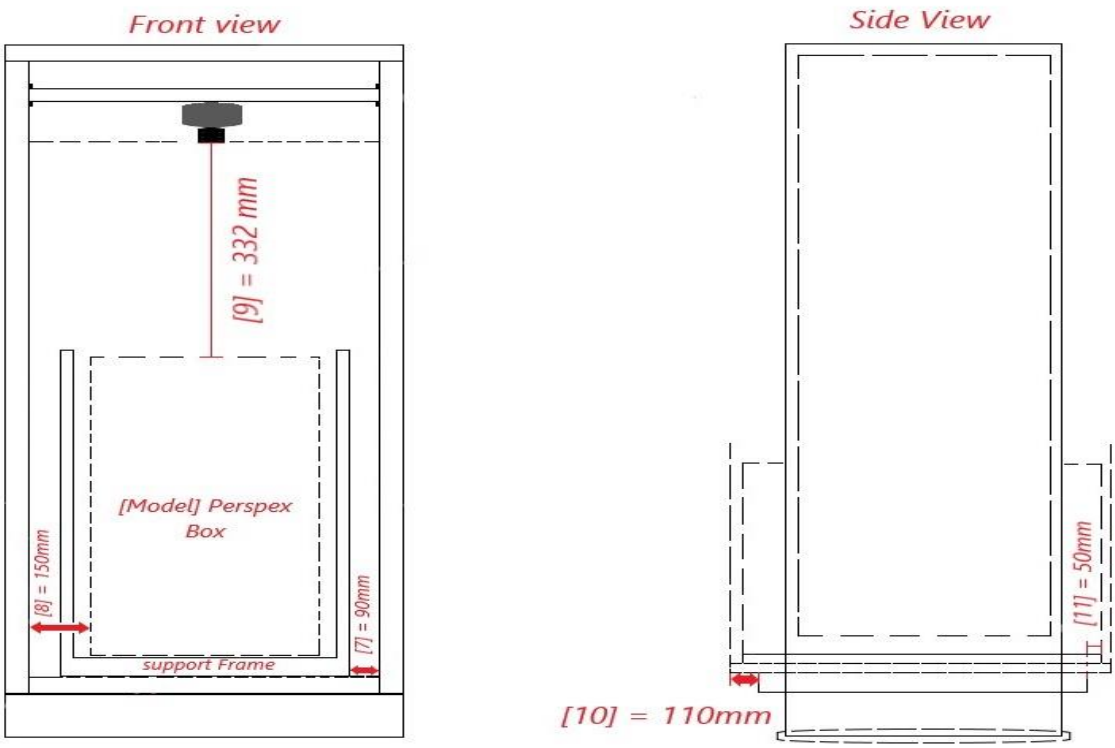

Figure 3-21.Experiments' schematic setup; testing machine, Perspex box and support frame.

Table 3-9 represents experiments' schematic setup.

• Total internal height
• Height for testing
• Height sum for safety distance, load cell and moving crosshead
• Width of the testing area
• Height of the machine from the ground
• Length of the testing area
• The distance between the support frame and the testing area
• The distance between the Perspex box wall and the testing area
• The separation distance between the Perspex box [top] and machine loading cell
• The length difference between the support frame & testing area
• The length difference between the Perspex box & testing area

Figure 3-22. The dimensions of the Perspex box to the machine testing area; the images from left to right are front sides [left and right] for length and left [front] and right front] sides for width.

Figure 3-23. The support frame dimensions-to- the machine testing area; images from left to right are front [left] and back [right] sides for length and left [front] and right [front] for width.

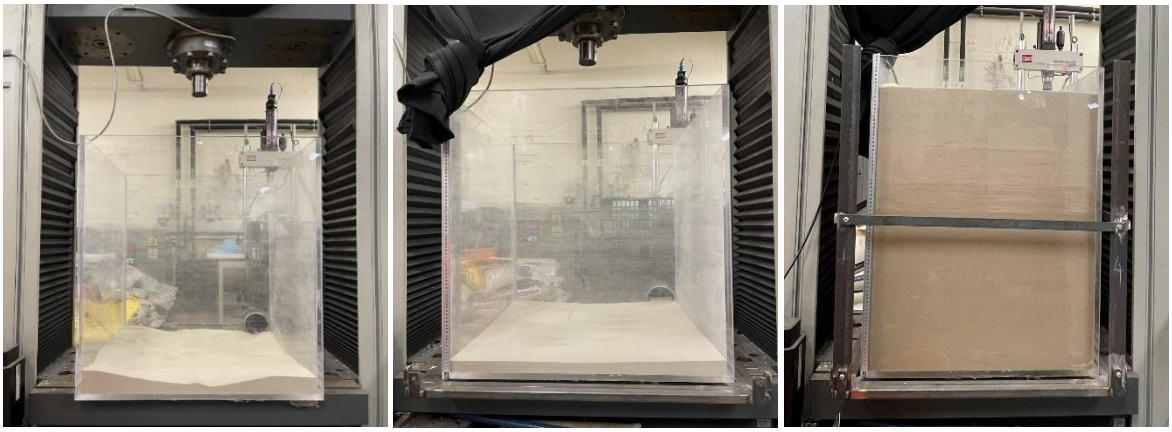

Figure 3-24. The final position of the Perspex box [left] and the support frame [middle and right] within the testing area.

Figure 3-25. The poured soil layer before and after levelling and compacting.

Figure 3-26. The positioning of the semi-submersible pressure transducer in the soil.

Figure 3-27. The 101.6mm pile diameter distance to the Perspex box's inner wall in saturated soil [experiment #]; the images from left to right are front, back, left, and right sides.

Table 3-10 exhibits the logged measurements for piles' distance to the perspex box's inner wall over different experimental tests.

				Pile to Perspex box internal wall distance [mm]			
Experiment number	***Pile diameter [mm]***	***Soil condition***	***Extraction method***	***Front***	***Back***	***Left***	***Right***
1	88.9	Unsaturated	D.E	290	300	300	290
14			F.E	300	300	300	290
24		Saturated	D.E	300	300	300	290
32			F.E	300	290	290	290
9	101.6	Unsaturated	D.E	290	290	290	290
19			F.E	290	290	290	290
28		Saturated	D.E	290	290	290	290
36			F.E	290	290	290	290

Figure 3-28. Starting positions for embedding piles' diameters in the two soil conditions; images from left to right are unsaturated and saturated soil for 88.9 and 101.6 mm.

The process of pouring sand into the Perspex box involved depositing layers that were 100 mm thick each, starting from the top edge. This procedure encompassed eight individual layers, with the height of fall diminishing as each subsequent layer was added. The internal height of the sand, once poured, reached 770 mm. In Figure 3-25 (left), it's evident that the layers were not entirely level due to the dimensions of the model box and the pouring technique. To address this unevenness, a wooden tool was utilised to level each layer before proceeding to compact it and add the subsequent layer. This process was repeated for each of the eight layers. Furthermore, a specialised tool was utilised to compact and form dense sand beds after levelling, as depicted in Figure 3-25 (right). Just like the levelling tool, this specialised tool was utilised after each layer to ensure the desired compactness and structure of the sand bed. Due to equipment limitations, the soil density achieved was not able to be measured.

During the preparation of soil beds for saturated conditions, an additional step was undertaken. A submersible pore pressure sensor was embedded in the centre of the sand within the Perspex box. This placement was at an internal height of 165 mm, extending to 405 mm from the top of the sensor. This arrangement resulted in an approximate separation distance of 15 mm from the bottom of the pile, as shown in Figure 3-26. In order to achieve complete saturation of the soil, a total of 216 litres of water was poured in a downward seepage manner. This was accomplished by pouring 12 litres of water 18 times, which facilitated the gradual saturation process. To ensure consistency in both density and results, the soil beds were prepared three times. Once for displacement test in unsaturated conditions, once for force control in unsaturated and once for all of the saturated tests due to the more intricate nature of this setup.

To guarantee the adherence to the design calculation for achieving the desired pile-to-wall diameter ratio, meticulous measurements were taken before each installation. These measurements encompassed the distance between the pile and the inner wall of the Perspex box from all sides. These measurements were then logged for record-keeping and to ensure consistency throughout the testing process. Visual representations of this measurement process can be found in Figure 3-27. Table 3-10 provides a summary of the recorded distances between the pile and the inner wall of the box for a selection of experimental tests. All the data presented in the summary table were rounded up to the nearest whole number. Numbers below 0.5 were rounded to 0% while numbers above 0.5mwere rounded to 1%. During testing, the initial position for embedding the pile into the soil was set to approximately 1 mm above the soil surface, as depicted in Figure 3-28.

3.7 Experimental Investigation Procedures

The experimental campaign encompassed a total of 39 tests, which were categorised into eight sets (as detailed in Table 3-12). These sets were structured based on three distinct variables: pile diameter, extraction method, and soil conditions. Each individual consisted of two stages, corresponding to two out of the three life stages/cycles outlined in the project. These stages comprised installation and extraction. The decision to solely focus on installation and extraction was primarily driven by time constraints. The experimental campaign was designed to be time-dependent, and therefore, the operational cycle was excluded from the scope due to these limitations. This approach is aimed to streamline the testing process and optimise resource utilization. Further details about the rationale behind this focus can be found in Table 3-11.

Table 3-11 summarises the executed stages' aim in the experimental campaign tests.

	Testing no.	***Aim***
Installation	39	The process of displacing or embedding the piles was designed to replicate real-world condition as closely as possible. This was done with the intention of simulating scenarios that would be encountered in practical situations. For instance, by creating conditions that mimic a soil plug, the installation process aimed to replicate actual impacts of pile installation. This approach allowed researchers to determine how these installations influence the corresponding tensile tests, if there were any discernible effects.
Extraction	39	The primary objective of employing "static" extraction of the novel strategy theory's feasibility or, in other words, to validate its efficacy. This was achieved by using static extraction methods to define the behaviour of extraction and establish a baseline measurement for the tensile capacity of the pile. These baseline measurements would serve as standards against which dynamic methods could be compared.

Table 3-12 summarises the sets' variables of the experimental campaign.

Variables	***Parameters/ set no.***	***1***	***2***	***3***	***4***	***5***	***6***	***7***	***8***
Pile diameter	88.9mm	✓		✓		✓		✓	
	101.6mm		✓		✓		✓		✓
Extraction method	Force			✓	✓			✓	✓
	Displacement	✓	✓			✓	✓		
Soil conditions	Unsaturated	✓	✓	✓	✓				
	Saturated					✓	✓	✓	✓

The installation process for embedding the piles to the desired depth of 350mm was carried out using a static displacement method known as "jacking". In contrast, two different static methods were employed for extraction phase: displacement control and force control, each with varying rates and velocities. In the displacement-control method, the name itself explains the approach. This displacement is incrementally altered, resulting in a corresponding force requirement, commonly referred to as the reaction force. This reaction force is directly linked to the specific displacement value. On the other hand, the force-control method, also known as load-control, involves incremental changes in the applied load. This can be achieved using various load forms, such as stress, pressure, or concentrated force. In the case of this experiment, the force-control method utilised the concentration force form, the resulting displacement is dependent on the load. By employing these methods, the study sought to understand how the incremental changes in displacement and force influenced the installation and extraction processes.

Across all the conducted tests, the consistent installation displacement velocity employed was 50 mm/min; maintained in a continuous manner. It's important to note that the experimental campaign predominately emphasises the extraction phase. Additionally, this velocity selection was driven by the aim to maintain consistency with other researchers' methodologies, such as the conducted by [4].

The extraction displacement velocity ranged between 5 to 100 mm/min, and the extraction rate by force-control ranged between 50 to 200 N/min. These ranges were chosen to balance thorough testing with practical time constraints. The goal was to ensure that both installation and extraction phases, as well as preparation for subsequent tests, could be managed effectively. These ranges were defined following a trial test with installation at 50 mm/min and extraction at 25 mm/min, which took a total of 21 minutes – 7 minutes for installation and 14 minutes for extraction. The longest test duration observed was 77 minutes, involving installation over 7 minutes and extraction spanning 70 minutes using displacement velocities of 50 and 5 mm/min for installation and extraction, respectively.

After estimating the total duration of tests through a trial run, additional tests in Table 3-14, primarily the initial ones, were conducted in multiple sets. The intention behind this approach was to ensure repeatability and consistency across various aspects, such as the setup and results. Table 3-13 shows the total count of tests conducted within each set. Repeatability tests were specifically carried out for two variables and were limited to unsaturated soil conditions. This

exclusion of saturated soil was due to its complex nature. Meanwhile, the consistent results obtained from the analysis of test data in sets 1 to 4 indicated confidence in achieving compatible and reliable outcomes for testing sets 5 to 8. It should be noted that set 1 encompassed the largest number of tests, six in total, three of each for 25 and 50 mm/min.

Table 3-13 depicts the number of tests carried out for each set.

	Set no.							
	1	2	3	4	5	6	7	8
Test no.	8	5	5	5	4	4	4	4

Throughout the entirety of the experimental campaign, both stages in all tests were subjected to a monotonic loading approach. This involved applying a continuous and constant velocity or rate without any waiting periods. This process began with a compression stage and then transitioned to the uplift tension stage. It's important to highlight that despite the capability of the testing apparatus to conduct and store each stage's data separately, a cyclic test option was chosen for the experiments. The rationale behind this decision was to ensure consistency in the testing process while eliminating potential human interference. By opting for the cyclic test approach, the need for precise timing during stage switches and concerns regarding data loss were addressed. This approach proved advantageous by effectively streamlining the testing process and enhancing data reliability, resulting in 78 sets of data being acquired instead of the initial 39.

The concept of cyclic loading tests involved the sequential application, removal, and subsequent reapplication of loads. To ensure accurate execution, it was ensured that each test represented a complete cycle. This entailed the test starting from 0 mm displacement, then proceeding to 350 mm for compression, followed by 350 mm back to 0 mm for tension. The test cycle then automatically terminated. In between the stages of compression and tension, there was a specified waiting period where no applied loads were present. This waiting time differed for saturated and unsaturated tests, set at 1 minute and 20 minutes, respectively.

Table 3-14 exhibits extraction repeatability tests in sets one to four.

Test code	***Ext. velocity [mm/min]***	***Ext. rate [N/min]***
D.E-MS-U-03	50	-
D.E-MS-U-04	50	-
D.E-LS-U-01	25	-
D.E-LS-U-03	25	-
F.E-MS-U-01	-	50
F.E-MS-U-02	-	50
F.E-LS-U-01	-	50
F.E-LS-U-02	-	50

Given the intricacies arising from the multitude of variables, parameters, and testing sets within the experimental campaign, a simplified notation system was adopted to label each aspect for ease of reference. To provide clarity and maintain consistency, certain conventions were established:

- Installation and Extraction Tests: Installation tests were marked with the prefix "I," and extraction tests with the prefix "E."
- Extraction Methods: Differentiated extraction methods were denoted as "D.E" for displacement control and "F.E" for force control.
- Soil Conditions: Unsaturated and saturated soil conditions were represented as "U" and "S," respectively.
- Pile Diameters: Pile diameters were referred to according to the notation provided in section 3-16.

For clarification, the notation "F.E-LS-U-01" refers to a force-control extraction test involving a large-steel pile in unsaturated soil, accompanied by an experiment number within a specific test set. Table 3-15 summarises all the conducted tests.

Table 3-15 shows the record of experiments.

Parameter						
Experiment Ref.	Pile Dia.	Ext. Vel/rate	Ext. app.	Soil cond.	Set No.	Test No.
D.E-MS-U-01: 25	88.9mm	25 mm/min	Displacement control	Unsaturated	1	1
D.E-MS-U-02: 25		25 mm/min				2
D.E-MS-U-03: 50		50 mm/min				3
D.E-MS-U-04: 50		50 mm/min				4
D.E-MS-U-05: 50		50 mm/min				5
D.E-MS-U-06: 5		5 mm/min				6
D.E-MS-U-07: 25		25 mm/min				7
D.E-MS-U-08: 100		100 mm/min				8
D.E-LS-U-01: 25	101.6mm	25 mm/min			2	1
D.E-LS-U-02: 50		50 mm/min				2
D.E-LS-U-03: 50		50 mm/min				3
D.E-LS-U-04: 5		5 mm/min				4
D.E-LS-U-05: 100		100 mm/min				5
F.E-MS-U-01: 50	88.9mm	50 N/min	Force control		3	1
F.E-MS-U-02 :50		50 N/min				2
F.E-MS-U-03: 100		100 N/min				3
F.E-MS-U-04: 150		150 N/min				4
F.E-MS-U-05: 200		200 N/min				5
F.E-LS-U-01: 50	101.6mm	50 N/min			4	1
F.E-LS-U-02: 50		50 N/min				2
F.E-LS-U-03: 100		100 N/min				3
F.E-LS-U-04: 150		150 N/min				4
F.E-LS-U-05: 200		200 N/min				5
D.E-MS-S-01: 5	88.9mm	5 mm/min	Displacement control	Saturated	5	1
D.E-MS-S-02: 25		25 mm/min				2
D.E-MS-S-03: 50		50 mm/min				3
D.E-MS-S-04: 100		100 mm/min				4
D.E-LS-S-01: 5	101.6mm	5 mm/min			6	1
D.E-LS-S-02: 25		25 mm/min				2
D.E-LS-S-03: 50		50 mm/min				3
D.E-LS-S-04: 100		100 mm/min				4
F.E-MS-S-01: 50	88.9 mm	50 N/min	Force control		7	1
F.E-MS-S-02: 100		100 N/min				2

Parameter						
Experiment Ref.	Pile Dia.	Ext. Vel/rate	Ext. app.	Soil cond.	Set No.	Test No.
F.E-MS-S-03: 150	101.6mm	150 N/min			8	3
F.E-MS-S-04: 200		200 N/min				4
F.E-LS-S-01: 50		50 N/min				1
F.E-LS-S-02: 100		100 N/min				2
F.E-LS-S-03: 150		150 N/min				3
F.E-LS-S-04: 200		200 N/min				4

During the course of the experimental campaign, human errors were encountered in two distinct forms. The first instance involved the loss of data for the D.E-MS-S-02 test conducted at a velocity of 25 mm/min test. Unfortunately, this data was inadvertently overridden by the data from the D.E-MS-S01 test performed at 5 mm/min. Consequently, the test data did for D.E-MS-S-02 was not included in the subsequent analysis of results due to data loss. The second form of human error was related to a delay in capturing pore pressure data during the installation phase of the D.E-LS-S-02 test conducted at velocity of 25 mm/min. This delay occurred because the external power supply for the transducer was off during this period. However, it is important to note that the pore pressure data was fully recorded during the extraction phase of the test. This occurred as the transducer was turned on approximately 4.03 minutes after the commencement of the installation phase.

3.8 Experimental Investigation Results

3.8.1 Pile Installation

During the entirety of the installation processes in unsaturated soil conditions, close observation revealed densification of the sand. However, the phenomenon of dilation was not observed. This absence of dilation could potentially be attributed to the effective boundary condition provided by the Perspex box. Both piles, regardless of their diameters, were effectively coring a soil column with a height approximately equivalent to the depth of penetration. Given the nature of the experimental setup, as depicted in Figure 3-29, measuring the soil column formed inside the pile during and after the installation process proved to be a challenge. This limitation hindered the ability to calculate the increment filling ratio (IFR).

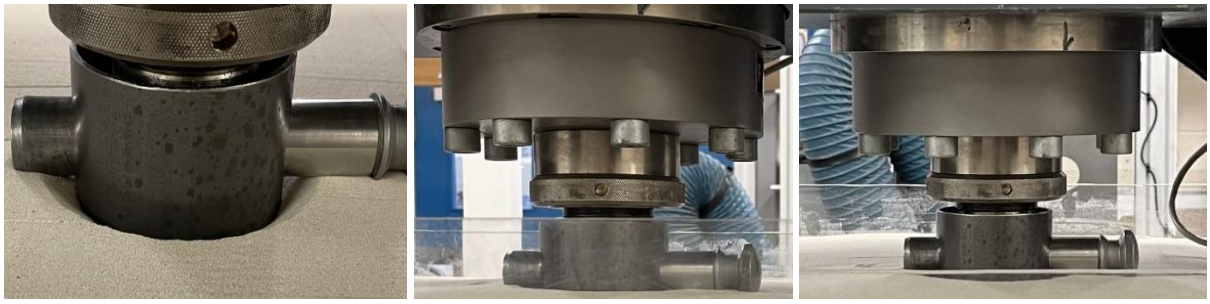

Figure 3-29. A close-up view of the distance tightness between the pile and machine load cell for accessing and measuring the developed soil column during and after the embedment.

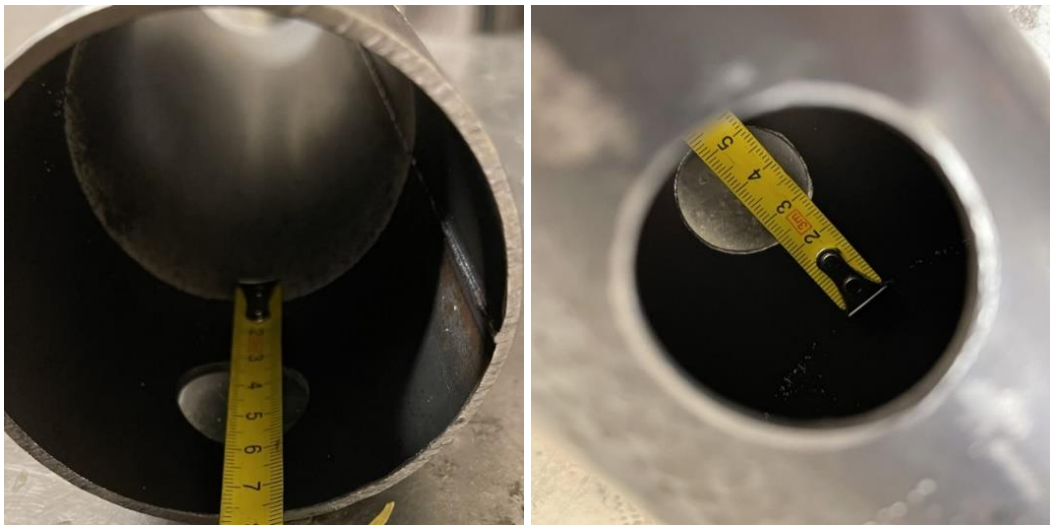

Figure 3-30. The height of the soil column resulting from the 88.9 mm pile installation in the unsaturated soil.

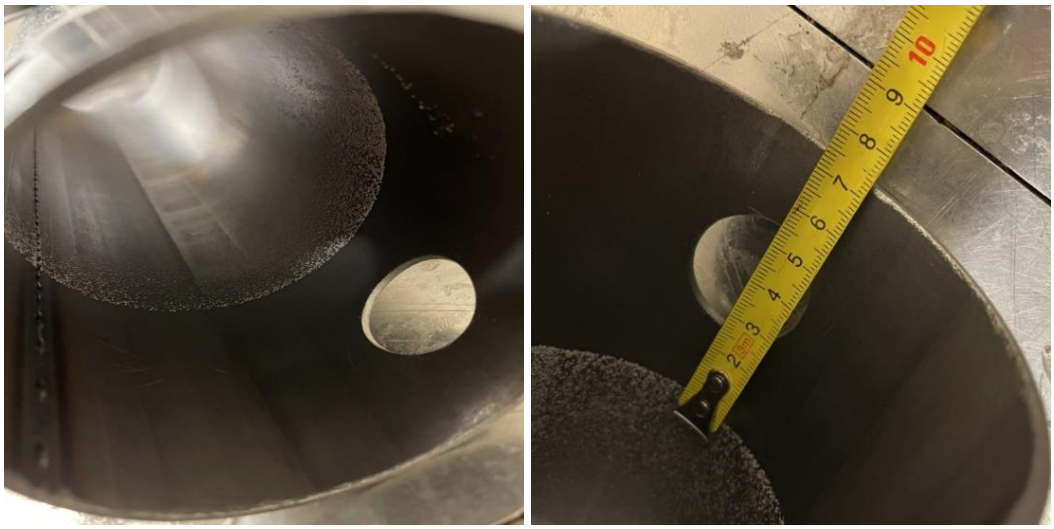

Figure 3-31. The soil column height developed inside the 101.6 mm pile in the unsaturated soil during installation.

Instead, the height of the soil column developed inside the pile was approximately measured after the completion of extraction and detachment of the pile from the testing machine, as shown in Figure 3-30 and Figure 3-31. However, it's worth noting that utilising a hammer had a drawback when attempting to remove the pin from the component holes and eventual

disconnection. Regardless of factors such as embedment duration, relative soil density, and pile surface roughness, hammering had the effect of erasing the remaining indications of the soil column height level within the pile. Although efforts were made to account for the impact of hammering, this phenomenon was observed in the majority of the pile disconnection instances, as evident in the left image of Figure 3-30.

The height of the soil plug within both pile diameters was equal, as depicted in Figure 3-30 and Figure 3-31, measuring at 325 mm above the tips of the piles. This height corresponded to a penetration length ratio (PLR) of 0.93. When measured from the top end of the piles, which was the adopted measurement approach, the height of the soil plug was found to be 25 mm lower than the actual penetration depth. This discrepancy is evident in the left image of Figure 3-30. Despite the advancement of the soil plug to this particular height, it did not align perfectly with the penetration depth. Consequently, both piles' diameters were considered as being partially plugged. This observation highlights the complexities of accurately measuring and assessing the soil plug formation within the piles and the importance of considering various measurement points and methods to capture the most comprehensive understanding of the phenomena.

Despite the suggestions made by [159] that the incremental filling Ratio (IFR) could be estimated from the Penetration Length Ratio (PLR), this approach was not adopted in the current study. The decision was based on the fact that the experiment was conducted at a model scale, which introduces the possibility of either underestimating or overestimating the actual IFR value due to scale effects. The study conducted by [4] supports the concern of potential estimation errors in a model-scale context. In their research, the observed final length of the soil plug above the pile tip was 220 mm and 249 mm, corresponding to PLR values of 0.55 and 0.62, respectively. The calculated IFR based on their results was 58% and 60%. However, when using the equation proposed by [159] to estimate the Incremental Filling Ratio (IFR), the calculated values were 37.95% and 48.85%. These estimations resulted in error percentages of 34.57% and 18.35% for the two cases.

In addition to the variability estimations, the outcomes of the model test conducted by [159] demonstrated a linear increase of IFR with PLR. However, considering the unique context of a model-scale experiment, the present study opted to use PLR as a defining factor for understanding the development of the final plug length, instead of relying on the IFR. The findings, when compared to other experiments conducted at different scales, revealed a

contradiction in terms of the PLR and the factors that govern the process. For instance, the research by [4] presented a PLR of 0.55 in loose sand and 0.62 in dense sand. They concluded that the dominant factor influencing the final plug length was the continuous jacking installation method without any suspension. This conclusion was drawn into their study involving a pile with an outside diameter of 60.33 mm and a wall thickness of 3 mm. Interestingly, the results of the current study indicated a different scenario. Despite maintaining consistent pile wall thicknesses, the controlling factor influencing the measured final plug length was found to be the pile diameter itself, surpassing the influence of the installation method (jacking) and the relative density of the soil.

Figure 3-32. The hammering effect on the soil column developed in 88.9 [left] and [right] 101.6 mm piles in saturated soil.

In the context of saturated soil conditions, as depicted in Figure 3-32, the evidence of the developed soil column length within the 88.9 mm and 101.6 mm piles became scattered following the hammering and disconnection process. As a result, the accurate measurement of the plug length ratio was hindered due to resulting uncertainty. As a result of this uncertainty, the determination of the plug length ratio could not be included in the analysis within this study.

3.8.2 Validating The Experimental Investigation Results

To establish the repeatability, consistency, and overall reliability and validity of the results of the experimental campaign's results, a series of eight tests were conducted. These results focused on two key variables: pile diameter and extraction method. Specifically, four tests were performed for each parameter in unsaturated soil conditions. However, testing in saturated soil was excluded from the subset of tests due to factors such as time limitations, among others.

Tests were systematically conducted for each combination of variable parameters in a consecutive manner. However, it's important to note that there was an exception with regards to the displacement extraction for the 101.6 mm pile due to a human error, which has been acknowledged, presented, and further analysed hereinafter. Among the variables, the extraction method was given prominence due to its central role in the setup and execution of the experimental campaign, as outlined in Sections 3.5 and 3.6. Nevertheless, for the sake of simplicity, the results have been organised based on the pile diameter variable. The figures, specifically Figure 3-33 and Figure 3-34, depict the outcomes for pile diameters of 88.9 mm and 101.6 mm, respectively. It's important to clarify that the results presented in this section and in subsequent sections illustrate the net tensile load, which has been obtained by subtracting the piles' self-weights from the measured extraction load.

All the testing was initiated at the outset of each testing set (Sets 1 to 4), ensuring that the extraction velocity or rate remained lower or equal to the installation velocity of 50 mm/min. This precaution was taken to prevent any potential influence of higher velocities or rates on the tensile capacity of the piles, irrespective of the extraction method, as illustrated in the preceding sections. After meticulous consideration of parameters that could lead to variations in results, even if only slight, such as the method of pile installation into the soil, a decision was made. Utilising pile displacement as an installation method has a compaction effect on the soil, which in turn affects the piles' tensile capacity. Achieving a consistent soil density by discharging and re-preparing the soil bed for each test was challenging due to the scale of the experiment. Hence, the point of pile failure displacement, or the displacement at which the pile failed, was chosen as the parameter to validate the repeatability and consistency of the experimental campaign's results. This decision was guided by the expectation that under constant extraction velocity or rate, the pile should fail at the same displacement. Any deviations that could occur due to the aforementioned parameters would likely be minimal to non-existent.

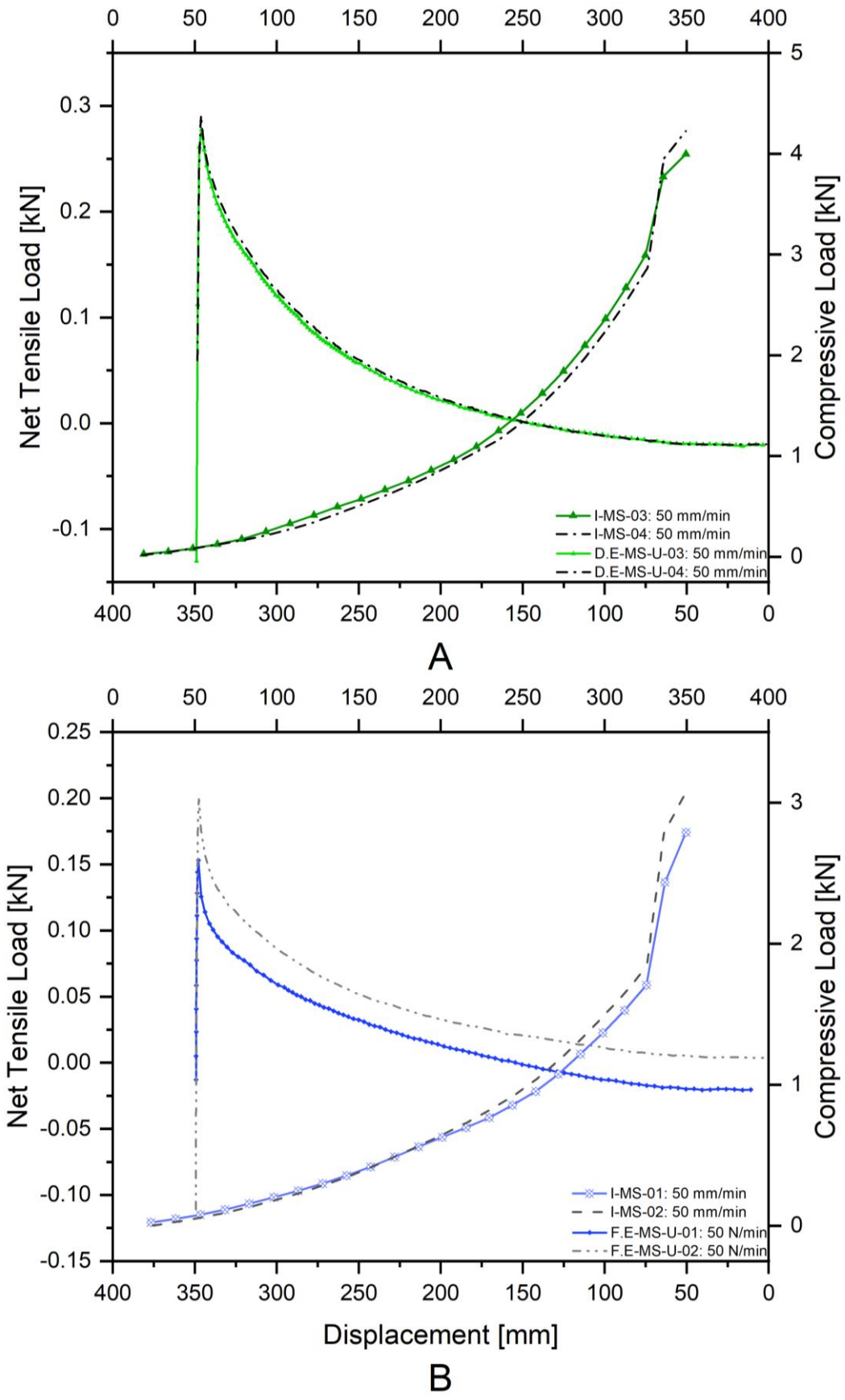

Figure 3-33. Load-displacement curves for the extracting 88.9 mm pile showing failure displacement consistency in testing extraction applications; [A] displacement and [B] force.

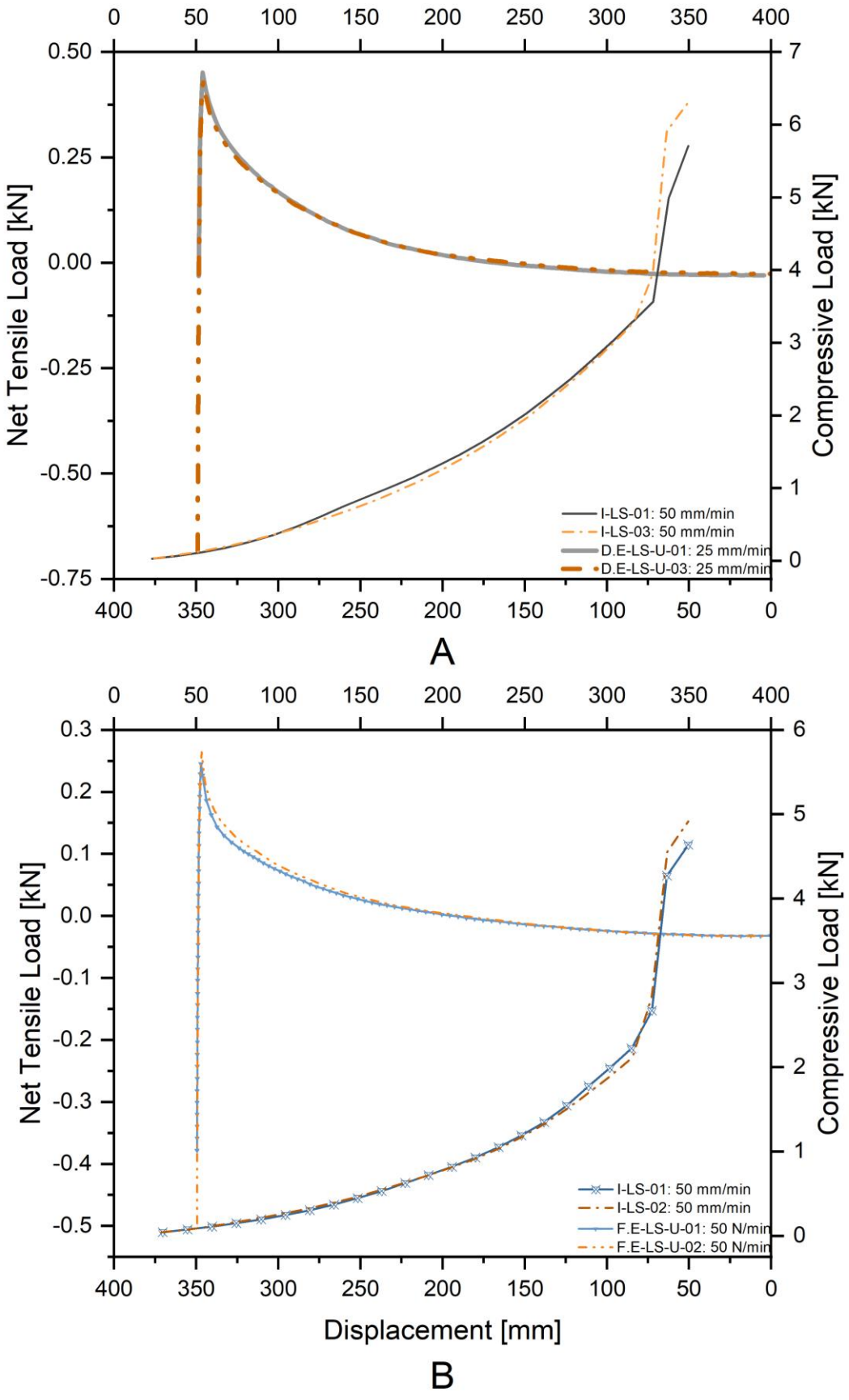

Figure 3-34. Load-displacement curves for the extracting 101.6 mm pile showing failure displacement consistency in testing extraction applications; [A] displacement and [B] force.

In the case of displacement extraction application, a slight increase in the tensile capacity of the 88.9 mm pile was observed. The capacity increased around 4% (3.6%) between tests D.E-MS-U-03 (0.28 kN) and D.E-MS-U-04 (0.29kN), as shown in Figure 3-33 A. This increase corresponds to a change in failure displacement from 345.9 mm to 346.4 mm, indicating a different of only 0.14%. Similarly, for the 101.6 mm pile, as depicted in Figure 3-34 A, the failure displacement was approximately 345.7 mm, in the D.E-LS-U-03 test, yielding a peak tensile capacity of 0.43 kN. This represented a decrease of about 4% in capacity compared to the D.E-LS-U-01 test, where the pile failed at 346.2 mm with a capacity of 0.45 kN. The difference in failure displacements between these two tests was also minimal, only 0.14%.

In the case of force extraction application testing, for the 88.9 mm pile, the failures in tests F.E-MS-U-01 and F.E-MS-U-02 occurred at displacements of 347.9 mm and 347.6 mm, respectively, signifying a very small 0.09% difference. The tensile capacity of the pile increased by a significant 26.6%, with capacities of 0.15 kN and 0.19 kN for the two tests as illustrated in Figure 3-33 B. Hypothetically, the difference in tensile capacity of the pile (26.6%) could result from the pile being stuck during the extraction. For the 101.6 mm pile in force extraction testing, the failure displacements were 347.1 mm and 346.7 mm in tests F.E-LS-U-01 and F.E-LS-U-02, respectively, with a 0.12% difference. The tensile capacity increased by 4%, resulting in capacities of 0.25 kN and 0.26 kN for the two tests, as illustrated in Figure 3-34 B.

In conclusion, the tests conducted on 88.9 mm and 101.6 mm piles using both displacement and force extraction applications showed consistent patterns in terms of failure displacement and change in tensile capacity. Under displacement extraction application, the difference in failure displacement was consistent at 0.14% and the change in tensile capacity was 4% for both pile diameters. On the other hand, for force extraction, while the change in tensile capacity varied between 4% and 26.6% for the two pile diameters, the difference in failure displacement remained relatively consistent at 0.09% and 0.12%. The high repeatability, consistency, and reliability observed in the tests conducted in unsaturated soil provide confidence in the validity of the results obtained from saturated soil testing. It should noted that it was challenging to conduct finite element analysis to understand the engineering of the decommissioning process in detail due to time limitations.

3.8.3 Tension Versus Compression

The debate regarding whether capacity of piles under tensile and compressive loads is equal or lower has been a subject of study by researchers. [162] applied plasticity theory to compute the pull-out force for shallow footings in ocean sediment and found it to be the same as the push (compression) force. In the context of free-draining soils like sand, [182] demonstrated that the tensile shaft capacity of driven piles is significantly lower than the compressive capacity. Analytically, this variation is attributed to factors such as dimensionless forms effects, Poisson's ratio, the ratio of tensile-to-compressive shaft capacity (which is influenced by slenderness and pile stiffness ratios (E_p/G_{avg} [26])), and changes in the total stress field due to loading direction. [183] conducted a comparative study of axial capacities for nine jacket platforms in the North Sea. The piles used in these platforms had varying diameters and embedment depths, ranging from 0.66 m to 2.13 m and 26 m to 87 m, respectively. Regardless of the method used for analysis (API and ICP methods), the tensile capacities were consistently lower than the compressive capacities, ranging from 14 to 100MN. [4] made a preliminary estimation that the extraction force required for piles studied by [183] could reach up to 70MN. This suggests that the tensile capacity of piles is generally lower than their compressive capacity, a finding that aligns with previous research and analytical models.

Since data was captured during the two processes, a comparison was carried out, notwithstanding it being outside the scope of the project. A few reasons for this were: to establish a benchmark against which future testing could be compared; for instance, installing piles dynamically and/or applying operational loads before extraction, with endless possible scenarios.

From each of the eight sets, results of one test were adopted, with four results for each soil condition. For ease of comparison, the results from testing the two extraction methods for each pile diameter in the same soil condition were combined into a single figure. Due to the number of variables, the selection of the results was based on the extraction velocity or rate as a baseline with a velocity of 50 mm/min for displacement and 50 N/min for force extraction applications, respectively. One reason for this choice was that other parameters, such as soil density, change with each installation process regardless of its condition. Selecting 50 mm/min as the extraction velocity ensured a consistent rate of impact on both the compressive and tensile capacities of

[26] G_{avg} is athe verage shear modulus over the depth range, and $E_P$is pile elastic modulus.

the piles during installation and extraction. On the other hand, the choice of 50 N/min for the force application was because it was the lowest extraction rate. Results in Figure 3-35 showed that in the tested soil conditions, the force required to extract the pile was lower than that needed for its installation.

1. In unsaturated soil:
    a. For the 88.9 mm pile (as shown in Figure 3-35 A):
        i. The tensile capacities were 0.3 kN (or approximately 0.29 kN) and 0.2 kN when extracted using displacement and force control applications, respectively.
        ii. This is approximately 92.8% (or 4.2 kN) less and 93.5% (or 3.1 kN) less of the compression capacities, respectively.
    b. For the 101.6 mm pile (as shown in Figure 3-35 B):
        i. The tensile capacities were 0.42 kN and 0.26 kN when extracted using displacement and force control applications, respectively.
        ii. These values are 92.9% (or approximately 5.9 kN less) and 94.7% (or approximately 4.9 kN less) of the compression capacities for each method, respectively.
2. In saturated soil:
    a. For the 88.9 mm pile with repeated compression capacities of 3.59 kN from two different sets (6 and 8), as illustrated in Figure 3-35 C:
        i. The tensile capacity saw a decrease of 96.7% (or 0.12 kN) for both force and displacement extraction methods.
        ii. Using the displacement extraction method, the reduction was 94.9% (or 0.18 kN).
    b. For the 101.6 mm pile (as presented in Figure 3-35 D):
        i. The tensile capacities decreased by 96.5% and 97% (resulting in 0.22 kN and 0.17 kN, respectively) for the displacement and force extraction methods.
        ii. These reductions are in comparison to the compression capacities of 6.1 kN and 5.7 kN for the respective methods.

This suggests that the observed reduction in the tensile capacities of piles, relative to their compressive capacities, might be attributed to the lack of operational loads and the duration of embedment.

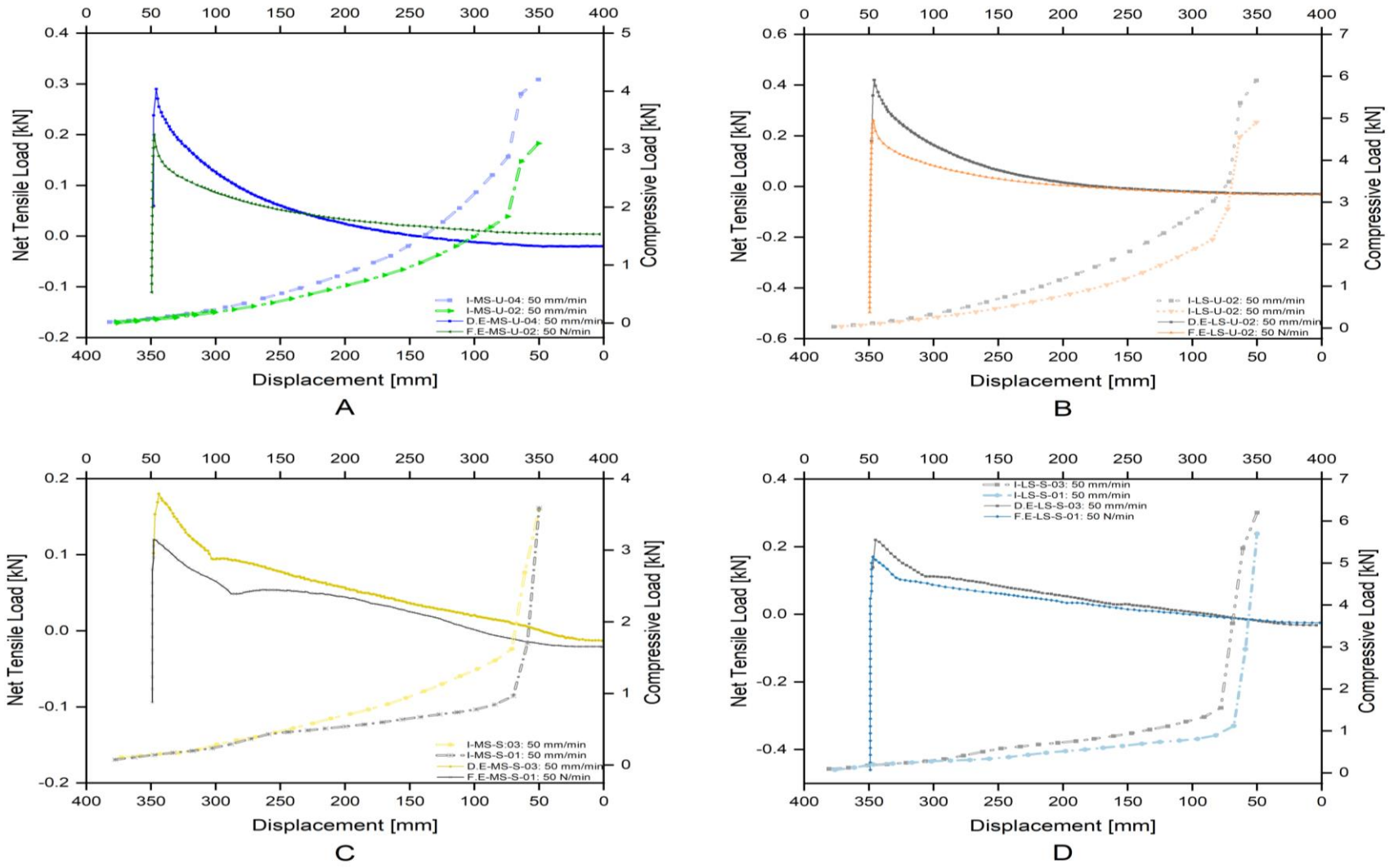

Figure 3-35. Load-displacement curves for installing and extraction of the tested piles' diameters in two soil conditions; A [88.9 mm] and B [101.6 mm] in unsaturated, and C [88.9 mm] and D [101.6 mm] in saturated.

3.8.4 Extraction in Unsaturated Soil

In the unsaturated condition, 13 tests were conducted using the displacement extraction application: 8 for the 88.9 mm pile (set 1) and 5 for the 101.6 mm pile (set 2). Both pile diameters were subjected to extraction velocities of 5 mm/min (lowest), 25 mm/min, 50 mm/min and 100 mm/min (highest). The load-displacement curves for the 88.9 mm and 101.6 mm piles can be found in Figure 3-36 and Figure 3-39, respectively. The data in Figure 3-36 and Figure 3-39 are further divided into separate graphs, each highlighting the effects of specific influencing factors, such as soil density and extraction velocity, on tensile capacity.

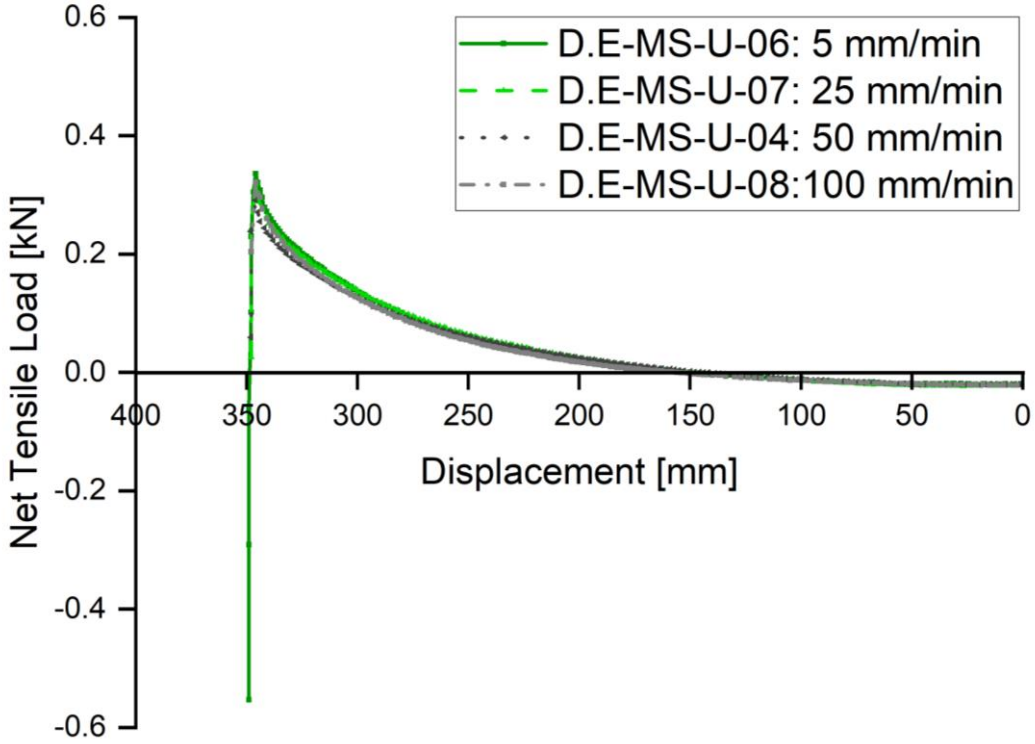

Figure 3-36. The load-displacement curve of displacement-extracting application testings for the 88.9mm pile in unsaturated soil.

The soil was observed to undergo slight densification during each installation and throughout the displacement extraction tests. This densification, as previously mentioned, is attributed to the method used for pile installation, specifically the static displacement method of jacking. It's essential to understand that soil densification is gauged by the measured compressive capacity; higher soil density correlates with higher capacity. For the 88.9 mm pile set, the compressive peak capacity varied from 3.51 kN (test 1) to 5.67 kN (test 8). In contrast, for the 101.6 mm pile set, it ranged from 5.71 kN (test 1) to 6.57 kN (test 5).

Results from Figure 3-37 illustrate the significant role soil densification plays in the tensile capacity of piles across various diameters. Delving deeper into this, we can consider tests D.E-MS-U-04 (with extraction velocity of 50 mm/min) and D.E-MS-U-07 (25 mm/min) for the 88.9 mm pile. Here, the compression capacities were 4.23 kN and 4.74 kN, respectively, marking a 12% increase. Notably, despite a reduction in extraction velocity of 25 mm/min, the pile's tensile capacity in terms of peak load still rose by approximately 8.8% (rounded to 9%).

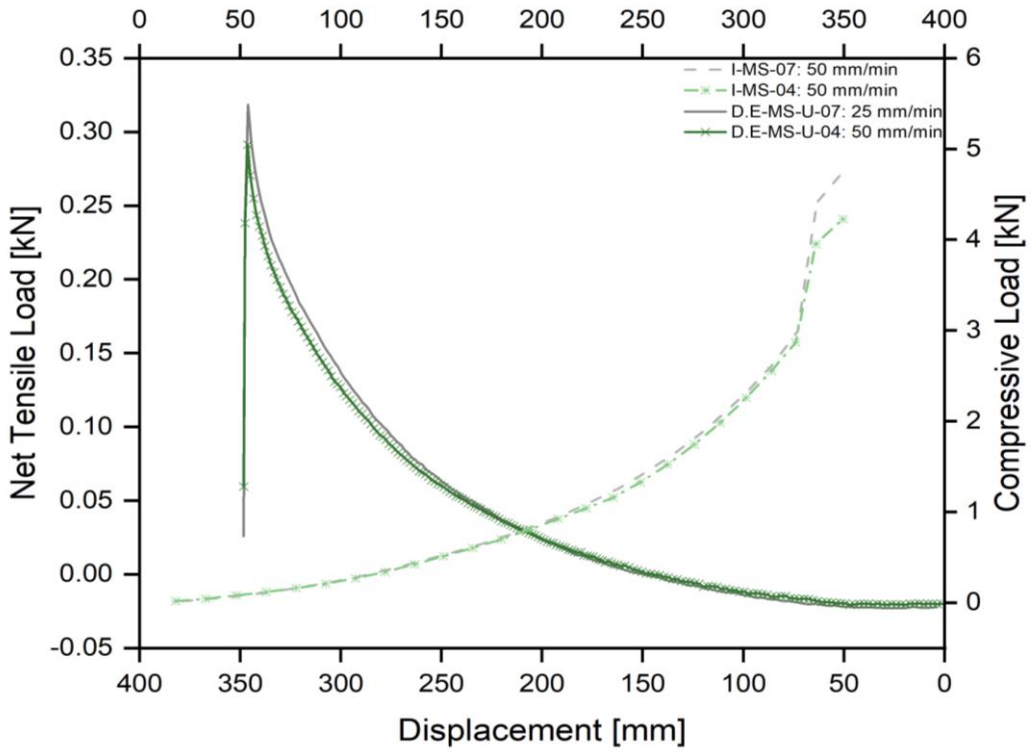

Figure 3-37 presents the load-displacement response to the impact of soil densification on the rate of extracting the 88.9 mm pile in unsaturated soil.

From the results pertaining to the 88.9 mm pile, determing the effect of the extraction rate on the tensile capacity proved difficult due to the broad spectrum of peak compression load values. For instance, the compression values from tests D.E-MS-U-07 (at 25 mm/min) and D.E-MS-U-08 (at 100 mm/min) stood at 4.74 kN and 5.67 kN, respectively. Even with this 20% increment increase in compression, the tensile capacity remained remarkably consistent - as presented in Figure 3-38, with 0.319 kN and 0.322 kN, respectively. This consistency might suggest that tensile capacity diminishes or plateaus upon, or after, reaching a specific velocity, especially at higher speeds like 100 mm/min. The credability of this hypothesis would be reinforced if a similar pattern is observed during the 101.6 mm pile tests.

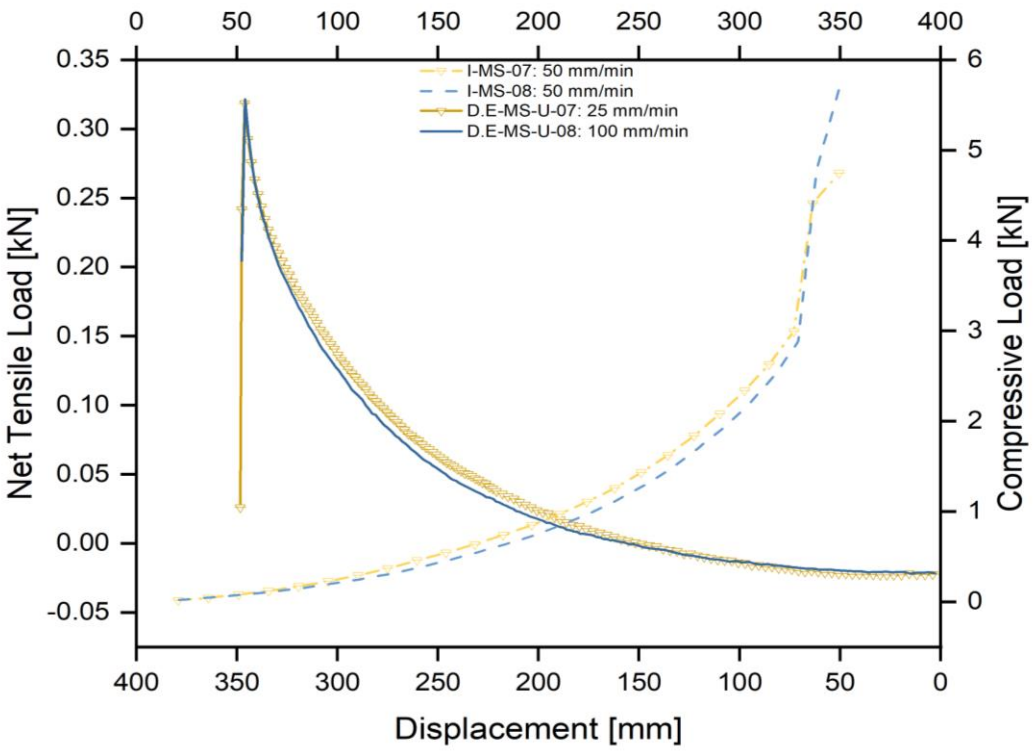

Figure 3-38. The load-displacement response for the impact of extracting the 88.9 mm pile with a higher velocity than 50 mm/min on the tensile capacity in the unsaturated soil.

Results from the 101.6mm pile tests, specifically D.E-LS-U-03 (25 mm/min) and D.E-LS-U-04 (5 mm/min), affirmed the influence of soil density on tensile capacity, albeit from a unqiue perspective. The peak compression capacities for these tests remained consistent at6.39 kN and 6.3 kN. However, a variation in tensile capacities was observed, with peak loads of 0.429 kN and 0.366 kN, respectively. This divergence underscores the direct relationship between the extraction rate on the pile's tensile capacity. Notably, the sequence indicated by the test notation reveals that the 5 mm/min test followed the 25 mm/min test.

In essence, while the experimental results confirmed the impact of soil density, they also highlighted the extraction rate as distinct factor influencing the tensile capacity, especially evident in the 101.6 mm pile tests. An analysis of these tests, as presented in Figure 3-40, revealed that the pile's tensile capacity decreased by 15% when a lower extraction velocity of 5 mm/min was applied under a consistent soil density.

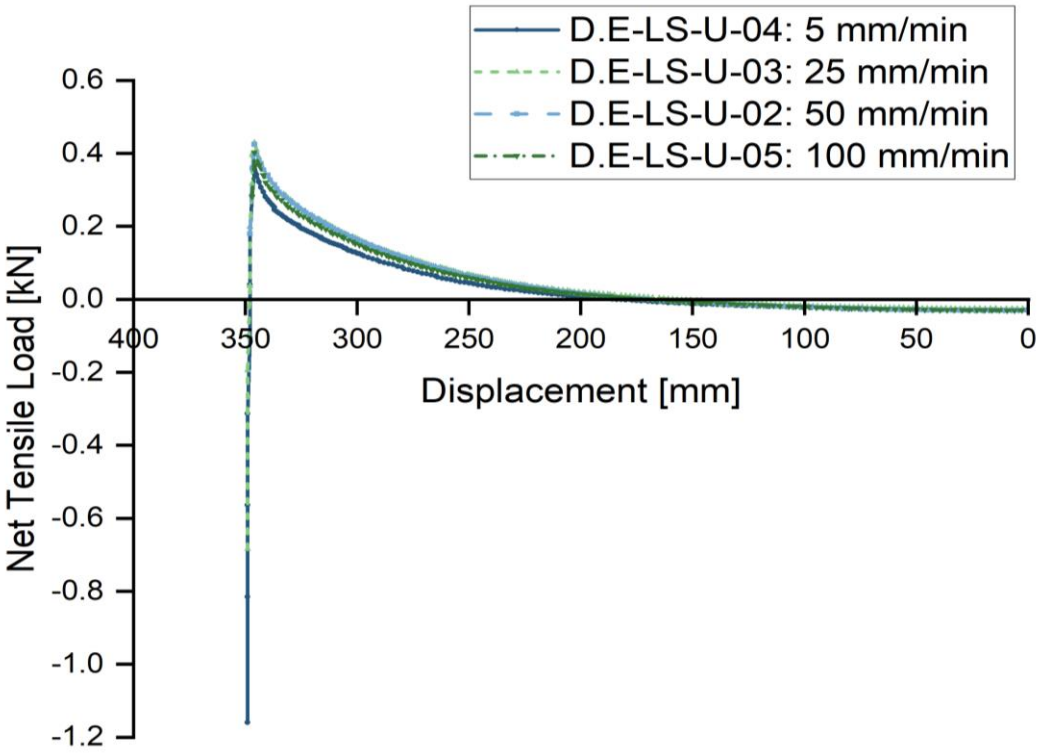

Figure 3-39. The load-displacement curve of each applied velocity to extract the 101.6 mm pile in unsaturated soil.

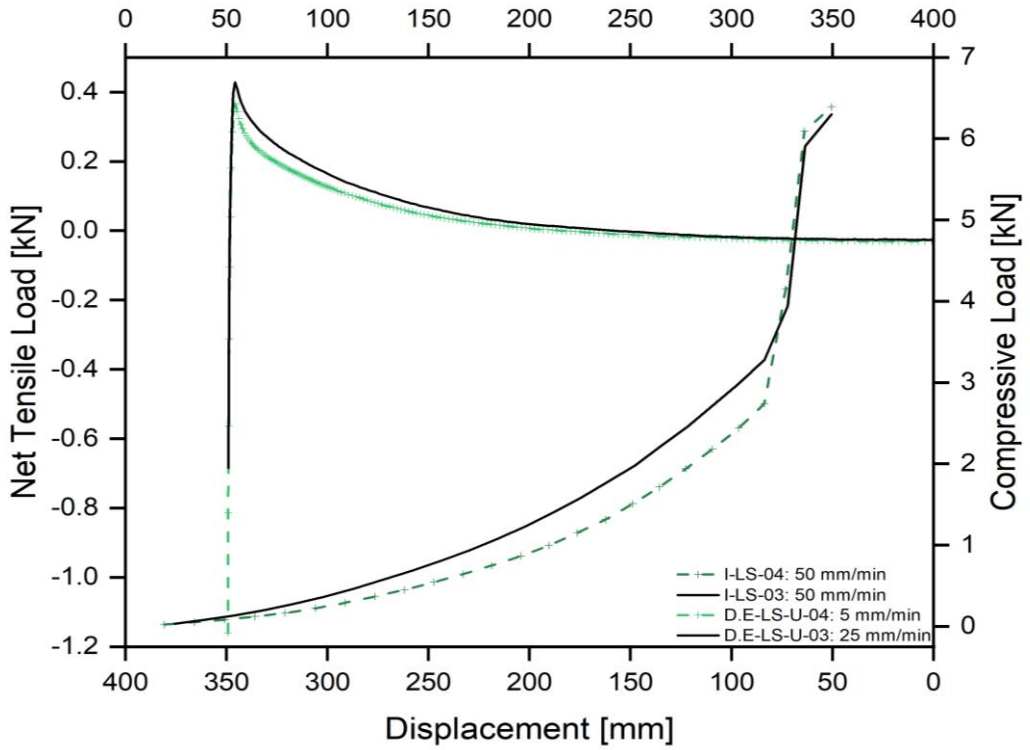

Figure 3-40. The load-displacement response to different rates of extracting the 101.6 mm pile in unsaturated soil with constant density.

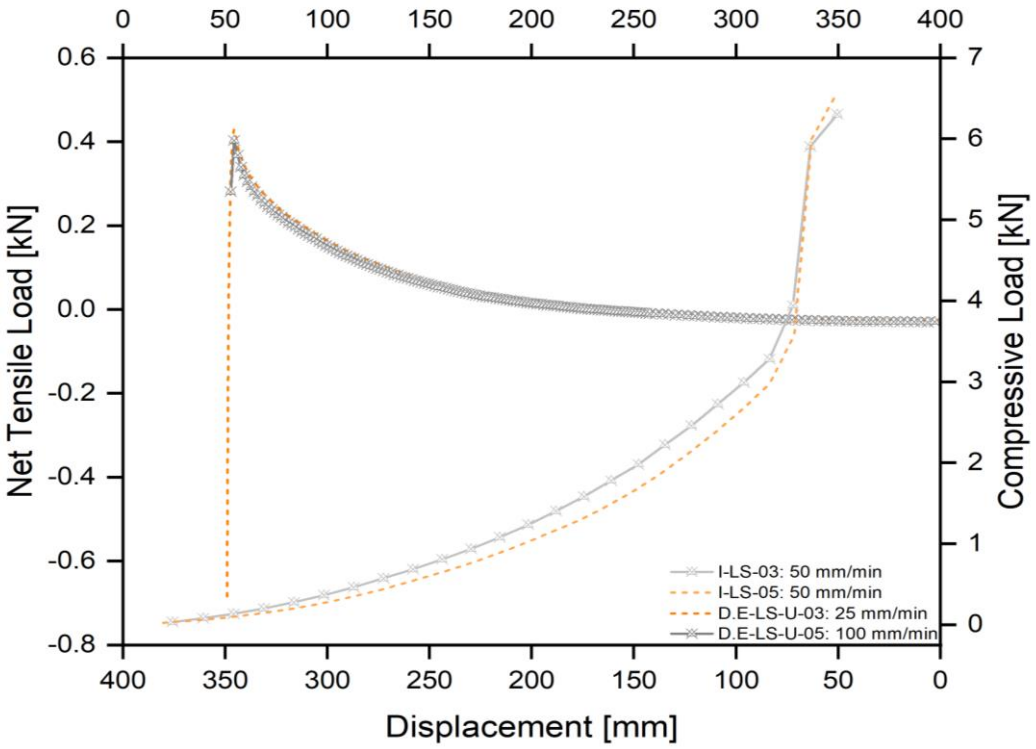

Figure 3-41. The response of the load-displacement curve when applying high displacement velocity, 100 mm/min, for 101.6 mm pile extraction in unsaturated soil.

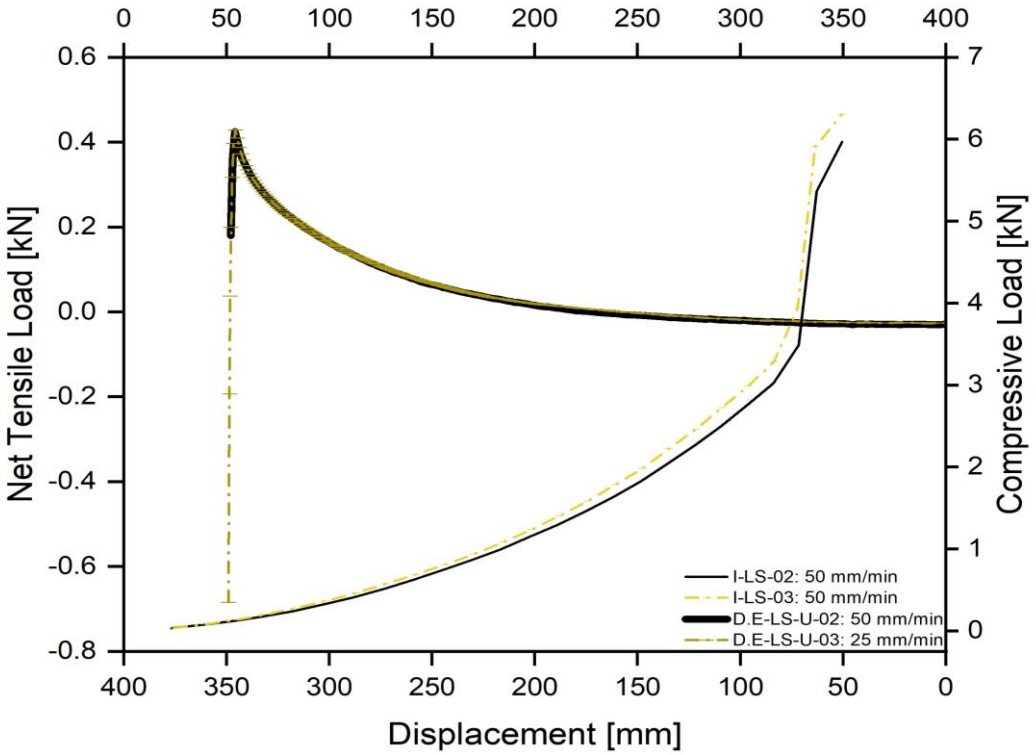

Figure 3-42 The load-displacement response for the impact of increasing the extraction rate on the tensile capacity of the 101.6 mm pile in unsaturated soil with lower density.

To verify the hypothesis drawn from 88.9 mm pile results – that the tensile capacity declines upon surpassing a particular extraction rate – the 101.6 mm pile tests for D.E-LS-U-03 (25 mm/min) and D.E-LS-U-05 (100 mm/min) were examined, as presented in Figure 3-41. The compression peak capacities were 6.3 kN and 6.57 kN for the 25 mm/min and 100 mm/min tests, respectively. While there was a 4% increase in compression, the tensile capacity of the 101.6 mm pile decreased by approximately (6.9%) (from 0.43 kN to 0.4 kN) at the 100 mm/min rate. This consistency in the 100 mm/min results across both pile diameters offers robust validation of the initial hypothesis.

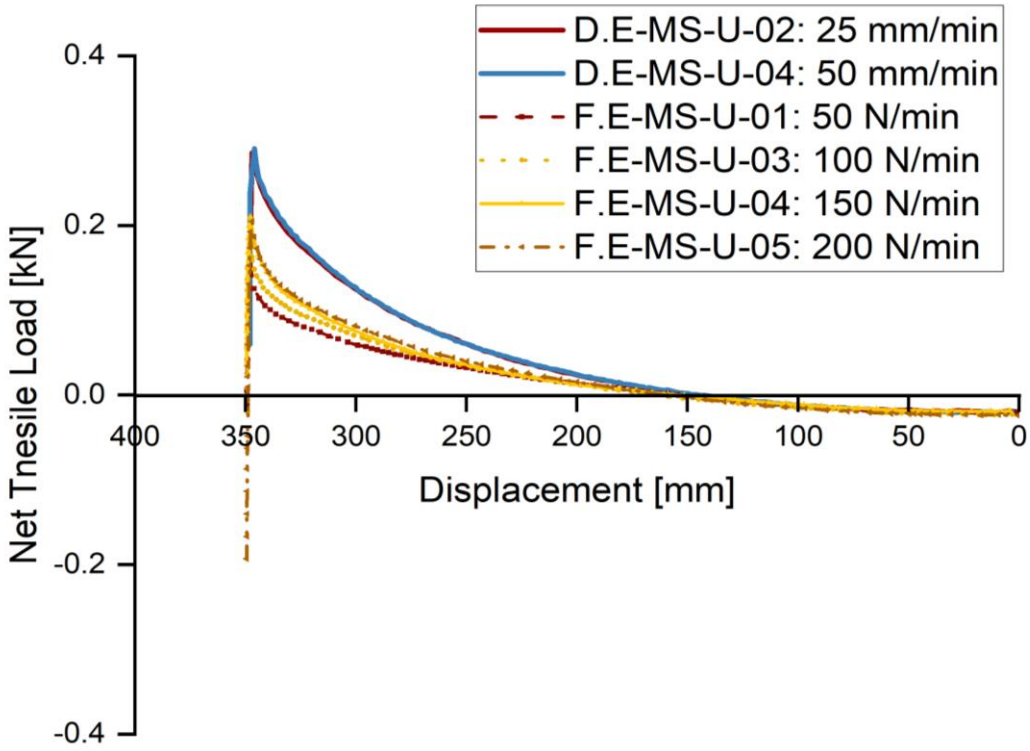

Figure 3-43. The load-displacement curves of the applied forces for extracting the 88.9 mm pile in unsaturated soil; two curves from displacement extraction tests had used for comparison.

The tests on the 101.6 mm pile, specifically D.E-LS-U-02 (50 mm/min) and D.E-LS-U-03 (25 mm/min), further endorsed by the proposed hypothesis, especially concerning the impacts of extraction rates under 100 mm/mn, albeit from a unique perspective. With an extraction velocity of 50 mm/min, the compressive and tensile capacities for the 101.6 mm pile stood at approximately 5.9kN and 0.42 kN, respectively, as given in Figure 3-42. These capacities were lower than those observed at a 25 mm/min velocity (6.3 kN and 0.43 kN) by margins of 5% and 2% respectively. Interestingly, despite the presence of a reduced soil density, the tensile capacity increased with the extraction rate, a finding which stands in contrast to the outcomes observed at 100 mm/min velocity.

Upon completing the displacement extraction tests in unsaturated soil, testing shifted focus to the force extraction application, this involved a total of 10 tests, with 5 tests designated for each pile diameter: set 3 (88.9 mm) and set 4 (101.6 mm). It's worth highlighting that before beginning the force extraction tests, the soil was removed and then freshly prepared as detailed in section 3.6. This procedure was adopted to reestablish the soil beds to the same density level as they were at the onset of the displacement extraction tests.

This process had dual objectives:

1. To compare the results of both extraction applications. In this regard, Figure 3-43 and Figure 3-44 showcase the load-displacement curves for the applied forces rates. These figures also incorporate two to three reference curves from the displacement extraction sets 1 and 2.
2. To ensure repeatability and maintain the consistency of soil preparation, with the resulting soil density gauged via its compressive capacity. Throughout the force extraction tests, the applied rates ranged from the lowest at 50 N/min to the highest at 200 N/min, also including intermediate rates of 100 and 150 N/min.

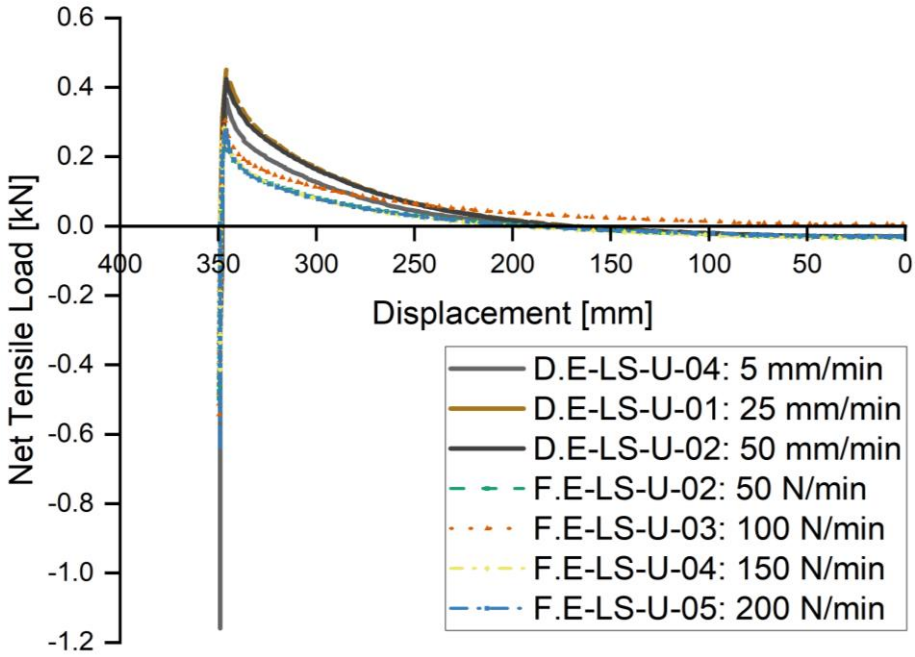

Figure 3-44. The load-displacement curves resulting from the applied rates to extract the 101.6 mm pile in unsaturated soil; for comparison, three curves were adopted for displacement extraction testing.

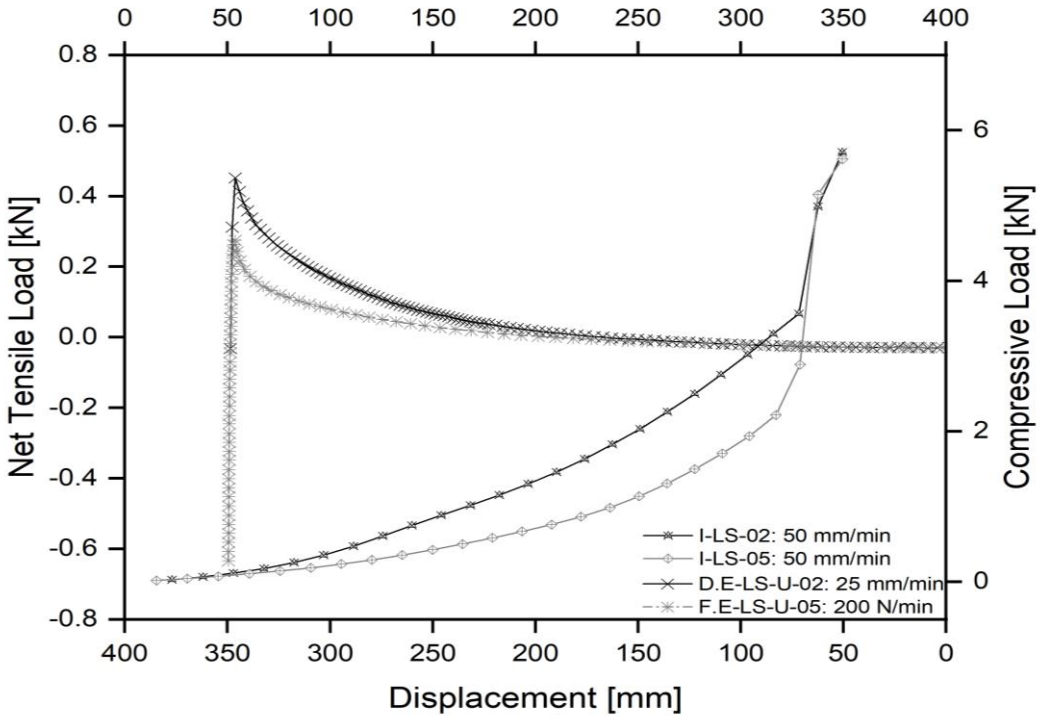

Figure 3-45. The peak tensile capacity of the 101.6 mm pile resulting from the employed force and displacement extraction applications in unsaturated soil.

- For the 88.9 mm pile, the peak load (compressive capcity) saw a significant decrease in set 3 compared to set 1 -observation the data is not presented within the research project.
- Test 1: A 15.3% reduction was observed. In set 1, the value was 3.51 kN/min, while it decreased to 2.97 kN/min in set 3.
- Test 2: An even greater decline was witnessed at 18.4%. The values for sets 1 and 3 were 3.76 and 3.07 kN/min, respectively.
- The 101.6 mm pile also exhibited a decline in compressive capacity.
- Test 1: The most significant drop of 18.7% was noticed, comparing values from set 2 (5.71 kN/min) to set 4 (4.64 kN/min)
- Notably, the highest reduction observed for the 88.9 mm pile (in test 2, set 3) was in line with the percentage reduction in the 101.6 mm pile.

The observed reduction prompted the selection of one test from each application. The primary criterion for this selection was a similar compressive capacity. This was done to validate whether the tensile capacities of piles under force extraction application, irrespective of their diameters, were influenced more by soil density or the applied extraction method. Using this criterion, the tests chosen were D.E-LS-U-02 (25 mm/min) and F.E-LS-U-05 (200 N/min) from

the 101.6 mm pile testing sets 2 and 4. These had compression capacities of 5.71 kN and 5.61 kN, respectively, showing a 1.75% (rounded to 2%) reduction. As depicted in Figure 3-45, the peak tensile capacity under force extraction (0.3044 kN) was significantly lower than that under displacement extraction (0.4812 kN), show a reduction of 37.5% (rounded to 38%). This indicates that the extraction method, specifically the force extraction application, played a predominant role in the decrease of the pile's tensile capacity, rather than any diminution in soil density.

The Influence of soil density on tensile capacity was prominently observed during the force extraction testing. This was especially evident when maintaining a consistent extraction rate of 50 N/min across two consecutive tests – specifically, tests 1 and 2 in both sets sets 3 and 4. This approach differed from previously mentioned methods. Referencing set 4 for the 101.6 mm pile, specifically F.E-LS-U-01 (50 N/min) and F.E-LS-U-02 (50 N/min), which are depicted in Figure 3-46, there was a notable increase. The peak compressive and tensile capacities of the pile in test 2 rose by 6% and 5%, respectively. Meanwhile, the 88.9 mm pile displayhed a significant increase in tensile capacity of 27% (rising from 0.1731 kN to 0.2193 kN) in contrast to a modest 3% increase in compressive capacity (shifting from 2.97 kN to 3.07 kN).

The significant difference observed might be attributed to the 88.9 mm pile becoming lodged during extraction. Such a rationale is plausible given that it experienced the highest increase among the trials with greater rates. For instance, the tensile capacity of the 88.9 mm pile stood at 0.199 kN under a 100 N/min rate, and this escalated to 0.2298 kN at a 150 N/min rate – a boost of roughly 15.47%. It's crucial to highlight that this 15% rise also incorporates the influence of densification, given that the compressive capacity surged by 9%.

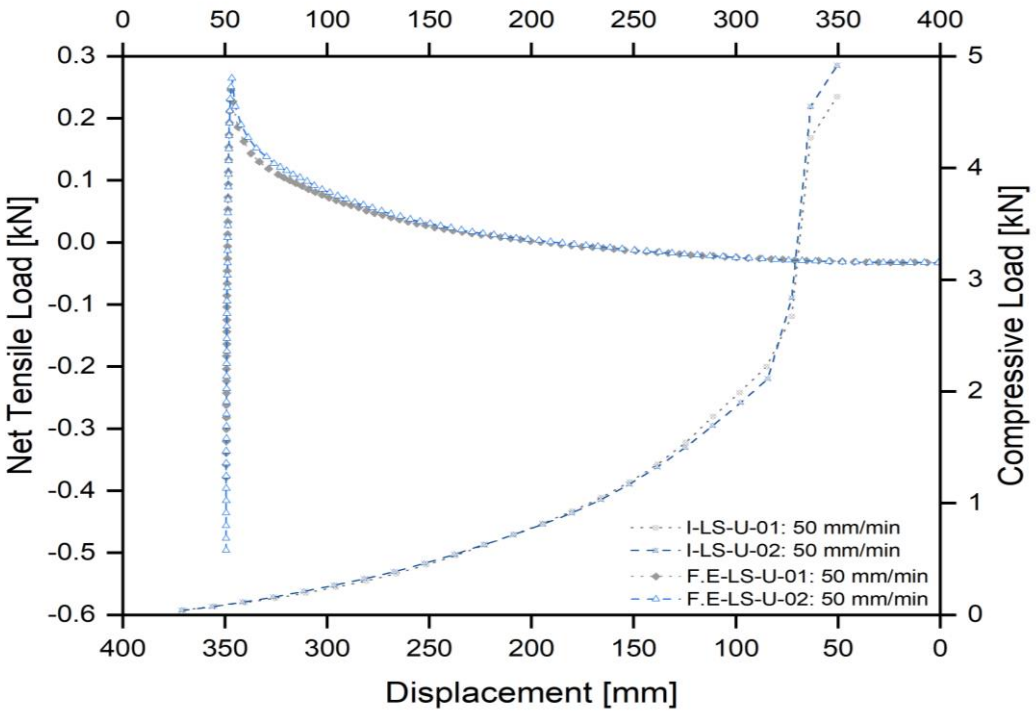

Figure 3-46. The load-displacement response to the influence of soil densification on the 101.6 mm pile's tensile capacity with a constant extraction force rate.

The ongoing densification of the soil during force extraction testing, was evident by the increasing compressive capacity with each test. This trend limited the potential for comparing the impacts of various extraction rates on tensile capacity under a consistent soil density. Notably, even with the continuous densification, the tensile capacities of both pile diameters either decreased or remained relatively stable after surpassing specific rates, mirroring trends observed in displacement extraction testing. For the 88.9 mm pile, as depicted in Figure 3-47, a decline was observed when applying rates higher than 150 N/min. Specifically, under the 200 N/min, the peak tensile capacity (0.2289 kN) decreased by 2% compared to the 150 N/min rate (0.2298 kN). In contrast, for the 101.6 mm pile, showcased in Figure 3-48, the reduction became evident following the 100 N/min rate (0.3342 kN). The tensile capacity dipped by 6.7% (to 0.3116 kN) at 150 N/min and by 8.9% (to 0.3044 kN) at 200 N/min. Importantly, the reduction percentage in tensile capacity, when increasing the rate from 150 to 200 N/min, remained consistent at 2% for both pile diameters.

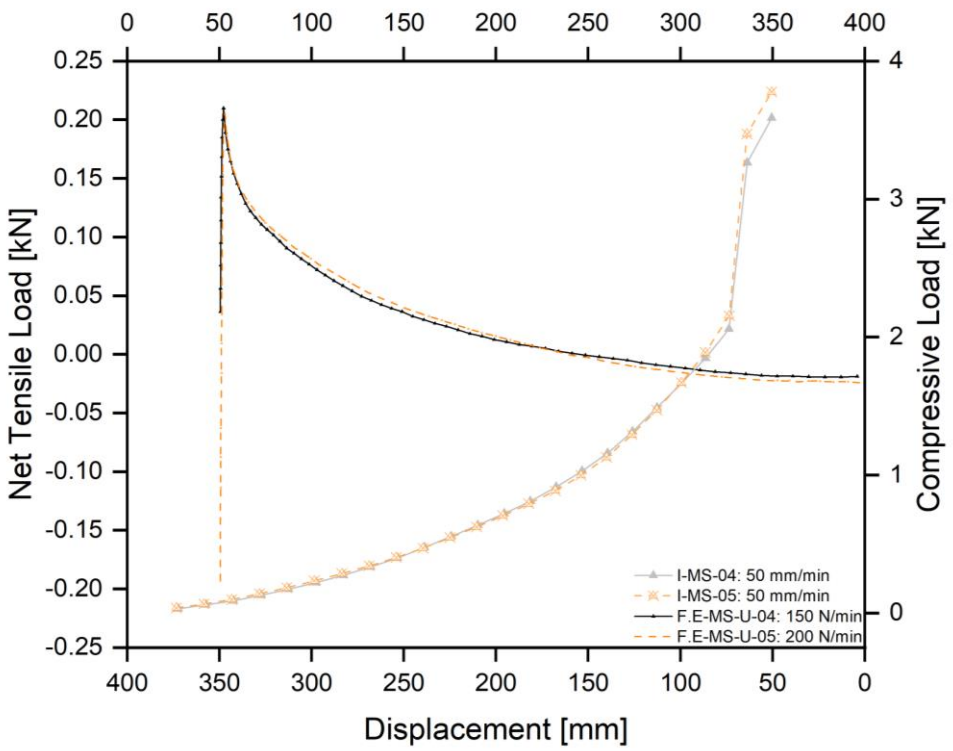

Figure 3-47. The response of the load-displacement curves at and after exceeding a specific force rate, 150 N/min, for 88.9 mm pile extraction in unsaturated soil.

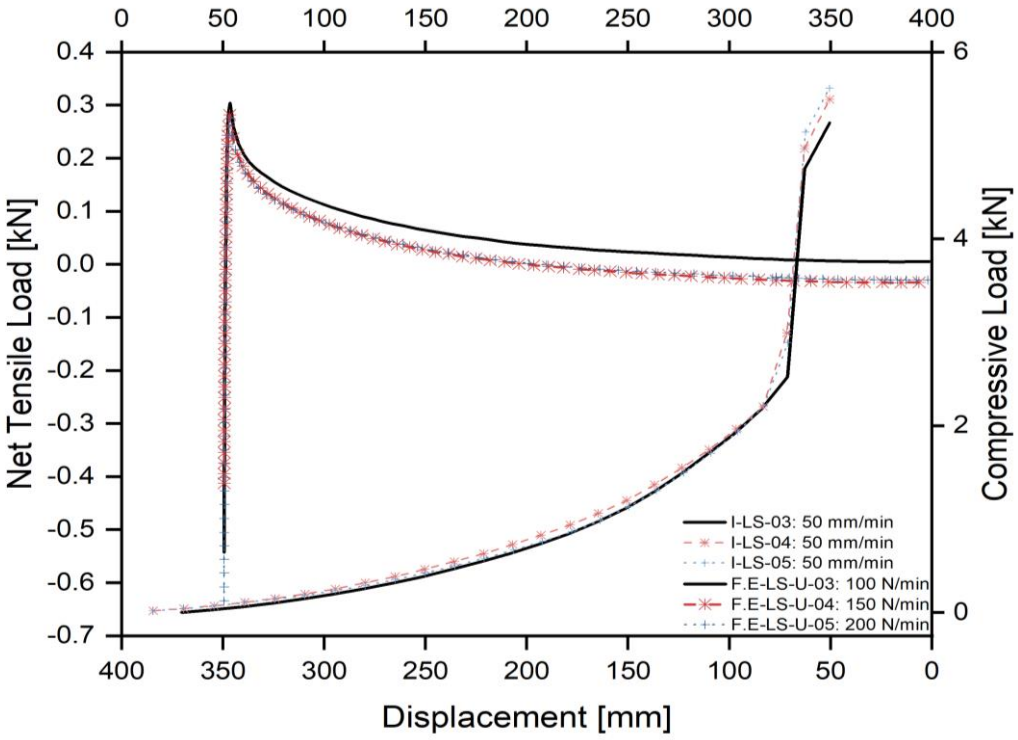

Figure 3-48. The effect of force-extracting rates at and surpassing 100 N/min on the tensile capacity of a 101.6 mm pile in unsaturated soil.

Compared to the reference curves from displacement extraction application testing, illustrated in Figure 3-43 and Figure 3-44, the tensile capacity of both pile diameters showed a significant reduction under the force extraction application. Using the D.E-MS-U-02 at velocity of 25 mm/min (0.3058 kN) as a reference curve, the tensile capacity of the 88.9 mm pile decreased by a range of 25% (lowest) to 43% (highest), irrespective of soil density. For the 101.6 mm pile, referencing the D.E-LS-U-04 at a velocity of 5 mm/min (0.396 kN) curve, the decline ranged from 23% (lowest) to 26% (highest). It's important to note that the results of tests in unsaturated soil provide an upper limit for extraction forces necessary in saturated soil, which will be discussed in the following section.

From the results for the testing sets in unsaturated soil, it can be concluded that the pile installation method influences soil density, typically resulting in an increase. This change in soil density can potentially mask the impact of different extraction rates. However, when soil density is held constant, the influence of the extraction rate on the pile's tensile capacity becomes much clearer. Therefore, to delve deeper into the effect of extraction rate – for example, to identify the optimal extraction rate - it's imperative to maintain a consistent soil density throughout all tests.

The results demonstrate that the method of extraction has a profound impact on the pile's tensile capacity, irrespective of the pile's diameter. The displacement extraction application consistently yielded a higher tensile capacity compared to the force extraction method. This disparity might stem from the inherent mechanisms of each extraction method. Independent of the application or pile diameter, it's evident that the pile's tensile capacity diminishes at or beyond a particular rate.

3.8.5 Extraction in Saturated Soil

In the saturated soil, a total of eight tests were conducted – four for each pile diameter of 88.9 mm (set 5) and 101.6 mm pile (set 6). This number is five tests fewer than in unsaturated conditions due to time constraints. The aim of testing in saturated soil was to examine the role of pore water pressure on extraction force and to study the influence of extraction applications mechanisms (particularly total energy, including velocity/ rate and time) on pore water pressure, which will be elaborated upon in the subsequent sections. For consistency, the extraction velocities used for both pile diameters in displacement control mirrored those in unsaturated conditions, ranging from a minimum of 5 mm/min to a maximum of 100 mm/min.

The load-displacement curves for the 88.9 mm and 101.6 mm pile diameters extracted at various displacement velocities are displayed in Figure 3-49 and Figure 3-51, respectively. The analysis strategy for the saturated soil test results paralleled that used for the unsaturated conditions. The results showcased in Figure 3-49 and Figure 3-51 were further dissected into separate figures, each representing the impact of individual factors on tensile capacity.

The presence of water complicated the behaviour of the soil. Under the displacement extraction application, the soil continued to densify with each installation process, just as observed in unsaturated conditions. For the 88.9 mm pile (set 5), the compressive peak capacity ranged from 2.53 kN to 4.12 kN, while for the 101.6 mm pile (set 6), it ranged from 4.83 kN to 6.22 kN. Conversely, in the testing sets for the force extraction application, the soil did not densify. Instead, it deformed. Efforts were made to restore the soil to its pre-extraction condition after each extraction process to achieve a consistent or nearly consistent density. For the 88.9 mm pile (set 7) and 101.6 mm pile (set 8), the compressive peak capacities were 3.59, 4.34, 3.3 and 5.09 kN for the former, and 5.74, 6.77, 5.06 and 4.42 kN for the latter, respectively.

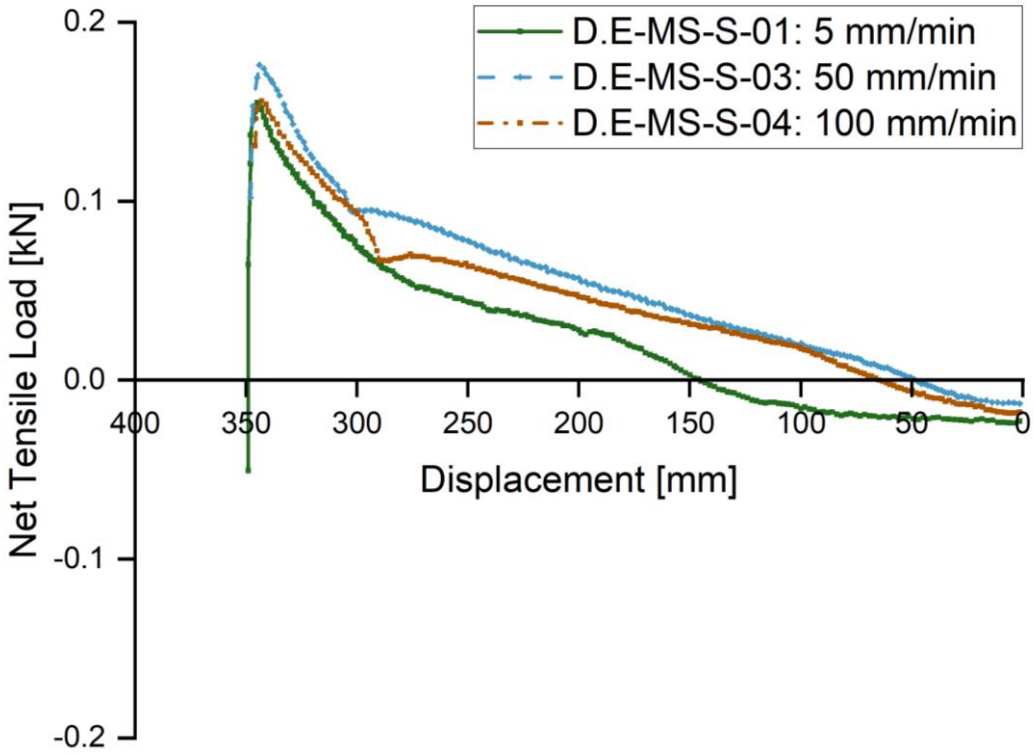

Figure 3-49. The load-displacement response for extracting the 88.9mm pile diameter in saturated soil by applying various displacement velocities.

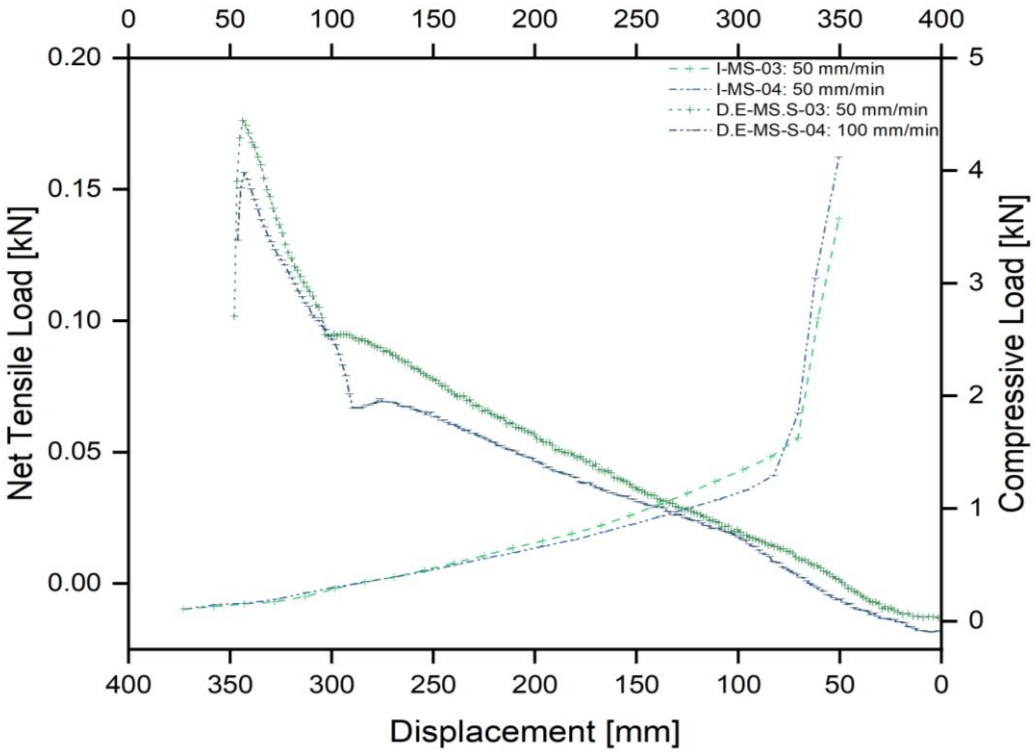

Figure 3-50. The response of the load-displacement curves for extracting the 88.9 mm pile with 50 mm/min or higher displacement.

Soil densification during displacement extraction testing posed challenges in clearly discerning the influence of extraction velocity on tensile capacity, mirroring observations in unsaturated conditions. Nonetheless, the influence was still evident. In the D.E-MS-S-04 at a velocity of 100 mm/min test for the 88.9 mm pile, the compressive capacity reached 4.12 kN, marking a 15.4% increase from the D.E-MS-S-03 at velocity of 50 mm/min test's capacity of 3.57 kN. Accompanying this increase, as depicted in Figure 3-50, the tensile peak capacity for the 88.9 mm pile at a velocity of 100 mm/min (0.1764 kN) saw a 10% reduction compared to the 50 mm/min velocity (0.1961 kN). A similar trend was noted for the 101.6 mm pile, albeit with variations. The recorded compressive capacities for D.E-LS-S-03 at a velocity of 50 mm/min and D.E-LS-S-04 at a velocity of 100 mm/min were relatively stable at 6.22 kN and 6.11 kN, respectively, reflecting a minor increase of 1.76%. At the 100 mm/min extraction velocity, the tensile capacity of the 101.6 mm pile, as given in Figure 3-52, stood at 0.2178 kN, marking a 13.94 % reduction from the 50 mm/min velocity (0.2531 kN). These results, specifically for D.E-MS-S-04 at velocity 100 mm/min and D.E-LS-S-04 at velocity 100 mm/min tests, align with findings from the tests D.E-MS-U-08 at velocity 100 mm/min (for 88.9 mm) and D.E-LS-U-05 at velocity 100 mm/min (for 101.6 mm) tests in unsaturated conditions. This validates the assumption that tensile capacity decreases upon reaching or surpassing a certain extraction rate, even in the presence of ongoing soil densification. In summary, when the extraction

velocity is capped at 50 mm/min, the tensile capacities of both pile diameters generally rise and as the pile diameter increases, so does the tensile capacity.

Results in Figure 3-53 showed that the presence of pore water pressure decreased the extraction force and tensile capacity for both pile diameters, in comparison with tests conducted in unsaturated soil. This is because the pore water pressure bore a significant part of the extraction load. To corroborate this reduction, nearly constant compressive capacities were utilised for the two types of soil, regardless of the extraction velocity. For tests conducted in unsaturated soil, compressives capacities for D.E-MS-U-01: 25 mm/min (from set 1) and D.E-LS-U-03:25 mm/min (from set 2) tests were adopted. The peak compressive capacities recorded were 3.51 kN for the 88.9 mm pile (D.E-MS-U-01: 25 mm/min) and 6.33 kN (D.E-LS-U-03: 25 mm/min) for the 101.6 mm pile, respectively.

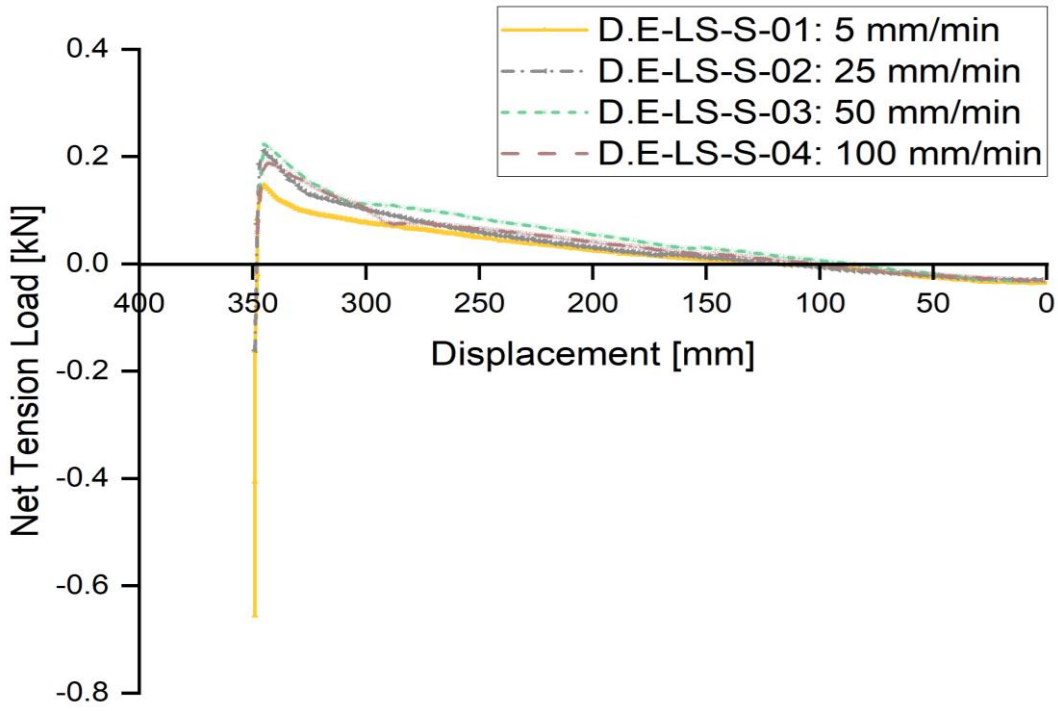

Figure 3-51. The load-displacement response for 101.6mm pile diameter extraction tests in saturated soil employing the displacement-control method.

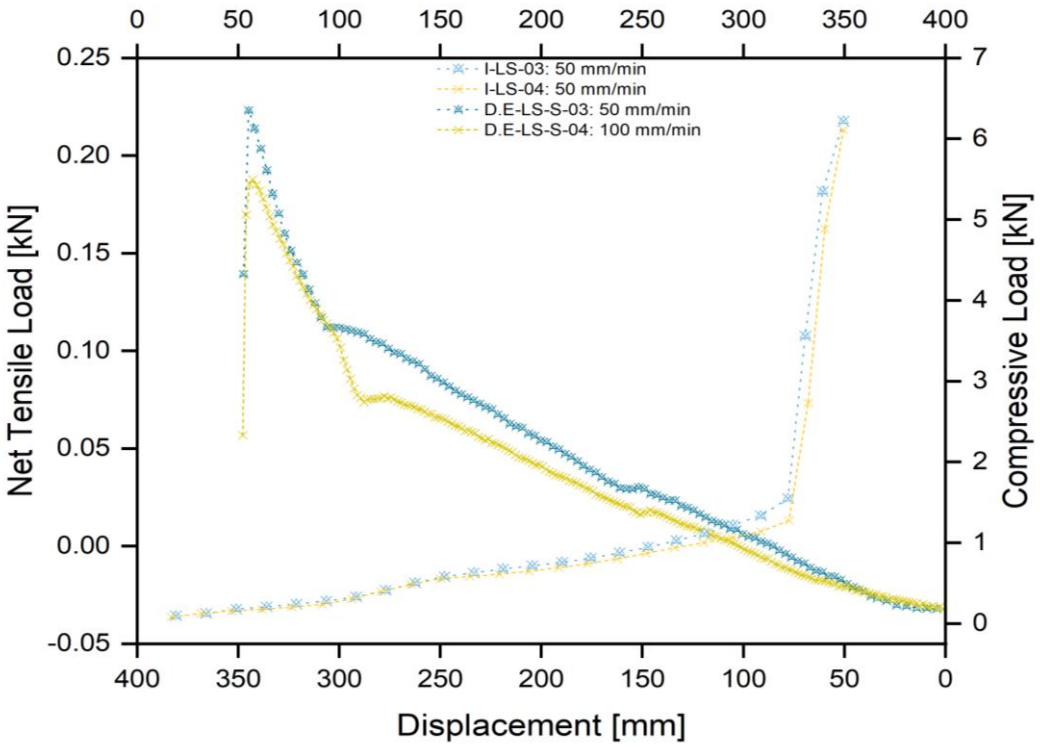

Figure 3-52. The influence of applying 50 and 100 mm/min extraction velocities on the 101.6 mm pile's tensile capacity in saturated soil.

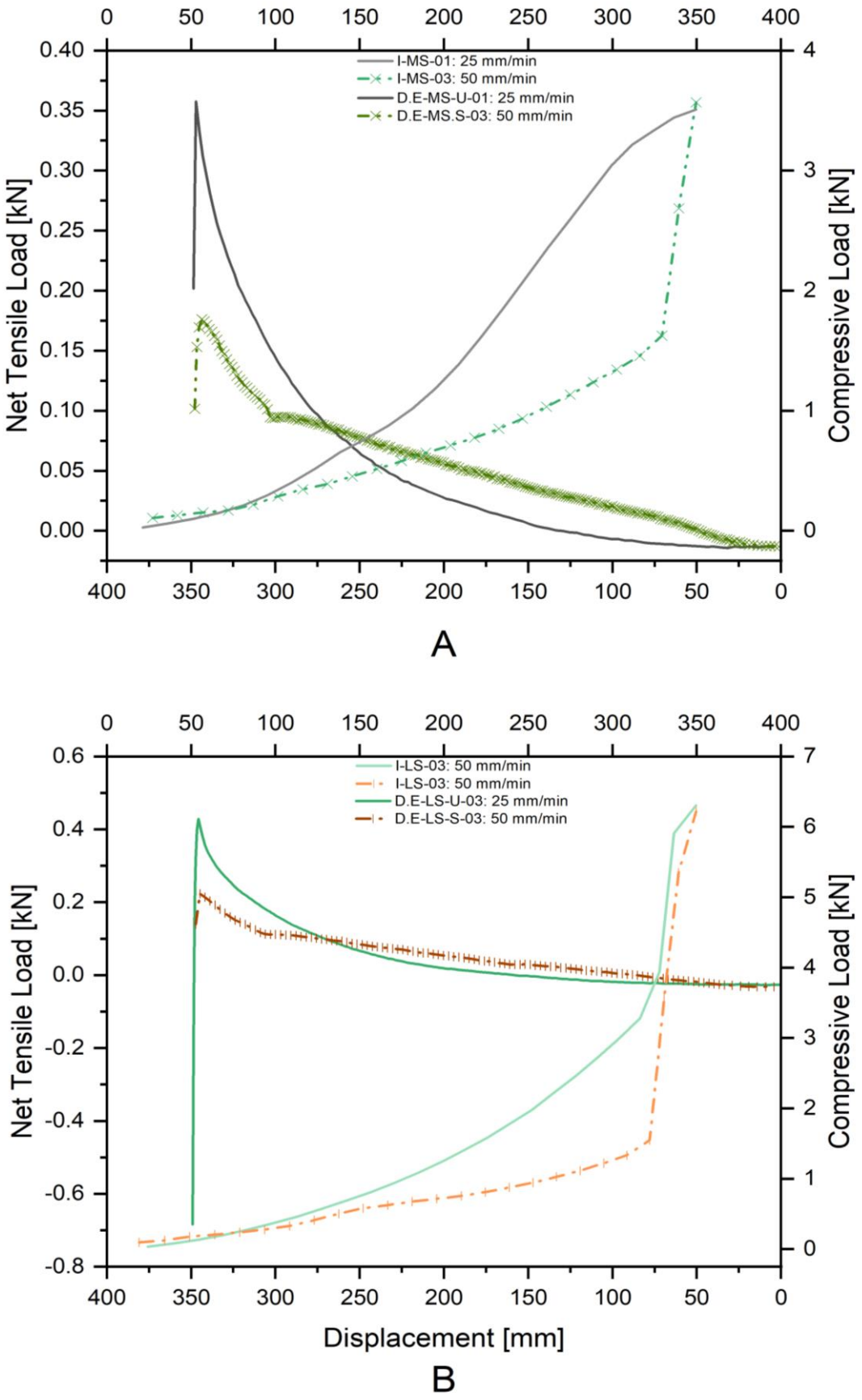

Figure 3-53. The load-displacement curves' response for extracting both piles' diameters in unsaturated and saturated soil with almost constant density; [A] 88.9 and [B] 101.6 mm piles.

When comparing D.E-MS-S-03 (velocity at 50 mm/min) with D.E-MS-U-01 (velocity at 25 mm/min) testing, as showcased in Figure 3-53-A, the compressive capacity of the 88.9 mm pile was 3.57 kN. This is nearly identical to the results from testing in an unsaturated condition, showing only a 1.7% increase. Even though a higher extraction velocity (50 mm/min) was applied in saturated soil, the tensile capacity of the 88.9mm pile (0.1961 kN) was 48.1% lower compared to the unsaturated condition (0.3776 kN). For the 101.6 mm pile testing, presented in Figure 3-53-B, the compressive capacities in tests D.E-LS-S-03 (velocity at 50 mm/min) and D.E-LS-U-03 (velocity at 25 mm/min) were nearly identical at 6.22 kN and 6.30 kN, respectively, marking a difference of 1.3%. In the saturated soil, the tensile capacity of the 101.6 mm pile (0.2531 kN) saw a 44.9% reduction compared to the result in the unsaturated condition (0.4593 kN).

After the displacement extraction tests, the sets for force extraction application were executed: sets 7 (88.9 mm) and 8 (101.6 mm). In total, there were eight tests, with four for each pile diameter. Unlike the tests in unsaturated soil, these tests were conducted without discharging and re-generating the soil bed due to the challenges of soil formation and time limitations. The extraction rates employed for testing in saturated soil were consistent with those in the unsaturated tests: 50 N/min as the lowest and 200 N/min as the highest, ensuring consistency when comparing results across the two soil conditions. For comparison with displacement extraction, a single reference curve from each pile diameter in the saturated soil (sets 6 and 7) was selected. These reference curves, along with the load-displacement curves for extracting the 88.9 mm and 101.6 mm piles by force, as illustrated in Figure 3-54 & Figure 3-55, respectively.

In the force extraction application tests in saturated soil, the soil did not densify but rather deformed, as mentioned earlier. This deformation manifested as the withdrawal of the soil column (plug) alongside the piles during extraction. The probable cause is the variance in the degree of suction force and shear failure brought about by the extraction applications, which will be elaborated in the subsequent section. Due to equipment constraints, such as the weight scale, and differences in lengths of the extracted columns, the weight of the soil extracted was not deducted from the net tensile load presented in Figure 3-54 and Figure 3-55. However, this weight was accounted for during the analysis. As a result of this deformation, the soil properties changed with each installation, evident from the compressive capacities of the piles' diameters.

For the 88.9 mm pile in set 7, the compressive capacities across tests 1 through 4 were 3.59, 4.34, 3.3 and 5.09 kN, respectively. For the 101.6 mm pile in sets 1, 2, 3, 4, and 8, they were, were 5.74, 6.77, 5.06 and 4.42 kN, respectively. Given these inconsistencies, comparing the results from saturated soil force extraction tests with those from unsaturated soil became challenging, particularly in verifying the assumption of a decrease in tensile capacity at or post a 100 N/min extraction rate. Thus, this comparison was omitted. The analysis primarily centered on contrasting the force extraction results in saturated conditions and with displacement extraction results in saturated conditions.

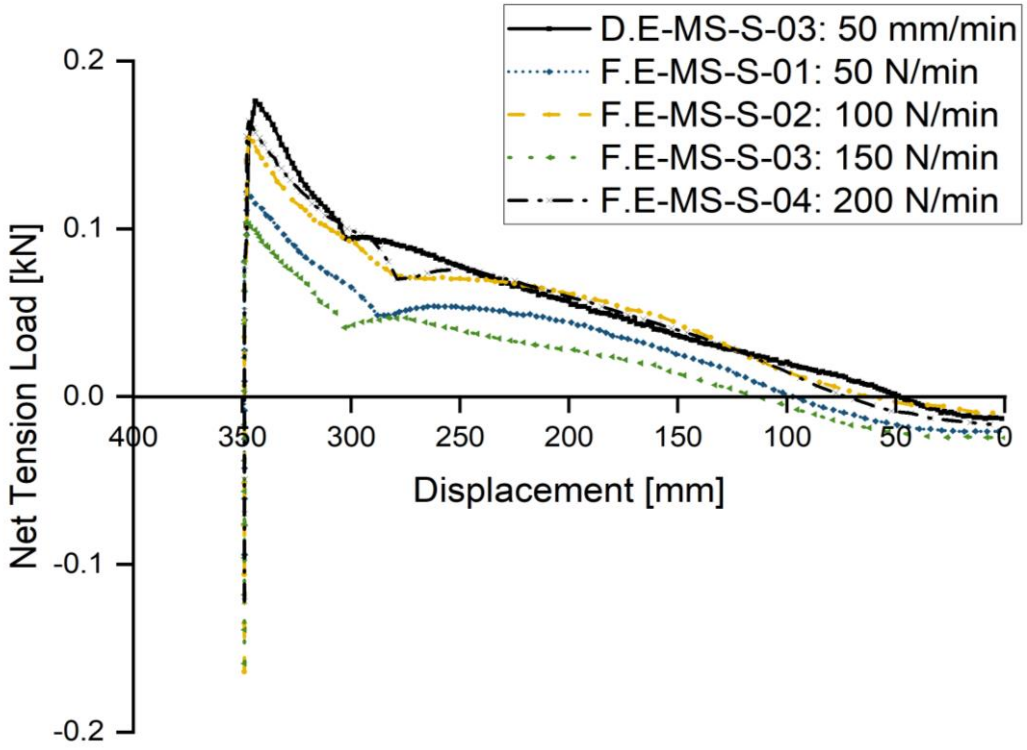

Figure 3-54. the load-displacement response in saturated soil for 88.9 mm pile extraction tests through the force-control method.

Despite the variation in compressive capacities of both pile diameters, the results in Figure 3-54 & Figure 3-55 clearly show that the tensile capacity generally increased with a rise in the extraction rate, with the exception of test F.E-MS-S-03 (velocity at 150 N/min). The discrepancy might be attributed to whether the soil column was extracted alongside the pile, and its associated weight. To support this, tests F.E-MS-S-01(velocity at 50 N/min) and F.E-MS-S-03 (velocity at 150 N/min) were chosen because their compressive capacities were nearly identical, at 3.59 kN and 3.3 kN, respectively. Moreover, the soil was extracted in the former test but not in the latter. Despite an 8.1% difference in compressive capacity, the tensile capacity for the 150 N/min (0.1243 kN), as depicted in Figure 3-56-A, was 12.8% lower than

that under the 50 N/min extraction rate, which was 0.1425 kN. This theory, suggesting that the soil column's weight might affect the tensile capacity, was further validated when testing the 101.6 mm pile, albeit from a different perspective. Here, the soil column was extracted in both reference tests. With compressive capacities of 6.77 kN for the F.E.-LS-02 (velocity at 11 N/min) and 5.06 kN for the F.E-LS-S-03 (velocity at 150N/min) test, there was a difference of 25.3%. Despite this significant difference, the tensile capacity of the 101.6 mm pile in F.E-LS-S-03: 150 N/min test was nearly equivalent to that in the F.E-LS-S-02: 100N/min, as showcased in Figure 3-56-B, representing a mere 1.2% difference. From the preceding, it is evident that the extraction rate can influence the length of the extracted soil column and, consequently, its weight, which in turn affects the tensile capacity.

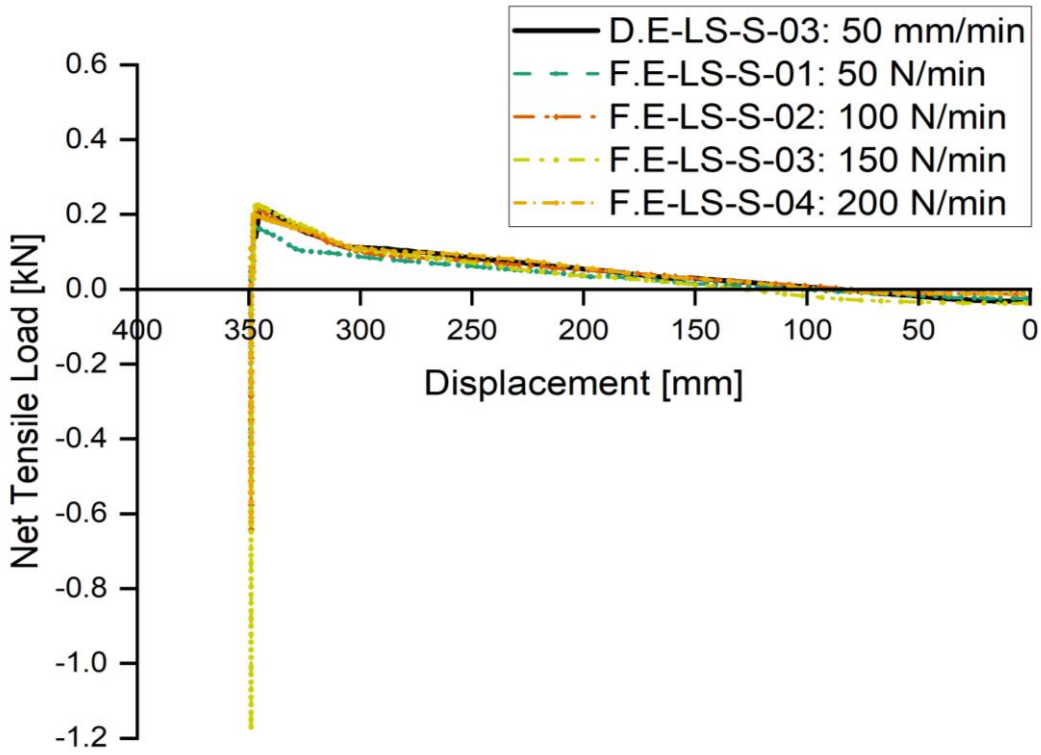

Figure 3-55.The 101.6 mm pile's load-displacement curve in saturated soil for the force-extracting method.

In comparison with the results from displacement extraction testing, reference curves included and displayed in Figure 3-54 and Figure 3-55, the tensile capacities of the 88.9 mm pile exhibited a reduction, regardless of soil density. In contrast, the capacities of the 101.6 mm pile were nearly equivalent to the capacity of the reference curve used for displacement extraction testing. Using the D.E-MS-S-01: 50 mm/min (0.1961 kN) as the reference curve, the tensile capacity of the 88.9 mm pile was 36.6% (highest) to 6.1% (lowest), irrespective of the soil density. On the other hand, the tensile capacities of the 101.6 mm pile were 0.4% and increased

by 0.8% at rates of 100 N/min (0.2522 kN) and 150 N/min (0.2552 KN), respectively, aligning closely with the reference curve D.E-LS-S-03: 50 mm/min (0.2531 kN). For the other rates, specifically 50 and 200 N/min, the reduction was 22.4% (highest) and 11.1% (lowest). The narrowing percentage gap between the two extraction applications in saturated soil, when compared to testing in unsaturated conditions, can be attributed to the retention or extraction of the soil column along with the pile during force extraction testing.

Despite the extraction of the soil column alongside the pile during force extraction testing, the tensile capacity of both piles' diameters decreased when compared to tests in unsaturated soil. As previously mentioned, this was due to the presence of pore water pressure. Two scenarios were utilised for analysis: extracting the pile without soil (scenario 1) and with soil (scenario 2). In Scenario 1, as illustrated in Figure 3-57-A, tests F.E-MS-S-03: 150 N/min and F.E-MS-U-03: 100 N/min for the 88.9 mm were chosen, as their compressive capacities were nearly identical at 3.3 kN and 3.29 kN, respectively. Despite the higher extraction rate applied in saturated soil conditions, the tensile capacity decreased by 35.5% to 0.1243 kN, as opposed to 0.199 kN in unsaturated conditions. In scenario 2, shown in Figure 3-57-B, the tests F.E-LS-S-03: 150 N/min and F.E-LS-U-03: 100 N/min were adopted. The compressive capacities for this pile were 5.06 kN in saturated soil and 5.24 kN in unsaturated soil - essentially constant with a minor reduction of 3.4%. There was a noticeable decline of 23.6% in tensile capacity, from 0.3342 kN in unsaturated conditions to 0.2552 kN in saturated conditions.

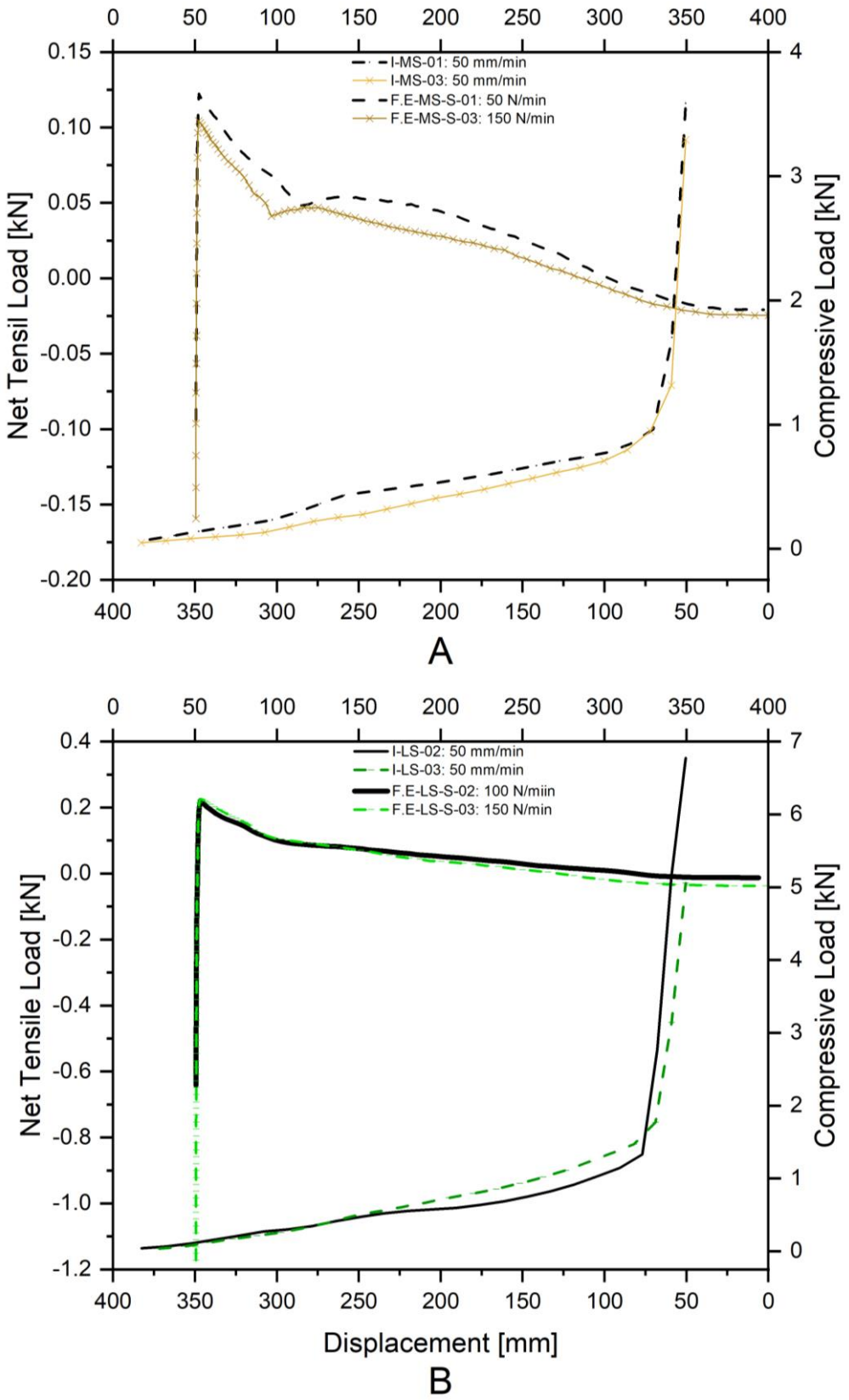

Figure 3-56. The impact of the weight and length of the soil plug pulled with the pile on the tensile capacity of the pile; [top] 88.9 mm and [bottom] 101.6 mm piles.

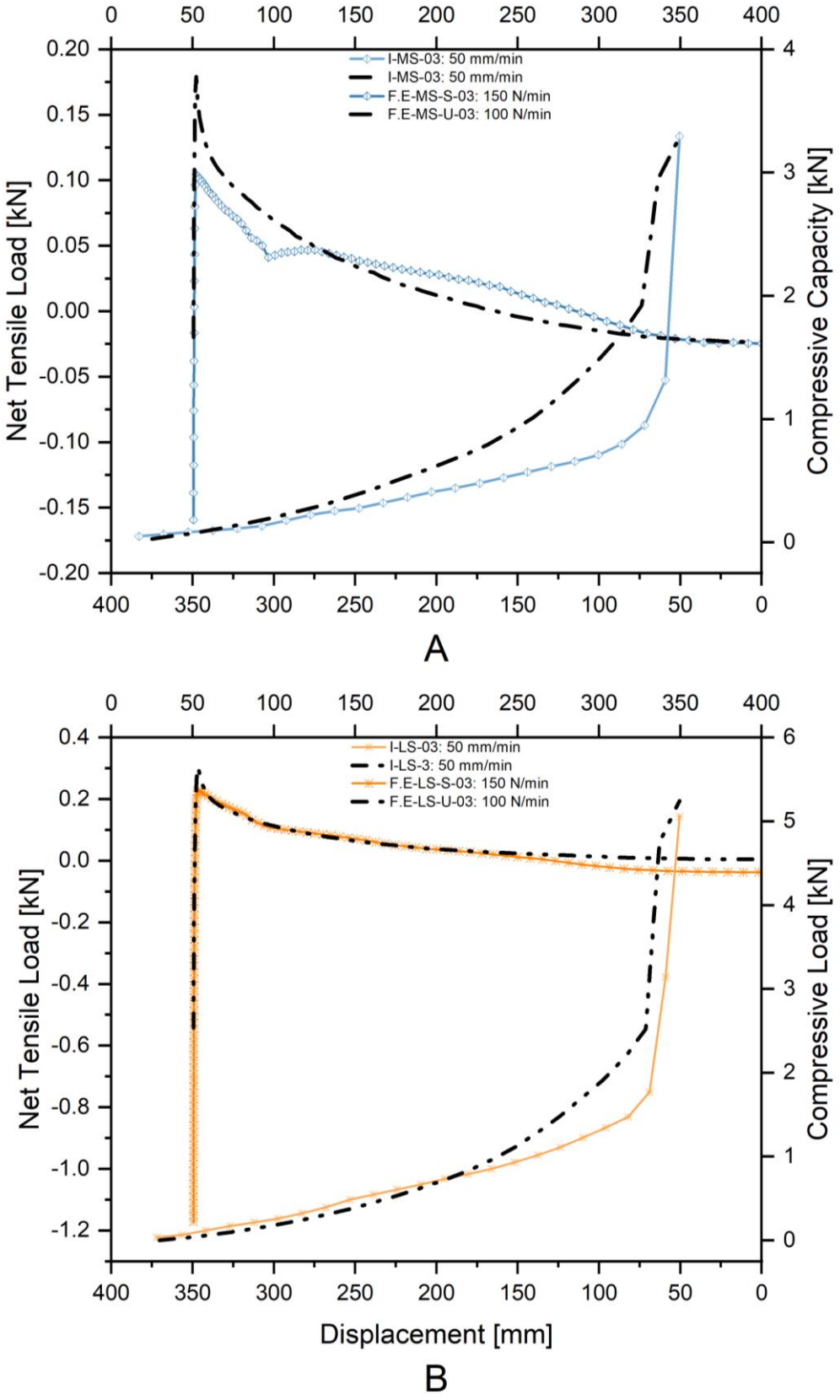

Figure 3-57.In testing force extraction application, the load-displacement curves for extracting both piles' diameters in unsaturated and saturated soil with almost constant density; [A] 88.9 and [B] 101.6 mm piles.

In tests conducted in saturated soil conditions with pore water pressure, both pile diameters showed reduced tensile capacities compared to unsaturated soil tests. However, using the displacement extraction yielded higher tensile capacities for both pile diameters compared to force extraction, mirroring findings in unsaturated conditions. This suggests that the type of extraction application, regardless of its velocity/rate, significantly affects soil behaviour, impacting factors like suction force and shear failure.

3.8.6 Suction Force

In saturated soil tests, both extraction methods resulted in a reduction of pore water pressure, leading to varying degrees of suction. As detailed in section 3.5.5, pore pressure levels were monitored using a semi-submersible pressure transducer. Importantly, the extraction process only began once real-time readings stabilised during the waiting periods that followed the installation phase. For displacement extraction, the waiting period was 300 seconds, while for force extraction, it was 60 seconds. Despite this reduction, primarily due to time limitations, the readings consistently stabilised within the designated waiting periods.

In the tests for displacement extraction application on both pile diameters, pore water pressure generally decreased under velocities ranging from the lowest at 5 mm/min to the highest at 100 mm/min. The pressure versus time curves for extracting piles with diameters of 88.9 mm and 101.6 mm at a 5 mm/min velocity are illustrated in Figure 3-58 and Figure 3-60, respectively. Meanwhile, Figure 3-59 and Figure 3-61 demonstrate the results of the other velocities applied for the 88.9 mm and 101.6 mm piles, respectively. The results from Figure 3-58 through Figure 3-61 highlight an immediate decline in pore pressure upon the application of the extraction load, regardless of the chosen velocity. This suggests that the water bore the brunt of the load. Furthermore, the figures depict how different extraction velocities impact the magnitude of the pore pressure reduction.

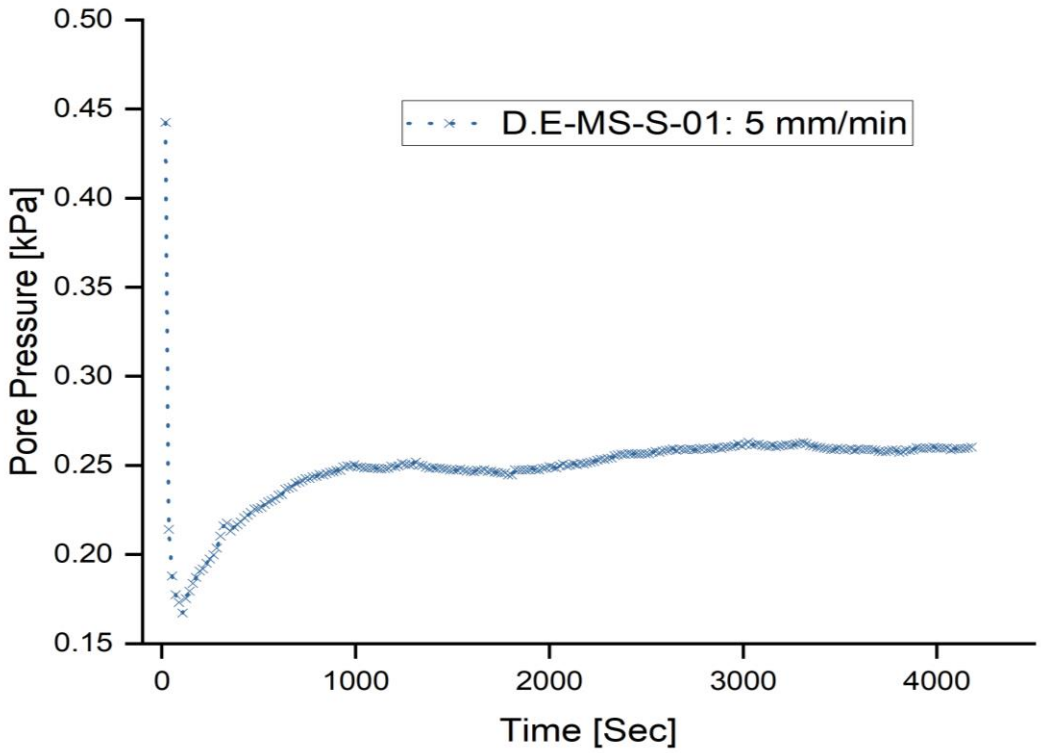

Figure 3-58. The pore pressure-time curve for extracting the 88.9 mm pile in saturated soil with a 5 mm/min velocity.

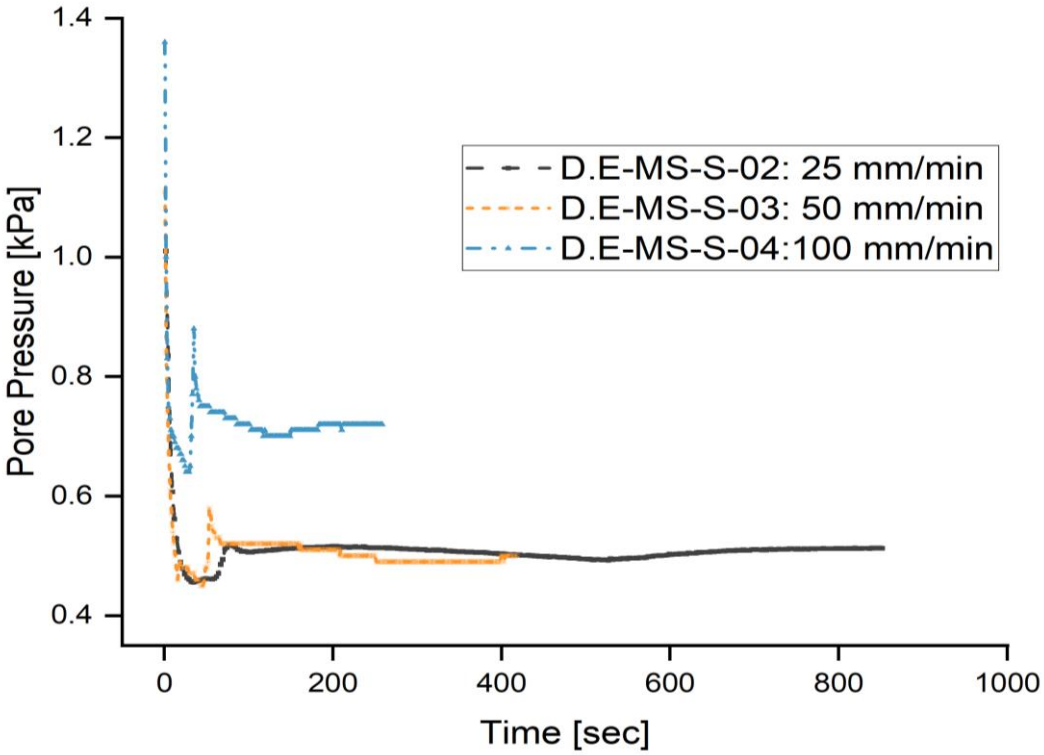

Figure 3-59. The pore pressure-time curves for the three velocities applied for extracting the 88.9 mm pile in saturated soil.

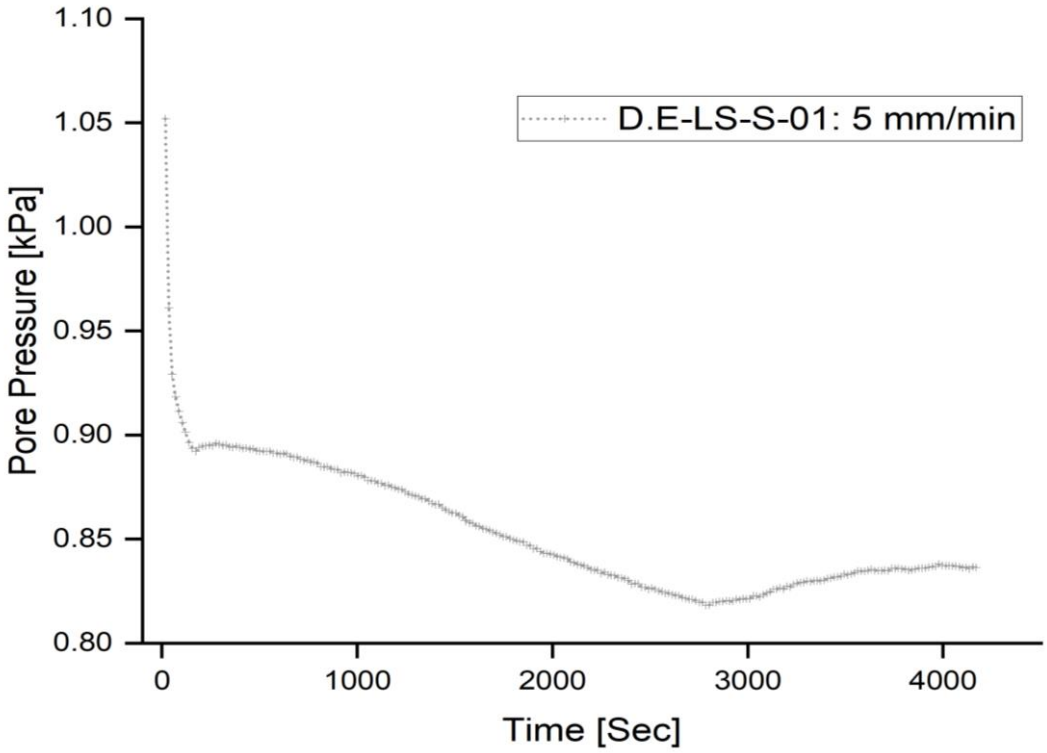

Figure 3-60. The pore pressure-time curve response for a 5 mm/min extraction velocity in testing the 88.9 mm pile in saturated soil.

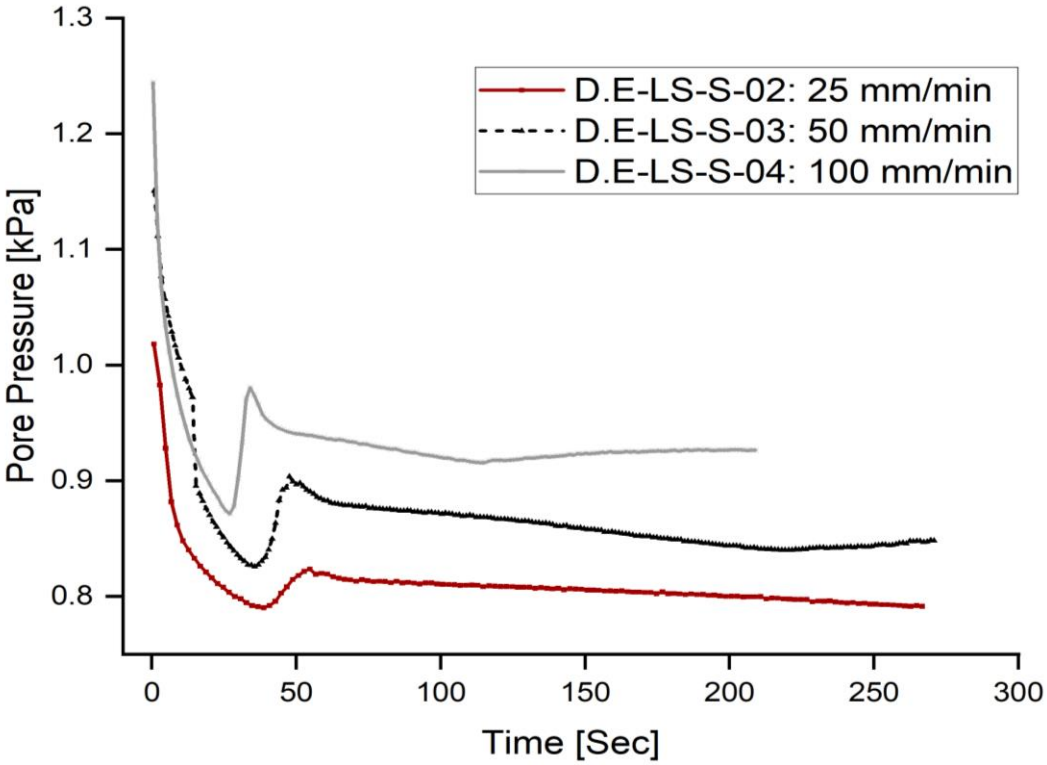

Figure 3-61. The pore pressure-time curves for the applied velocities for extracting the 101.6 mm pile in saturated soil.

At a velocity of 5 mm/min, both pile diameters exhibited the least reduction in pore pressure levels. The reduction from the onset of extraction to failure was 0.3 kPa for the 88.9 mm pile and 0.2 kPa for the 101.6 mm pile. As extraction velocities increased, the reduction in pore pressure levels also reduced, with the most significant decline observed at the velocity of 100 mm/ min. Here, the pore pressure reduction was 0.7 kPa for the 88.9 mm pile and 0.3 kPa for the 101.6 mm pile. From these observations, the 88.9 mm pile consistently showed a higher degree of pore pressure reduction compared to the 101.6 mm pile. The increase in reduction, when comparing velocities from 5 mm/min to 100 mm/min, was 133% for the 88.9 mm pile and 50% for the 101.6 mm pile. This disparity may be attributed to the diameter-to-wall thickness ratio of the piles: 30 (or 29.6 precisely) for the 88.9 mm pile and 34 (or 33.8 to be exact) for the 101.6 mm pile. This theory finds some validation in the observed pore pressure curves. The curves for the 88.9 mm pile showed a steep decline (as seen in Figure 3-58 and Figure 3-59), while those for the 101.6 mm pile descended more gradually (as depicted in Figure 3-60 and Figure 3-61). These trends indicate that the induced pore pressure dissipated more intensely during the extraction of the 88.9 mm pile than the 101.6 mm pile. Despite the variations in the magnitude of pore pressure reductions, the ratio of pore pressure decrease - from the start of extraction to the point of failure – remained fairly consistent across both pile diameters, as summarised in Table 3-16.

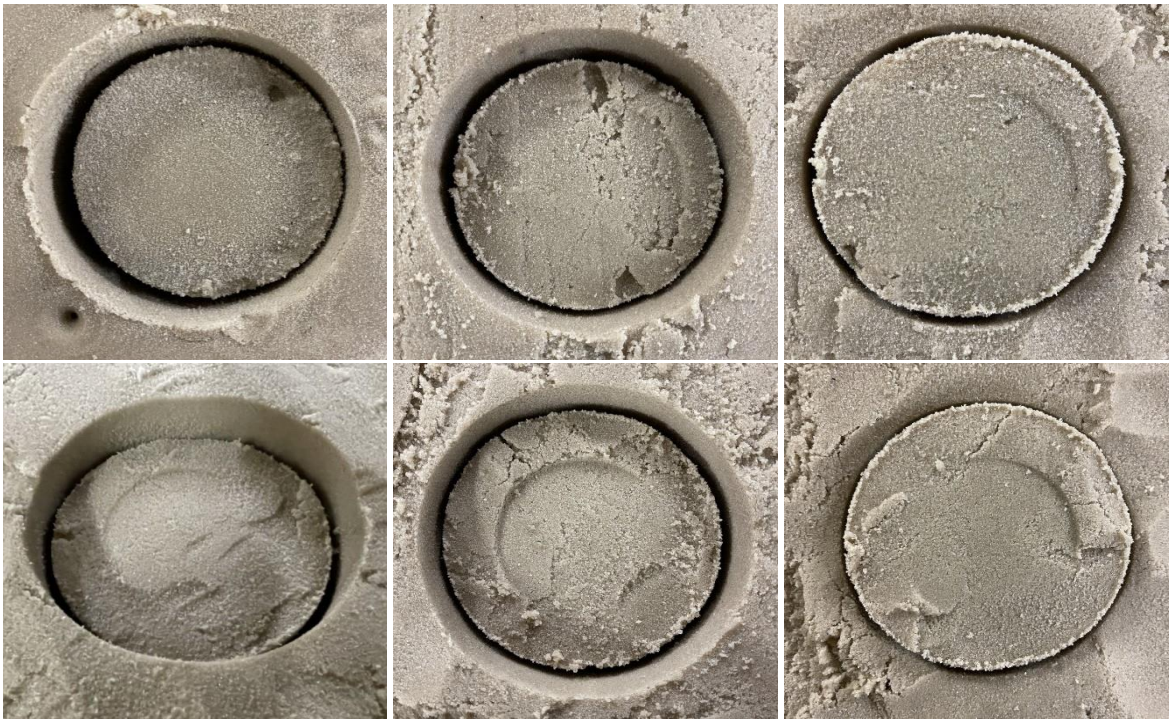

Figure 3-62. The elevation level of the plug to the soil surface for extracting both piles' diameters by applying various displacement velocities; [top] 88.9 mm and [bottom] 101.6 mm piles.

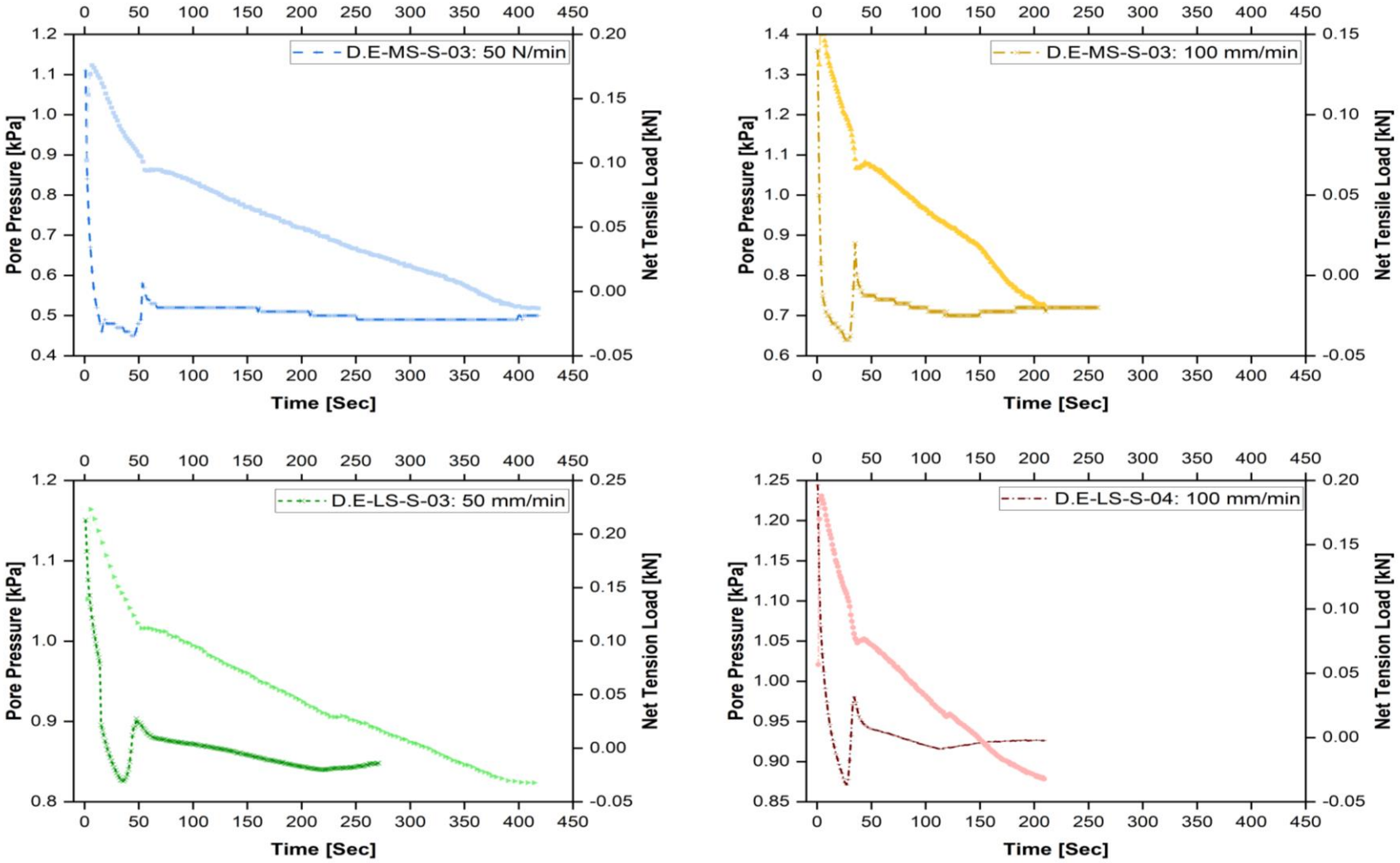

Figure 3-63. The pore water pressure level during extracting both piles' diameters under 50 and 100 mm/min displacement velocity; [top] 88.9 mm and [bottom] 101.6 mm pile.

Table 3-16 summarises the ratio of reduction in pore water pressure from the start of the extraction process until failure in testing displacement extraction application.

Pile diameter [mm]/ velocity [mm/min]	***5***	***25***	***50***	***100***
88.9	2.6	2.2	2.5	2.1
101.6	1.3	1.3	1.4	1.4

Figure 3-62 illustrates that during the testing of the displacement extraction application, both piles' diameters were extracted with walls free of soil, leaving the plug behind. This supports the assumption of partial dissipation and indicates the formation of a partial drainage path, which subsequently reduced the suction force. There are two potential hypotheses to explain the development of these drainage conditions, characteristic of local shear failure, under the displacement extraction application: the chosen extraction velocities and/or the application mechanism itself. When considering the displacement application mechanism, the load (or force) is the variable factor, which typically rises incrementally until the desired displacement is reached. Importantly, as the force required to achieve the stipulated displacement grows, the extraction rate will decelerate. Therefore, upholding a consistent displacement rate, irrespective of the necessary load (both its initial magnitude and rate of application) to attain it, and the time intervals between loading stages, could profoundly influence soil behaviour.

Given the inherent high permeability of sand, the chosen extraction velocities were deliberately low. This allowed the extraction process to extend over an extended period, facilitating the dissipation of induced pore water pressure and leading predominantly to drained conditions. For instance, at an extraction velocity of 5 mm/min, it took over one hour (more than 4,000 seconds) to extract both pile diameters. In contrast, at a velocity of 100 mm/min, it took between 209-258 seconds to extract the 88.9 mm and 101.6 mm piles, respectively. However, even with these slower velocities, the elevation of the soil plug increased as extraction velocities rose, as illustrated in Figure 3-62. Notably, under the 100 mm/min velocity (as seen in the top right image), which displayed the most significant reduction in pore pressure level, the soil plug's top either closely or slightly exceeded the height of the soil surface. This indicates that if even higher extraction velocities were employed than those currently adopted, soil behaviour would likely shift to an undrained state, resulting in heightened suction. Overall, these results underscore the critical interplay between time and extraction velocity in managing the soil's pore water pressure level, revealing a direct correlation.

Under the force extraction application, the behaviour of pore water pressure exhibited patterns similar to those observed during displacement extraction. This similarity pertains particularly

to the correlation between the degree of reduction in pore water pressure and the extraction rate, with the lowest observed at 50 N/min and the highest at 200 N/min. Figure 3-64 and Figure 3-65 provide insights into the pore water pressure-time curves during the extraction of 88.9 mm and 101.6 mm diameter piles, respectively, across most force rates. It's crucial to highlight that there were deviations in the behaviour of pore water pressure during two specific tests: F.E-MS-S-03: 150 N/min for the 88.9 mm pile and F.E-LS-S-01: 50 N/min for the 101.6 mm pile. The reasons for these anomalies remain undetermined, leading to their exclusion from the general analysis. However, the pore pressure-time curves for these particular extraction rates are presented separately in Figure 3-66 (for the 88.9 mm pile) and Figure 3-67 (for the 101.6 mm pile).

In the force extraction testing, Figure 3-64 to Figure 3-67 clearly illustrate that the moment the extraction load is applied, a substantial portion of this load is borne by the water, resulting in an immediate drop in pore pressure, consistent across all rate settings. Excluding the unique behaviour seen at the 150 and 50 N/min rates for the 88.9 mm and 101.6 mm piles respectively, the minimal decrease in pore pressure was evident at the slower rates of 50 and 100 N/min, as showcased in Figure 3-64 and Figure 3-65. Even with variations in rate settings, the range of pore pressure difference from the start of extraction to the point of failure remained consistent across both pile diameters. Specifically, the difference was 0.12 kPa for the 88.9 mm pile and approximately 0.1 kPa (exact 0.095 kPa) for the 101.6 mm pile. A slight uptick in pore pressure reduction was noticed as the extraction rates increased, with the most prominent decrease manifesting at the maximum rate of 200 N/min. Here, the pore pressure differences for the 88.9 mm and 101.6 mm piles were 0.15 kPa and 0.14 kPa, respectively, marking them as virtually identical. This consistent ratio of pore pressure decreases from the outset of extraction to the point of failure mirrored the trends observed during displacement extraction. All of these results have been collated and tabulated in Table 3-17 for ease of reference.

Table 3-17 summarises the ratio of reduction in pore water pressure from the start of the extraction process until failure in testing force extraction application.

Pile diameter [mm]/ force rate N/min]	***50***	***100***	***150***	***200***
88.9	1.1	1.1	1.1	1.2
101.6	1.1	1.1	1.2	1.2

When comparing force extraction testing with displacement extraction testing, there was a noticeable yet slight increase in the degree of reduction. Specifically, for the 88.9 mm pile, there was a 25% increase across the 50 to 200 N/min rates. For the 101.6 mm pile, this

increment was 40% between 100 to 200 N/min rates, excluding the values at 150 and 50 N/min. The smaller percentage increase in force testing can be attributed to the inherent mechanism of the extraction method. In force-controlled testing, there is a direct control over the rate of load application. The force is applied consistently at a predetermined rate and controlled, with the displacement being the variable factor. Consequently, force-controlled extraction is generally faster than displacement-controlled extraction, evidenced by the reduced extraction times seen in force extraction. To elucidate, despite varying extraction rates, the overall duration for force extraction remained relatively close. For the 88.9 mm pile, extraction times varied between 53 seconds (at 150 N/min) and 135 seconds (at 50 N/min). For the 101.6 mm pile, the times ranged from 73 seconds (at 150 N/min) to 88 seconds (at 50 N/min).

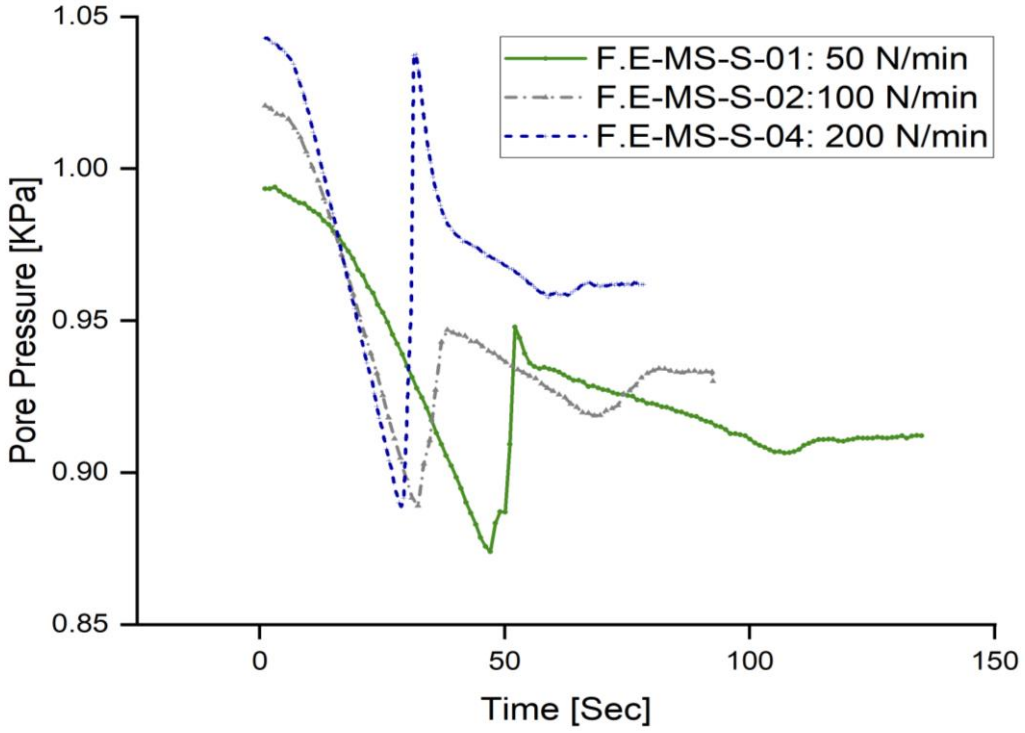

Figure 3-64. The response of the pore pressure-time curves for extracting the 88.9 mm pile in saturated soil under various force rates.

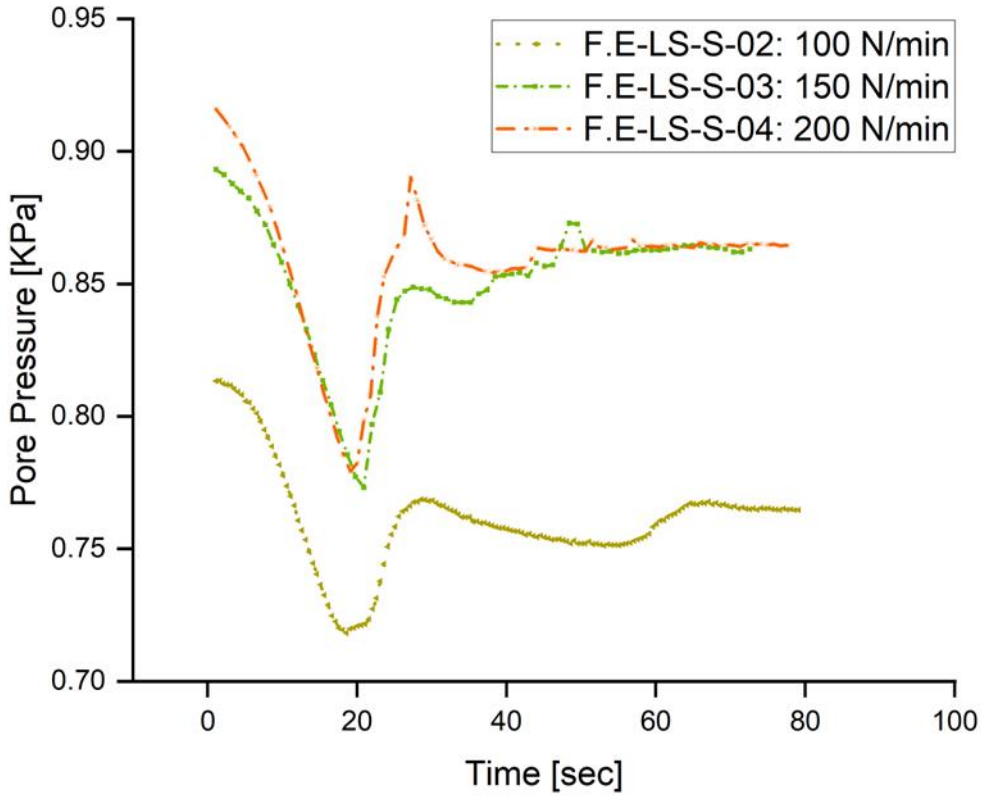

Figure 3-65. The response of the pore pressure-time curves for extracting the 101.6 mm pile in saturated soil under various force rates.

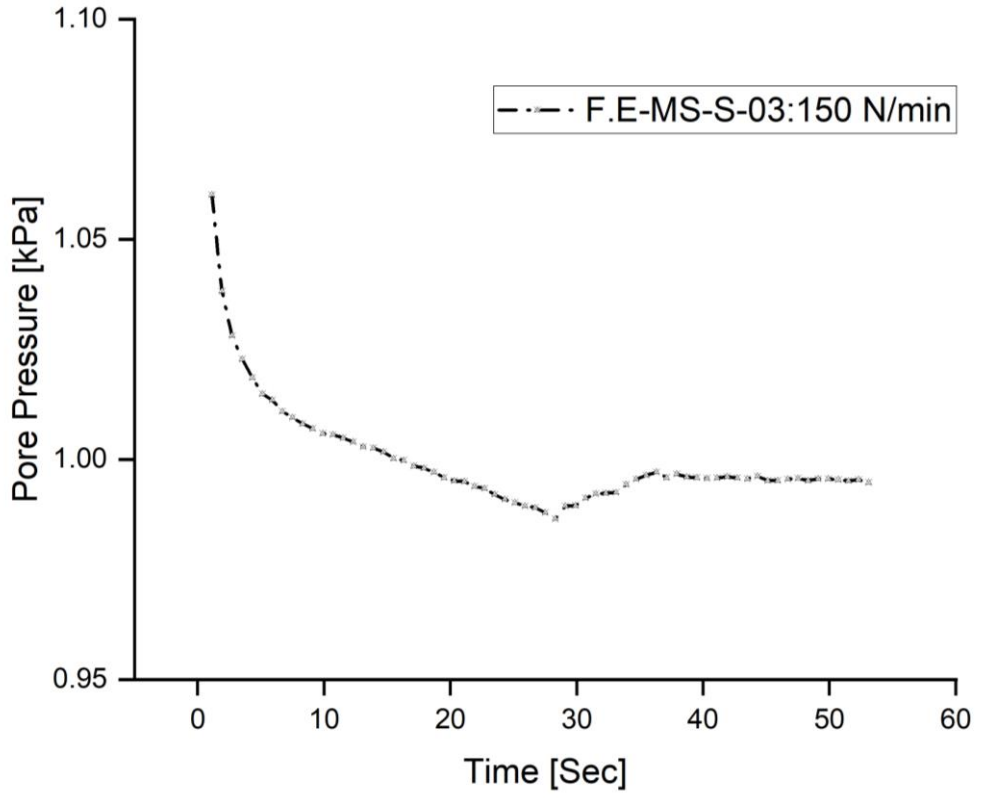

Figure 3-66. The pore pressure-time curve response for extracting the 88.9 mm pile under the rate of 150 N/min in saturated soil.

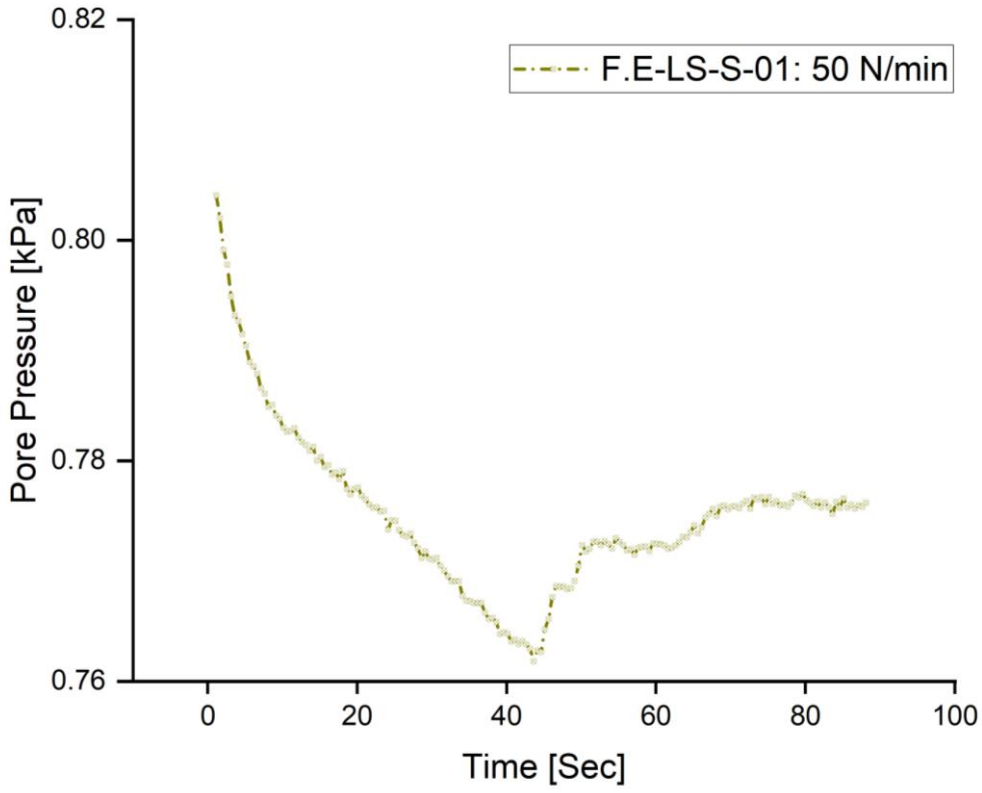

Figure 3-67. The pore pressure-time curve for extracting the 101.6 mm pile in saturated soil with 50 N/min rate.

Figure 3-68. The conditions of the soil and 88.9 mm pile after terminating force-extraction application testing.

Figure 3-69. The conditions of the soil and 101.6 mm pile after terminating force-extraction application testing.

Figure 3-68 to Figure 3-69 highlight the effects of the force application mechanism combined with the adopted extraction rates. Due to the speed of this extraction method, there was a swift extraction of both pile diameters. This rapid extraction meant that the soil plug remained inside the piles. This observation indicates the creation of a strong suction force, leading to an un-drained condition. This behaviour is indicative of a general shear failure. Upon failure, there was a rapid and significant dissipation of the induced pore pressure, as observed in Figure 3-64 and Figure 3-65. the level of pore pressure post-failure was between 25% and nearly the original level observed before the extraction process began. However, the outcomes from the force extraction testing do not discredit the method entirely. Its effectiveness can be modified by adjusting various factors. For instance, allowing a sufficient waiting or consolidation period between loading stages can help in the dissipation of the pore water pressure. Furthermore, using slower extraction rates, such as rates less than or equal to 1 N/min, might lead to better results. Notwithstanding, with a more profound understanding of displacement control applications, it is believed it could replicate the installation and decommissioning of mono-piles.

3.8.7 Failure Surface Shape

The detailed investigation of the shape of the failure surface necessitates a distinct experimental setup, specifically an axis-symmetrical one, which was not utilised in this research project and thus was beyond its scope. Despite this limitation, during testing in unsaturated soil conditions, there was a consistent observation of a circular pattern of failure on the sand's surface. However, the current experimental setup did not provide the means to accurately determine the initial formation and subsequent propagation of the failure shape through the soil – be it curved or conical – especially during the extraction process. This limitation stemmed from the absence of advanced imaging tools such as time-exposure photography.

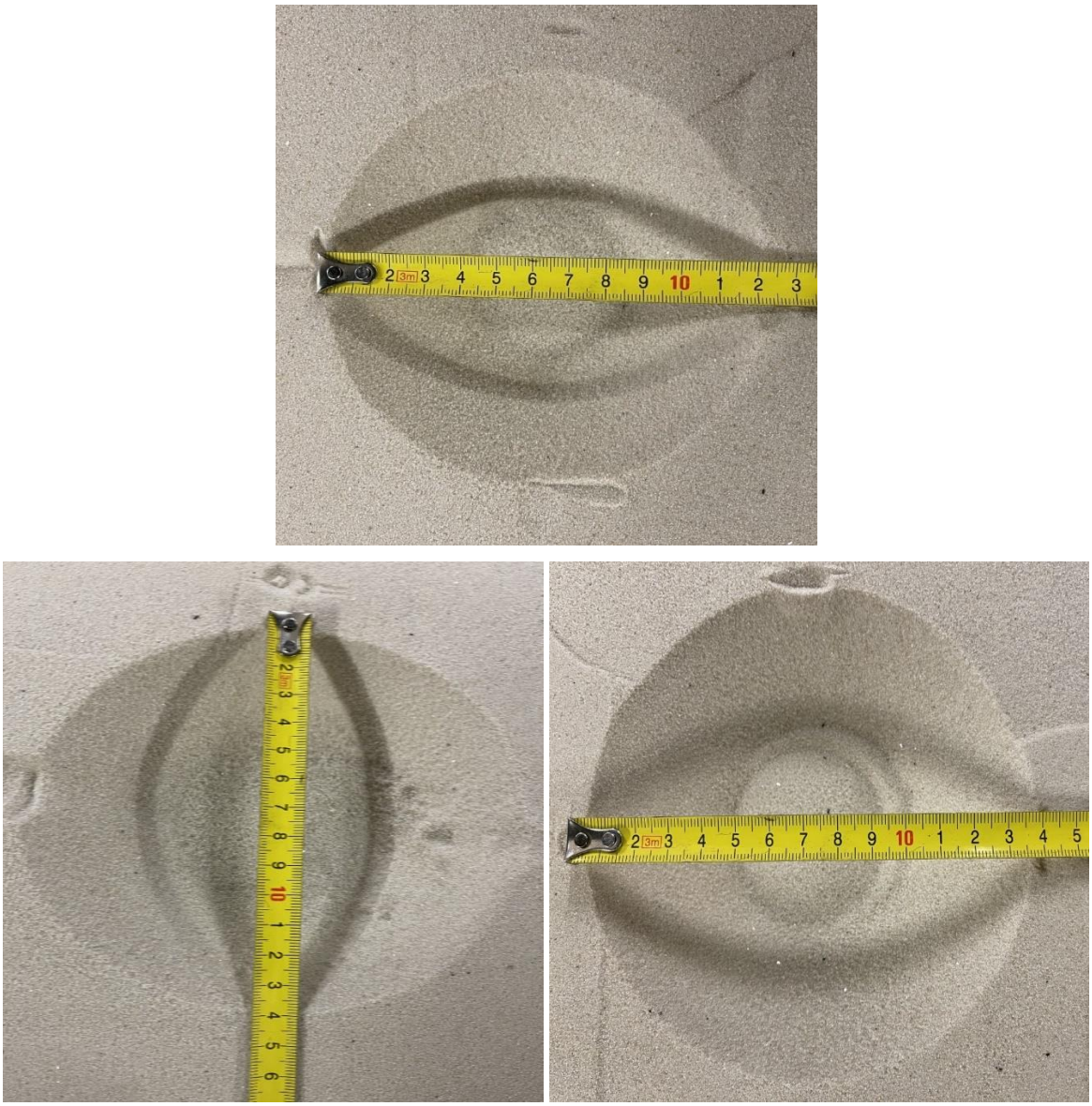

Figure 3-70. The top view of the failure surface shape and its diameter in unsaturated soil; [top] 88.9 mm - force- and [bottom] 101.6 mm piles –[left] displacement and [right] force.

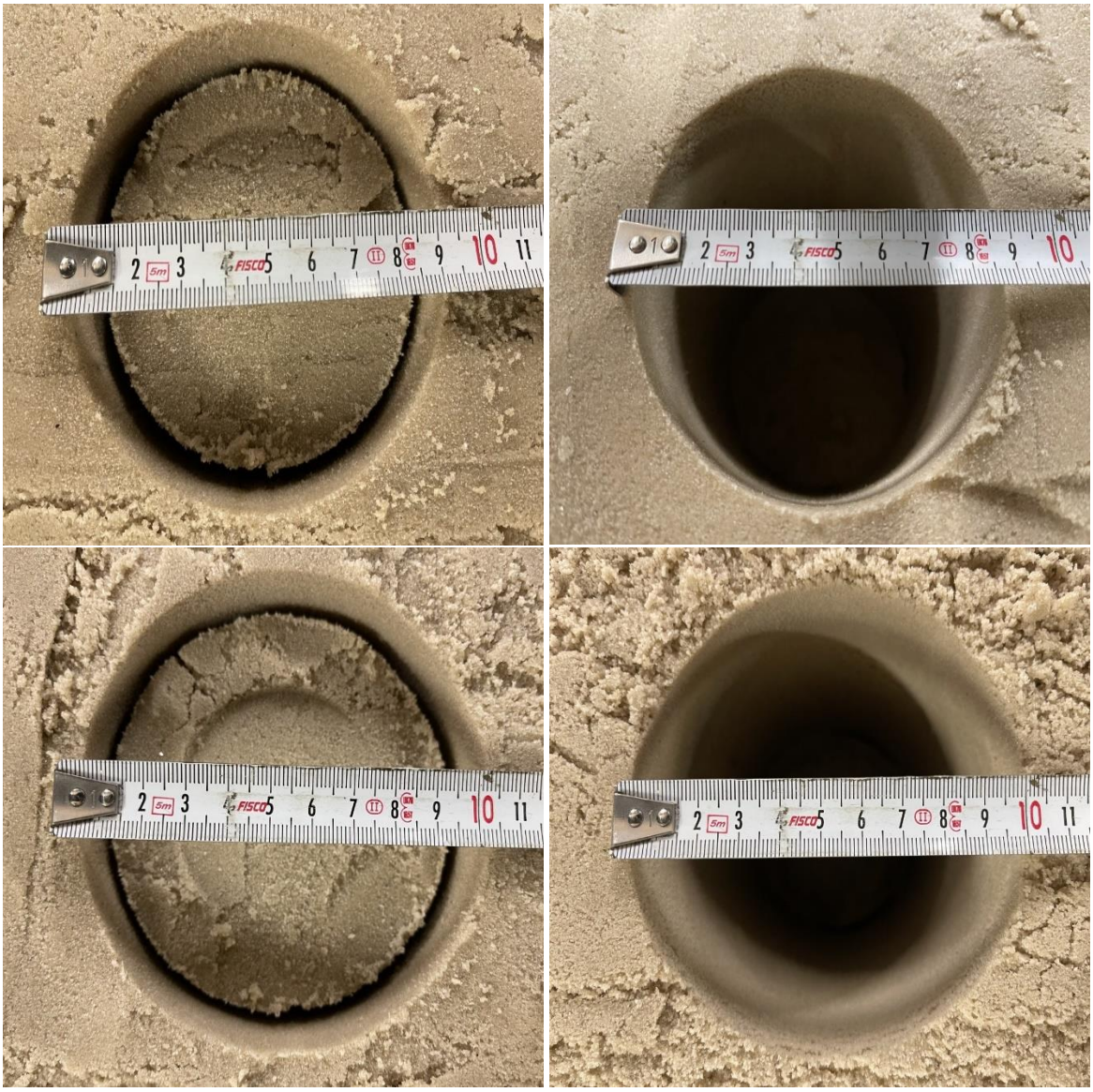

Figure 3-71. The top view of the failure surface shape [vertical] and its diameter in saturated soil; [top] 88.9 mm, [bottom] 101.6 mm piles, [left] displacement and [right] force.

In the unsaturated soil tests, the observed failure circles showed a diameter proportionate to the pile diameter being examined:

1. For the 88.9 mm pile, as shown in Figure 3-70 (top), the failure circle's diameter was approximately 120 mm. This is about 1.35 times the pile diameter.
2. For the 101.6 mm pile, depicted in Figure 3-70 (bottom), the failure circle exhibited a diameter of roughly 140 mm, which is approximately 1.38 times the pile diameter.

When analysing both piles' diameters in unsaturated soil conditions, the ratios of the failure circle diameters were essentially consistent, hovering around a multiplier of 1.35 to 1.38 times the respective pile diameter.

Changes in soil saturation levels did lead to alterations in the failure surface's shape, transitioning from an assumed curved from in unsaturated conditions to a vertical cylindrical shape in saturated conditions.

With no embedment duration and operational load, the diameters of the failure and the piles were equal in nature. For the 88.9 mm pile shown in Figure 3-71 (top), that the failure diameter was approximately 90 mm which correlated to 1.01 times the pile's diameter. Results indicated within Figure 3-71 (bottom), illustrate that the diameter for the vertical cylinder was roughly equal to 101.9 mm which equated to 1.0 times the diameter of the 101.6 mm pile. From the investigated variables, the most significant factors influencing the failure surface's extent and shape were the diameters of the piles and the soil's conditions.

3.9 Conclusion

Extraction, in general, is influenced by factors such as installation, embedment duration, and operational loads. Installation affects the structure-soil interaction both during and after the process, and this interaction is further strengthened by the duration of embedment, irrespective of operational loads, as depicted in Figure 3-72. The process of extracting a structure can be seen as the reverse of its installation, with several common factors between the two, such as the applications used for both processes. Various industries, from onshore to near- and offshore, have been and continue to investigate extraction, irrespective of their practice. These industries include construction, marine salvage, offshore oil and gas, highlighting that extraction is not as thoroughly understood or researched as installation. In the context of the offshore wind industry, which is a newer entrant, there is ongoing experimental work aimed at examining the feasibility of extracting fixed single steel pile-foundations, also known as mono-piles, using vibration and/or pressure applications. However, the data from this research remains confidential. The focus on these specific applications might stem from their previous use in pile and suction bucket installations. Other extraction techniques, such as displacement or force-control, have not been widely applied, investigated, or reported in academic literature.

A preliminary theoretical review has been conducted to understand the mechanics of the extraction phenomenon and to identify the factors that influence or control it. In other words, the aim was to discern the components that impact the extraction load. Regardless of the type of object or structure embedded in the seabed – whether it's suction caissons or anchor plates - several factors can influence the extraction load. These factors include the weight of the object and soil, suction force, soil resistance along the failure surface, and the adhesion force between the object and its surrounding soil (often referred to as skin friction). It's essential to recognise that while these factors are consistent, they can vary depending on the structure's specific configuration. For open-ended piles, the adhesion force or skin friction is influenced by the interaction between the pile surface and the soil both inside and outside the pile, known as shaft resistance. A hypothetical visualisation of the factors influencing extraction load for an open-ended pile is illustrated in Figure 3-73. Excluding the weight factor, each factor is affected by a set of parameters, some of which are shared across factors. Parameters like soil properties and conditions, embedment ratio, and pile friction angle influence both the failure surface and shaft resistance. As for suction, key influencing parameters include the velocity and duration of extraction.

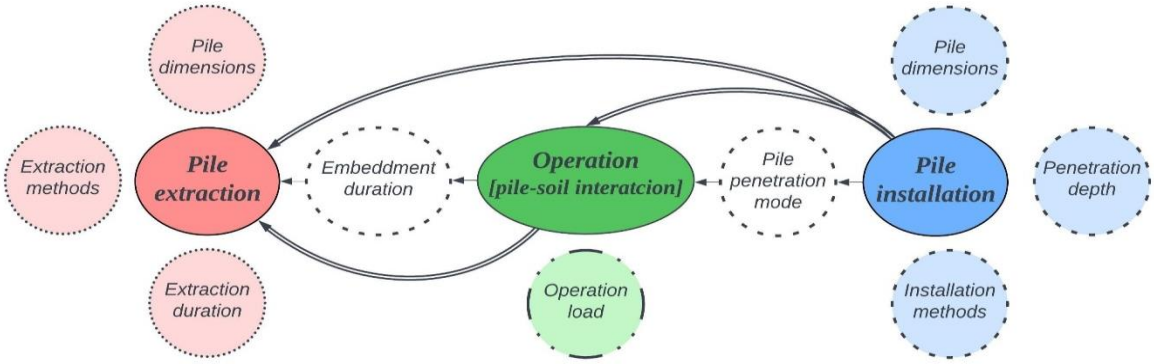

Figure 3-72. An overview of a few factors of the processes that influence extraction.

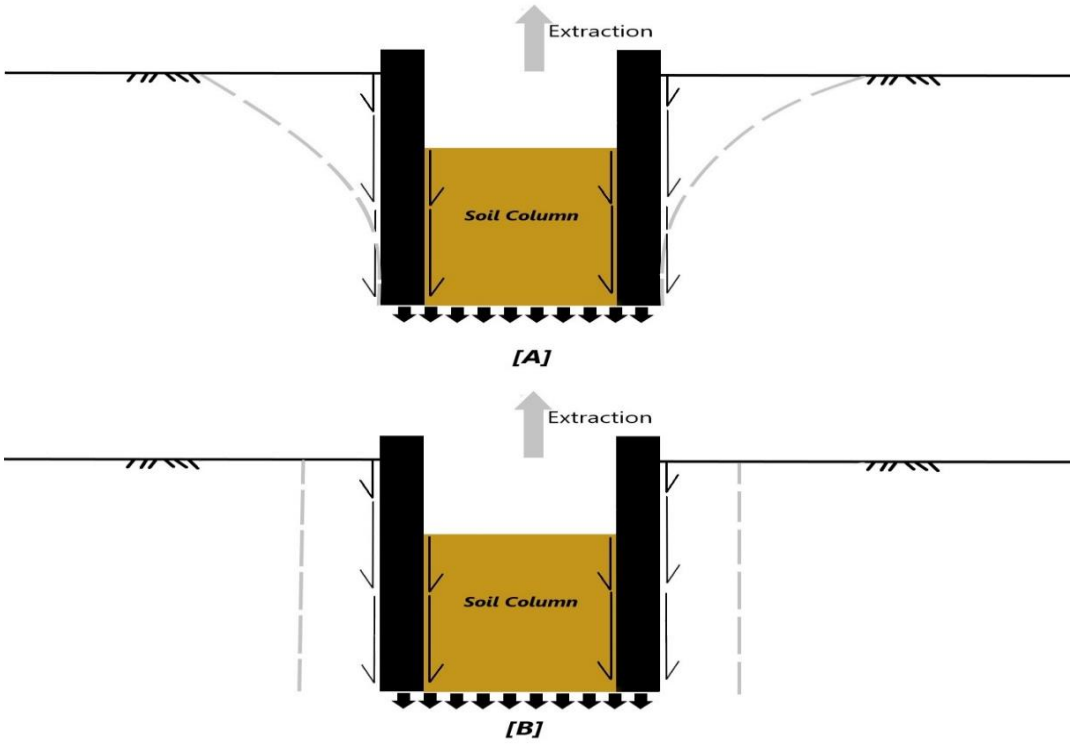

Figure 3-73. The potential influencing factors on the extraction load of open-ended piles in different soils; [A] dense sand and stiff clay and [B] loose sand and soft clay.

A series of 1g model pile extraction tests were conducted using displacement and force control on 400mm-long open-ended steel piles with diameters of 88.9 and 101.6 mm in both in unsaturated and saturated soil. The experimental investigation aimed to validate whether the identified factors and their parameters consistently influence extraction, regardless of the application. Additionally, the feasibility of the two aforementioned extraction methods was examined and confirmed.

In both unsaturated and saturated soil conditions, the experimental investigation results confirmed that the pile's tensile capacity is lower than its compressive capacity. The tensile capacity of the 88.9 mm and 101.6 mm piles was more than 90% lower. One contributing factor to this significant reduction was the lack of embedment duration and operational loads. In the absence of excess pore pressure in unsaturated soil, the tensile capacities of both pile diameters were higher than in saturated conditions. It was crucial to maintain a constant soil density across both conditions, which in turn, confirmed the impact of extraction velocity/rate on piles' tensile capacity. For pile diameters that remained constant in wall thickness and embedment ratio, tensile capacity increased with the enlargement of the pile diameter.

When comparing the force and displacement extraction applications under constant soil density, the displacement extraction in both unsaturated and saturated soils yielded a higher

tensile capacity for the 88.9 mm and 101.6 mm piles. Despite the greater capacity resulting from displacement extraction, both pile diameters in saturated soil were extracted without any soil, indicating the development of a low suction degree. This is because the mechanism and rate of the application, which both influence extraction time, were slow. This allowed for the dissipation of the induced pore water pressure, and thus the drained condition predominated. However, this was not observed under force extraction. Due to its faster mechanism and rate, force extraction led to a high degree of suction, resulting in the pile being extracted with the soil plug intact. Beyond the influence of the extraction applications, the ratio of the pile's diameter to its wall thickness was confirmed to be a significant factor affecting the degree of drainage: the higher the ratio, the quicker the drainage.

The experimental investigation pinpointed the optimal velocity or rate within the range of applied extraction rates for both displacement and force applications. For displacement extraction, the optimal velocity remained consistent for both pile diameters in unsaturated and saturated soils, at $\leq$ 50 mm/ min. In contrast, for force extraction, the optimal rate differed based on the pile diameter: $\leq$ 150 N/min for the 88.9 mm pile and $\leq$ 100 N/min for the 101.6 mm pile in unsaturated soil. In saturated soil, determining the optimal rate for force extraction proved challenging due to the influence of the soil plug weight on tensile capacity during the testing of both the 88.9 mm and 101.6 mm piles. The results from this experimental campaign confirmed the feasibility of fully removing offshore wind's fixed single steel pile foundations (mono-piles) using both displacement and force extraction methods. The experimental campaign results aided in identifying parameters that need investigation to understand extraction mechanics further. The parameters are summarised in Table 3-18.

Table 3-18 summarises parameters for future investigation.

Testing parameter	***Description***
Soil material	• Single soil bed (clay) • Mixed soil bed (clay & sand)
Pile type & dimensions	• Closed-ended pile • Open-ended piles with constant diameters and variable wall thickness
Installation method	• Dynamic (e.g., impact-hammering & vibration)
Embedment time	• Varies from a day to year+
Operational duration	• Apply static load (vertical and horizontal) with varying durations (e.g., a day to year+)
Extraction method	• Force • Displacement & force • Vibration • Vibration & Displacement • Vibration & force

All parameter values should be known to calculate the net ultimate pile pullout capacity analytically; equations are presented below. However, this was not the case herein due to limitations in defining a few of the parameters.

According to [159] Incremental Filling Ratio [IFR] determines by increment of soil plug length [ΔL] and increment of pile penetration depth [ΔD]

$$IFR = \frac{\Delta L}{\Delta D} \cdot 100\ (\%)$$

According to [4] the pile shaft capacity [$Q_s, [N]$] determines by unit shaft friction [$F(z)$, [N/m^2] and side surface of the pile [A_s, [m^2]

$$Q_s = F(z) \cdot A_s$$

To calculate the unit skin friction [$F(z)$] determines by effective vertical stress [σ'_v, [N/m^2], lateral earth pressure coefficient and interface friction angle [$tan\delta, [°]$]

$$F(z) = \sigma'_v \cdot K \cdot \tan\delta$$

To calculate the effective stress [σ'_v, [N/m^2]]; effective unit weight of soil [γ, [kN/m^3]] and pile embedment depth [m]

$$\sigma'_v = \gamma \cdot Z$$

According to [164] the effective weight of the soil (γ') involved in the extraction determines by the specific gravity of solids (G_s), unit weight of water (γ_w), and the soil void ratio.

$$\gamma' = \frac{(G_s - 1) \cdot \gamma_w}{1 + e}$$

Acccording to [164] calculate the soil void ratio

$$e = w \cdot G_s$$

Empirical equations to calculate the net uplift capacity of pile:

Net ultimate pile pullout capacity [Q_0] determines by lateral earth pressure coefficient [K_s], pile diameter [D], unit weight of the soil [γ], embedded length of pile [L] and interface friction angle [$tan\delta$]

$$Q_0 = \frac{\pi}{2} \cdot K_s \cdot D \cdot \gamma \cdot L^2 \cdot tan\delta$$

Net ultimate pile pullout capacity [Q_0] determines by theortical uplift coefficient factor [K_u], pile diameter [D], unit weight of the soil [γ], pile length [L] and interface friction angle [$tan\delta$]

$$Q_0 = \frac{\pi}{2} \cdot K_u \cdot D \cdot \gamma \cdot L^2 \cdot tan\delta$$

According to [173]

$$Q_0 = \frac{\pi}{2} \cdot K_u \cdot D \cdot \gamma \cdot L \cdot tan\delta$$

Accrording to [166] the ultimate pile pullout capacity [Q_0] determines by net uplift capacity factor [A_1], effective weight of the soil [γ], pile diameter [d] and embedded length of pile.

$$Q_0 = A_1 \cdot \gamma \cdot \pi \cdot d \cdot L^2$$

Chapter Four

4 Decommissioning Techno-Economic Assessment of Offshore Wind Fixed Foundations

4.1 Background

In generic terms, decommissioning expenditures (DecEx), also referred to as decommissioning and disposal (D&D) costs or asset retirement costs, represent the costs incurred to undo modifications made on either land [184] or sea-scape. These modifications can include the development, erection, or setup of an asset or plant. As stated by BVG Associates (2019), DecEx encompasses the expenses, at the conclusion of a project's designated life, to remove offshore infrastructure, ensure its safety, and dispose of its components.

DecEx is a significant expenditure in the offshore wind industry that contributes to the levelised cost of energy (LCOE), along with other costs such as capital (CAPEX) and operational (OPEX) expenses. Figure 4-1 depicts the percentages of these three primary expenditures incurred throughout the offshore wind farm's life cycle. Among them, CAPEX and DecEx have the highest and lowest percentages, respectively. The indicated percentage for DecEx is estimated to range between 1% [126], [185] and 1.8% (~2%) [68]. In contrast, the Climate Change Capital (2006) (CCC) estimates DecEx to fall between 2 - 3%. Figure 4-2 provides a detailed breakdown of the main cost elements associated with offshore wind expenditures.

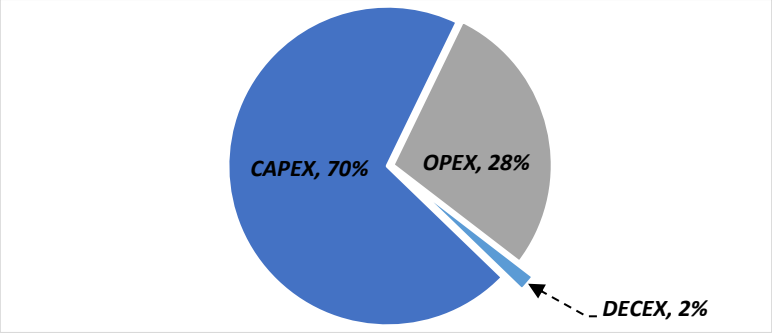

Figure 4-1. Offshore wind expenditures' percentage breakdown.

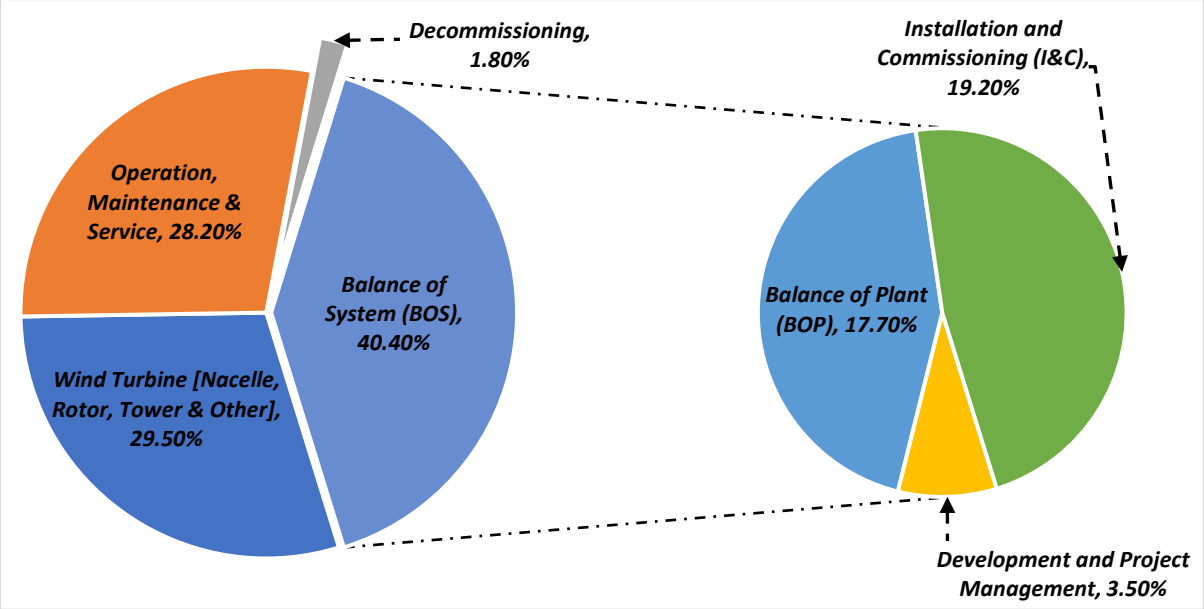

Figure 4-2. Offshore wind cost elements' contribution percentage to levelised cost of Energy (LCOE).

DecEx, as outlined in publicly published offshore wind farm decommissioning programmes, encompasses three stages: pre-decommissioning, decommissioning operations, and post decommissioning. Figure 4-3 illustrates some of the activities associated with these stages. Only a few of the published programmes provide estimates for the expenditures and timelines related to decommissioning, which are summarised in Table 4-1 and

Table 4-2, respectively.

Table 4-1 summarises estimated decommissioning expenditures of offshore wind farms.

Specifications - Authors	[186]	***[108]***	[187]	***[109]***
Wind farm	Thanet	Lincs	Gwynt y M*ô*r	Sheringham Shoal
No. of Tubrines	100	75	160	88
Foundation Type	Mono-piles	Mono-piles	Mono-piles	Mono-piles
Total Capacity [MW]	300	270	576	316.8
DecEx [£]	12,000,000	27,322,000[27]	64,000,000[28]	122,991,592[29]

[27] The estimated costs included vessel time and ancillary activities; furthermore, assumes the disposal costs of the bulk materials once transported to onshore equate to the scrap value of the assets. The estimated costs included 12% contingency.

[28] The estimated costs predict to increase to 106,000,000 because of inflation and interest rate over ten years from 2011.

[29] In 2014, the estimated decommissioning costs, for Sheringham Shaol OWF, are 1,415,515 kNOK; exchange rate used was: 1 NOK = 0.087 GBP. The estimated costs included 30% contingency.

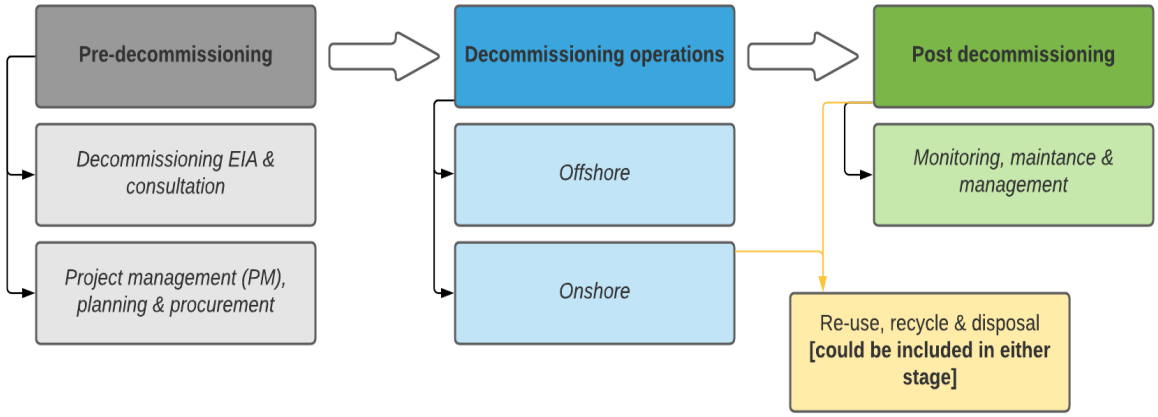

Figure 4-3. Some of the decommissioning stages' activities.

Table 4-2 summarises the estimated time for the first two decommissioning stages' activities.

Authors - specifications	***Wind farm***	***Foun. Type [Turbine No.]***	***Decom. EIA & Consultation***	***PM, planning & procurement***	***Decom. operations***	***Total [days]***
[**186**]	Thanet	MP [100]	-	-	Nine months (270 days) [offshore]	270
[108]	Lincs	MP [75]	12 months (360 days)	36 months (1,080 days)	Six months (180 days[30]) [offshore]	1,650
[109]	Sheringham Shoal	MP [88]	12 months (360 days)	36 months (1,080 days)	Nine months (270 days[31]) average [offshore]	1,710

[30] The estimated duration for offshore decommissioning operations (WTG & foundations) are 258.45 ~ (259) days.

[31] The estimated duration for offshore decommissioning operations range between six to 12 months.

[110]	Greater Gabbard	MP [140]	-	90 days	170 days[32]	260
[187]	Gwynt y Môr	MP [160]	-	-	-	720[33]
[132]	London Array	MP [175]	-	-	360 days	360

Table 4-1, in conjunction with publicly published industrial reports on offshore wind decommissioning costs [68], [112], [188], demonstrates that the decommissioning cost per MW is on the rise. The increase in decommissioning cost per MW since CCC (2006) initial prediction is illustrated in Figure 4-4[34][35]. Additionally, CCC provided a breakdown of decommissioning costs at each stage, as shown in Figure 4-5. It is noteworthy that the cost estimation for decommissioning the Sheringham Shoal wind farm is significantly higher compared to other projects. This discrepancy could be due to calculation errors, a conservative estimation approach, or the complexity of the project.

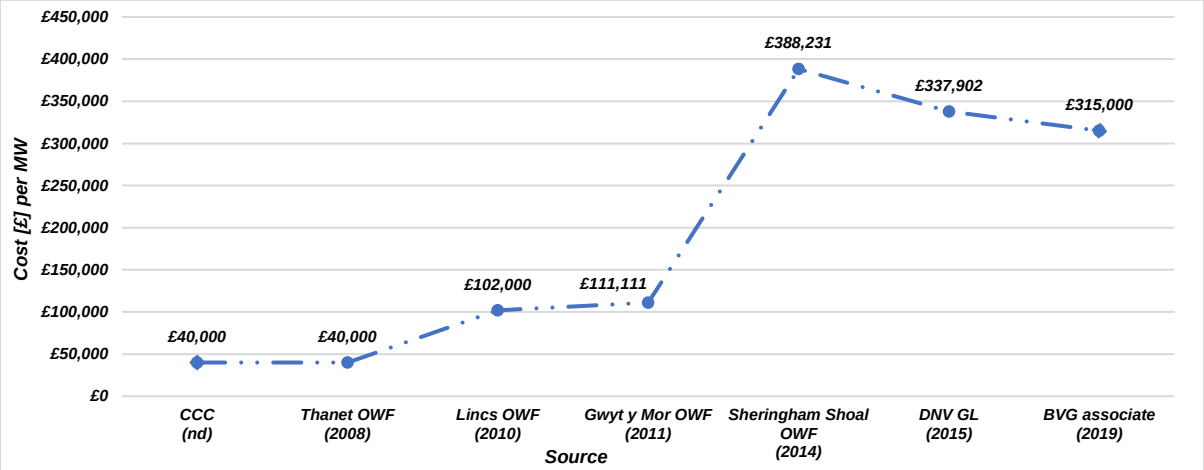

Figure 4-4. The increase in decommissioning cost per MW.

[32] The decommissioning operations' duration for Greater Gabbard offshore wind farm is; 140 days for offshore operations and 170 for onshore operations, including dismantling and disposal, where off and onshore operations will perform parallel.

[33] The duration declared for decommissioning Gwynt y Môr wind farm is 2 years.

[34] The estimation for DNV GL for decommissioning costs ranged between 200,000 - 600,000 euros [excluding transmission assets]; however, the indicated value, in figure [4], had based on the average of the values. The exchange rate used was: 1 Euro = 0.84 GBP.

[35] For 1GW wind farm, the decommissioning cost estimation per MW ranged between 300,000 [68] to 330,000 GBP [231].

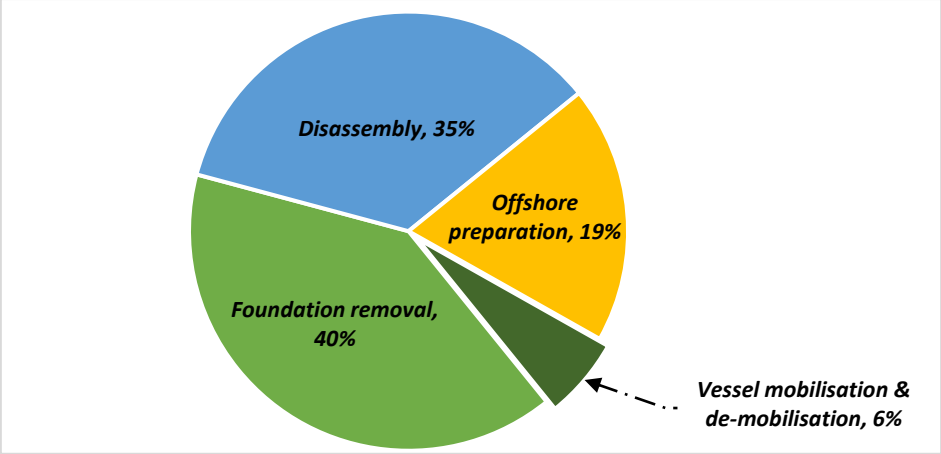

Figure 4-5. Breakdown of decommissioning costs.

[Arup (2018)], commissioned by the Department of Business, Energy and Industrial Strategy (BEIS), estimated a range for the total decommissioning costs of 37 offshore wind farms in the UK, irrespective of projects status, up to 2045. The estimate was based on understanding the forecast costs presented by developers and asset owners. Using a cost model they developed, Arup projected the total decommissioning costs (using 2017 rates and excluding inflation) to be £1.82bn at the baseline, with a range between £1.28bn and £3.64bn[36].

Concurrently with industry initiatives, DecEx has been investigated by various authors using two main approaches. One approach involved the development of a cost and time model that focused exclusively on the decommissioning operations of offshore wind components [99], [189]. The other approach viewed DecEx as a parameter in the development of diverse life cycle models for offshore wind [126], [185]. [Kaiser and Synder (2012)] provided a comprehensive look at all aspects of the installation and decommissioning phases of offshore wind. They assessed related costs by developing a methodological framework. Selected results from these studies are presented in Table 4-3.

Table 4-3 summarises DecEx estimation by scholars.

Authors - specifications	*Total capacity (MW)*	*DecEx (£)*	*Cost (£) per MW*
[185]	**500**	**202,369,500**	**404,739**
[99]	**150 – 1,200 [8 OWFs]**	**-**	**+200,000[37]**
[126]	**504**	**122,860,000**	**243,700**

[36] Arup excluded OFTO costs.

[37] The stated cost is the average cost for all the means of transport. Transprotation methods employed are self transportation (one WTIV & two WTIVs) and multi vessel transportation (non-propelled jack up & two barges).

The extracted data from Table 4-1 to Table 4-3 demonstrates that there is no standardisation or baseline methodology employed by either the industry or academic literature for estimating offshore wind decommissioning time and costs. This leads to inconsistencies in the results. Notably, all the studied sources have adopted the same decommissioning methodologies for offshore wind components, as summarised in Table 4-4.

Table 4-4 summarises decommissioning strategies and methodologies adopted by the studied sources.

Specifications - OWComponents	***OWFoundations***	***WTG***	***Offshore cables***	***Offshore substation foundations***
Decommissioning strategy	Partial removal	Full removal	Left in-situ	Partial removal
Decommissioning methodology	Cut at or below the seabed [1 or 2m]	Reverse of installation	Cut & buried below the seabed [1 - 2m]	Cut at or below the seabed [1 - 2m]

The discrepancies arise because certain projects, such as Sheringham Shoal wind farm [109], provided more detailed data concerning cost estimates compared to others like Gwynt y Môr [187]. Meanwhile, some projects did not conduct a thorough analysis of decommissioning costs and instead relied on forecasted decommissioning costs from neighbouring projects, as seen with the Lincs offshore wind farm [108].

This led to the formulation of the question: "How likely will the following decommissioning methodologies reduce the removal costs of foundations?" This question was posed to experts in both offshore wind and oil and gas industries. The methodologies discussed included: internal or external cutting of the pile (partial removal), and excavation and extraction (full removal), Figure 4-6 illustrates the responses from the experts.

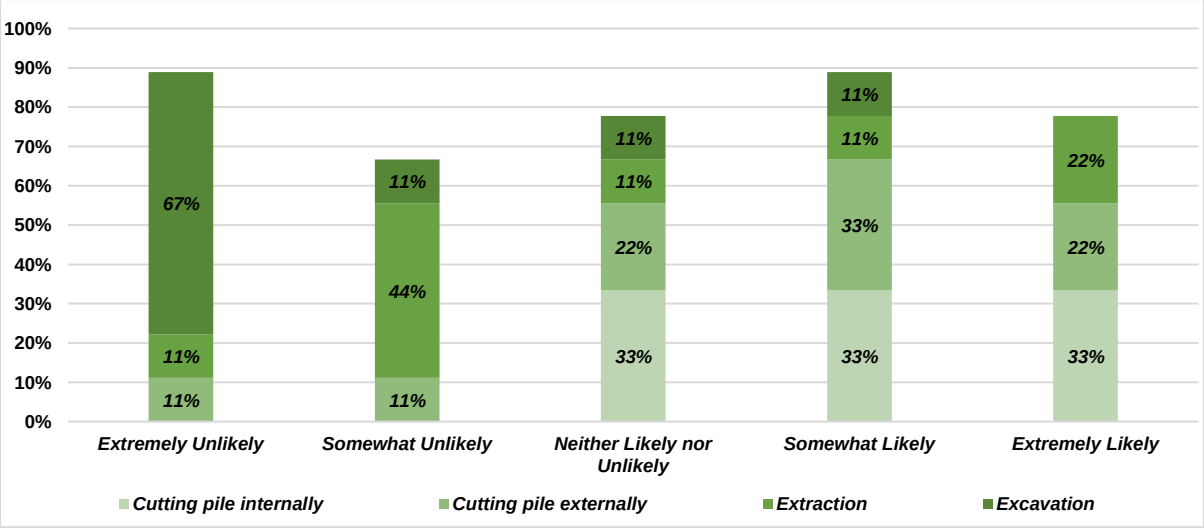

Figure 4-6. How likely each of the covered decommissioning methodologies will reduce foundations removal costs.

Additionally, a techno-economic model framework for decommissioning was developed, focusing solely on OWFoundations. This model aimed to investigate and compare two decommissioning methodologies: the preferred and the proposed. The objective was to ascertain whether a novel methodology would be more cost-effective and time-efficient than the current preferred method, taking various factors into account. Specifically, the goal was to identify parameters or factors that influence time and costs, either increasing or decreasing them, in relation to the preferred decommissioning methodology. Another aim was to explore if there could be a noticeable reduction in decommissioning time and cost by employing a novel methodology. These factors include considerations such as vessels and durations of removal operations, among others. The current preferred methodology involves cutting the pile either internally or externally at or below the seabed level, whereas the proposed method suggests extracting the pile.

The rationale for focusing on OWFoundations includes expanding the definition of decommissioning to encompass not only wind turbines but also their foundations, as decommissioning is essentially the reverse process of installation. Additionally, foundation removal costs represent one of the highest percentages of the total decommissioning costs when using the preferred decommissioning methodology, as illustrated in Figure 4-5. This cost is notable, especially when compared to the removal costs of Wind Turbine Generators (WTG) [68].

4.2 OWFoundations' Removal Operations Duration

The strategies and methodologies for decommissioning offshore wind components significantly influence the duration of removal operations. This, in turn, affects the duration of vessels on-site and, more specifically, their costs, which has broader implications for DecEX overall [53]. This perspective aligns with the feedback received from experts in the offshore oil & gas and wind industries, as illustrated in Figure 4-7. They responded to the question: "To what extent do the durations of removal operations, as determined by decommissioning strategies and methodologies, influence the decision-making process?"

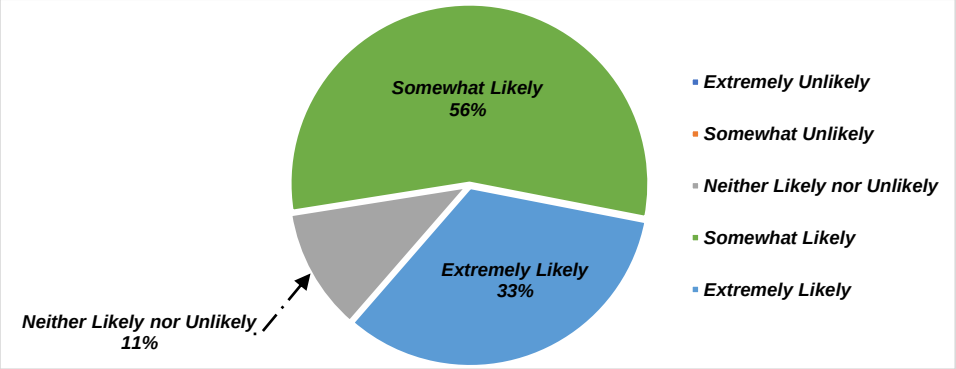

Figure 4-7. How likely offshore oil & gas and wind industries' experts consider removal operations duration in their decision-making process?

To date, decommissioning has only occurred at the earliest offshore wind farms; large-scale decommissioning has not yet been undertaken. Therefore, for currently operating offshore wind farms, the time needed for removal operations – irrespective of the specific decommissioning strategies and methodologies - is still uncertain. Additionally, technologies needed to dismantle the larger structures that currently exist are either undeveloped or not yet available. For example, while existing cutting technologies can handle pile with a diameter up to 3 metres, there are no available technologies to cut piles with a diameter greater than 3 metres [53], [109]. For instance, abrasive water jet cutting could cut $\leq$ 3 meters diameter piles [109].

Consequently, with the research project focusing exclusively on OWFoundations, the removal operations/activities for both the preferred and proposed decommissioning strategies and methodologies have been studied in-depth to establish an approximate duration range.

The preferred decommissioning strategy, out of the two existing strategies, is the partial removal, as evidenced by the publicly published decommissioning programmes, as shown in Table 4-5. This preference largely stems from the fact that the duration of soil excavation operation, even without considering its environmental impact, is shorter for partial removal than it is for full removal. Notably, with the current excavation method for full removal, the excavation diameter increases by 2 meter around the pile for every 1 meter of depth [108], [110]. As a consequence, the full removal strategy through excavation has been omitted here. However, its duration is categorised alongside other foundation removal strategies later in this section.

In essence, the removal operations for the partial removal strategy - irrespective of the methodology – consist of excavation, cutting, and lifting. For the partial removal of

OWFoundations - whether cut internally or externally – excavation occurs either within the pile, around it, or in some cases, both, as illustrated in Table 4-5.

Table 4-5 summarises the proposed decommissioning strategies & methodologies for OWFoundations.

OWFoundations' decommissioning - Authors	[108]	[109]	[110]	[111]
Wind farm name	Lincs	Sheringham Shoal	Greater Gabbard	Burbo Bank Extension
Decommissioning Strategy	Partial removal	Partial removal	Partial removal	Partial removal
Cutting method	Internally	Internally	Externally	-
Excavation method – depth(m)	Internally – 2m	Internally – 2m	Externally – 2m	Internally & externally – 1.5m
Cutting depth (m)	1m (initial)	1m (initial)	1m (initial)	1m (initial)

The method, depth, duration, and equipment used for soil excavation vary depending on the cutting depth, removal methodology, and seabed conditions. For instance, despite the cutting method, the cutting depth is influenced by specific localised factors at each site, such as soil conditions. This leads to variations in excavation depth and duration [108]. Cutting depths for piles embedded in hard rock and sandbanks are 1 – 2 m and 5 – 10 m below the seabed, respectively. This distinction is due to the potential movement of sand over extended time periods [112]. As a result, the initial excavation depth will be 1 metre below the cutting depth for all seabed conditions.

Furthermore, the equipment and methods used for excavation vary based upon pile cutting methods, as demonstrated in Table 4-6. The data presented in Table 4-6 was extracted from the offshore oil and gas industry, mainly from the Brent Field -Alpha Jacket decommissioning programme. This reliance on data from the oil and gas sector arises due to a lack of comprehensive data in publicly published OWFs decommissioning programmes and the offshore wind industry's prospective reliance on offshore O&G in terms of decommissioning strategies, technologies, equipment, experience and methods, among others [109]. The Brent Alpha jacket platform comprises of 32 hollow steel piles with a 1.82m diameter and other legs, such as pontoons, with varying diameters, the largest being 7.32m [113].

Table 4-6 demonstrates proposed excavating equipment for partial removal methodologies in the offshore oil and gas industry.

Excavation - cutting method	***Cutting internally***	***Cutting externally***	***Reference***
Equipment	Drill string (drill pipe, bottom hole assembly & drill pit), OR	Subsea/ seabed dredger; supported by ROV for restricted area	[113]

Excavation - cutting method	*Cutting internally*	*Cutting externally*	*Reference*
	high-pressure water jetting (HPWJ)		
Duration (hr)	Drilling/milling 48h per pile	-	

For the cutting operations of OWFoundations, each cutting method, whether internal or external, involves distinct activities and tools, leading to variations in the duration of removal operations [53], as shown in Table 4-7. Furthermore, there is no standardised procedure for conducting activities for any of the decommissioning methodologies associated with OWFoundations. For instance, while both the Burbo Bank Extension and Lincs wind farms proposed cutting the pile internally, they each outlined different activities and sequences, as illustrated in Table 4-8.

Table 4-7 summarises the proposed equipment for cutting piles internally and externally in offshore oil & gas and wind industries.

Cutting Method	*Cutting equipment*	*Deployment method*	*Duration (hr)*
Cutting internally	Abrasive mechanical jetting (AWJ)	Lowering from the vessel	12
Cutting externally	Diamond wire cutting (DWC)	ROV or sea crawler	7
Reference	[99], [109], [113]	[113]	

Table 4-8 compares removal activities proposed for cutting the pile internally.

Scenario 1: Burbo Bank Extension wind farm [111]	***Scenario 2: Lincs wind farm*** [108]
Cut & lift the TP, and load it to the vessel/barge	Excavating within the MP
Inspect the foundation or/ and re-instate lifting attachment	Deploying cutting tool
Excavating with the MP	Attach TP & MP to vessel's crane
Deploying cutting tool	Cut the pile internally
Cutting the pile internally	Lift & load the MP & TP to the vessel/ barge
Lift & load the MP to the vessel/ barge	-

The activities outlined in Table 4-8 clearly indicate that scenario one will take longer than scenario two. Furthermore, there may be a need for an additional vessel for the removal of the transition piece, which will influence DecEx. This estimation with the foundation removal operations' duration estimated in the decommissioning programmes of Lincs and Sheringham Shoal wind farm, as depicted in Table 4-9.

Table 4-9 summarise the estimated duration for offshore wind foundations removal operations.

Removal duration – References	[108]	[109]
Wind farm name	Lincs	Sheringham Shoal
TP	-	Minimum 4 – maximum 7 [average 5]

MP	Average 0.5 days for one foundation[38] (include TP) [12 hrs]	Minimum 8 – maximum 15 hrs [average 11]

The data provided earlier indicates that the duration of removal operations for OWFoundations, regardless of the cutting methods used, is likely to exceed 11 hours as a minimum. This introduces a significant degree of uncertainty. The uncertain nature of the duration, combined with the current unavailability of technologies for partial removal methodologies, prompted the following questions: How likely is it that the industry will consider decommissioning OWFoundations through existing and proposed removal methodologies? Moreover, which technology or method, whether it's existing, proposed, or entirely new, will likely see development in the coming years?

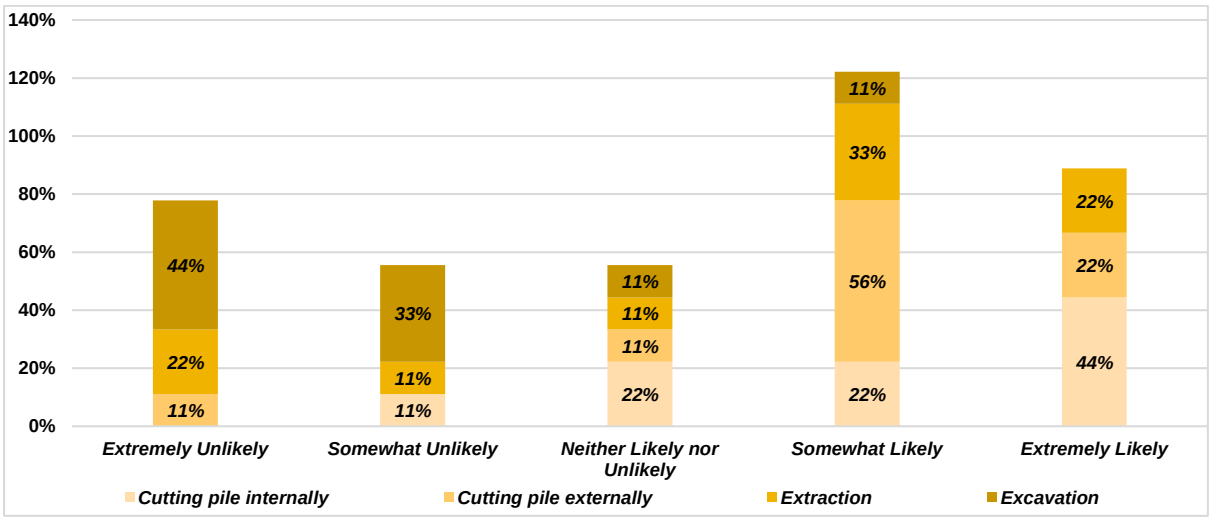

Figure 4-8. How offshore O&G and wind industries experts will likely utilise existing and proposed removal methodologies for offshore wind foundations, relying on their durations.

[38] For Lincs wind farm, the estimated duration for the removal of ten foundations is five days.

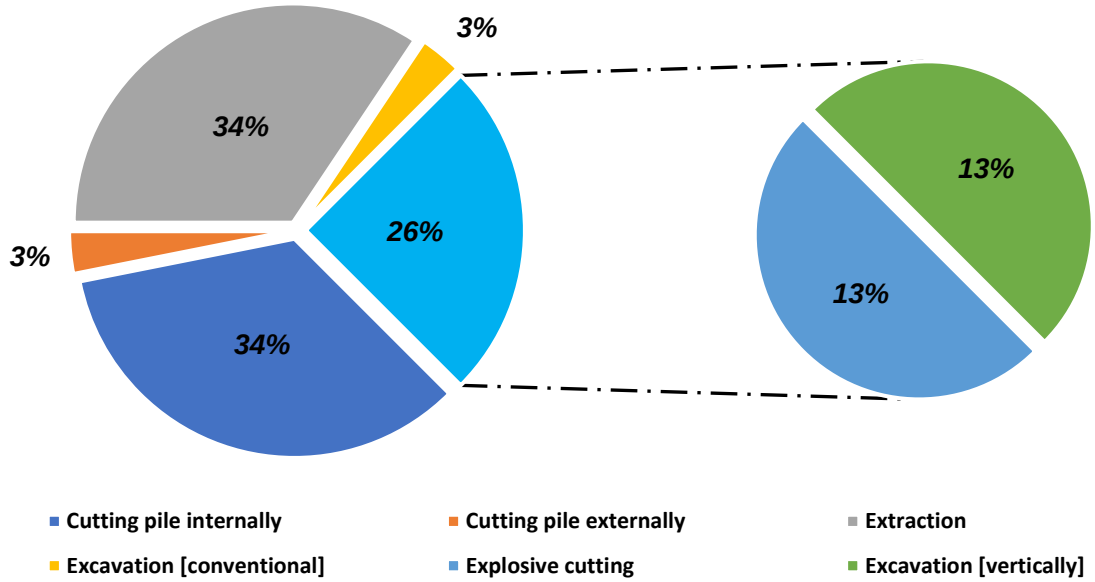

Figure 4-9. The percentage of OWFoundations decommissioning methodologies supported by offshore oil & gas and wind industries' experts.

The questions raised align with the BEIS recommendation, emphasizing the need to innovate and develop new decommissioning methodologies to reduce costs and time [53]. Moreover, the intent was to gauge the offshore wind industry's acceptance of the proposed decommissioning method, specifically extraction, for OWFoundations. Responses to the questions, shown in Figure 4-8 & Figure 4-9, were sourced from experts in both the offshore oil & gas and wind industries.

The feedback received suggests that the most probable method for OWFoundations removal is first cutting the pile internally, followed by extraction, and then external pile cutting. Moreover, the responses indicated the potential development of diverse methodologies, such as vertical excavation and explosive cutting, in addition to refining existing and proposed methods. Notably, the experts predominately favoured the extraction method and the internal pile cutting approach, with both methods each receiving 34% support.

Extraction is essentially the inverse of the installation process. Consequently, it is hypothesised that its duration will align closely with that of installation. The key activities involved in extraction include break plus pull-out and lifting. Possible methods for pile extraction encompass the use of vibro-hammers [190], hydraulic mechanisms [191], or through force or displacement control.

Extraction was first executed in the offshore wind sector at the Lely wind farm. The Lely wind farm comprises of four foundations, each measuring 26 metres in height, with diameters

ranging between 3.2 - 3.7 metres. A vibratory hammer was used to extract all of its foundations from the seabed, taking only three hours in total, which averages to about 45 minutes for each foundation [190].

Table 4-10 categorises the duration range for the existing and proposed removal methodologies for OWFoundations.

OWFoundations decommissioning methods – duration (hr)	***Minimum***	***Maximum***	***Average***
Cutting methodologies [partial removal]	11	24	18
Excavation [full removal]	24	-	-
Extraction [full removal][39]	6	10	8

The discrepancies in activities, sequencing, and tools for OWFoundations removal methodologies, as demonstrated earlier, combined with the limited data in the publicly published decommissioning programmes and the unavailability of removal methodologies' technologies, led to the following simplifications, exclusions, and assumptions:

1. Duration and costs associated with personnel and removal tools, such as seabed crawlers, ROVs, and seabed dredgers, were excluded from the OWFoundations decommissioning cost and time model. It should be noted that excluding these costs will result in reduction of the total expenditures of decommissioning offshore wind foundations, regardless of whether the reduction amount was a fraction or substantial.
2. To maintain consistency across all removal strategies and methodologies for OWFoundations, it was assumed that transition pieces would be removed before the foundations.
3. Due to the lack of specific data regarding the durations for excavation and cutting operations, it was assumed for simplicity that the durations for all partial removal methodologies were the same.
4. Given the uncertainties surrounding the duration of foundation removal operations, the durations for all removal methodologies were grouped within a specific range, as shown in Table 4 10. The default duration for foundation removal operations, in this context, represents the average and encompasses both excavation and cutting for partial removal strategies and extraction operations for full removal strategies.

[39] Foundations of Greater Gabbard OWFarm installed within 6 to 8 hours [average of 7 hours].

Bullet 4-1

Up to this point, none of the studies, including the ones mentioned earlier, have delved deeply into the effects of various decommissioning strategies and methodologies on a single structure, be it existing or new, with respect to DecEx and time. Instead, a limited number of studies, notably reference [53], have explored the consequences of the removal operations' duration for one specific decommissioning methodology – typically the preferred one – for different offshore wind components, such as the WTG, tower, and foundation. An example would be the partial removal methodology applied to offshore wind foundations.

4.3 Wait-on-Weather

Weather is a pivotal factor influencing the total cost and the scheduling and duration of offshore activities throughout a project's lifecycle. The harshness of the marine environment poses risks to the safety of personnel and the vessel in use, which can lead to project delays that span days or even weeks. In essence, offshore tasks at various phases of a project might be postponed owing to weather-related interruptions. This influence of weather on vessel operations is evident in Figure 4-10.

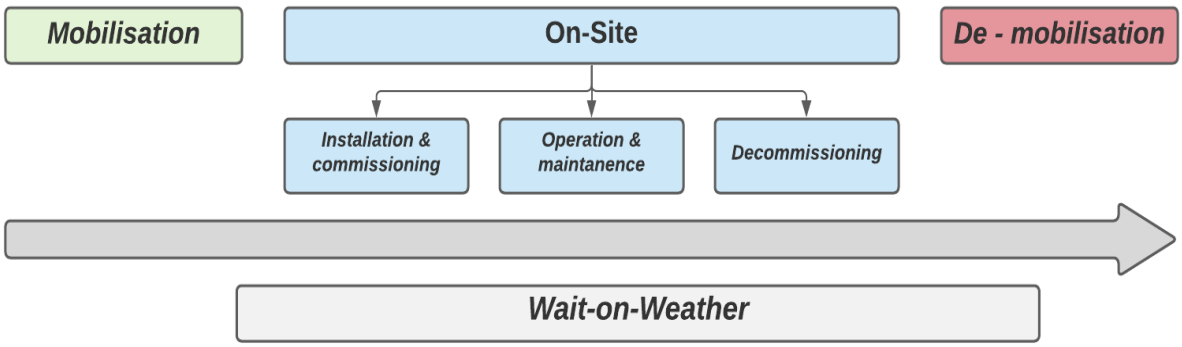

Figure 4-10. The stages where the utilised vessels could experience potential delays due to wait-on-weather.

Wait-on-weather (WOW), also termed as weather downtime, occurs when specific weather conditions exceed the standard or permissible operating limits of vessels for conducting offshore activities [71]. Such weather conditions primarily encompass wind speed and wave height.

Wave height plays a crucial role in restricting the movement of vessels. Regardless of the vessel type, an excessive wave height can hinder the transit from one location to another and affect the elevation of jack-up vessels or barges at a particular site. This constraint is often related to the vessel's significant wave height [H_s], commonly referred to as the wave height limit [71],

[192]. Conversely, wind speed significantly affects the operational capacity and safety of crane vessels. Specifically, it impacts their ability to securely hold, instal, or remove components [71], [99].

Wait-On-Weather (WOW) can differ considerably depending on several factors related to the wind farm. For instance, the farm's location, size, and metocean data play pivotal roles in determining the frequency and intensity of WOW incidents. Wind farms located farther from the shore and at greater depths in the sea or ocean tend to face more extreme weather conditions compared to those closer to the shore. As a result, offshore farms in deeper and more remote locations often necessitate the use of vessels equipped to handle higher environmental criteria, ensuring safety and operational efficiency in such challenging conditions.

Using the vessels with higher environmental criteria in deep or open sea regions can significantly extend the operational weather window. For instance, in an area where the wave height is typically around 2 metres but can rise or exceed 3 metres during specific times of the year. Wind Turbine Installation Vessels (WTIVs) would theoretically be operational for about 70 - 80% of the year. This is because their significant wave height tolerance falls between 1.8 m - 2.5 m, as illustrated in Figure 4-11. On the other hand, self-elevating jack-up barges, which have a significant wave height range of 1.2 m – 1.5 m, would be operational only about 40% of the year, or even less. This highlights the importance of selecting the right vessel for the specific conditions of the project site to optimise operational efficiency and manage costs.

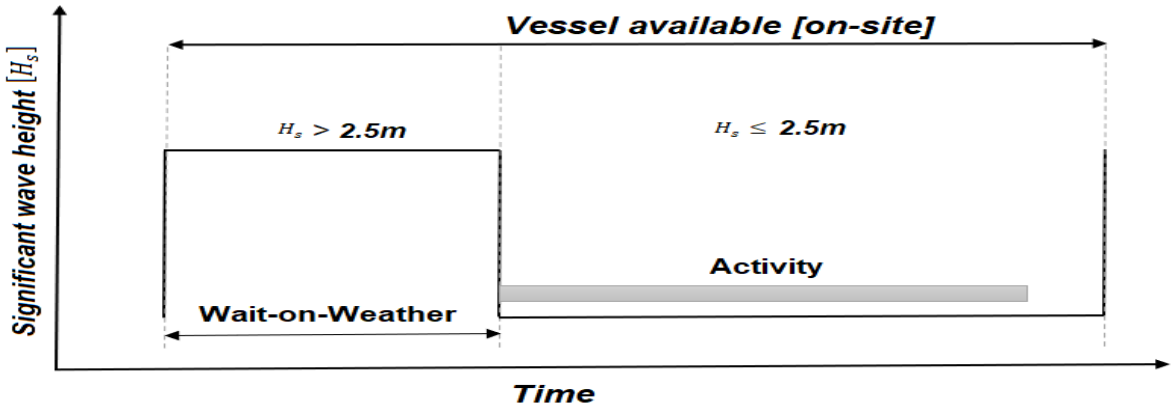

Figure 4-11. The impact of H_s on-site on completing offshore activities utilising Wind Turbine Installation Vessels.

Moreover, not all jack-up vessels/barges currently in operation have the capability to remain elevated on-site during extreme weather conditions. This often necessitates their mobilisation to a safer location. As a result, weather conditions are a paramount consideration in offshore wind projects, influencing not only vessel selection but also the overall project cost, schedule,

and duration of its phases. This underscores the necessity of meticulous planning and robust decision-making to ensure project efficiency and safety.

In the decommissioning phase of offshore wind farms, there is variability in how different projects account for the impact of wait-on-weather on operations. A few publicly available decommissioning programmes have factored in the influence of WOW on their projected decommissioning timelines. For instance, in the Thanet offshore wind farm's projections, the average time allotted for the decommissioning, removal, and loading of a WTG onto a transport barge – including the time allowance for WOW - totals two days [186]. Contrastingly, for the Lincs wind farm, the average allowance for WOW spanned three days for the removal of nine WTGs, and two days for the removal of eight foundations [108]. However, this consideration is not universal. Other published decommissioning programmes, such as those for the Greater Gabbard and Sheringham Shoal wind farms, have not incorporated WOW contingencies into their estimated durations for component removal [109], [110]. This inconsistency in planning underscores the need for a standardised approach to account for weather-related uncertainties during decommissioning, ensuring both safety and efficiency in project timelines.

Given the preceding data, it's clear that meticulous planning and consideration for WOW is paramount for all activities across all phases of a project. In this context, WOW was duly incorporated into the removal operations' duration for offshore wind foundations. For the sake of clarity and consistency, the adjustment weather factor, denoted as $ADJWEATHER$, was employed to gauge the operative window for vessels. This methodology is in line with the approaches adopted by other researchers in the field [70], [126]. The adjustment weather factor serves as a metric to estimate the amount of time the vessels can operate. For example, an $ADJWEATHER$ value of 100% signifies an uninterrupted operational flow with no weather-induced delays. On the other hand, an $ADJWEATHER$ value of 75% suggests that vessels are non-operational 25% of the time due to weather constraints. Adopting such a standardised approach facilitates more accurate project planning and ensures all potential weather-related delays are factored into the operational timeline.

Despite the profound influence of WOW on the duration and cost of project phases, there was an imperative need to moderate the impact of the adjustment weather factor in this context, without completely negating the effect of WOW. One rationale behind this decision was to ensure that the influence of critical inputs, such as the duration of vessels and foundation removal operations, on decommissioning expenditures remains paramount. As a result, a

pragmatic baseline for adjustment weather factor was set at 80%. This offers a balanced approach, ensuring that while the impact of WOW is accounted for, it does not overshadow other vital components of the project. Nevertheless, to comprehensively understand the ramifications of WOW on the duration and cost associated with OWFoundations' removal operations, a sensitivity analysis was undertaken. This analysis utilised a spectrum of adjustment weather factors, spanning from 50% - 100%, offering a holistic view of potential scenarios and their implications.

Statement 4-1

By consensus, summer months are the preferable window for offshore activities, given that the WOW in June is not the same as in December [71], [126], [186], [187]. However, there's always a risk of not finishing the activities before winter sets in, potentially extending the activities over two years or more, regardless of the project phase or the efficacy of planning. Should offshore activities spill over into the autumn or winter months, the vessels will have fewer operating days, leading to increased non-working days and costs. The foundation installation at the Greater Gabbard offshore wind farm illustrates this point. Specifically, 69 and 71 mono-piles were installed in the autumn [3 months] and winter [3 months] of 2009 and summer [3 months] 2010, respectively [193]. This underscores the fact that weather remains a formidable challenge in the offshore wind industry.

4.4 Vessels

4.4.1 Background

The installation and decommissioning of offshore wind farms' super and sub-structures necessitate specialised vessels. This is primarily because the unique challenges posed by the towering heights above and the significant depths below the mean sea level demand tailored solutions for each component across its lifecycle. Consequently, the availability and appropriateness of vessels to undertake transportation and various activities throughout the project's designated lifetime are fundamental to offshore wind development.

The term "Vessels" is used interchangeably with "installation vessels" and "decommissioning vessels" throughout this document. This usage is because, regardless of the terminology, one or more types of vessels might be employed for both the installation and decommissioning of a component. As such, the term "vessels" encompasses all appropriate vessel types, which are

detailed in subsequent sections, used for the installation and/or decommissioning of OWFoundations.

Throughout the evolution of offshore wind development, it has been evident that there is not – and never has been – a definitive answer regarding the most suitable vessel type(s) for use [99]. This assertion is especially valid during the installation of offshore wind farm components. For example, OWFoundations, such as mono-piles and jackets, can be installed using either heavy-lift (floating) vessels or jack-up vessels [68].

Furthermore, vessels have consistently emerged as one of the primary bottlenecks[40] in the offshore wind sector. This issue became particularly noticeable during the dawn of the large-scale commercial project development era, as exemplified during the installation of the Middelgrunden wind farm.

From a historical perspective, the installation of initial offshore wind projects (Middelgrunden wind farm) projects was relatively straightforward and unproblematic because they were on a smaller scale. As such, projects utilised what was readily available at a minimal cost. However, during the installation of the Middelgrunden wind farm, several challenges arose, including weather-related delays and vessels running aground in shallow depths, among others.

These challenges highlighted a crucial realisation within the industry: vessels used for the installation of initial projects were ill-equipped to handle the installation of larger, future commercial projects. Limitations in the lifting and transporting capacities of these vessels, along with their inability to operate in open seas and under challenging offshore conditions, were some of the primary concerns [71].

The aforementioned reasons, combined with other factors, led companies such as Mayflower Energy to design new, advanced wind turbine installation vessels (WTIVs) tailored to meet the specific needs of the offshore wind sector. Several contributing factors to this shift include that many of the vessels previously used were seen as temporary solutions, having been originally built for other marine industries. Additionally, much of the state-of-the-art vessel equipment was unavailable for wind projects because it was predominately booked by the oil and gas industry [46], [71].

[40] Bottlenecks are supply chain shortage/ unevenness, whereby the demand outgrows the supply chain capacity.

The current offshore wind market features a diverse range of vessel types, making up large fleets available for charter to either install or decommission offshore wind components. Globally, the vessel fleet stands at 137 vessels, with 82 being jack-ups and 55 being heavy-lift (floating) vessels. Of these, 61% and 39% are in Europe and China [40].

Despite the current size of the global fleet and the anticipation of more vessels entering the market, vessel availability will continue to be a bottleneck in offshore wind due to its rapid expansion. For example, offshore wind is breaking into new markets like Asia and North America, while simultaneously expanding in capacity in Europe.

The offshore wind market in China underscores this point, as there is ongoing installation rush with a capacity of over 10GW under construction. The goal is to connect offshore wind projects to the grid before the end of 2021. However, the country's existing vessel capacity can only support the installation of approximately 6GW per year [40]. China successfully installed a new offshore wind capacity of 17 GW in 2021.

In Europe, the current fleet of vessels, regardless of their types, is well-suited for installation of offshore wind turbines with capacities up to 8MW [194]. Only a handful of these vessels are equipped to handle turbines with capacities of 10MW or more, for instance, turbines like GE's Haliade-X [12 – 14MW] [40], [195]. Drawing from the inaugural global offshore vessel database, as presented by GWEC Market Intelligence, the operational jack-ups have been delineated. Out of more than 50 jack-ups, specific ones are earmarked for installing turbines of various capacities [40], as demonstrated in Figure 4-12.

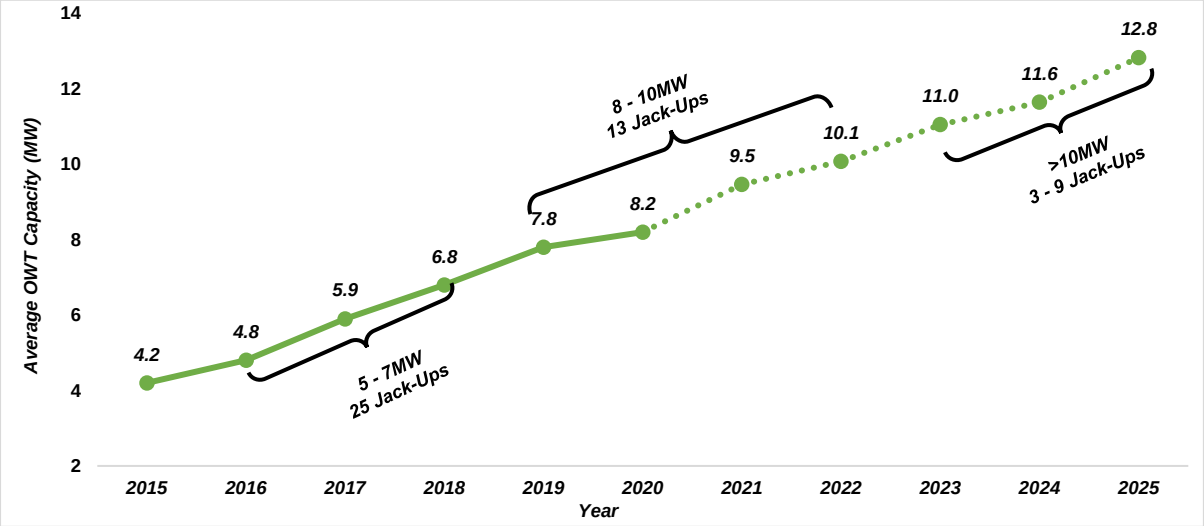

Figure 4-12. The number of in-operation Jack-Ups capable of installing wind turbine capacities.

Therefore, for Europe, both from current and forward-looking perspectives, given the rapid pace of innovation in offshore win and the expansion of its structures, coupled with the onset of the next generation (mega-sized) turbine capacity era, the existing vessel fleet might fall short of the projected demands in the coming years. This could lead the offshore wind industry to consider converting oil and gas heavy-lift (floating) vessels [195], as was done in the early stages of offshore wind development. Simultaneously, the smaller vessels currently in use may find opportunities in emerging markets or be repurposed for other roles, such as maintenance and servicing jobs [194].

Statement 4-2

Throughout the evolution of offshore wind energy, vessels have consistently played a pivotal role in market growth. Yet, paradoxically, they have also emerged as a significant bottleneck for both the expansion and cost optimisation of offshore wind. For example, with a limited supply of vessels that cannot keep pace with the surging demand of the offshore wind sector and its escalating infrastructural needs, there's a theoretical risk that the growth trajectory of offshore wind structures might plateau. Additionally, this imbalance could lead to persistent escalation in the construction costs and charter rates (e.g., daily rates) for vessels.

Bullet 4-2

Up to this point, the offshore wind industry has primarily centered its attention on the influence of vessels in terms of costs, availability, among other factors, on its growth and expansion. Conversely, there has been minimal focus on the impending decommissioning phase and its potential implications.

4.4.2 Vessel Strategies

To date, two vessel strategies have been employed in the offshore wind industry: feeding and transiting. These strategies aim to utilise a combination of vessel types and quantities for the transportation and installation [46], [196] or eventual decommissioning of wind farm components.

For example, the OWFoundation, such as a mono-pile, can be both transported and installed using jack-up vessels. Alternatively, transportation can be carried out by either tugs or platform supply vessels, while installation can be done by heavy-lift (floating) vessels like sheerleg [68]. A comparison of these strategies can be found in Table 4-11.

Table 4-11 compares feeding and transiting strategies.

Vessel strategies in offshore wind			***Reference***
Strategy	***Feeding***	***Transiting [one vessel type only]***	
Purpose	Transit Only	Transit and either install or decommission	[196]
Vessel utilisation degree	High	Low	
Advantage	Time-Saving [components continuous flow]	No additional vessels	
Disadvantage	High cost and risk	Time-consuming	

The decision to select a specific vessel strategy depends on and is influenced by various factors. These factors encompass the risks associated with transportation and operation, the number, type, and charter costs of the utilised vessels and/or barges, the size and weight of the components, and the distance to the shore, among others [46], [68], [70].

The feeding strategy has not been as prevalent in the offshore wind industry as the transiting strategy. A primary reason for this is the associated risks of loading operations from the feeder to the installation vessel and vice-versa. Nonetheless, the feeding strategy may be considered if the charter rate for the feeder is lower than that for the installation vessel and does not result in an increased risk.

In this context, while the term "feeder" is used to describe one of the vessels strategies during installation, the term "sender" is the antonym to the term "feeder" – is introduced and used in reference to decommissioning activities.

Statement 4-3

The prevailing use of the transiting strategy in the offshore wind installation market potentially provides insights into the vessel strategy that might be preferred for future decommissioning operations. This perspective is consistent with the vessel strategy proposed for the removal operations of turbines and foundations at the Sheringham Shoal wind farm, where two self-propelled jack-up vessels are planned to work concurrently [109].

4.4.3 Vessel Types

Offshore wind utilises a variety of vessel types for both the installation and decommissioning of wind farm components. Some of these vessels were originally constructed for other offshore industries, such as marine civil engineering and oil and gas. However, in response to the

specific needs and growth of the offshore wind sector, many have been freshly designed and built [46], [196].

The roster of vessels used encompasses a range, including but not limited to, cable laying and burial vessels, offshore substation transport and installation vessels, turbine and foundation installation vessels, and those dedicated to operations and maintenance, among others. Importantly, it should be noted that a single vessel type might be employed for the installation and/or decommissioning of multiple components of an offshore wind farm. For example, heavy-lift (floating) vessels, such as semi-submersibles and crane ships (e.g., sheerlegs), can be used both for installation and decommissioning of offshore substations and OWFoundations.

The emphasis in this context is strictly on vessel types that have the capacity to install offshore wind turbines and their foundations. An important rationale for focusing on turbine installation vessels is the fact that a significant proportion of operational vessels, have been and continue to be used for the installation of both foundations and turbines. This demonstrates the versatility and multi-purpose functionality of these vessels in the offshore wind industry.

However, with the current and anticipated advancements in the specifications of turbines and foundations, such as foundations weighing in excess of 1,000 tonnes - there will be a pronounced divergence in the fleets of installation vessels. As a result, heavy-lift (floating) vessels are expected to see increased utilisation in the installation of OWFoundations. This is largely due to the limited number of self-propelled jack-up vessels possessing the requisite lifting capacities [68]. Given these dynamics, the primary vessel types designated for the installation of turbines and foundations are Wind Turbine Installation Vessels (WTIVs) and Multi-Purpose Vessels (MPVs).

The types of MPVs encompass self-propelled jack-up vessels and barges, self-elevating jack-up barges, and heavy-lift vessels (HLVs). MPVs were originally constructed for diverse fields of activity. However, many underwent partial conversions to be temporarily utilised in the offshore wind sector; such as, they are often considered as the first generation of vessels tailored for offshore wind projects [196]. A case in point is A2SEA, now known as the DEME Group, which converted two feeder vessels specifically for the installation of turbines at the Horns Rev 1 wind farm [46].

While WTIVs (Wind Turbine Installation Vessels) are, as the name suggests, vessels explicitly built to perform offshore wind activities, particularly installation. WTIVs and multi-purpose self-propelled jack-up vessels share design similarities, which will be detailed in subsequent sections. For the sake of clarity and simplicity, WTIVs are categorised under the self-propelled jack-up type in this context.

4.4.3.1 Self-Propelled Jack-Up

Self-propelled jack-up vessels, barges and WTIVs are all subtypes of self-propelled jack-up (SPJU) [192]. A comparison between these types is provided in Table 4-12. These types of vessels can operate independently when it comes to propulsion, positioning, and elevation, without depending on the availability or limitation of tugboats or towing vessels. In essence, they have the capability to perform all operations - from loading and transportation to installation - without assistance or dependence on other vessels [71], [196].

However, designs vary; for example, jack-up vessels and WTIVs have a ship-like shape, while jack-up barges feature a flat bottom. It is important to highlight that the design of both vessels is similar, with the distinction being in the optimisation of deck space and load capacity, transit speed, and lifting capability in the case of WTIVs.

Table 4-12 compares self-propelled jack-up types.

Specifications	***Multi-purpose Self-Propelled Jack-Ups***	***WTIVs***
Generation	first	second
Field/ purpose	multi-fields (e.g., offshore oil and gas and offshore wind)	single field (offshore wind only)
Example	Kraken	Wind -previously known as Pacific- Orca
Offshore wind projects	Walney wind farm (1 & 2) & Greater Gabbard	Rampion
Reference	[193], [197], [198]	[199]–[202]

The subsequent discussion will be centered exclusively on WTIVs, as they were intentionally designed and built for offshore wind, in contrast to multi-purpose self-propelled jack-up types. The motivation behind the development of WTIVs was to guarantee efficient and rapid turbine installations in response to the surging demand for offshore wind farm installation processes. Additionally, the expansion in offshore super and sub-structures specifications, their numbers, distance from the shore, and water depth all played a role [46], [203]. With ongoing enhancements in their capabilities, WTIVs can now install a turbine in less than two days.

The first WTIV to enter the market was the MPI Resolution in 2003, with specifications summarised in Table 4-13. Formerly known as Mayflower Resolution, it was later followed by the Resolution and TIV Resolution.

Table 4-13 summarises the specifications of MPI resolution.

MPI Resolution Specification		***Reference***
Maximum transit speed (Knot)	11	[196], [204]
Maximum transport capacity - turbines	10 - 3.5MW	
Lifting Capacity (Tonnes)	Upgraded from 300 to 600	
Minimum/ Maximum Water Depth (m)	5/ 33.5 - 35	
Maximum Wind Speed (m/s)	15.5	
Maximum Wave Height (m)	3	
Number of linked Projects	~23	[205]
Countries [Offshore Wind Farms]	UK [Burbo Bank, London Array], Germany [Arkona]	

Currently, there are between 16 and 32 in-operation WTIVs globally, excluding China, with an additional 5 to 7 under construction or ordered [195], [206], [207]. However, there is inconsistency regarding the number of vessels capable of installing or supporting wind turbines with capacities greater than 10MW. For instance, some sources report there are three [194], others say four [195], while some even mention nine [40] such vessels worldwide.

4.4.3.2 Jack-Up Barge

The jack-up barge (JUB) is a self-elevating, non-self-propelled barge that can either be self-positioning [71] or tugged–positioning [196]. JUBs depend on tugboats, specifically towing tugs, for transit to and from the site, making their movement comparatively slow. Nonetheless, under certain weather conditions, self-positioning JUBs are capable of on-site movement [71].

JUBs differs from SPJU types in terms of manoeuvrability and size. A comparison between JUBs and Self-propelled Jack-Up types is presented in Table 4-14. Typically, JUBs are smaller than WTIVs since they are designed to remain on-site to facilitate the installation of offshore wind turbines or foundations.

Table 4-14 compares a few specifications of JUB and SPJU.

Specification	*JUB*	*SPJU*	*Reference*
Self-propulsion	No	Yes	[70], [71], [196]
Self-elevating	Yes	Yes	
Self-positioning	Varies	Yes	
Speed (Knots)	Four - Eight [depending on tugboats speed]	+10	
Capacity - turbines	Two - eight	+8	

A JUB positioned on-site for installation will necessitate one or more barges, either self-propelled or towed, serving as feeders. This approach ensures a continuous flow of components, thereby eliminating any waiting or transit times. Consequently, JUBs can be viewed as either installation platforms or feeder barges [196]. For example, during the Robin Rigg wind turbine installation, A2SEA's Sea Energy vessel served as a feeder, transporting turbines to the SeaWorker barge for installation [71], [208].

Statement 4-4

To date, there is no single jack-up vessel or barge that can operate effectively on all seabed types, whether soft or hard. In addition, those that cannot remain securely elevated on-site in extreme weather conditions and need to be moved to a safer location are not suitable for use. One reason for this is the unpredictability of the time needed to extract the penetrated legs of the jack-up vessels or barges from the seabed [192].

4.4.3.3 Heavy-Lift Vessels

Heavy-lift vessels (HLVs), also referred to as crane ships, floating HLVs, or floating equipment, are non-elevating, self-propelled hull vessels. These can have a flat-bottomed or ship-shaped hull and are equipped with high-capacity cranes. To maintain their position offshore, HLVs either use dynamic positioning (DP) or anchor-based mooring. It's important to note that larger HLVs are self-propelled, smaller ones require tugboats for towing to the site.

In the early 2000s, HLVs began to play a role in the offshore wind industry, primarily for the installation of foundations and substations. One reason HLVs were chosen for foundation installation is that the crane's height is not a crucial factor. However, they are seldom used for turbine installation due to limitations in lifting height and sensitivity to conditions [70], [196]. There are several types of HLVs, but only four are typically used for foundation installation, irrespective of their unique specifications and cost. These are illustrated in Table 4-15, where some of their specific features are also listed.

Table 4-15 summarises a few specifications for HLVs' four types.

HLV Types	*Speed (knot)*	*Positioning*	*Example*	*Reference*
Sheerleg	6 - 7	-	Rambiz	[209]
Semi-Submersible	6	Dynamic - DP3	Thialf	[210]
Mooring Heavy Lift Crane	10	Mooring – Anchor	Stanislav Yudin	[211]
DP2 Heavy Lift Crane	17	Dynamic – DP2	Jumbo Javelin	[212]

When employing HLVs (e.g., sheerlegs) for installing OWFoundations, the feeding strategy will typically be used. This involves transporting foundations either by feeder vessels (like platform supply vessels) or by towing with tugs [68], [70]. For a more cost-effective approach, other heavy-lift vessels, such as the Seaway Yudin, can offer an alternative to the typical feeder strategy. This is achieved by leveraging its transit speed to transport offshore structures directly on-board [211]. At present, there are 55 HLVs in operation worldwide, with 32 of them located in Europe. Additionally, five more are currently under construction, specifically designed for the industry [40].

4.4.4 Vessels Costs

The costs associated with vessels, irrespective of the types previously discussed and the project phases (be it installation, operation and maintenance, or decommissioning), can be categorised into three main components: mobilisation, charter rate, and de-mobilisation [192]. Figure 4-12 provides a detailed breakdown of vessel costs specifically for the decommissioning phase of offshore wind projects.

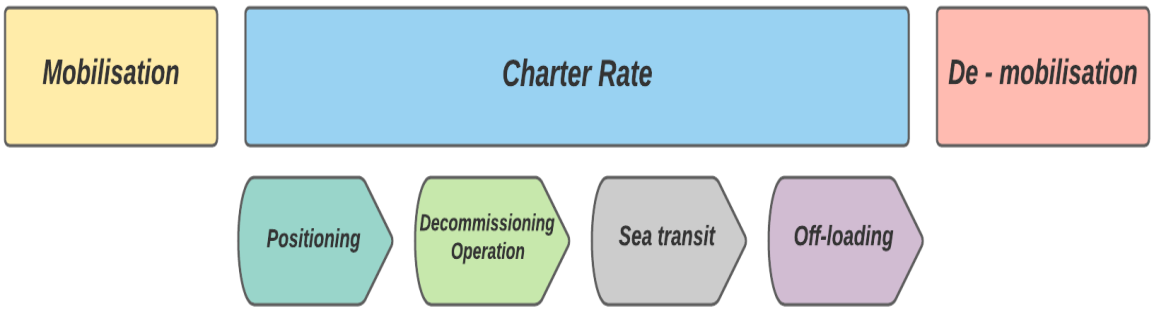

Figure 4-13. Vessels' cost breakdown for the offshore wind decommissioning phase.

At its core, mobilisation and de-mobilisation costs pertain to the expenses incurred to position the vessel at the necessary location. Specifically, mobilisation cost involves the expense of moving the vessel from its existing location to the location specified by the charterer, which

could be a port or a specific site [70], [71]. Additionally, it's worth noting that the costs for mobilisation and demobilisation are often several times the charter rate.

The charter rate, often referred to as the day rate, represents the cost of leasing a vessel for a single day. This rate is influenced by several factors including market conditions, vessel availability, and the duration of the charter (or contract length). For example, charter rates are likely to be higher in a spot market or for short-term charter periods (such as 30 days) in comparison to longer contract durations, like three months or more [71], [192].

In summation, the costs or rates mentioned above are shaped by various determinants, including but not limited to, market availability, vessel usage duration, vessel specifications such as type, speed, crane capacity and deck size. Other influencing factors are waiting due to weather conditions, site specifics like location, the number and specifications of turbines, the nature of the seabed, water depth, among others [192], [213].

4.4.5 Vessels in Offshore Wind Decommissioning

The decommissioning plans for offshore wind farms have outlined diverse vessel strategies and types for the removal operations of mono-pile foundations, as illustrated in Table 4-16.In this context, the letters "R" and "T" denote "removal" and "transportation", respectively.

The vessel types proposed have been selected on the technological specifications available during the formulation of these decommissioning programmes to secure approval for project development. However, it's imperative to recognise that vessel technologies and their specifications might evolve by the time decommissioning is undertaken. Consequently, the vessel types initially proposed could undergo changes or modifications.

Table 4-16 illustrates proposed vessel strategies and types for offshore wind farms' foundations decommissioning.

Reference	***Offshore wind farm***	***Vessel strategies***	***Vessel types***
[186]	*Thanet*	Transiting or sender	Jack-up barge (R & T), or jack-up barge (R) & support barge (T)
[108]	*Lincs*	-	Jack-up vessel or floating barge
[109]	*Sheringham Shoal*	Transiting	Jack-up vessel (R & T)
[187]	*Gwynt y Môr*	Transiting or sender	Jack-up, barge or heavy lift [floating] vessel (R or, & T), or buoyant tow (T)

Within the industry, several researchers have supported diverse vessel strategies and types for the removal operations of foundations. For instance, [Ioannou, Angus and Brennan (2018)] championed the transiting strategy, opting to employ self-propelled jack-up vessels. In contrast, [Topham and McMillan (2017)] explored both transiting and sending strategies. For their approach, they employed just one type of vessel, specifically, one non-propelled jack-up and several barges.

Bullet 4-3

So far, none of the studies, including those mentioned, have explored the available vessel types in terms of cost and duration for decommissioning methods of offshore wind foundations other than the method of cutting the pile at or 1 – 2m below the seabed. Moreover, the vessels employed for decommissioning have been confined to jack-up vessels/barges, with the noticeable exclusion of HLVs.

4.5 Cost and Time Modelling for OWFoundations Decommissioning

The publicly published offshore wind farm decommissioning programmes indicate that the offshore wind sector predominately focuses on a single decommissioning strategy for its foundations: partial removal. This involves either internally or externally cutting the pile at or up to 2 metres below the seabed. Furthermore, there is a noticeable lack of data and inconsistencies in estimating the timing and costs for decommissioning in these published programmes. Additionally, one vessel strategy, transiting, appears to be posted to dominate the future offshore wind decommissioning market. These factors underscore the need to develop a cost and time model tailored for decommissioning offshore wind fixed foundations.

The model's objective is to pinpoint the most cost-effective strategy and methodology for decommissioning offshore wind foundations in terms of both time and expense. This is achieved by investigating and comparing the favoured and proposed decommissioning strategies and methodologies, as well as employing a variety of vessel types and strategies.

For the purposes of this model, the decommissioning methodologies considered involve either cutting the pile at or 1 to 2 metres below the seabed or extraction, which correspond to partial and full removal strategies, respectively. The relevant data inputs, such as the time required for cutting or extracting, have been detailed in earlier sections. As for vessel strategies, the model

considers both transiting and sending, with the vessel types being WTIVs, jack-up barges, and HLVs.

The selection of the vessel was based on several factors, including its specifications (such as crane capacity, deck space, and speed), the water depth at the site, market availability, among others. The data for the vessels was sourced from various types of references. Table 4-17 presents the types of sources studied, categorised based on data availability. In this table, the letters Y, N and S represent "available", "unavailable", and "supporting", respectively.

Table 4-17 summarises data availability status in the studied sources.

Source Type	*Basic specifications*	*Technical specifications*	*Costs*	*Days*
Vessel owners/ operators' websites	*Y*	*N*	*N*	*N*
Literature review	*S*	*Y*	*Y*	*Y*
OWFs decommissioning programme	*S*	*Y or S*	*Y or S*	*Y*

Basic specifications for vessels encompass dimensions, transit speed, crane capacity, and jacking speed, among other features. On the other hand, technical specifications delve into details such as positioning, as well as the duration required for loading and off-loading. Cost-related specifications cover aspects like mobilisation, day rates and de-mobilisation.

The existing decommissioning programmes and literature reviews are either deficient in or vary regarding vessels' basic and technical specifications and costs. For example, literature reviews predominately centre on vessels' transit speed, deck space capacity and costs [68], [99], [126]. In contrast, the Sheringham Shoal wind farm provided confident estimates for the majority of the durations associated with foundation removal operations as well as the technical specifications of vessels [109]. Given this variability and lack of consistent information, establishing a baseline for vessels selection and costs became imperative to ensure a consistent, reliable, and realistic modelling model.

Regardless of their type, the baseline for vessels' basic specifications was derived from the MPI Resolution specifications, as illustrated in section 4.4.3.1. This choice was made because the MPI Resolution is the first vessel specifically designed for offshore wind. The technical specifications and costs for vessels were determined based on the average values extracted from available decommissioning programmes and literature reviews. Certain technical specifications, such as the duration of loading and off-loading, were kept constant across all

vessel types. This decision was influenced by the fact that the average crane capacity considered for all selected vessel types in this study is 900 T and above.

In instances where there was inconsistency in the vessels' day rates, the cost estimation was grounded on the average costs available for the vessel. If there was a deficiency or uncertainty surrounding a particular vessel type's cost, it estimated cost would either be increased or decreased from the available cost of a different vessel type. The cost, in theory, could surge or drop by a minimum of £50,000 and a cap of £100,000. For example, if the discrepancy between two vessel types' day rate amounts to £100,000, then the day rate for a third type, where the rate remains ambiguous, will either increase or decrease by £100,000. The magnitude of this increment or decrement would be determined based on the vessel's type, avalaibility and its relative development/advancement. For the sake of consistency and simplicity, if the daily rate of the Wind Turbine Installation Vessel (WTIV) is £100,000 less than that of the Heavy Lift Vessel (HLV), the Jack-up Barge (JB) daily rate will be estimated as £100,000 less than that of the WTIV.

£100,000 difference between the day rates of a Jack-up Barge (JB) and a Wind Turbine Installation Vessel (WTIV),

The following equations, labelled [1] - [17], illustrated below, were developed to calculate the vessels' total time and cost for the removal operations for the offshore foundations. To calculate the total foundation decommissioning time needed per trip $[T_F, Decom; hour\ [h]]$, equation [1] can be utilised.

$$\begin{matrix}\textit{Foundations' total decommissioning time per trip } [T_F, Decom] \\ \\ \end{matrix} = \begin{matrix}[Travel\ time + foundation\ decommissioning\ time \\ + intra - field\ movement\ time \\ + Unloading\ time]\end{matrix} \quad (1)$$

The total travel time, $[T_{Travel};\ hour\ [h]]$, has determined by the distance between the port and site, $[D;\ nautical\ miles\ [nm]]$; and the average vessel speed $\left[V_{Speed};\ Knot\ [Kn]\right]$.

$$\textit{Total travel time } [T_{Travel}] = 2 \cdot \left[\frac{D}{V_{Speed}}\right] \quad (2)$$

Foundations total removal time, $[T_{Time}, Removal; hour\ [h]]$; has determined by The foundation removal time $[T_F, \text{Removal};\ hour\ [h]]$; and vessel capacity $[V_{Capacity}]$.

$$\text{Foundations total removal time per trip } [T_{Time}, Removal] = \left[T_F, Removal \cdot V_{Capacity}\right] \quad (3)$$

The foundation removal time, $\left[T_F, \text{Removal}; hour\ [h]\right]$; for WTIVs and heavy lift [floating] vessels had calculated using equations [3] & [4], respectively.

$$\text{Foundation removal time, WTIVs } [T_F, Removal, WTIVs] = [Positioning + Jacking\ up + Removal\ operations + Loading\ (lift + place) + Jacking\ down] \quad (4)$$

$$\text{Foundation removal time, HLVs } [T_F, Removal, HLVs] = [Positioning + Removal\ operations + Loading\ (lift + place)] \quad (5)$$

For WTIVs and jack-up barges, the jacking time at the site, $\left[T_{Jacking}, \text{site}; hour\ [h]\right]$; has determined by the site's water depth, $\left[WD_{Site}; meter\ [m]\right]$; and the vessel jacking speed $\left[V_{Jacking}; meters\ per\ minute\ [m/min]\right]$. It is worth noting that the jacking time -down- had hypothetically estimated to decrease by a certain percentage, herein 20%, after placing each foundation on the vessels' deck.

$$\text{Jacking time at the site } [T_{Jacking}, Site] = \left[\frac{WD_{Site}}{[V_{Jacking}]}\right]/60 \quad (6)$$

The total intra-field movement time, $\left[T_{Time}, \text{Intra} - \text{field}; hour\ [h]\right]$, has calculated by intra-field movement time, $\left[T_{Intra-field}; hour\ [h]\right]$; and vessel capacity $\left[V_{Capacity}\right]$.

$$\text{Total intra-field movement time } [T_{Time,}\ Intra - field] = \left[T_{Intra-field} \cdot V_{Capacity}\right] \quad (7)$$

Intra-field movement time, $\left[T_{Intra-field}; hour\ [h]\right]$, has determined by the turbines' separation distance, $\left[D_{Turbine}; \text{nautical miles } [nm]\right]$; and the average vessel speed $\left[V_{Speed}; Knot\ [Kn]\right]$.

$$\text{Intra-field movement time } \left[T_{Intra-field}\right] = \left[\frac{D_{Turbine}}{V_{Speed}}\right] \quad (8)$$

The unloading time at port, $\left[T_{Unloading}, \text{port}; hour\ [h]\right]$; for WTIVs, jack-up barges and heavy lift [floating] vessels had calculated using equations [9] & [10], respectively.

$$\text{Unloading Time, WTIVs \& Jack-up barges } [T_{Unloading}, Port, WTIVs\ \&\ Jack-up\ barges] = [Positioning + Jacking\ up + Unloading + Jacking\ down] \quad (9)$$

$$\underset{[T_{Unloading}, Port, HLVs]}{\textit{Unloading Time, HLVs}} = [Positioning + Unloading] \quad (10)$$

For WTIVs and jack-up barges, the jacking time at port, $\left[T_{Jacking}, \text{port; } hour\ [h]\right]$; has determined by the port's water depth, $\left[WD_{Port};\ meter\ [m]\right]$; and the vessel jacking speed $\left[V_{Jacking};\ meters\ per\ minute\ [m/min]\right]$.

$$\underset{[T_{Jacking}, Port]}{\textit{Jacking time at port}} = \left[\frac{WD_{Port}}{V_{Jacking}}\right]/60 \quad (11)$$

The total number of trips, $[N_{Trips}]$, has calculated by the total number of offshore wind turbines, $[N_{OWTs}]$; and vessel capacity $[V_{Capacity}]$.

$$\textit{Total number of trips } [N_{Trips}] = \frac{N_{OWTs}}{V_{Capacity}} \quad (12)$$

The adjustment weather per trip, $\left[ADJWEATHER_{Trip}; hour\ [h]\right]$, has determined by foundations' total decommissioning time per trip, $\left[T_F, Decom; hour\ [h]\right]$; and adjustment weather factor, [ADJWEATHER]. The adjustment weather factor was set < 1 [0.8]

$$\underset{[ADJWEATHER_{Trip}]}{\textit{Adjustment weather per trip}} = \frac{T_F, Decom}{ADJWEATHER} \quad (13)$$

The decommissioning time per foundation by adjusted weather, $\left[ADJWEATHER_{Decom}, Foundation; hour\ [h]\right]$, has calculated by adjustment weather per trip $\left[ADJWEATHER_{Trip}\right]$; and vessel capacity $\left[V_{Capacity}\right]$. Adjustment weather factor was set < 1 [= 0.8]

$$\underset{[ADJWEATHER_{Decom}, Foundation]}{\textit{Decommissioning time per foundation by adjusted weather}} = \frac{ADJWEATHER_{Trip}}{V_{Capacity}} \quad (14)$$

Total decommissioning time for offshore wind farm foundations, $\left[T_{Decom}, \text{OWFFs; } hour\ [h]\right]$; calculated by the total number of trips $\left[N_{Trips}\right]$ and adjustment weather per trip $[ADJWEATHER_{Trip}]$.

$$\underset{[T_{Decom}, OWFFs]}{\textit{Total decommissioning time for offshore wind farm foundations}} = N_{Trips} \cdot ADJWEATHER_{Trip} \quad (15)$$

Total decommissioning cost for offshore wind farm foundations, $[C_{Decom}, OWFFs; Pound\ [£]]$, has determined by the total decommissioning time for offshore wind farm foundations, $[T_{Decom}, OWFFs; hour\ [h]]$; and vessels daily cost $[V_{Cost}, Daily\ rate; Pounds\ [£]]$. Total decommissioning cost for offshore wind farm foundations for transit and sending strategies had calculated using equations [16] & [17], respectively.

$$\text{Total decommissioning cost for offshore wind farm foundations}[C_{Decom,}\ OWFFs, Transit] = \left[\frac{T_{Decom}, OWFFs}{24} \cdot V_{Cost}\right] \quad (16)$$

$$\text{Total decommissioning cost for offshore wind farm foundations}[C_{Decom,}\ OWFFs, Sender] = \left[\frac{T_{Decom}, OWFFs}{24} \cdot T_{Vessels}, Costs\right] \quad (17)$$

For sender strategy, total vessels costs, $[T_{Vessels}, Costs]$; have determined by the sum of vessels for decommissioning, $[V_{cost}, Decommissioning]$ and transportation $[V_{cost}, Transportation]$.

4.5.1 Transiting Strategy

For the transiting strategy, WTIVs and heavy lift (floating) vessels – with mooring HLV cranes – were chosen to execute removal operations, storage, and transportation of foundations from the site to the port.

The rationale behind selecting mooring heavy lift cranes lies in their ability to load the foundations and transport them to the port, exemplified by vessels like the Seaway Yudin [211]. It is worth noting that sheering vessels, such as Svanen [68], [214], do not share this capability. In contrast, heavy-lift (floating) vessels, like semi-submersible vessels, were developed primarily for the oil and gas industry and command day rates exceeding £450,000 [68], [203]. The choice of WTIVs, as previously mentioned, stems from their specific construction to support offshore wind activities.

4.5.1.1 Wind Turbine Installation Vessels

The fundamental specifications of the WTIVs used in this study were based on the average specifications of seven operational vessels, summarised in Table 4-18. The details of these seven vessels were gathered from vessel owners/operators' websites, which are provided in

Appendix B. The remaining inputs for the model – pertaining to vessels' technical specifications and costs – were derived from existing decommissioning programmes and a literature review, as summarised in Table 4-19 &

Table *4-20*.

Table *4-21* presents the consistently applied average values for the WTIVs inputs used in the vessels' cost and time model.

Table 4-18 summarises the average WTIV fundamental specifications.

Fundamental Specifications	***Average Value***
Transit Speed (Knot)	*12*
Jacking Speed (m/s)	*1.1*
Crane capacity (T) at radius (m)	*1,240 at 27.5*[41]
Foundation capacity (avg.)	*5*
Wave height (m)	*2.4*[42]
Wind speed (m/s)	*20*[43]
Water depth(m)	*56*

[41] The crane capacity average value was based on the specifications of five vessels.
[42] The wave height average value was based on the specifications of six vessels.
[43] The wind speed average value was based on the specifications of two vessels due to the lack of other vessels' specifications.

Table 4-19 summarises WTIVs technical specifications utilised by the decommissioning programme and the literature review available.

Authors/ Specifications	***[99]***	***[126]***	***[68]***[44]	***SSOWF [109]***
Crane capacity (T)	*1,500*	-[45]	*1,500*	*1,200 at 25 m radius*
Number of turbines or foundations	*Ten turbines or eight foundations*	*Five Units*[46]	*Five sets*[47]	*Five Units*
Speed (Knot)	*10*	*10*	*12*	*13*
Jacking speed	-	*30m/h*	*1m/min*	*2.4m/min*[48]
Jacking duration (h)	-	-	-	*10*[49]
Positioning (h)	-	-	*4*[50]	*6*
Loading duration (h)	-	*11*	-	-
Off-loading duration (h)	-	*8*	*1*[51]	*4*
Number of vessels	*One to two*	*Three*	-	*Two*

Table 4-20 summarises WTIVs costs.

Authors/ Cost	[206]	[194]	[68]	[126]	[99]
Daily Cost	*$220,000*[52]	*€150,000 – 200,000*[53]	*£110,000*[54]	*£112,600*	*£150,000*
Mobilisation costs (£)	-	-	-	*405,000*	*300,000*
Mobilisation duration (h)	-	-	-	*720*	-
Demobilisation costs (£)	-	-	-	-	-

[44] The illustrated data employed for the installation process; however, it would utilise for decommissioning process.
[45] If no data is available, a"- "used.
[46] A unit equals complete wind turbine generator with foundation.
[47] A set equals wind turbine component.
[48] The publicly published decommissioning programme for Sheringham Shoal wind farm indicated that vessel equivalent to Pacific Orca would utilise for decommissioning. Relying on Pacific Orca vessel technical specifications, the jacking speed is 2.4m/min.
[49] The duration for jack-up and pre-loading, and jack-down is 8 and 2 hours, respectively.
[50] The duration is for Transport and positioning.
[51] The duration is for lifting and pile positioning.
[52] Exhange rate used was: 1 USD = 0.7214 GBP.
[53] Exchange rate used was: 1 EUR = 0.8587 GBP.
[54] Daily costs range between £90,000 to £130,000 excluding equipment, fuel and crew.

Demobilisation duration (h)	-	-	-	*48*	-

Table 4-21 summarises the WTIVs implemented values in vessels' cost and time model.

WTIV Specifications	***Average Value***
Foundation capacity	*5*
Transit speed (Knot)	*12*
Jacking speed (m/min)	*1.1*
Wave height (m)	*2.4*
Crane Capacity (T) at radius (m)	*1,240 at 27.5*
Water depth (m)	*56*
Wind speed (m/s)	*20*
Positioning duration (h)	*5*
Loading duration (h)	*4*
Off-loading duration (h)	*4*
Daily cost (£)	*136,316*
Mobilisation cost (£)	*352,500*
Demobilisation cost (£)	*-*

Some of the extracted data, such as the duration for loading and off-loading, showed inconsistencies – some vessels seemed to either underestimated or overestimated, for example, 1 and 8 hours for unloading, and 11 hours for loading. As a result, the off-loading duration value, shown in

Table *4-21,* is based solely on the Sheringham Shoal wind farm decommissioning programme. Accordingly, the loading duration was estimated to be equal to the off-loading duration, as both processes involve similar actions: lifting and placing.

4.5.1.2 Mooring HLV Cranes

The fundamental specifications of the mooring HLV cranes utilised in this study are based on the specifications of the Seaway Yudin, as detailed in Table 4-22. The technical specifications and cost-related data for the vessels were sourced from available resources, as compiled in Table 4-23.

Table 4-22 summarises mooring HLV cranes fundamental specifications based on Seaway Yudin specifications.

Fundamental Specifications	***Value***
Transit Speed (Knot)	*10*
Crane capacity (T)	*2,500*

Wave height (m)	*1.8*
Water depth(m)	*Unrestricted*

Table 4-23 summarises mooring HLV cranes available technical specifications and costs.

Technical specification(s) and costs/ Author(s)	[68]
Positioning (h)	2 (duration for transport and positioning)
Daily cost (£)	200,000

It's important to note that the data presented in Table 4-23 is not exclusive to mooring HLV cranes. Instead, the values are generalised for heavy lift (floating) vessels, with the exception of semi-submersible vessels. The values adopted for mooring HLV crane inputs in the vessels' cost and time model were derived from Table 4-22 & Table 4-23.

Statement 4-5

DP (Dynamic Positioning) heavy lift cranes, like the Bokalift 1 – which was repurposed from a semi-submersible vessel to a DP-2 crane vessel – are equipped to handle removal operations, storage and transportation of foundations from the offshore site to a port [215], similar to the capabilities of mooring HLV cranes.

4.5.2 Sender Strategy

For the sender strategy, two scenarios were utilised. In each scenario, a self-elevating jack-up barge was employed alongside either one heavy-lift (floating) vessel or a WTIV. It is worth noting that for the feeder strategy (referred to as "sender" here), self-elevating jack-up barges remain at the site to conduct installation activities. Meanwhile, transportation as handled by two feeder barges, a strategy explored by several scholars for both installation [68], [71] and decommissioning [99].

For simplicity, consistency, and a reliable comparison between the two scenario outcomes, self-propelled vessel types, specifically, WTIVs and heavy-lift (floating, sheerleg) vessels, were selected to perform removal operations. Meanwhile, self-elevating, self-positioning jack-up barges were utilised for the storage and transportation of foundations from the site to the port.

The selection of heavy-lift (floating, sheerleg) vessels was influenced by their limited deck space, making them an ideal candidate for sender or feeder strategies. On the other hand, opting for self-elevating, self-positioning jack-up barges minimises the number of required tugboats to just one for transportation. Conversely, using self-elevating, non-self-positioning jack-up

barges would necessitate a minimum of two or three tugs: one for transportation and one or two for positioning, either at the site or port.

4.5.2.1 WTIVs and Self-Elevating Jack-up Barges

The foundational and technical specifications, as well as the costs of the WTIVs used in this study, were derived from the average values detailed in

Table *4-21,* as described in section 4.5.1.1. The basic specifications of the self-elevating jack-up barges used in this study were modelled after the JB-117 specifications, as referenced in [192], [216], [217], and are compiled in Table 4-24. The input data regarding the costs of the vessels were sourced from available resources and are presented in Table 4-25.

Table 4-24 summarises self-elevating jack-up barges fundamental specifications based on JB-117 specifications.

Fundamental Specifications	***Average Value***
Transit Speed (Knot)	*6 (average tugboat speed)*
Jacking Speed (m/s)	*0.4*
Crane capacity (T) at radius (m)	*1,000 at 22*
Wave height (m)	*1.5*
Wind speed (m/s)	*10*
Water depth(m)	*45*

Table 4-25 summarises self-elevating jack-up barges costs.

costs/ Author(s)	[99]
Daily cost (£)	75,000
Mobilisation cost (£)	200,000

The average speed for self-elevating jack-up barges was assumed based on the speeds of the following tugboats: 5 knots [192], 6 knots [71], and an average of 6 knots (ranging between 4-8 knots) [70].

There's a noticeable absence of data regarding the technical specifications for self-elevating jack-up barges, such as the duration required for positioning. As a consequence, it was estimated to be 25% longer than the specifications for WTIVs. For example, if the positioning duration for WTIVs is 5 hours, then for self-elevating jack-up barges, it would be approximately 6.25 hours (round down to 6 hours for simplicity). Furthermore, the deck capacity of self-elevating jack-up barges was estimated to be 25% less than that of WTIVs. The

reason for increasing or decreasing values by 25% is the understanding that self-elevating jack-up barges are not technologically advanced as WTIVs.

4.5.2.2 Floating Sheerleg and Self-elevating Jack-Up barges

The fundamental specifications for floating sheerlegs used in this analysis were based on the average specifications of five operational vessels, as presented in Appendix C. These specifications are summarised in

Table 4-26. Data related to the vessels' costs inputs were extracted from available resources and are presented in Table 4-27.

Table 4-26 summarises floating sheerleg fundamental specifications.

Fundamental Specifications	***Value***
Transit Speed (Knot)	*8*
Crane capacity (T)	*2,980*
Water depth(m)	*N.A.*

Table 4-27 summarises floating sheeleg vessels costs.

costs/ Author(s)	[68]
Average daily cost (£)	185,000

Floating sheerleg vessels are employed for the installation of substations and foundations. Accordingly, their average daily cost was determined based on the day rates for vessels involved in substation installation and foundation installation, being £175,000 and £200,000, respectively [68].

Due to the absence of specific technical specifications for floating sheerlegs, such as the duration of positioning, it was increased by 25% compared to the positioning duration of mooring HLVs. The fundamental, technical specifications, and costs of the self-elevating jack-up barges used in this study were derived from values presented in Table 4-24 and Table 4-25, as detailed in section 4.5.2.1.

4.6 Results

The model developed facilitated the comparison of OWFoundations' decommissioning strategies and methodologies – both existing and proposed. It also allowed for the comparison of vessel types, strategies, and quantities in terms of cost and time. It should be noted that the

costs presented henceforth do not include the vessels' mobilisation and de-mobilisation costs due to the absence of the necessary data.

The results from the model indicate that using a single vessel, whether a WTIV or mooring HLV, for the transit strategy will require more time to complete the foundation decommissioning activities compared to the sender strategy, as illustrated in Figure 4-14 and Figure 4-15. Furthermore, Figure 4-14 & Figure 4-16 and Figure 4-15 & Figure 4-17 provide insights into the number of vessels, their types and strategies for cutting the pile at or below 1 to 2 metres and extraction, respectively. These figures also illustrate the associated costs and time for the decommissioning of foundations.

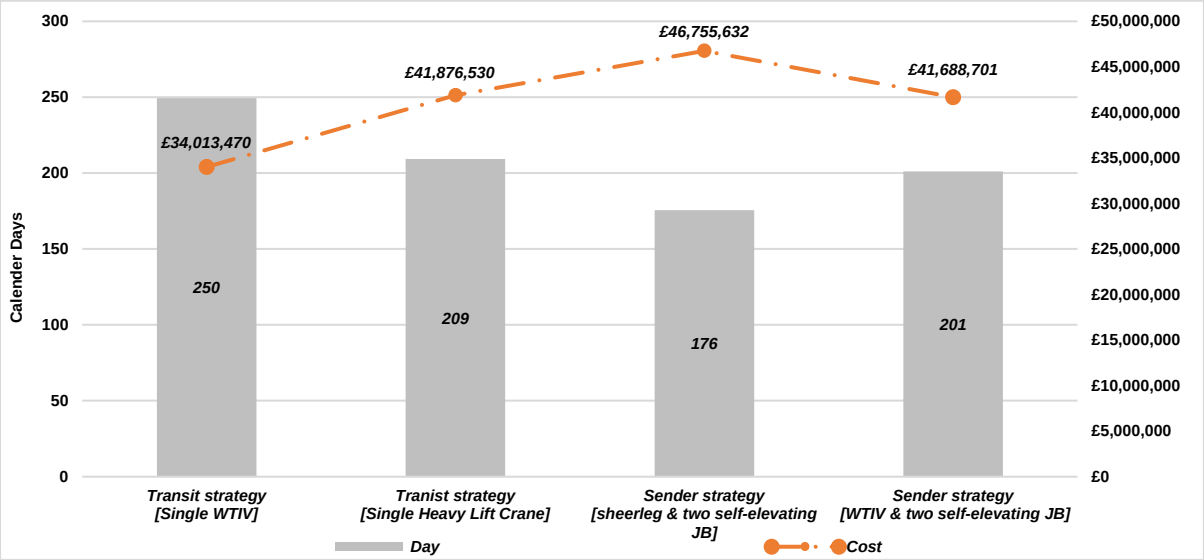

Figure 4-14. The time and cost of a single vessel for transit strategy for foundations partial removal options by cutting the pile at or 1 to 2m below the seabed.

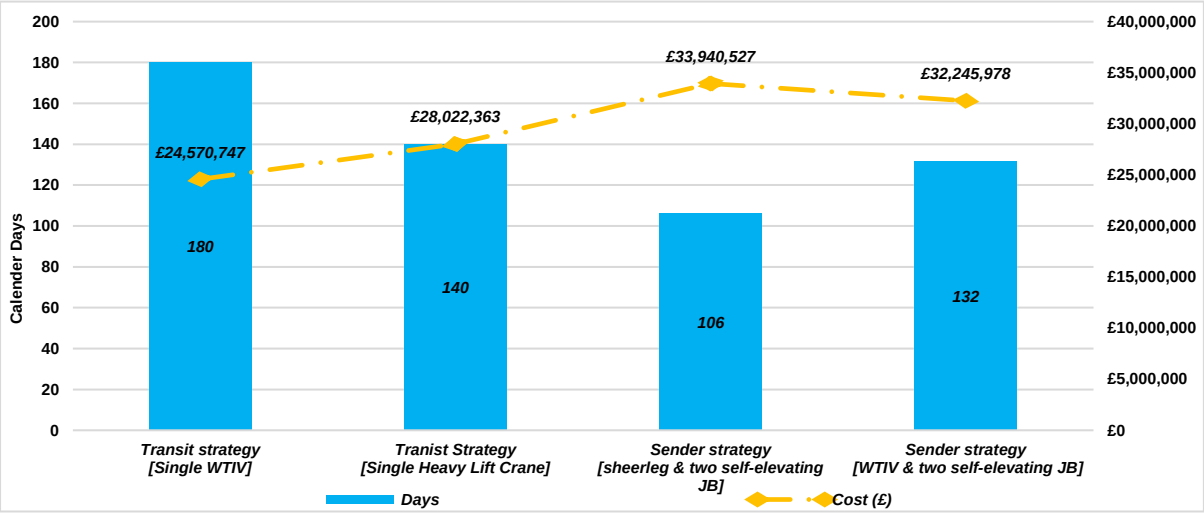

Figure 4-15. The time and cost of a single vessel for transit strategy for foundations full removal option by extraction.

However, when two vessels operate concurrently, the duration decreases significantly, as depicted Figure 4-16 and Figure 4-17. Analysis of the results confirms that executing foundation decommissioning activities – regardless of the strategy and methodology - using heavy-lift (floating) vessels is faster than using WTIVs. This is mainly because heavy-lift (floating) vessels require less positioning time compared to WTIVs and negate the need for jacking up and down at either the site or port.

In terms of overall vessel costs, employing heavy-lift (floating) vessels – whether mooring or sheerleg – incurs the highest expenses for the partial removal decommissioning option under both transit and sender strategies. This can be attributed to the limited availability of heavy-lift (floating) vessels - irrespective of their type – which results in steeper charter rates. On the other hand, for the full removal decommissioning option, the sender strategy is more costly than the transit strategy. This is due to the use of either one WTIV or one heavy-lift (floating) sheerleg vessel, in conjunction with two self-elevating jack-up barges and two tugboats, each priced at £8000 each.

It is worth pointing out that within the transit strategy, the overall costs for vessels - whether one or two WTIVs or mooring HLVs - remained consistent, even with a 50% reduction in the duration. As a result, within the transit strategy framework, the duration could be further minimised, maintaining the same total costs as with a single vessel, by employing three or more vessels.

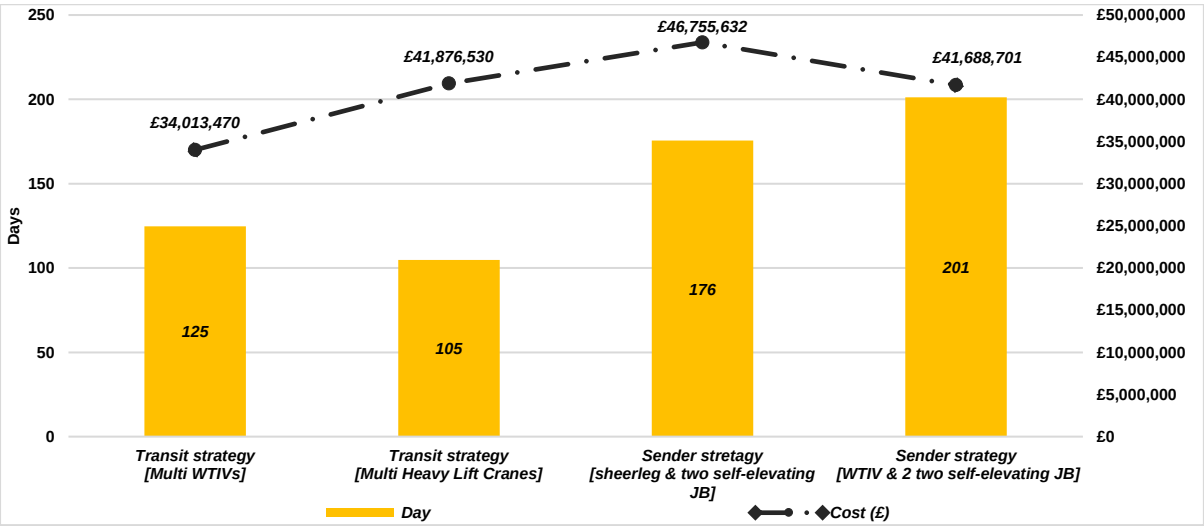

Figure 4-16. The time and cost of multi vessels for transit strategy for foundations partial removal options by cutting the pile at or 1 to 2 m below the seabed.

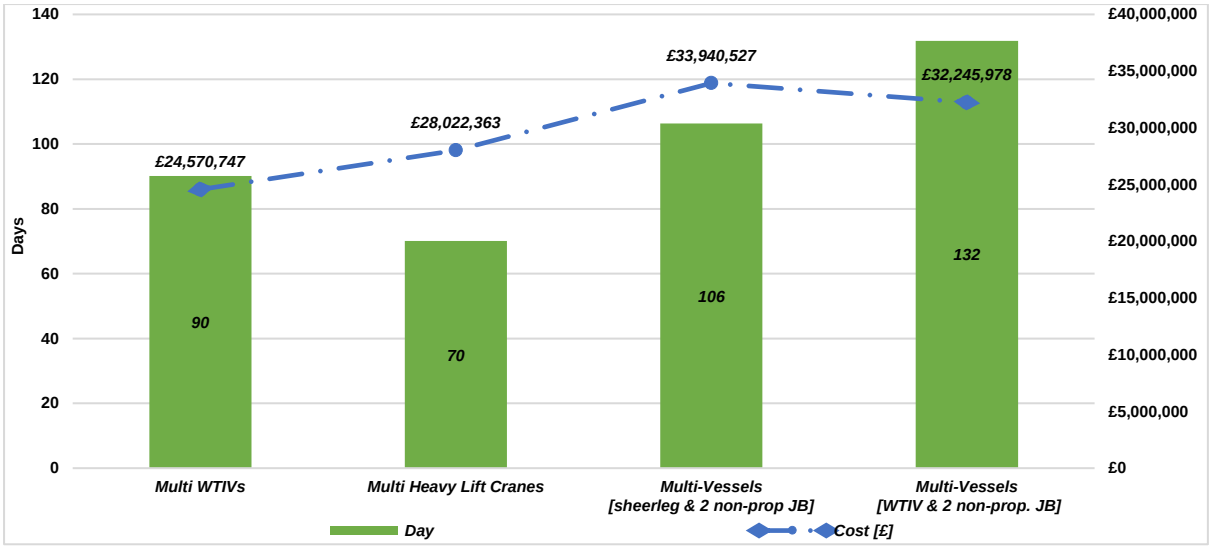

Figure 4-17. The time and cost of multi vessels for transit strategy for foundations full removal by extraction.

The results presented above confirm that, irrespective of the decommissioning strategy and methodology, the transit strategy using WTIVs is the most cost-effective approach for decommissioning OWFoundations. In terms of time efficiency, the ideal scenario involves using at least two or more vessels operating concurrently, regardless of their type. Furthermore, employing heavy-lift (floating) vessels for either transit or sender strategies ensures the quickest duration for both full or partial removal decommissioning approaches, compared to using WTIVs.

4.7 Sensitivity Analysis

The model was designed to accommodate modifications to certain factor assumptions – regardless of their level of certainty – that significantly influence the cost and duration of decommissioning OWFoundations. This adaptability is essential for visualising various scenarios. Each scenario can produce distinct impacts – either significant or minimal - on the estimated decommissioning cost and time. These pivotal factors encompass the duration of OWFoundations' removal operations, wait-on-weather conditions, vessels' day rates, and the learning curve.

4.7.1 OWFoundations' Removal Operations Duration

The duration of removal operations for OWFoundations' decommissioning strategies and methodologies, as previously mentioned, possesses a high degree of uncertainty. This is primarily because many offshore wind farms, especially the large-scale ones, have not yet

undergone or even initiated decommissioning activities. Consequently, the estimated average duration for all removal methodologies pertaining to offshore wind foundations under investigation has been amplified by 100%. This percentage represents a conservative estimate, derived from BEIS's assessment for factors with high uncertainty, such as the duration of removal methodologies for OWFoundations [53].

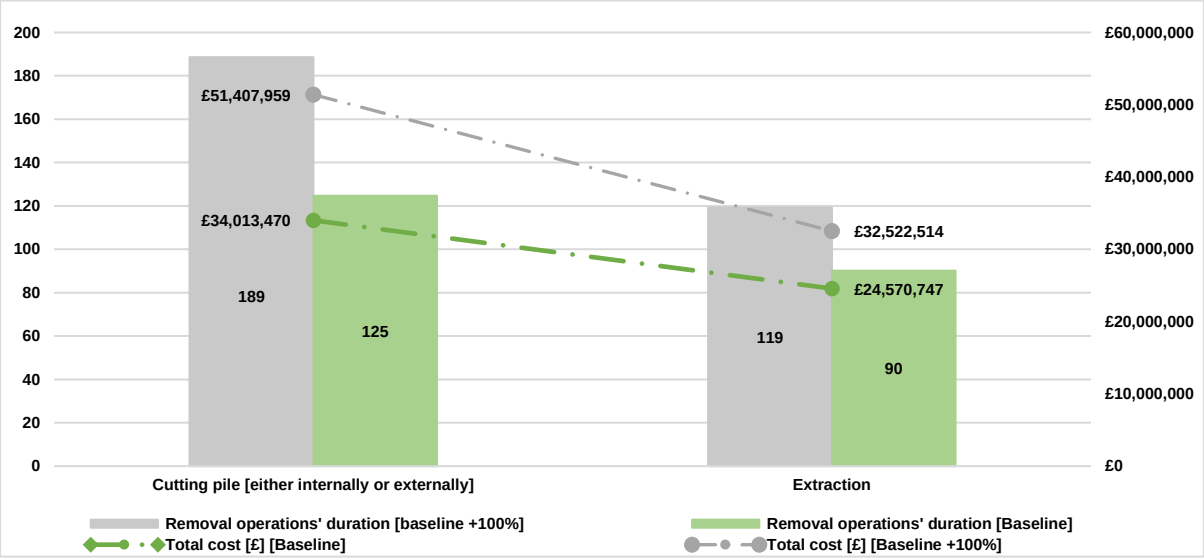

Figure 4-18. The impact of incrementing removal methodologies operations duration for offshore wind foundations utilising two WTIVs on decommissioning cost and time.

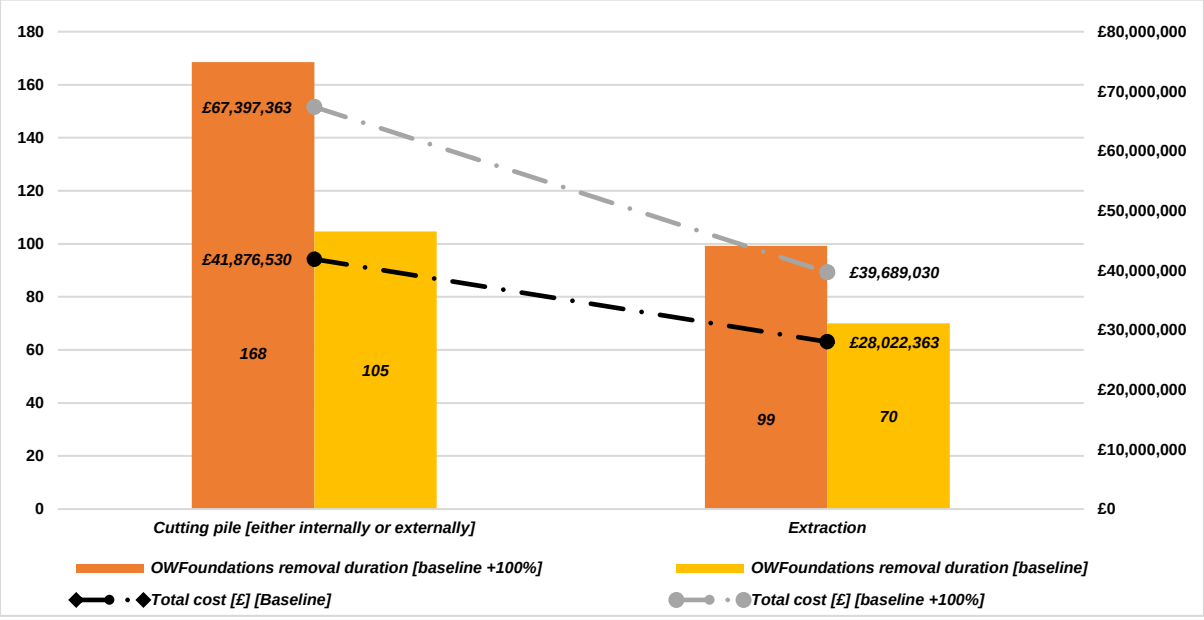

Figure 4-19. The impact of incrementing removal methodologies operations duration for offshore wind foundations utilising two HLVs on decommissioning cost and time.

An anticipated 100% escalation in the removal operations duration for the examined decommissioning methodologies has led to a rise in the decommissioning cost and time for OWFoundations, as depicted in Figure 4-18 & Figure 4-19. For extraction methods, the

removal operations duration has surged by 32.2% and 41.4% when using WTIVs and HLVs, respectively. This has culminated in a corresponding rise in costs by equivalent percentages. For methodologies that involve cutting the pile and employ WTIVs, there has been an elevation in both duration and cost by 51.2% and 51.1%, respectively. Meanwhile, when HLVs are used, these figures have climbed by 60% for duration and 60.95% for cost, respectively.

4.7.2 Wait-on-Weather

Wait-on-weather (WOW), previously addressed in section 4.3, influences the duration and cost of OWFoundations' removal operations. As a result, a sensitivity analysis was conducted on WOW by adjusting the weather factor range. The explored range was set between 50% and 100% and applied to the transit strategy, incorporating two types of vessels. Figure 4-20 and Figure 4-21 depict the relationship between wait-on-weather and the duration and costs associated with the vessels: WTIVs and the mooring heavy-lift (floating) crane, respectively, for both the partial and full removal decommissioning options.

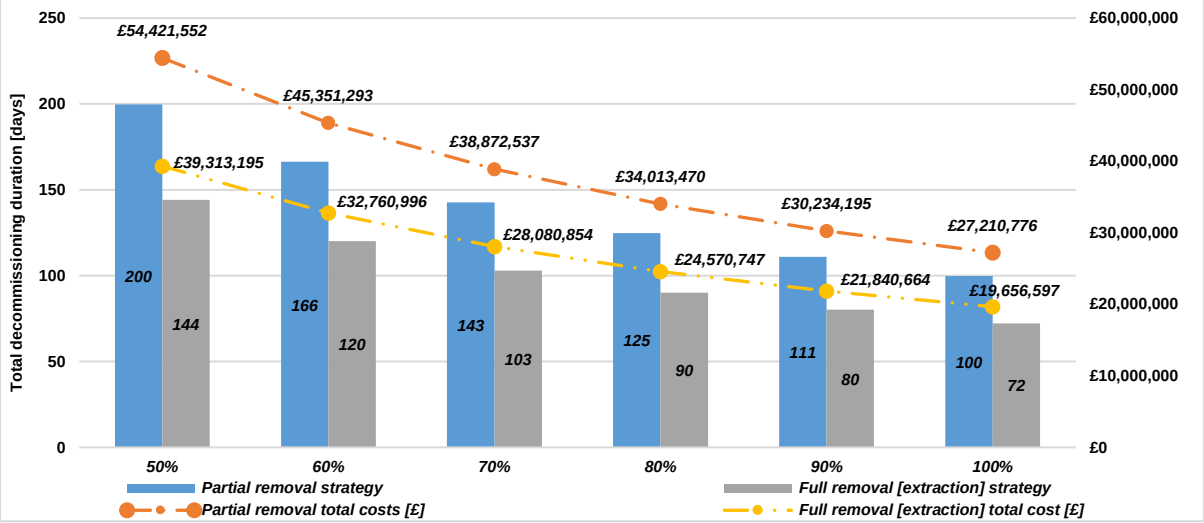

Figure 4-20. The time and cost of the sensitivity of the wait-on-weather factor for decommissioning removal strategies utilising two WTIVs.

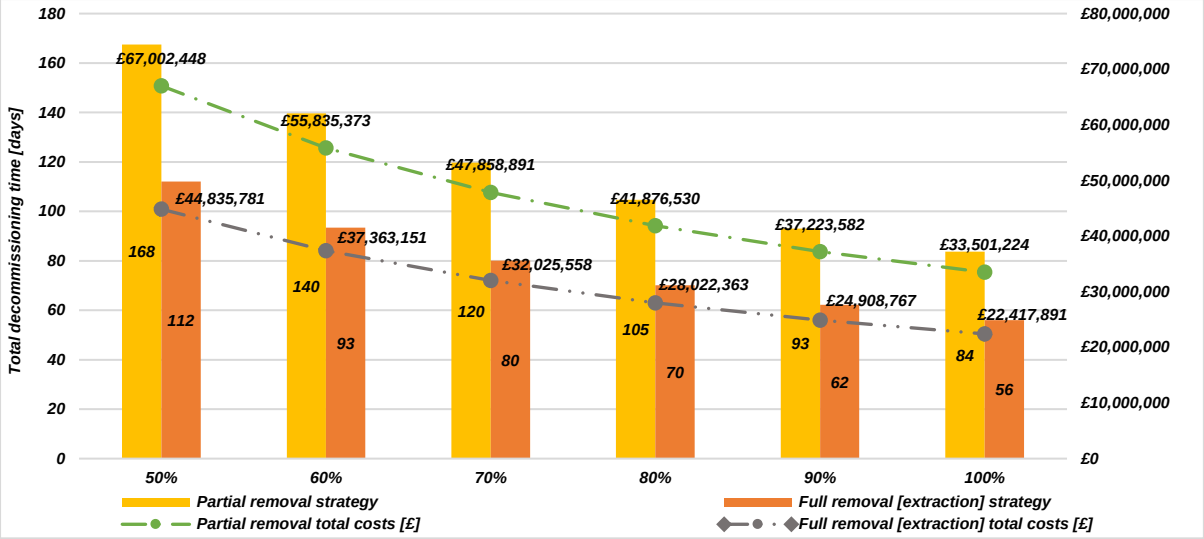

Figure 4-21. The time and cost of the sensitivity of the wait-on-weather factor for decommissioning removal strategies utilising two mooring HLVs.

The model's findings indicated that WOW has a considerable impact on the costs and time associated with vessels executing foundation removal operations, as anticipated, regardless of the decommissioning strategies and methodologies used. Even when vessels operate only 50% of the time, extracting foundations proves to be more economical than cutting the pile either at or 1 – 2 metres below the seabed. Furthermore, despite the shorter duration required for executing decommissioning methodology with heavy-lift (floating) – mooring – vessels, their costs are higher compared to WTIVs.

4.7.3 Vessel Day Rates

Vessels, as previously discussed, form the backbone of offshore wind development. Their associated costs, especially day rates, play a significant role in determining the overall project cost. It is anticipated that vessel costs will experience high volatility as demand for offshore wind decommissioning grows. This increase in demand will likely result in competition between offshore wind decommissioning, oil and gas operations, offshore wind installation, and other marine developmental activities. Given this backdrop, the day rates for vessels used in the transit strategy, namely WTIVs and mooring heavy-lift vessels, have been adjusted by ± 20% to assess the potential financial implications for foundation decommissioning strategies and methodologies. This adjustment also serves to test the model's sensitivity to variations in the vessel day rates.

Figure 4-22. Impact of setting vessels day rates on foundations partial removal options costs.

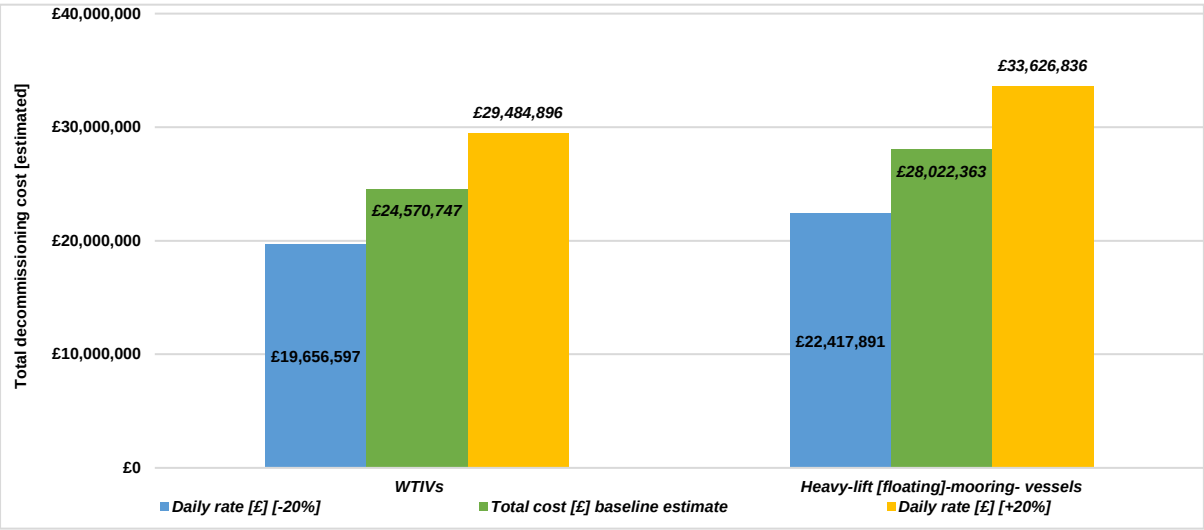

Figure 4-23. Impact of setting vessels day rates on foundations full removal option [extraction] costs.

The figures, namely Figure 4-22 and Figure 4-23 clearly demonstrate the direct relationship between the vessels' day rates and the overall costs associated with the decommissioning of offshore wind foundations, be it for partial or full removal options. As day rates rise of fall, there's a corresponding increase or decrease in the total decommissioning costs.

This emphasises the crucial nature of day rates in the overall financial planning and budgeting of decommissioning projects. As such, when formulating estimates for decommissioning projects – irrespective of the specific structure, strategy, or methodology being considered - it becomes paramount to make well-informed assumptions about vessels' day rates. Decision-makers need to understand and be prepared for the inherent uncertainties associated with these assumptions. Furthermore, it is worth stressing that the chosen 20% adjustment range for day rates, used in this model for sensitivity analysis, might be surpassed in real-world scenarios,

especially over an extended period. Given the myriad factors influencing day rates – from the global economic situation to technological advancements and market demand – there exists a significant likelihood that day rates could fluctuate beyond this predefined range in the longer run.

4.7.4 Learning Curve

Learning is the change that results from experience and knowledge. For instance, in industries, learning grows through the repeated execution of projects and activities, leading to a reduction in costs over time. Put simply, as a task is repeated, the time required to complete it decreases with each repetition, resulting in reduced costs.

The standard or conventional definition of the learning curve is the reduction of costs by a certain percentage when the cumulative quantity of produced, manufactured, or delivered units doubles [53], [218]. The purpose of the learning curve, also known as the efficiency curve, cost curve, or experience curve, is to predict future cost reductions [219].

The learning curve is more pronounced in manufacturing compared to other processes due to the production of numerous sub-components within a unit. This offers continuous and incremental opportunities for improvement. Consequently, decommissioning presents fewer opportunities for significant learning [53]. In the context of offshore wind, “units” refer to, but are not limited to, WTGs.

Learning opportunities will primarily emerge from removal operations, regardless of decommissioning strategies and structures, as these operations are major contributors to decommissioning costs. Therefore, to achieve cost reduction, it’s essential to enhance the efficiency of removal operations, stimulate market competition, and drive innovations [53], [69], [220]. This has been evidenced in European offshore wind installation.

For example, market competition has spurred the development of vessels both in quantity and specifications. This led to a temporary reduction in vessels’ day rates due to an oversupply in the market. The evolution of vessels, combined with improvements in installation methodologies, particularly for offshore wind superstructures, has reduced installation times. An example is the Sandbank turbines installation, where the time decreased to one day per turbine [221], in contrast to the previous four days [70].

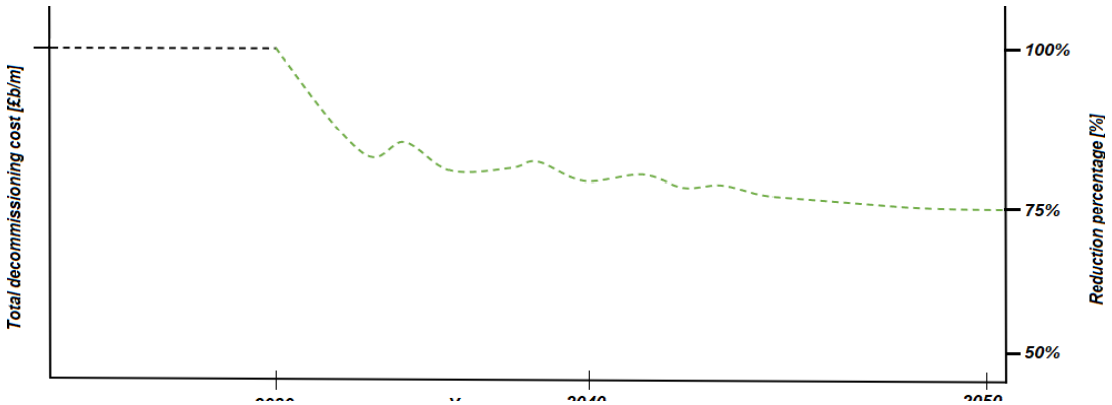

Figure 4-24. Hypothetically, the learning rates' impact on the total decommissioning cost.

Hypothetically, the initial impacts of learning on decommissioning will be minimal or remain steady in the short term. However, as decommissioning activities are scaled up in the long term, the benefits of learning will become more pronounced, leading to a greater percentage reduction in costs. Yet, this reduction will eventually plateau, reaching a steady level as depicted in Figure 4-24.

Based on the foregoing, an analysis of the learning rate was conducted to determine the impact of efficiency improvements on OWFoundations' decommissioning cost and time. The learning rates explored ranged from 5% up to 35%. This range aligns with the rates observed in energy sectors like wind and biomass, where rates can reach up to 35% [53]. Decommissioning activities have already occurred in the offshore O&G sector. Here, learning-through-doing and economies of scale, especially in well plugging and abandonment, have been evident [53], [222]. As a result, the industry's goal to reduce decommissioning costs by 35% is within sight, given that costs have already decreased by 23%, averaging a 6% reduction over the past four years.

The learning rates were applied to the removal operations of the partial removal strategy for OWFoundations, specifically for cutting the pile either internally or externally, using the transit strategy. For clarity, these rates were applied only to the average duration of operations associated with cutting the pile – such as– excavating and cutting - while other parameters were kept constant. The reason the proposed OWFoundations decommissioning method, extraction, was excluded from the analysis is because it is considered an innovative approach for for cost reduction, distinct from cost reduction achieved through learning.

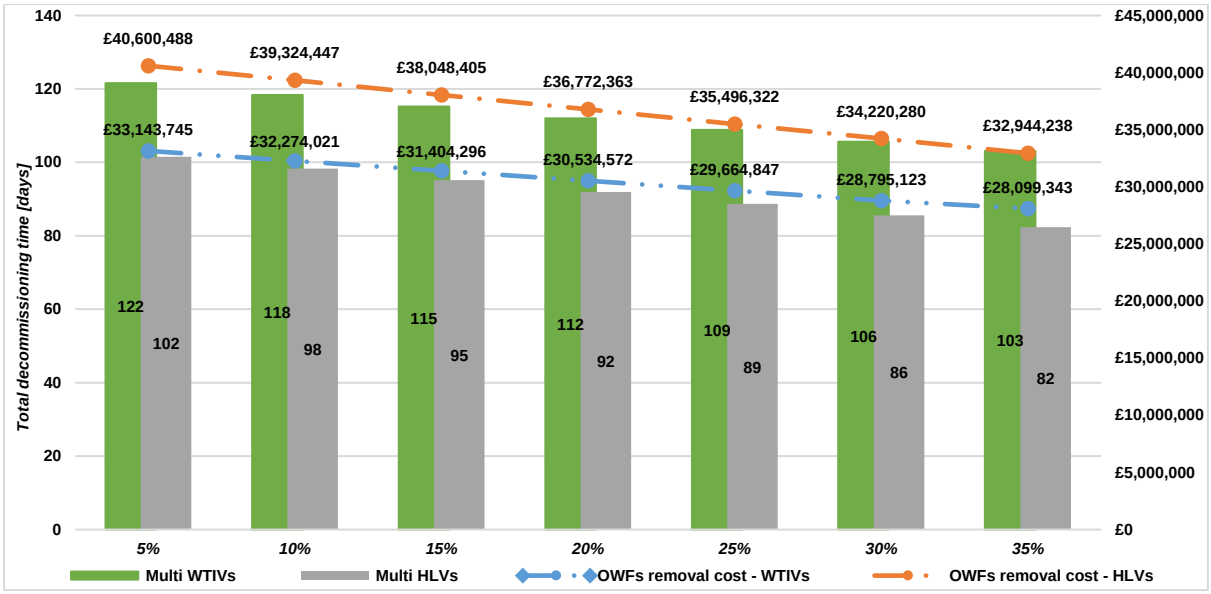

Figure 4-25. The effects of learning rates on OWFs decommissioning cost and time utilising transit strategy.

The results, as demonstrated in Figure 4-25, clearly highlight the direct impact of learning rates on the decommissioning time and cost for OWFoundations. With a learning rate of 35% (the maximum), the decommissioning cost decreased by 17.4% from the baseline estimated cost of £34,013,470 when utilising two WTIVs. Meanwhile, when using two HLVs, the decommissioning cost decreased by 21.3% from £41,876,530. The findings presented in this section, as well as in section 4.7.3, affirm that there are viable opportunities to reduce the costs of currently available decommissioning strategy for OWFoundations, which is partial removal.

4.8 Conclusion

To date, there is no standardised methodology for calculating DecEx for the most favoured decommissioning methods for offshore wind structures. The reason is that offshore wind decommissioning remains in its infancy, characterised by a lack of experience, knowledge, technology, and compounded by numerous uncertainties. As a result, the estimated DecEx, along with time assessments, tend to be inconsistent, incomplete, and inaccurate.

The inconsistency of DecEx arises because projected costs in published decommissioning programmes are derived over various periods and under different market conditions, with a consistent trend towards increase. Moreover, these costs are either determined through optimistic or conservative approaches, often overlooking prevailing market conditions at the actual time of decommissioning and appropriate inflation adjustments. However, as the

industry gains experience, offshore wind decommissioning is anticipated to become more specific, consistent, and comparable across projects.

The reduction of time, and primarily costs, are pivotal factors in decision-making regarding the selection of decommissioning methodologies. Consequently, a techno-economic assessment model was developed to pinpoint the primary cost drivers of offshore wind decommissioning, with a sole focus of OWFoundations. The aim was also to broaden the scope of OWFoundations' decommissioning methodologies by integrating and contrasting novel methodologies with currently preferred ones.

The model's foundation was based on two key OWFoundations decommissioning methodologies and the critical factors influencing the precision of decommissioning time and cost estimations. The chosen methodologies involve cutting the pile at or below the seabed and extracting it; corresponding to partial and full removal strategies, respectively. Key influencing factors encompass project complexity (such as site specifications and project size), industry maturity, uncontrollable external factors, and prevailing market conditions, including aspects like vessel availability. Additionally, the model was designed to accommodate adjustments to some of its variables, allowing for a visualisation of their sensitivity impact on decommissioning cost and duration.

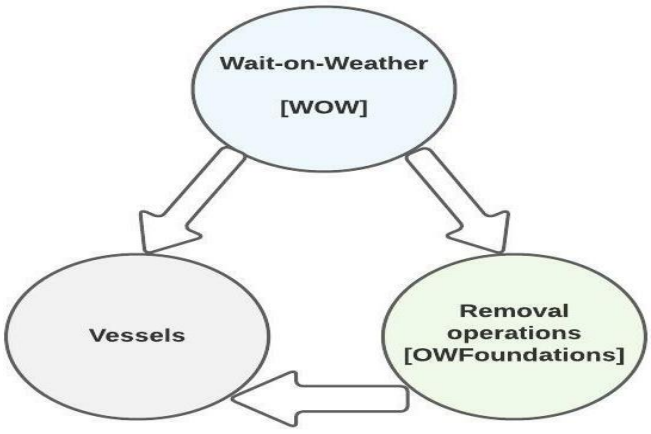

Figure 4-26. The impact of WOW and removal methodologies' operations on vessels.

Model results, as depicted in Figure 4-26, indicate that weather conditions (an uncontrollable factor) significantly influence the duration of removal operations, regardless of the methodologies chosen. This, in turn, impacts the on-site duration of vessels. Moreover, weather conditions play a pivotal role in vessel selection. In terms of removal operations duration, extracting the pile proved to be quicker than cutting it at or below the seabed, regardless of

whether WTIVs or heavy lift (mooring) vessels were used, taking into account various factors. Partial removal tends to be lengthier due to its multifaceted processes, which include excavating and cutting prior to lifting the pile, steps that are absent during extraction.

Although vessels are fundamental to offshore wind operations, their availability and appropriateness remain significant challenges in the industry. Two strategies for vessel operations, sender, and transit, have been modelled. The model's findings suggest that the time and costs of decommissioning OWFoundations using the sender strategy exceed those of the transit strategy. Put differently, regardless of the decommissioning methodology chosen, decommissioning using one HLV (sheerleg) and two self-elevating jack-up vessels (the sender strategy) incurs higher time and cost than using two HLVs (mooring) – the transit strategy.

The model's sensitivity analysis highlighted factors that both increase and decrease DecEx, as depicted in Figure 4-27. Regardless of these factors, decommissioning costs when employing HLVs always surpass those of WTIVs, even though HLVs complete removal operations more swiftly. This is attributed to the heightened demand for heavy-lift vessels, especially from the oil and gas sectors, coupled with their limited availability. Moreover, the selection of vessels is intricately tied to prevailing weather conditions.

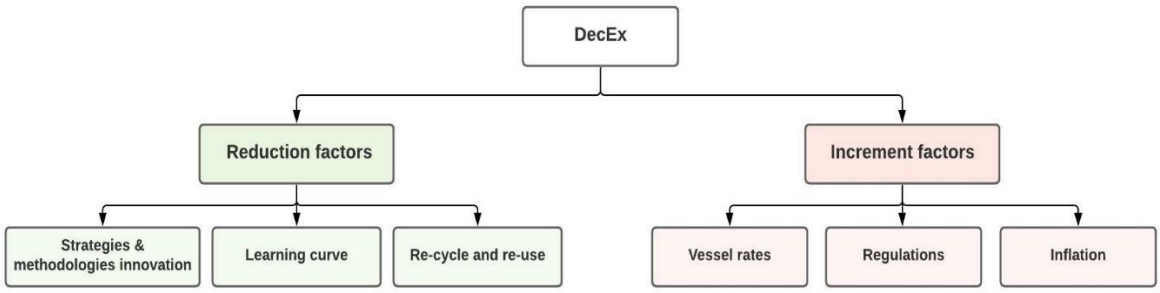

Figure 4-27. Decommissioning expenditures reduction and increment factors.

Beyond introducing a novel decommissioning methodology, the model has identified additional factors, such as the learning curve, that could further reduce costs for the preferred decommissioning approach. In the near future, the model will be expanded to explore more factors, as well as considerations like recycling, reuse, and inflation.

Chapter Five

5 Conclusion

Decommissioning represents the final stage of a project's lifecycle. In the energy sector, the development and submission of a preliminary plan is a prerequisite for project approval before construction begins. The primary objective of decommissioning is to restore the site to its original condition, as closely as possible, prior to project construction or installation. This process also aims to eliminate any risks introduced during the project's lifecycle, ensuring the site or area can be repurposed for future developments or, at a minimum, does not adversely affect other industries. Decommissioning is intricate, and the chosen strategy significantly influences the industry's potential for long-term sustainability. This strategy is influenced by various factors, including regulatory, engineering, economic, environmental and social considerations, among others. This research project focuses on decommissioning within the offshore energy sector, with a particular emphasis on offshore wind.

In the offshore energy sector, the decommissioning of structures or platforms is often considered the reverse of the installation process. This entails dismantling the most recently installed component first and continuing in this manner until the first component installed is last to be removed. This reversal concept extends beyond just the order, also applying to the decommissioning methods for structures like suction bucket foundations and gravity bases. From the inception of its earliest regulations, such as the 1958 Geneva Convention on the Continental Shelf, the decommissioning objective for the offshore energy sector (primarily oil and gas) was consistent with the onshore energy sector: a mandate for the complete removal of all offshore installations. Notably, at this juncture, the concepts of decommissioning and abandonment were largely synonymous. However, this understanding remained static only until the Brent Spar incident in the mid-1990s, which ushered in significant shifts in concepts, objectives, and methods. Decommissioning began to be viewed as a broader phase, with abandonment being just one of its constituent processes or activities. While the overarching objective of decommissioning has remained consistent, adjustments have been introduced to accommodate exceptions to the full removal of offshore installations. These exceptions allow for strategies like partial removal or leaving installations in-situ, provided they pose no risks posed to navigation, marine ecosystems, or other sea users. Intriguingly, these updated regulations were swiftly incorporated and applied to marine projects with structural designs

similar to offshore oil and gas, such as offshore wind, without accommodating potential industry-specific variations like purpose, risk, or scale.

Upon analysing both the offshore wind and oil and gas sectors, it is evident that their differences significantly outnumber their similarities. Offshore wind serves as a cornerstone in the global energy transition, essential for realising the objectives set forth in the 2015 Paris Agreement's climate action framework. Specifically, offshore wind is pivotal for Europe's ambition to achieve carbon neutrality by 2050. The success and impact of offshore wind are largely contingent on the scale and volume of installations, while the offshore oil & gas sector emphasises the number of wells. From a risk perspective, offshore wind installations are perceived as relatively benign; they primarily contain a minimal volume of fluids, translating to a reduced risk of spills during the decommissioning phase. This stands in stark contrast to offshore oil and gas installations, which house an array of hazardous materials, from hydrocarbon residues to radioactive substances. Given this disparity, directly applying the updated decommissioning regulations - emphasising partial removal, the favoured method for decommissioning single fixed-steel pile foundations or “mono-piles” in the offshore wind sector – might inadvertently diminish seabed availability. Over time, this could severely limit the space required to sustain the growth of offshore wind projects.

5.1 Decommissioning By Extraction

The primary objective of this research project is to explore and advance the full removal techniques for fixed-steel pile foundations in the offshore wind sector. More specifically, the study aims to innovate and implement an extraction method tailored for decommissioning single fixed-steel pile foundations in offshore wind installations. By broadening the scope of decommissioning to encompass these specific structures, the research hopes to foster the sustainable, long-term growth of the offshore wind industry and reduce its reliance on methodologies derived from the offshore oil and gas sector. Given the multifaceted nature of decommissioning, this study delves into two of its core aspects: engineering and economics.

From the engineering standpoint, the literature review unveils a significant knowledge gap regarding the extraction of offshore foundations, with a narrow focus on anchor plates. Moreover, there remains an undefined spectrum of factors influencing or resisting the extraction process. This research brings a pioneering and academically rigorous contribution by conceptualising an extraction mechanism primarily for open-ended piles. This mechanism

assumes consistent extraction resistance factors across various fixed foundation types that may be studied in the future. By examining industries where extraction plays a role, such as salvage and construction, several primary extraction resistance factors have been identified. These include:

1. Effective Soil and Object Weight: This encompasses the combined weight of the soil mass, the object to be extracted, and the mechanism facilitating force transmission.
2. Soil Resistance along the Failure Surface: This represents the resistance provided by the soil when an object is being pulled from it.
3. Adhesion Force: The binding force that occurs between the surface of the object and the surrounding soil.
4. Soil Suction Force: Influenced by factors such as soil properties, extraction speed, and the duration of extraction.

In the context of open-ended piles, this research defines parameters impacting these factors:

- The extension of the failure surface shape to the soil surface is influenced by the embedment ratio, and soil properties and conditions.
- The horizontal dimension of the failure shape is dictated by the pile friction angle and embedment ratio.
- Skin friction determinants encompass the embedment ratio, relative soil density, soil-pile friction angle, and soil shear resistance angle.
- Soil suction force is impacted by soil properties, extraction velocity/ rate, and extraction duration.

In essence, this study meticulously charts the parameters and factors pivotal to the extraction of offshore foundations, laying a foundational framework for future research in the domain.

To validate the developed theoretical method for aiding the extraction of offshore wind's single fixed-steel pile foundations (mono-piles) that are displaced/driven into soil, a series of 1g experimental tests using scaled models were undertaken. These experiments were conducted at two scales: 1:73 and 1:64. The outside diameters of the piles for the 1:73 and 1:64 scales were 88.9 mm and 101.6 mm, respectively. To mitigate the impact of piles' dimensions, both the wall thickness and the embedment ratio for both piles' diameters were kept constant at 3 mm and 350 mm, respectively. The feasibility of the extraction method was investigated

through two novel applications in the offshore wind context: force and displacement, applied at varying rates. The force-extraction rates used were 50 (minimum), 100, 150 and 200 N/min (maximum). In terms of displacement control, the extraction velocities ranged from 5 mm/min (minimum) to 100 mm/min (maximum), with intermediary values of 25 and 50 mm/min. The investigation were carried out under two soil conditions: unsaturated and saturated.

The experimental investigations in both unsaturated and saturated soil conditions verified that the pile's tensile capacity is notably less than its compressive capacity. This discrepancy was especially pronounced in the 88.9 mm and 101.6 mm piles, where the tensile capacity saw a reduction of over 90%. This marked decline can be ascribed to the lack of embedment duration and operational loads. In the case of taking into account the operational loads, along with embedment duration, there will be an increase in the tensile capacity of the pile, as the factors will strengthen the structure-soil interaction. Nonetheless, the increase will not exceed or equal the compressive capacity of the pile.

In unsaturated soil conditions, where there is no excess pore pressure, the tensile capacities of both pile diameters exceeded those in saturated soil. It was also imperative to maintain a consistent soil density across both conditions. This consistency further underscored the influence of extraction velocity or rate on the pile's tensile capacity.

In a comparison of force and displacement extraction techniques under consistent soil density, displacement extraction showed high tensile capacity for the 88.9 mm and 101.6 mm piles in both unsaturated and saturated soil conditions. However, in saturated soil, both pile diameters were extracted soil-free, pointing to the development of minimal suction. This phenomenon can be linked to the gradual mechanism and the rate of displacement extraction approach, which facilitated the dissipation of the induced pore water pressure, resulting in a prevailing drainage condition. Such a behaviour was not observed during force extraction, which, due to its swifter mechanism and rate, resulted in pronounced suction and the subsequent extraction of the soil plug alongside the pile. Additionally, the ratio of the pile diameter to wall thickness emerged as a significant determinant of drainage speed, with a larger ratio accelerating the drainage process.

The experimental investigation pinpointed the optimal extraction velocities or rates for both displacement and force applications. For displacement extraction, the optimal velocity remained consistent for both pile diameters in unsaturated and saturated soils, standing at ≤ 50

mm/min. In the case for force extraction, the optimal rate was contingent on the pile diameter. In unsaturated soil, rates of ≤ 150 N/min and ≤ 100 N/min were optimal for the 88.9 mm and 101.6 mm piles, respectively. However, in saturated soil conditions, pinpointing the optimal rate for force extraction became complex due to the influence of the soil plug weight on tensile capacity during the tests.

The findings from the experimental phase affirmed the viability of completely removing offshore wind's single fixed steel pile foundations (mono-piles) via extraction, leveraging both displacement and force methods.

5.2 Decommissioning Techno-Economic Assessment

From an economic perspective, the literature review revealed a noticeable gap in the comprehensive examination of decommissioning expenditures associated with offshore wind turbine structures. Most studies either centered around developing a cost and time model to explore a single vessel strategy (transiting) across various scenarios for decommissioning wind components - as proposed by the industry – or they utilised DecEx as a parameter to formulate diverse life cycle models for offshore wind. Given that foundation removal represents the largest chunk of decommissioning expenses, this research ventured to craft a cost and time model specifically for the decommissioning of offshore wind fixed foundations. The primary objective of this modelling effort is to determine the most economical strategy and methodology for decommissioning offshore wind foundations. This involves a thorough comparison of favoured and suggested decommissioning strategies and methodologies, combined with an analysis of various vessel types and strategies.

The decommissioning methodologies examined for single fixed-steel pile foundations include cutting the pile at the seabed or 1 to 2 metres below it, and extraction methods encompassing both partial and full removal strategies. The input data for these methodologies focused primarily on the duration of associated activities. For the partial removal strategy, activities involved excavation and cutting, while the full removal strategy utilised extraction. In terms of vessels, two strategies were adopted: transiting and sending. The vessel types considered were WTIVs, jack-up barges, and HLVs. Furthermore, the model was designed to allow modifications to certain factors, enabling an assessment of their sensitivity and impact on decommissioning cost and time.

The model's findings highlight the pronounced influence of weather, an uncontrollable variable, on the duration of removal operations. This effect is evident irrespective of the methodology employed and significantly impacts the time vessels spend on-site. In terms of removal operation duration, partial removal proves to be lengthier due to multiple processes it involves, such as excavation and cutting, a series of steps not necessary in extraction.

Despite vessels playing a pivotal role in offshore wind operations, their availability and suitability remain major challenges in the industry. The findings show that, regardless of the scenario pursued, the sender strategy accrues higher time and costs for OWFoundations compared to the transit strategy. Furthermore, under the transit strategy, the results suggest that HLVs complete OWFoundations decommissioning operations more quickly than WTIV, albeit at a greater expense.

By increasing the estimated baseline values by conservative percentages – specifically, increasing the estimated duration of offshore wind foundation decommissioning methods' activities by 100%, adjusting the weather factor by 50 – 100%, and varying vessels' day rate by ± 20% - the results of the sensitivity analysis clearly indicate that extraction as a decommissioning method is more economical than the industry-proposed method. Additionally, the sensitivity analysis results demonstrate a direct impact of the learning curve on the decommissioning time and cost of OWFoundations. This evidence underscores opportunities for cost reductions in the industry's preferred decommissioning method, partial removal.

The model has identified factors that can influence Decommissioning Expenditure (DecEx) both positively and negatively. Factors that can lead to a reduction in DecEx include the development of innovative decommissioning strategies and methods, recycling and reusing materials, and benefits derived from the learning curve. Conversely, factors that contribute to an increase in DecEx include vessel rates, inflation, and regulatory requirements.

5.3 Future Research

From the theoretical and experimental researched showcased within this thesis, it is apparent the impact the novel method created has had on decommissioning offshore single-steel fixed piles for the wind sector. One can also see the direct correlation this has on other offshore

structures and the clear transition that this created methodology could be implemented for other offshore structures within oil and gas and other renewable sectors.

Future work should not only validate the methodology presented herewith by a field trial but also look at laboratory testing of other offshore structures to achieve similar results. The potential for this approach to be adopted across sectors for the efficient and effective method for decommissioning should not be underestimated. A brief breakdown of the potential objectives is presented in the Table 5-1 looking at the decommissioning perspectives of engineering, environmental and economics.

Table 5-1 summarises the required future work for decommissioning offshore wind mono-pile foundations.

Decommissioning	***Aspect***	***Description***	***Aim***
Engineering	Experimental	• Test in various types of soil, e.g., clay only and mix layers [clay and sand]	• To further understand the extraction [breakout] mechanics in cohesive soil [e.g. clay] • To determine and compare the impact of different soil types on the tensile capacity of the pile
		• Test further extraction applications, e.g., vibration only, vibration with displacement, displacement with force, and vibration with force	• To define the optimised/ efficient extraction application for offshore wind mono-pile foundations
		• Test welded piles	• To define the impact of welding on extraction
	Finite element model	• Model the experimental campaign using the testing data	• To validate the results
		• Scale up the experimental model	• To simulate loads of a field case throughout the farm's designated lifetime to assess the impact on the tensile capacity of the pile, along with carrying out pile extraction through the vessel
Environmental	Environmental impact assessment	• Carry out a study comparing the impact of different decommissioning	• To define the best decommissioning method

Decommissioning	***Aspect***	***Description***	***Aim***
		methods for monopile foundations on the environment through different attributes	
Economics	Techo-economic assessment	• Carry out a study comparing the recoverable material [e.g. steel] from extracting and cutting the pile	• To determine the value impact of recycling or reusing the recoverable material on decommissioning costs.

6 Reference

[1] GWEC, “Global Wind Report 2021,” *Glob. Wind Energy Counc.*, p. 80◘, 2021.

[2] OREAC, “The Power of our Ocean,” *Ocean Renew. Energy Action Coalit. (OREAC)*, vol. 47, no. 1, p. 92, 2020.

[3] WindEurope, “Our Energy Our Future - How offshore wind will help Europe go carbon-neutral,” *Wind. Mark. Intell.*, 2019.

[4] C. Davidson, M. J. Brown, A. J. Brennan, and J. Knappett, “Decommissioning of Offshore Piles Using Vibration,” *Proc. Twenty-seventh Int. Ocean Polar Eng. Conf.*, pp. 666–673, 2017.

[5] H. Ritchie and M. Roser, “Energy,” 2020. [Online]. Available: https://ourworldindata.org/electricity-mix. [Accessed: 14-Mar-2022].

[6] IRENA, “Wind energy,” *International Renewable Energy Agency*. [Online]. Available: https://www.irena.org/wind. [Accessed: 18-Mar-2022].

[7] Worley, “Energy transition - Turning our net-zero ambitions into reality.” [Online]. Available: https://www.worley.com/sustainability/energy-transition. [Accessed: 08-Mar-2022].

[8] C. Arlota and H. K. de M. Costa, *Climate change, Carbon Capture and Storage (CCS), energy transition, and justice: where we are now, and where are (should be) we headed?* INC, 2021.

[9] IRENA, “Energy Transition.” [Online]. Available: https://www.irena.org/energytransition. [Accessed: 11-Mar-2022].

[10] S&P Global, “What is Energy Transition? ,” 2020. [Online]. Available: https://www.spglobal.com/en/research-insights/articles/what-is-energy-transition. [Accessed: 11-Mar-2022].

[11] C2ES, “Renewable Energy,” *Center for Climate and Energy Soilutions*. [Online]. Available: https://www.c2es.org/content/renewable-energy/. [Accessed: 14-Mar-2022].

[12] United Nations, “The paris agreement,” 2015.

[13] European Commission, “Paris Agreement.” [Online]. Available: https://ec.europa.eu/clima/eu-action/international-action-climate-change/climate-negotiations/paris-agreement_en#ecl-inpage-598. [Accessed: 11-Mar-2022].

[14] IRENA, *World energy transitions outlook - 1.5 degrees pathway*. Abu Dhabi, 2021.

[15] IRENA, “Reaching Zero With Renewables: Eliminating CO2 emissions from industry and transport in line with the 1.5C climate goal,” *Int. Renew. Energy Agency*, p. 216, 2020.

[16] IRENA, “Industry & Transport,” *International Renewable Energy Agency*. [Online]. Available: https://www.irena.org/industrytransport. [Accessed: 23-Mar-2022].

[17] EPA, “Overview of Greenhouse Gases ,” *United States Environmental Protection Agency*. [Online]. Available: https://www.epa.gov/ghgemissions/overview-greenhouse-gases. [Accessed: 23-Mar-2022].

[18] IRENA, *Renewable capacity statistics 2021 - International Renewable Energy Agency*. 2021.

[19] IRENA, “Climate Change,” *International Renewable Energy Agency*. [Online]. Available: https://www.irena.org/climatechange. [Accessed: 22-Mar-2022].

[20] IRENA, “Renewable Energy Highlights,” *Int. Renew. Energy Agency*, 2021.

[21] IEA, “Global Energy Review 2021,” *IEA*, 2021.

[22] IRENA, “Capacity and Generation - Technologies,” *International Renewable Energy Agency*. [Online]. Available: https://www.irena.org/Statistics/View-Data-by-Topic/Capacity-and-

Generation/Technologies. [Accessed: 25-Mar-2022].

[23] IEA, “World Energy Outlook 2021,” *Int. Energy Agency*, p. 386, 2021.

[24] GWEC, “Global Wind Energy Report: Annual Market Update 2017,” p. 72, 2018.

[25] A. Kessler, “Gone with the wind: When Crotched Mountain had a wind farm,” 2017. [Online]. Available: https://www.ledgertranscript.com/When-Crotched-Mountain-had-a-wind-farm-7910099. [Accessed: 31-Mar-2022].

[26] D. Brooks, “Remembering the worlds first wind farm - in New Hampshire - Granite Geek,” *Granite geek*, 2016. [Online]. Available: https://granitegeek.concordmonitor.com/2016/02/24/remembering-worlds-first-wind-farm-new-hampshire/. [Accessed: 31-Mar-2022].

[27] Siemens Gamesa, “Onshore Wind Turbine SG 6.6-155 .” [Online]. Available: https://www.siemensgamesa.com/products-and-services/onshore/wind-turbine-sg-5-8-155. [Accessed: 31-Mar-2022].

[28] GE Renewable Energy, “Cypress Onshore Wind Turbine Platform .” [Online]. Available: https://www.ge.com/renewableenergy/wind-energy/onshore-wind/cypress-platform. [Accessed: 31-Mar-2022].

[29] Power Technology, “The world’s 10 biggest wind turbines ,” 2022. [Online]. Available: https://www.power-technology.com/features/featurethe-worlds-biggest-wind-turbines-4154395/. [Accessed: 31-Mar-2022].

[30] A. Durakovic, “GE Haliade-X Offshore Wind Turbine Reaches 14 MW Output ,” *Offshore Wind*, 2021. [Online]. Available: https://www.offshorewind.biz/2021/10/05/ge-haliade-x-offshore-wind-turbine-reaches-14-mw-output/. [Accessed: 31-Mar-2022].

[31] J. Tempel, N. Diepeveen, D. Sakzmann, and W. Vries, “Design of support structures for offshore wind turbines,” *WIT Trans. State Art Sci. Eng.*, vol. 44, pp. 1755–8336, 2010.

[32] Ørsted, “1991-2001 The First Offshore Wind Farms (Chapter 2/6),” *Ørsted*. [Online]. Available: https://orsted.com/about-us/whitepapers/making-green-energy-affordable/1991-to-2001-the-first-offshore-wind-farms. [Accessed: 01-Apr-2022].

[33] BP, “BP Statistical Review of World Energy,” *BP Energy outlook 2021*, vol. 70, 2021.

[34] IEA, “Renewable Energy Market Update - outlook for 2021 and 2022,” *IEA*, no. Paris, 2021.

[35] IRENA, *Global Renewables Outlook: Energy transformation 2050*. Abu Dhabi, 2020.

[36] IRENA, *Future of Wind: Deployment, investment, technology, grid integration and socio-economic aspects (A Global Energy Transformation paper)*. Abu Dhabi, 2019.

[37] IEA, “Net Zero by 2050: A Roadmap for the Global Energy Sector,” *Int. Energy Agency*, p. 224, 2021.

[38] IEA, “Offshore Wind Outlook 2019,” *IEA*, 2019.

[39] GWEC, “What if one of the key solutions to fighting climate change was in our ocean?,” *Global Wind Energy Council*. [Online]. Available: https://gwec.net/offshore-wind/. [Accessed: 08-Apr-2022].

[40] GWEC, “GWEC Market Intelligence releases Global Offshore Wind Turbine Installation Database,” 2020. [Online]. Available: https://gwec.net/gwec-market-intelligence-releases-global-offshore-wind-turbine-installation-database/. [Accessed: 19-Jan-2021].

[41] GWEC, “Global Wind Report 2022,” *Glob. Wind Energy Counc.*, 2022.

[42] European Commission, “Boosting Offshore Renewable Energy for a Climate Neutral Europe,” *European Commission*, 2020. [Online]. Available:

https://ec.europa.eu/commission/presscorner/detail/en/IP_20_2096. [Accessed: 04-May-2022].

[43] European Commission, “Energy - Onshore and offshore wind,” *European Commission*. [Online]. Available: https://energy.ec.europa.eu/topics/renewable-energy/onshore-and-offshore-wind_en. [Accessed: 04-May-2022].

[44] Adnan Durakovic, “EU Streamlining Path to 300 GW by 2050 Offshore Wind Target | Offshore Wind,” 2022. [Online]. Available: https://www.offshorewind.biz/2022/02/16/eu-streamlining-path-to-300-gw-by-2050-offshore-wind-target/. [Accessed: 04-May-2022].

[45] WindEurope, “Offshore Wind Energy - 2021 Statistics,” *Wind. Mark. Intell.*, 2022.

[46] EWEA, “Oceans of opportunity - Harnessing Europe’s largest domestic energy resource,” vol. 105, no. 11, pp. 1–69, 2009.

[47] WindEurope, “Overview of national permitting rules and good practices,” *Wind. Mark. Intell.*, vol. 1, 2021.

[48] WindEurope, “Wind energy in Europe: Outlook to 2023,” no. September, p. 44, 2019.

[49] Department of Energy and Climate Change, “Decommissioning of offshore renewable energy installations under the Energy Act 2004 - Guidance notes for industry,” 2011.

[50] Department of Energy and Climate Change, “Energy Act 2004,” *UK Public Gen. Acts - 2004 C.20*, p. 296, 2004.

[51] EuropeanCommission, “COMMUNICATION FROM THE COMMISSION TO THE EUROPEAN PARLIAMENT, THE COUNCIL, THE EUROPEAN ECONOMIC AND SOCIAL COMMITTEE AND THE COMMITTEE OF THE REGIONS - An EU Strategy to harness the potential of offshore renewable energy for a climate neutral future,” 2020.

[52] EU, “Directive (EU) 2018/2001 of the European Parliament and of the Council on the promotion of the use of energy from renewable sources,” *Off. J. Eur. Union*, vol. 2018, no. L 328, pp. 82–209, 2018.

[53] Arup, “Department of Business, Energy and Industrial Strategy - Cost Estimation and Liabilities in Decommissioning Offshore Wind Installations - Public Report,” p. 39, 2018.

[54] SiemensGamesa, “Siemens Gamesa pioneers wind circularity: launch of world’s first recyclable wind turbine blade for commercial use offshore,” *Siemens Gamesa Newsroom*, 2021. [Online]. Available: https://www.siemensgamesa.com/en-int/newsroom/2021/09/launch-world-first-recyclable-wind-turbine-blade. [Accessed: 26-May-2022].

[55] J. A. Schneider and M. Senders, “Foundation design: A comparison of oil and gas platforms with offshore wind turbines,” *Mar. Technol. Soc. J.*, vol. 44, no. 1, pp. 32–51, 2010.

[56] J. A. Pratt, “Offshore at 60: Remembering the Creole field ,” 2014. [Online]. Available: https://www.offshore-mag.com/home/article/16757220/offshore-at-60-remembering-the-creole-field. [Accessed: 22-Apr-2022].

[57] PetroWiki, “History of offshore drilling units ,” 2015. [Online]. Available: https://petrowiki.spe.org/History_of_offshore_drilling_units. [Accessed: 22-Apr-2022].

[58] 4C Offshore, “Middelgrunden Offshore Wind Farm - Fully Commissioned - Denmark,” *4C Offshore - Research & Intelligence*. [Online]. Available: https://www.4coffshore.com/windfarms/denmark/middelgrunden-denmark-dk08.html. [Accessed: 22-Jun-2022].

[59] J. H. M. Larsen, H. C. Soerensen, E. Christiansen, S. Naef, and P. Vølund, “Experiences from Middelgrunden 40 MW Offshore Wind Farm,” *Copenhagen Offshore Wind*, 2005.

[60] 4C Offshore, “Horns Rev 1 Offshore Wind Farm - Fully Commissioned - Denmark,” *4C Offshore - Research & Intelligence*. [Online]. Available: https://www.4coffshore.com/windfarms/denmark/horns-rev-1-denmark-dk03.html. [Accessed: 22-Jun-2022].

[61] Orsted, “Horns Rev 1 wind turbine has reached the 100GWh mark,” *Orsted - Media*, 2015. [Online]. Available: https://orsted.com/en/media/newsroom/news/2018/10/horns-rev-1-wind-turbine-has-reached-the-100gwh-mark. [Accessed: 22-Jun-2022].

[62] WindEurope, “Offshore Wind in Europe - Key trends and statistics 2017,” *Wind. Mark. Intell.*, 2018.

[63] WindEurope, “The European offshore wind industry - Key trends and statistics 2016,” *Wind. Mark. Intell.*, 2017.

[64] WindEurope, “Offshore wind in Europe - Key trends and statistics 2019,” *Wind. Mark. Intell.*, 2020.

[65] WindEurope, “Offshore wind in Europe - Key trends and statistics 2018,” *Wind. Mark. Intell.*, 2019.

[66] EWEA, “The European offshore wind industry - key 2015 trends and statistics,” *Eur. Wind Energy Assoc.*, 2016.

[67] WindEurope, “Offshore Wind in Europe - Key trends and statistics 2020,” *Wind. Mark. Intell.*, 2021.

[68] BVG Associates, “A Guide to an Offshore Wind Farm - Updated and extended - Published on behalf of The Crown Estate and the Offshore Renewable Energy Catapult,” no. January, pp. 1–70, 2019.

[69] M. J. Kaiser and B. Synder, *Offshore Wind Energy Costing Modeling: Installation and Decommissioning*. 2012.

[70] M. J. Kaiser and B. Snyder, “Offshore wind energy installation and decommissioning cost estimation in the U.S. outer continental shelf,” p. 340, 2010.

[71] K. E. Thomsen, *Offshore Wind - A comprehensive Guide to Successful Offshore Wind Farm Installation*, 2nd ed. Elsevier, 2014.

[72] DNV.GL, “Assessment of Offshore Wind Farm Decommissioning Requirements,” *Ontario Minist. Environ. Clim. Chang.*, 2016.

[73] A. Spyroudi, “End-of-life planning in offshore wind,” *CATAPULT*, 2021.

[74] O. Y. Miñambres, “Assessment of current offshore wind support structures concepts – challenges and technological requirements by 2020,” *Karlshochschule Int. Univ.*, 2012.

[75] DNV, “Offshore Standard - DNV-OS-J101 - Design of Offshore Wind Turbine Structures,” 2013.

[76] DNV GL, “DNVGL-ST-0126 - Support structures for wind turbines,” p. 182 pp, 2016.

[77] M. Keene, “Comparing offshore wind turbine foundations,” 2021. [Online]. Available: https://www.windpowerengineering.com/comparing-offshore-wind-turbine-foundations/. [Accessed: 03-Feb-2022].

[78] X. Wu *et al.*, “Foundations of offshore wind turbines: A review,” *Renew. Sustain. Energy Rev.*, vol. 104, no. December 2018, pp. 379–393, 2019.

[79] A. Kielkiewicz, A. Marino, C. Vlachos, F. Maldonado, Javier Lopez, and I. Lessis, “The Practicality and Challenges of Using XL Monopiles for Offshore Wind Turbine Substructures,” 2015. [Online]. Available: https://www.esru.strath.ac.uk//EandE/Web_sites/14-15/XL_Monopiles/index.html. [Accessed: 07-Mar-2022].

[80] WindFacts, “Offshore support structures,” 2009. [Online]. Available: https://www.wind-energy-the-facts.org/offshore-support-structures.html. [Accessed: 09-Mar-2022].

[81] MENCK, “Alpha Ventus Wind Farm.”

[82] Tube, “FA 09 Tripods , Jackets and Tripiles : Innovative Tube Systems for Offshore Wind Energy Systems,” pp. 1–5, 2018.

[83] E. de Vries, “Exploring the trends in foundation design,” 2012. [Online]. Available: https://www.windpowermonthly.com/article/1190827/exploring-trends-foundation-design. [Accessed: 10-Mar-2022].

[84] Offshore Wind, “Bard gets off the ground offshore,” 2009. [Online]. Available: https://www.modernpowersystems.com/features/featurebard-gets-off-the-ground-offshore/. [Accessed: 10-Mar-2022].

[85] 4C Offshore, “Hooksiel Offshore Wind Farm.” [Online]. Available: https://www.4coffshore.com/windfarms/germany/hooksiel-germany-de76.html. [Accessed: 09-Mar-2022].

[86] 4C Offshore, “BARD Offshore 1 Offshore Wind Farm.” [Online]. Available: https://www.4coffshore.com/windfarms/germany/bard-offshore-1-germany-de23.html. [Accessed: 09-Mar-2022].

[87] Power Technology, “BARD Offshore I Wind Farm, North Sea,” 2013. [Online]. Available: https://www.power-technology.com/projects/bard-offshore-i-north-sea-german/. [Accessed: 09-Mar-2022].

[88] E. de Vries, “Heading offshore - fast: ‘We want to be fully independent!’ says BARD Engineering,” 2007. [Online]. Available: https://www.renewableenergyworld.com/wind-power/heading-offshore-fast-we-want-to-be-fully-independent-says-bard-engineering-51472/#gref. [Accessed: 10-Mar-2022].

[89] FoundOcean, “Beatrice Offshore Wind Farm.”

[90] BOWL, “Beatrice Offshore Wind Farm Consent Plan - Construction Method Statement,” *Beatrice Offshore Wind Farm Ltd*, 2016.

[91] R. Strancich, “GeoSea: New technology drives down turbine foundation installation costs ,” *Reuters Events*, 2010. [Online]. Available: https://www.reutersevents.com/renewables/wind-energy-update/geosea-new-technology-drives-down-turbine-foundation-installation-costs. [Accessed: 15-Mar-2022].

[92] M. M. Luengo and A. Kolios, “Failure mode identification and end of life scenarios of offshore wind turbines: A review,” *Energies*, vol. 8, no. 8, pp. 8339–8354, 2015.

[93] WindEurope, “Repowering and Lifetime Extension: making the most of Europe’s wind energy source,” *Wind. Mark. Intell.*, 2017.

[94] A. Gokhale, “Concept for repowering OWF -Comparison of CO2 and costs with decommissioning,” 2021.

[95] Michele Admin, “Extending the Lifetime of Wind Turbines ,” *Wind Systems Magazine*, 2019. [Online]. Available: https://www.windsystemsmag.com/extending-the-lifetime-of-wind-turbines/. [Accessed: 27-May-2022].

[96] DNV, “Wind farm life-extension.” [Online]. Available: https://www.dnv.com/services/wind-farm-life-extension-5383. [Accessed: 27-May-2022].

[97] L. Ziegler, E. Gonzalez, T. Rubert, U. Smolka, and J. J. Melero, “Lifetime extension of onshore wind turbines: A review covering Germany, Spain, Denmark, and the UK,” *Renew. Sustain. Energy Rev.*, vol. 82, no. October 2017, pp. 1261–1271, 2018.

[98] A. Buljan, “Keeping Turbines Turning for Longer: How Offshore Wind Can Address Ageing Assets Smartly to Extract Hidden Value ,” *Offshore Wind*, 2021. [Online]. Available: https://www.offshorewind.biz/2021/06/07/keeping-turbines-turning-for-longer-how-offshore-wind-can-address-ageing-assets-smartly-to-extract-hidden-value/. [Accessed: 27-May-2022].

[99] E. Topham and D. McMillan, “Sustainable decommissioning of an offshore wind farm,” *Renew. Energy*, vol. 102, pp. 470–480, 2017.

[100] Momentum, “Bockstigen Offshore Repowering.” [Online]. Available: https://momentum-gruppen.com/case/bockstigen-offshore-repowering/. [Accessed: 15-Jun-2022].

[101] J. Gredes, “World’s First Offshore Wind Repowering Completed in Sweden ,” *Greentech Media*, 2018. [Online]. Available: https://www.greentechmedia.com/articles/read/worlds-first-offshore-wind-repowering-completed-in-sweden. [Accessed: 15-Jun-2022].

[102] 4C Offshore, “Bockstigen Offshore Wind Farm - Fully Commissioned - Sweden,” *4C Offshore*. [Online]. Available: https://www.4coffshore.com/windfarms/sweden/bockstigen-sweden-se02.html. [Accessed: 15-Jun-2022].

[103] The Crown Estate, “Offshore Wind Leasing Round 4 - Unlocking new areas of seabed for the generation of low carbon energy for millions more homes by 2030.” [Online]. Available: https://www.thecrownestate.co.uk/round-4/. [Accessed: 02-Jun-2022].

[104] 4C Offshore, “Key project dates for Yttre Stengrund - Sweden ,” *4C Offshore - Research & Intelligence*. [Online]. Available: https://www.4coffshore.com/windfarms/sweden/project-dates-for-yttre-stengrund-se04.html. [Accessed: 16-Jun-2022].

[105] T. Russell, “Yttre Stengrund completely decommissioned,” *4C Offshore*, 2016. [Online]. Available: https://www.4coffshore.com/news/yttre-stengrund-completely-decommissioned-nid3199.html. [Accessed: 16-Jun-2022].

[106] R. Welstead, J., Hirst, R., Keogh, D., Robb G. and Bainsfair, “Research and guidance on restoration and decommissioning of onshore wind farms,” *Scottish Nat. Herit.*, 2013.

[107] 4C Offshore, “Global Offshore Wind Farms Database ,” *4C Offshore - Research & Intelligence*. [Online]. Available: https://www.4coffshore.com/windfarms/. [Accessed: 14-Jul-2022].

[108] Centrica Energy, DONG, and Siemens, “LINCS Offshore Wind Farm Decommissioning Plan - On behalf of Lincs Wind Farm Limited - Produced in association with RPS,” p. 41, 2010.

[109] Scira Offshore Energy, *Decommissioning Programme - Sheringham Offshore Wind Farm - Statoil*. 2014.

[110] Greater Gabbard Offshore Winds Ltd, *Decommissioning Programme - Greater Gabbard Offshore Wind Farm Project*. 2007.

[111] Dong Energy, “Burbo Bank Extension Offshore Wind Farm,” vol. 1, no. March, 2013.

[112] Climate Change Capital, “Offshore Renewable Energy Installation Decommissioning Study,” 2006.

[113] Shell U.K. Limited, “BRENT ALPHA JACKET DECOMMISSIONING TECHNICAL DOCUMENT,” no. February, 2017.

[114] FPS, “NOTES FOR GUIDANCE ON THE EXTRACTION OF TEMPORARY CASINGS AND TEMPORARY PILES WITHIN THE PILING INDUSTRY,” 2010.

[115] Dieseko Group, “Decommissioning Lely offshore wind farm,” *Dieseko Group - Projects*. [Online]. Available: https://www.diesekogroup.com/project/decommissioning-lely-offshore-wind-farm/. [Accessed: 19-Jul-2022].

[116] Delfares, “Industry joins forces to study the sustainable decommissioning of offshore wind

turbine foundations - Deltares," 2019. [Online]. Available: https://www.deltares.nl/en/news/industry-joins-forces-study-sustainable-decommissioning-offshore-wind-turbine-foundations/. [Accessed: 25-Jun-2019].

[117] M. Coronel, "Hydraulic pile extraction scale tests for testing the removal of piles from the soil at the end of their operational life - Public report," 2020.

[118] GROW, "Slip Joint Offshore Research project (SJOR) ," *GROW - Projects*. [Online]. Available: https://grow-offshorewind.nl/project/sjor. [Accessed: 20-Jul-2022].

[119] S. Killoh, "History made by Heerema with offshore testing campaign," *HEEREMA*, 2021. [Online]. Available: https://www.heerema.com/insights/history-made-by-heerema-with-offshore-testing-campaign. [Accessed: 20-Jul-2022].

[120] J. Jonkman, S. Butterfield, W. Musial, and G. Scott, "Definition of a 5-MW Reference Wind Turbine for Offshore System Development," *Natl. Renew. Energy Lab. - A Natl. Lab. U.S. Dep. Energy - Off. Energy Effic. Renew. Energy*, p. 75, 2009.

[121] C. Desmond, J. Murphy, L. Blonk, and W. Haans, "Description of an 8 MW reference wind turbine," *J. Phys. Conf. Ser.*, vol. 753, no. 9, p. 17, 2016.

[122] C. Bak *et al.*, "The DTU 10-MW Reference Wind Turbine," p. 22, 2013.

[123] E. Lozano-Minguez, A. J. Kolios, and F. P. Brennan, "Multi-criteria assessment of offshore wind turbine support structures," *Renew. Energy*, vol. 36, no. 11, pp. 2831–2837, 2011.

[124] W. N. Wandji, A. Natarajan, N. Dimitrov, and T. Buhl, "Design of monopiles for multi-megawatt wind turbines at 50 m water depth," *Eur. Wind Energy Assoc. Annu. Conf. Exhib. 2015, EWEA 2015 - Sci. Proc.*, pp. 8–12, 2015.

[125] A. Myhr, C. Bjerkseter, A. Ågotnes, and T. A. Nygaard, "Levelised cost of energy for offshore floating wind turbines in a lifecycle perspective," *Renew. Energy*, vol. 66, no. June, pp. 714–728, 2014.

[126] A. Ioannou, A. Angus, and F. Brennan, "A lifecycle techno-economic model of offshore wind energy for different entry and exit instances," *Appl. Energy*, vol. 221, no. November 2017, pp. 406–424, 2018.

[127] Vattenfall, "Power plants: Horns Rev 1 ." [Online]. Available: https://powerplants.vattenfall.com/horns-rev/. [Accessed: 24-Mar-2021].

[128] Power Technology, "Horns Rev Offshore Wind Farm, Denmark," 2008. [Online]. Available: https://www.power-technology.com/projects/hornsreefwind/. [Accessed: 24-Mar-2021].

[129] Ørsted, "Our Offshore Wind Farms." [Online]. Available: https://orsted.com/en/our-business/offshore-wind/our-offshore-wind-farms. [Accessed: 24-Mar-2021].

[130] H. Craven, "Decommissioning Programme for Dudgeon Offshore Wind Farm - Statoil," p. 40, 2015.

[131] GreaterGabbardOffshoreWindsLtd, "Greater Gabbard Offshore Wind Farm - environmental statement - Airtricit Flour, PMSS," p. 672, 2005.

[132] London Array Limited, "Decommissioning Programme for London Array," p. 29, 2013.

[133] Scira Offshore Energy LTD, "Sheringham Shoal wind farm - Environmental Statement," p. 722, 2015.

[134] Yumpu, "Galloper Wind Farm Project." [Online]. Available: https://www.yumpu.com/en/Galloper_Wind_Farm_Project. [Accessed: 11-Apr-2021].

[135] SSE Renewables, "Greater Gabbard Offshore Wind Farm." [Online]. Available: https://www.sserenewables.com/offshore-wind/operations/greater-gabbard/. [Accessed: 18-

Mar-2021].

[136] FLOUR, “Greater Gabbard Offshore Wind Farm - United Kingdom.” [Online]. Available: https://www.fluor.com/projects/offshore-wind-farm-epc. [Accessed: 31-May-2020].

[137] 4C Offshore, “Greater Gabbard Offshore Wind Farm.” [Online]. Available: https://www.4coffshore.com/windfarms/united-kingdom/greater-gabbard-united-kingdom-uk05.html. [Accessed: 31-May-2020].

[138] Power Technology, “The Greater Gabbard Offshore Wind Project, UK,” 2010. [Online]. Available: https://www.power-technology.com/projects/greatergabbardoffsho/. [Accessed: 14-Apr-2021].

[139] Designing Buildings, “Pile foundations ,” 2021. [Online]. Available: https://www.designingbuildings.co.uk/wiki/Pile_foundations#Introduction. [Accessed: 02-Feb-2022].

[140] Designing Buildings, “Building foundations ,” 2021. [Online]. Available: https://www.designingbuildings.co.uk/wiki/Building_foundations#Types_of_shallow_foundations. [Accessed: 02-Feb-2022].

[141] UWE, “Foundations.” [Online]. Available: http://environment.uwe.ac.uk/geocal/foundations/fountype.htm. [Accessed: 02-Feb-2022].

[142] DNV GL, “Standard - DNVGL-ST-0119 - floating wind turbines,” p. 162, 2018.

[143] A. S. Vesic, *Design of pile fundations - National Cooperative Highway Research Program, Synthesis Highway Practice.*, vol. I. 1977.

[144] B. Wrana, “Pile Load Capacity – Calculation Methods,” *Stud. Geotech. Mech.*, vol. 37, no. 4, 2015.

[145] R. Rajapakse, *Pile Design and Construction Rules of Thumb*, Second Edi. Elsevier Inc., 2008.

[146] Nucor Skyline, “Piling Accessories,” *Nucor - Pile Accessories*. [Online]. Available: https://www.nucorskyline.com/globalnav/products/accessories. [Accessed: 31-Aug-2022].

[147] B. Byrne, “Driven pipe piles in dense sand,” *Aust. Geomech. J.*, vol. 27, pp. 72–80, 1995.

[148] B. R. D. Raines, O. G. Ugaz, and M. W. O. Neill, “Driving characteristics o f o p e n - t o e p i l e s in d e n s e sand,” vol. 118, no. 571, pp. 72–88, 1992.

[149] E. Pohland, “Pile Driving Part II: Pile Types and Guidelines,” *Pile Buck Magazine - Deep Foundation*, 2021. [Online]. Available: https://pilebuck.com/foundation/pile-driving-part-ii-pile-types-guidelines/. [Accessed: 31-Aug-2022].

[150] A. De Nicola and M. F. Randolph, “The plugging behaviour of driven and jacked piles in sand,” *Geotechnique*, vol. 47, no. 4, pp. 841–856, 1997.

[151] K. Paik, R. Salgado, J. Lee, and B. Kim, “Behavior of open- and closed-ended piles driven into sands,” *J. Geotech. Geoenvironmental Eng.*, vol. 129, no. 4, pp. 296–306, 2003.

[152] O. A. Purwana, C. F. Leung, Y. K. Chow, and K. S. Foo, “Influence of base suction on extraction of jack-up spudcans,” *Geotechnique*, vol. 55, no. 10, pp. 741–753, 2005.

[153] M. S. Hossain, Y. Hu, and D. Ekaputra, “Extraction response of skirted foundations and a spudcan on sand-over-clay deposits,” *Geotechnique*, vol. 67, no. 5, pp. 460–465, 2017.

[154] G. T. Houlsby, R. . Kelly, and B. W. Byrne, “The tensile capacity of suction caissons in sand under rapid loading,” *Proc. 1st Int. Symp. Front. Offshore Geotech. (ISFOG 2005)*, no. 1, pp. 405–410, 2005.

[155] Dieseko Group, “Offshore ,” *Dieseko Group - Markets: Offshore*. [Online]. Available: https://www.diesekogroup.com/markets/offshore/. [Accessed: 07-Sep-2022].

[156] GIKEN LTD., “Press-in Principle,” *GIKEN LTD. - Press-in Method*. [Online]. Available: https://www.giken.com/en/press-in_method/press-in-principle/. [Accessed: 08-Sep-2022].

[157] F. Brucy, J. Meunier, and J. F. Nauroy, “Behavior of pile plug in sandy soils during and after driving,” *Proc. Annu. Offshore Technol. Conf.*, no. 1, pp. 145–154, 1991.

[158] B. M. Lehane and K. G. Gavin, “Base Resistance of Jacked Pipe Piles in Sand,” *J. Geotech. Geoenvironmental Eng.*, vol. 127, no. 6, pp. 473–480, 2001.

[159] K. Paik and R. Salgado, “Discussion of ‘determination of bearing capacity of open-ended piles in sand,’” *J. Geotech. Geoenvironmental Eng.*, vol. 130, no. 6, pp. 656–656, 2003.

[160] C. L. Liu, “Ocean Sediment Holding Strength Against Breakout of Embedded Objects,” 1969.

[161] S. G. Paikowsky, R. V Whitman, and M. M. Baligh, “A new look at the phenomenon of offshore pile plugging,” *Mar. Geotechnol.*, pp. 213–230, 1989.

[162] W. D. L. Finn and P. M. Byrne, “The evaluation of the break-out force for a submerged ocean platform,” *Proc. Annu. Offshore Technol. Conf.*, vol. 1972-May, pp. I863–I868, 1972.

[163] M. A. Foda, “On the extrication of large objects from the ocean bottom (the breakout phenomenon),” *J. Fluid Mech.*, vol. 117, no. 24885, pp. 211–231, 1982.

[164] S. A. Vesic, “Breakout Resistance of Objects Embedded in Ocean Bottom,” 1969.

[165] L. Pliskin, “Removal of concrete gravity platforms,” 1979.

[166] B. C. Chattopadhyay and P. J. Pise, “Uplift Capacity of Driven Piles in Sand.,” *J. Inst. Eng. Civ. Eng. Div.*, vol. 68, no. 2, pp. 89–91, 1987.

[167] G. G. Meyerhof and J. I. Adams, “The Ultimate Uplift Capacity of Foundations,” *Can. Geotech. J.*, vol. 5, no. 4, pp. 225–224, 1968.

[168] W. H. Baker and R. L. Konder, “Pullout load capacity of a circular earth anchor buried in sand.pdf,” *44th Annu. Meet. Highw. Res. Board*, pp. 1–10, 1966.

[169] E. J. Murray and J. D. Geddes, “Uplift of anchor plates in sand,” *J. Geotech. Eng.*, vol. 114, no. 12, pp. 1461–1462, 1988.

[170] H. B. Sutherland, “Uplift resistance of soils,” *Geotechnique*, vol. 38, no. 4, pp. 493–516, 1988.

[171] D. R. Levachrer and J.-G. Sieffert, “Tests on model tension piles,” *J. Geotech. Eng.*, vol. 110, no. 12, pp. 1735–1748, 1984.

[172] M. F. Randolph, J. Dolwin, and R. Beck, “Design of driven piles in sand,” *Geotechnique*, vol. 44, no. 3, pp. 427–448, 1994.

[173] B. M. Das, G. R. Seeley, and T. W. Pfeifle, “Pullout Resistance Of Rough Rigid Piles In Granular Soil,” *Soils Found.*, vol. 17, no. No. 3, pp. 72–77, 1977.

[174] B. M. Das, “A Procedure for Estimation of Uplift Capacity of Rough Piles,” *Soils Found.*, vol. 23, no. 3, pp. 122–126, 1983.

[175] S. El-Gharbawy and R. Olson, “Pullout capacity of suction caisson foundations for tension leg platforms,” *Proc. Int. Offshore Polar Eng. Conf.*, vol. 1, pp. 531–536, 1998.

[176] J. Jeffrey, “Investigating the performance of continuous helical displacement piles Investigating the performance of continuous helical displacement piles,” *Univ. Dundee*, 2012.

[177] R. Phillips and A. J. Valsangkar, “Experimental Investigation of Factors Affecting Penetration Resistance in Granular Soils in Centrifuge Modelling.,” *Cambridge University, Engineering Department, (Technical Report) CUED/D-Soils*. 1987.

[178] E. Heins, M. F. Randolph, B. Bienen, and J. Grabe, “Effect of installation method on static and dynamic load test response for piles in sand,” *Int. J. Phys. Model. Geotech.*, vol. 20, no. 1, pp.

1–23, 2020.

[179] Omega, “Submersible Pressure Transducers: for level, depth or ground water measurements,” pp. 0–5.

[180] Omega, “Omega User’s Guide: PX709 series - Submersible Pressure Transducers.”

[181] GWI, “GW Intsruments - Instrunet Data Acquisition: iNet-512 instruNet Wiring Box (i512),” 2017. [Online]. Available: http://www.gwinst.com/p/i512/index.html. [Accessed: 02-Nov-2022].

[182] B. A. De Nicola and M. F. Randolph, “Tensile and Compressive Shaft Capacity of Piles In Sand,” *Geotech. Eng.*, vol. 119, no. 12, pp. 1952–1973, 1993.

[183] R. Overy, “The use of ICP design methods for the foundations of nine platforms installed in the UK North Sea.,” *Proc. 6th Int. Offshore Site Investig. Geotech. Conf. Confronting New Challenges Shar. Knowl.*, 2007.

[184] WIKI ACCOUNTING, “Accounting for decommissioning costs - Fixed Assests.” [Online]. Available: https://www.wikiaccounting.com/accounting-decommissioning-costs/. [Accessed: 09-Mar-2021].

[185] M. Shafiee, F. Brennan, and I. A. Espinosa, “A parametric whole life cost model for offshore wind farms,” *Int. J. Life Cycle Assess.*, vol. 21, no. 7, pp. 961–975, 2016.

[186] Thanet Offshore Wind Limited, “Thanet offshore wind farm - Offshore Decommissioning Plan,” p. 33, 2008.

[187] RWE npower Renewables, “Decommissioning strategy Gwynt Môr Offshore Wind Farm Ltd,” 2011.

[188] Chamberlain Kerry, “Offshore operators act on early decommissioning data to limit costs - Reuters Events - Renewables,” 2016. [Online]. Available: https://www.reutersevents.com/renewables/wind-energy-update/offshore-operators-act-early-decommissioning-data-limit-costs. [Accessed: 27-Oct-2021].

[189] E. Topham, D. McMillan, S. Bradley, and E. Hart, “Recycling offshore wind farms at decommissioning stage,” *Energy Policy*, vol. 129, no. January, pp. 698–709, 2019.

[190] Diesko Group, “Decommissioning Lely offshore wind farm.” [Online]. Available: https://www.diesekogroup.com/desommissioning-lely-offshore-wind-farm/. [Accessed: 31-Dec-2019].

[191] GROW, “Hydraulic Pile Extraction Scale Tests (HyPE-ST) .” [Online]. Available: https://grow-offshorewind.nl/project/hype-st. [Accessed: 04-Nov-2021].

[192] The crown estate, “Jack-up vessel optimisation,” 2014.

[193] 4C Offshore, “Vessels working on Greater Gabbard - United Kingdom.” [Online]. Available: https://www.4coffshore.com/windfarms/united-kingdom/vessels-on-greater-gabbard-uk05.html. [Accessed: 29-Jul-2021].

[194] C. Naschert, “Global shortage of installation vessels could trouble waters for offshore wind,” *S&P Global Market Intelligence*, 2019. [Online]. Available: https://www.spglobal.com/marketintelligence/en/news-insights/trending/LPC6P4u-UC9qVTTB4V05Cg2. [Accessed: 19-Jan-2021].

[195] A. Durakovic, “Offshore Wind Faces Installation Vessel Shortage - Rystad Energy,” 2020. [Online]. Available: https://www.offshorewind.biz/2020/11/26/offshore-wind-faces-installation-vessel-shortage-rystad-energy/. [Accessed: 19-Jan-2021].

[196] J. Bard and F. Thalemann, “Offshore Infrastructure : Ports and Vessels - a report of the off-shore renewable energy conversion platforms - coordination action,” *ORECCA*, 2011.

[197] Seajacks, “Seajacks Kraken.” [Online]. Available: https://www.seajacks.com/self-propelled-jack-up-vessels/seajacks-kraken/. [Accessed: 29-Jul-2021].

[198] 4C Offshore, “Seajacks Kraken - Jack-up vessel | 4C Offshore.” [Online]. Available: https://www.4coffshore.com/vessels/vessel-seajacks-kraken-vid51.html. [Accessed: 29-Jul-2021].

[199] 4C Offshore, “Wind Orca - Jack-up vessel.” [Online]. Available: https://www.4coffshore.com/vessels/vessel-wind-orca-vid536.html. [Accessed: 29-Jul-2021].

[200] Ship Technology, “Pacific Orca Wind Farm Installation Vessel.” [Online]. Available: https://www.ship-technology.com/projects/pacific-orca-wind-farm-installation-vessel/. [Accessed: 29-Jul-2021].

[201] Cadeler, “Technical secifications - Windfarm Installation Vessel (WIV) Wind Orca,” 2021.

[202] 4C Offshore, “Vessels working on Rampion - United Kingdom.” [Online]. Available: https://www.4coffshore.com/windfarms/united-kingdom/vessels-on-rampion-uk36.html. [Accessed: 29-Jul-2021].

[203] FOWIND, “Supply chain , port infrastructure and logistic study - for offshore wind development in Gujarat and Tamil Nadu,” p. 124, 2016.

[204] MPI OFFSHORE, “Offshore installation and maintenance vessel MPI Resolution,” 2019.

[205] 4C Offshore, “MPI Resolution Heavy Maintenance and Construction.” [Online]. Available: https://www.4coffshore.com/vessels/vessel-mpi-resolution-vid35.html. [Accessed: 03-Feb-2021].

[206] J. Hartkopf-Mikkelsen, “Offshore wind turbine manufacturer: We are missing installation ships now,” 2020. [Online]. Available: https://www.soefart.dk/article/view/736115/havmolleproducent_vi_mangler_installationsskibe_nu. [Accessed: 19-Jan-2021].

[207] Offshore Engineer, “Booming Offshore Wind Market Faces Shortage of Installation Vessels,” 2020. [Online]. Available: https://www.oedigital.com/news/483533-booming-offshore-wind-market-faces-shortage-of-installation-vessels. [Accessed: 09-May-2021].

[208] 4C Offshore, “Vessels working on Robin Rigg - United Kingdom .” [Online]. Available: https://www.4coffshore.com/windfarms/united-kingdom/vessels-on-robin-rigg-uk20.html. [Accessed: 16-May-2021].

[209] DEME Group, “Rambiz.” [Online]. Available: https://www.deme-group.com/technologies/rambiz. [Accessed: 31-Jul-2021].

[210] Heerema, “Thialf.” [Online]. Available: https://hmc.heerema.com/fleet/thialf. [Accessed: 12-May-2021].

[211] Seaway Heavy Lifting, “Seaway Yudin,” 2019.

[212] Jambo, “Vessel, Jumbo Javelin - DP2 Heavy Lift Crane,” pp. 0–3, 2015.

[213] T. Stallard, *Economics of ocean energy*, vol. 8. Elsevier Ltd., 2012.

[214] Van Oord, “Heavy Lift Installation Vessel - Svanen.” 2018.

[215] Boskalis, “Heavy lift vessels.” [Online]. Available: https://boskalis.com/about-us/fleet-and-equipment/offshore-vessels/heavy-lift-vessels.html. [Accessed: 07-Aug-2021].

[216] J-UB, “JB-117 Self Elevating Platform.” [Online]. Available: https://www.jackupbarge.com/fleet/detail/jb-117-self-elevating-platform/. [Accessed: 07-Aug-2021].

[217] 4C Offshore, “JB - 117 - Jack-up barge .” [Online]. Available:

https://www.4coffshore.com/vessels/vessel-jb---117-vid81.html. [Accessed: 07-Aug-2021].

[218] T. P. Wright, “Factors Affecting the Cost of Engineering,” *J. Aeronaut. Sci.*, vol. 3, no. 4, pp. 122–128, 1936.

[219] J. Kagan, “Learning Curve,” 2020. [Online]. Available: https://www.investopedia.com/terms/l/learning-curve.asp. [Accessed: 14-Oct-2021].

[220] Catapult, “Cost reduction monitoring framework 2016 - Qualitative summary report,” 2017.

[221] Offshore Wind, “Siemens and MPI Adventure Install All Sandbank Turbines,” 2017. [Online]. Available: https://www.offshorewind.biz/2017/01/23/siemens-and-mpi-adventure-install-all-sandbank-turbines/. [Accessed: 18-Oct-2021].

[222] OGA, “UKCS Decommissioning- Cost Estimate 2021,” no. July, pp. 1–32, 2021.

[223] Z. Shahan, “History of Wind Turbines ,” 2014. [Online]. Available: https://www.renewableenergyworld.com/2014/11/21/history-of-wind-turbines/#gref. [Accessed: 21-Jan-2021].

[224] N. Nixon, “Timeline: The history of wind power,” *The Guardian*, 2008. [Online]. Available: https://www.theguardian.com/environment/2008/oct/17/wind-power-renewable-energy. [Accessed: 21-Jan-2021].

[225] B. N. Owens, *The Wind Power Story: A Century of Innovation That Reshaped the Global Energy Landscape*. Wiley, 2019.

[226] WindEurope, “Wind industry calls for Europe-wide ban on landfilling turbine blades,” *WindEurope Newsroom - Press releases*, 2021. [Online]. Available: https://windeurope.org/newsroom/press-releases/wind-industry-calls-for-europe-wide-ban-on-landfilling-turbine-blades/. [Accessed: 26-May-2022].

[227] T. Russell, “MPI ADVENTURE Decommissioning Robin Rigg Turbines | 4C Offshore News,” *4C Offshore News*, 2015. [Online]. Available: https://www.4coffshore.com/news/mpi-adventure-decommissioning-robin-rigg-turbines--nid2512.html. [Accessed: 14-Jul-2022].

[228] G. Smith and G. Lamont, “Decommissioning of Offshore Wind Installations - What we can Learn - What we can Learn,” *Offshore Wind Energy 2017*, no. June 2017, 2017.

[229] A. S. Vesic, “Bearing Capacity of Deep Foundations in Sand,” *Highw. Res. Rec.*, vol. 39, pp. 112–153, 1963.

[230] H. Niroumand and K. A. Kassim, *Horizontal Anchor Plates in Cohesionless Soil*. 2016.

[231] Catapult Offshore Renewable Energy, “Wind farm costs – Guide to an offshore wind farm.” [Online]. Available: https://guidetoanoffshorewindfarm.com/wind-farm-costs. [Accessed: 23-Feb-2021].

7 Appendix

7.1 Appendix A

Global wind statistics for 2021 are shown under the appendices because had been published after chapter two -literature review- writing-up. Furthermore, the stats had published only by GWEC, resulting in a lack of comparison to ensure consistency and reliability. The statistics herein demonstrate on and off-shore wind cumulative installed capacity; globally [Figure 7-1] and in geographical regions [Figure 7-2].

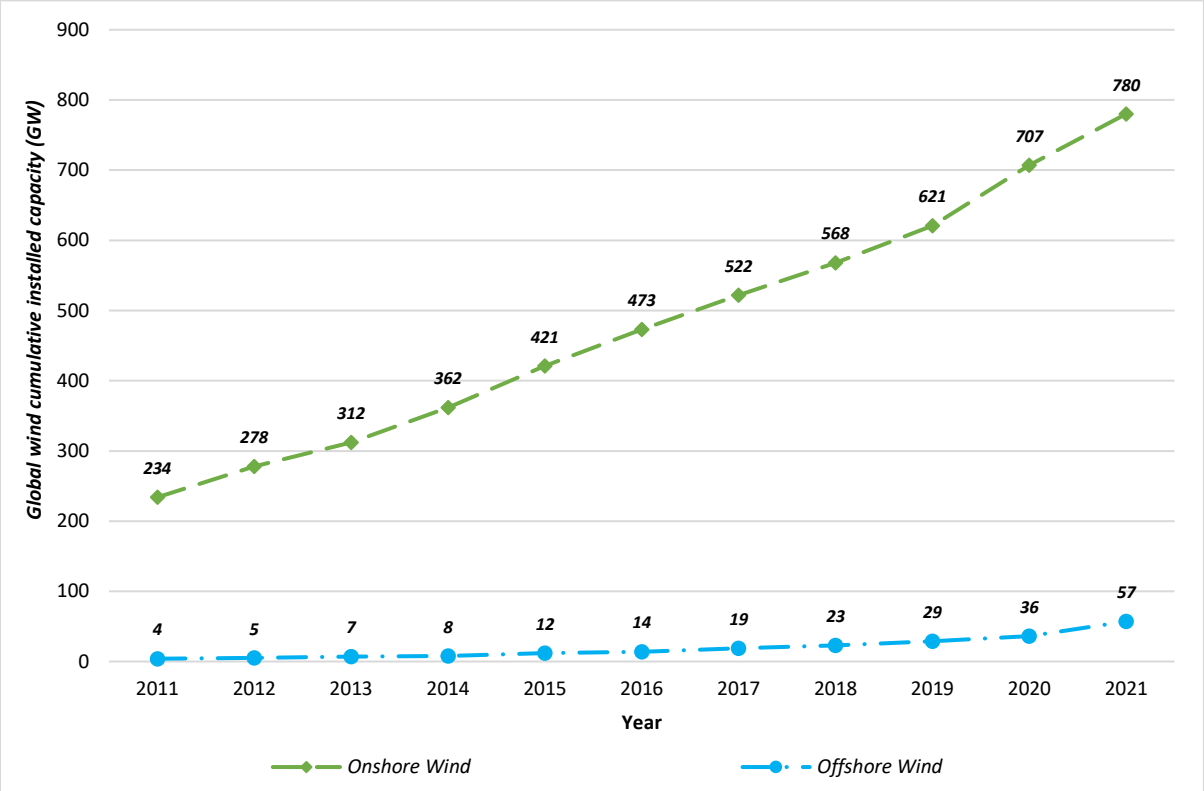

Figure 7-1. Up-to-date [2021] global wind cumulative installed capacity - source: author analysis edited based on [GWEC, 2022].

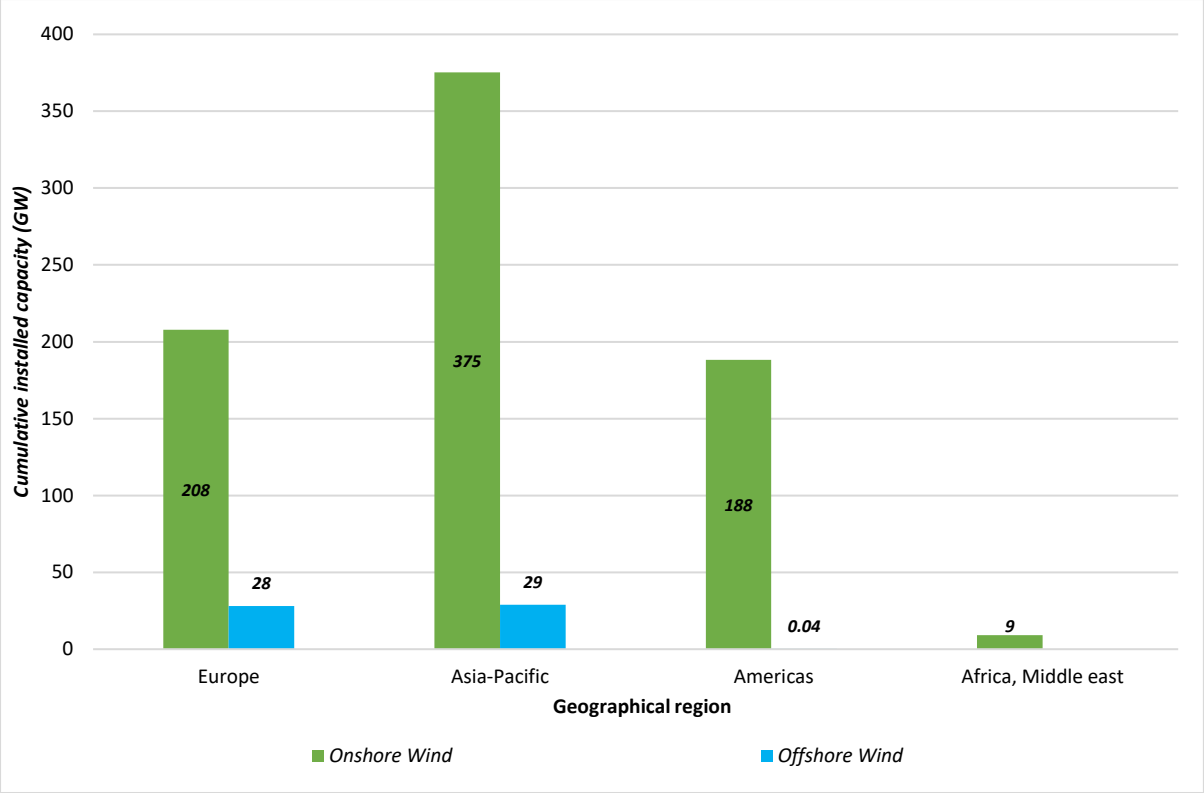

Figure 7-2. Geographical regions cumulative wind installed capacity, on and offshore – source: author edited based on [GWEC, 2022].

7.2 Appendix B

Wind Turbine Installation Vessels' Fundamental Specifications

Vessel Name/ Specifications	***Sea Installer***	***Sea Challen -ger***	***MPI Adventure***	***Pacific Osprey***	***Pacific Orca***	***Scylla***	***Aeolus***
Current owner/ operator	Geo-Sea	GeoSea	Van Oord	Cadeller	Cadeller	Sea-Jacks	Van Oord
Country	DK	DK	NL	DK	DK	UK	NL
Number of legs	-	-	6	6	6	4	4
Transit Speed (Knot)	10	12	11.7 ~12	13	13	10	11
Max. water depth (m)	55	55	40	70	60	65	45
Crane capacity (t) at radius (m)	900 at 24	900 at 24	1,000 at 24	1,200 at 25	1,200 at 31	1,500 at 31.5	1,600 at 32
Jacking speed (m/min)	0.4	0.4	1	2.4	2.4	0.8	0.6
Wind speed (m/s)	-	-	-	20	20	-	-
Max. operable significant wave height (m)	2	1.8	2.8	2.5	2.5	2.5	-

7.3 Appendix C

Floating Sheeleg Vessels Fundamental Specifications

Vessel Name/ Specifications	***Taklift 7***	***Taklift 4***	***Rambiz***	***Asian Hercules II***	***Asian Hercules III***
Current owner/ operator	Boskalis (Royal Boskalis Westminster)	Boskalis (Royal Boskalis Westminster)	Scaldis Salvage and Marine Contractors NV	Smit	Smit
Country	NL	NL	BE	NL	NL
Transit Speed (Knot)	10	10	6	7	7
Crane capacity	1,200	2,200	3,300	3,200	5,000